

A Thesis Submitted for the Degree of PhD at the University of Warwick

Permanent WRAP URL:

<http://wrap.warwick.ac.uk/163097>

Copyright and reuse:

This thesis is made available online and is protected by original copyright.

Please scroll down to view the document itself.

Please refer to the repository record for this item for information to help you to cite it.

Our policy information is available from the repository home page.

For more information, please contact the WRAP Team at: wrap@warwick.ac.uk

**Heterologous expression and *in-vitro* analysis of
Streptococcus pneumoniae FtsEX divisome
complex with peptidoglycan (PG) hydrolase
PcsB and actin homologue FtsA, required for PG
remodelling and cell separation**

Souvik Naskar

A thesis submitted in partial fulfilment of the requirements
for the degree of

Doctor of Philosophy

Warwick Medical School

University of Warwick

November 2019

Table of Contents

| | |
|---------------------------------------|--------------|
| Table of Contents | II |
| List of Figures | XI |
| List of Appendix Figures | XIV |
| List of Tables | XV |
| Acknowledgements | XVI |
| Declaration | XVIII |
| Abstract | XIX |
| List of Abbreviations | XX |

CHAPTER 1. Towards bacterial cell division mechanisms in the quest for finding new antibiotic targets1

| | |
|--|----|
| 1.1. Bacterial cell envelopes and their differential organization in Gram-positive and Gram-negative bacteria..... | 4 |
| 1.2. Cell division in the <i>E. coli</i> , a model for Gram-negative and rod-shaped bacteria | 6 |
| 1.2.1. <i>E. coli</i> elongation complexes, their assembly and roles during cell elongation..... | 6 |
| 1.2.2. <i>E. coli</i> Z-ring positioning and its regulators..... | 9 |
| 1.2.2.1. The Min system in <i>E. coli</i> | 10 |
| 1.2.2.2. The Nucleoid Occlusion system in <i>E. coli</i> | 12 |
| 1.2.3. <i>E. coli</i> divisome complexes, their assembly and roles during septation and cell separation | 14 |

| | |
|---|----|
| 1.3. Cell division in the <i>S. pneumoniae</i> , a model for Gram-positive and oval-shaped cocci bacteria | 20 |
| 1.3.1. Locating division site and Z-ring positing in <i>S. pneumoniae</i> | 20 |
| 1.3.2. <i>S. pneumoniae</i> elongation complexes, their assembly and roles during cell elongation..... | 23 |
| 1.3.3. <i>S. pneumoniae</i> divisome complexes, their assembly and roles during septation and cell separation | 29 |
| 1.4. Cell division in <i>Bacillus subtilis</i> , a model for Gram-positive and rod-shaped bacteria | 33 |
| 1.4.1. Vegetative cell cycle of <i>B. subtilis</i> | 34 |
| 1.4.1.1. <i>B. subtilis</i> elongasome complexes, their assembly and roles during cell elongation | 35 |
| 1.4.1.2. <i>B. subtilis</i> Z-ring positioning and its regulators | 42 |
| 1.4.1.2.1. The Min system in <i>B. subtilis</i> | 42 |
| 1.4.1.2.2. The Nucleoid Occlusion (NO) system in <i>B. subtilis</i> | 45 |
| 1.4.1.2.3. EzrA, is one of the major regulators of Z-ring positioning in <i>B. subtilis</i> .. | 47 |
| 1.4.1.3. <i>B. subtilis</i> divisome complexes, their assembly and roles during septation and cell separation | 48 |
| 1.4.2. Asymmetric cell cycle and sporulation of <i>B. subtilis</i> | 57 |
| 1.4.2.1. Formation of <i>B. subtilis</i> endospore..... | 57 |
| 1.4.2.2. Germination of <i>B. subtilis</i> endospore | 62 |
| 1.5. <i>Streptococcus pneumoniae</i> as pathogen and organism specific issues in AMR | 63 |
| 1.6. The divisome as a target for new antibiotics..... | 64 |
| 1.7. An ABC-transporter and hydrolase complex could potentially be a good target for novel antibiotics. | 69 |
| 1.8. Challenges in studying membrane lipid bound divisome proteins and new tools to address these challenges | 72 |

| | |
|---|----|
| 1.9. AIMS and OBJECTIVES: Studying a macromolecular complex involves FtsAZ, FtsEX and PcsB complex in membrane lipid bound SMALP nanodisc | 75 |
|---|----|

CHAPTER 2. Materials and Methods76

| | |
|---|-----|
| 2.1. Materials..... | 76 |
| 2.1.1. Media of bacterial culture | 76 |
| 2.1.2. Buffers and solutions..... | 77 |
| 2.1.3. Bacterial strains..... | 80 |
| 2.1.4. Plasmids used for cloning, mutagenesis and expression..... | 81 |
| 2.1.5. Primers/Oligonucleotides..... | 86 |
| 2.2. Microbiology methods | 93 |
| 2.2.1. Preparation of competent cells..... | 93 |
| 2.2.2. Preparation of agarose plates with selective antibiotic(s)..... | 94 |
| 2.2.3. Synchronization of bacterial culture | 94 |
| 2.3. Molecular biology methods..... | 95 |
| 2.3.1. Gene cloning techniques | 95 |
| 2.3.1.1. Polymerase chain reaction (PCR)..... | 95 |
| 2.3.1.2. Restriction enzyme digestion of DNA | 97 |
| 2.3.1.3. Dephosphorylation of linearized plasmid DNA to prevent its re-ligation | 97 |
| 2.3.1.4. DpnI digestion of template plasmid DNA..... | 98 |
| 2.3.1.5. Agarose gel electrophoresis..... | 98 |
| 2.3.1.6. Cleaning PCR product..... | 99 |
| 2.3.1.7. Extraction and purification of amplified PCR product..... | 99 |
| 2.3.1.8. Ligation..... | 99 |
| 2.3.1.9. Transformation in <i>E. coli</i> | 100 |
| 2.3.1.10. Colony screening by PCR | 100 |
| 2.3.1.11. Isolation of plasmid DNA and minipreparation | 102 |
| 2.3.1.12. Measurement of DNA concentration..... | 102 |
| 2.3.1.13. Restriction enzyme mapping | 102 |

| | | |
|------------|---|-----|
| 2.3.1.14. | DNA Sequencing..... | 103 |
| 2.3.2. | Plasmid construct assembly by Gibson cloning method..... | 103 |
| 2.3.3. | Plasmid construct mutagenesis | 104 |
| 2.4. | Protein expression, extraction and purification..... | 105 |
| 2.4.1. | Small-scale induction and membrane preparation | 105 |
| 2.4.2. | Large-scale induction and membrane preparation | 106 |
| 2.4.3. | Extraction and purification of Membrane protein (MP) and/ or membrane associated protein (MAP)..... | 107 |
| 2.4.3.1. | MP and/or MAP extraction using SMALP and purification using affinity (IMAC) and size-exclusion chromatography (SEC)..... | 107 |
| 2.4.3.1.1. | Reconstitution of SMALP extracted protein from separate inductions . | 110 |
| 2.4.3.1.2. | Co-expression, co-extraction and co-purification (Co-EEP) of SMALP- Proteins | 110 |
| 2.4.3.2. | MP and/or MAP extraction using detergent and purification using IMAC and SEC | 110 |
| 2.4.4. | Protein purification techniques | 111 |
| 2.4.4.1. | Immobilised metal affinity chromatography (IMAC)..... | 111 |
| 2.4.4.2. | Size-exclusion chromatography (SEC) | 113 |
| 2.4.5. | Protein measurement..... | 114 |
| 2.4.6. | Protein characterisation and analysis using biochemical and biophysical techniques | 115 |
| 2.4.6.1. | Native polyacrylamide gel electrophoresis (Native-PAGE) analysis | 115 |
| 2.4.6.2. | Sodium dodecyl sulphate polyacrylamide gel electrophoresis (SDS- PAGE) | 116 |
| 2.4.6.3. | Western blot (WB) and immunoassay..... | 117 |
| 2.4.6.4. | In-gel protein digestion and mass-spectrometry..... | 118 |
| 2.4.6.5. | ATP-binding assay | 119 |
| 2.4.6.6. | ATP-hydrolysis assay | 119 |
| 2.4.6.7. | Dynamic light scattering (DLS) | 120 |
| 2.4.6.8. | Analytical ultracentrifugation (AUC)..... | 120 |
| 2.5. | Microscopy techniques..... | 120 |
| 2.5.1. | Visualizing cells using confocal airy-scan microscopy | 120 |

| | |
|--|-----|
| 2.5.2. Visualizing proteins using Negative staining and electron microscopy (EM) | 121 |
| 2.5.3. Visualizing proteins using Cryo-EM | 121 |

CHAPTER 3. Heterologous expression and purification of individual proteins involved with ABC-transporter and PG hydrolase complex.....122

| | |
|---|-----|
| 3.1. INTRODUCTION..... | 122 |
| 3.2. RESULTS..... | 123 |
| 3.2.1. Heterologous expression of <i>Streptococcus pneumoniae</i> FtsE, FtsX, FtsA and PcsB has their distinct phenotypes | 123 |
| 3.2.2. <i>In-vitro</i> characterisation of FtsE, FtsX, FtsA, PcsB in lipid bound SMALP nanodiscs..... | 126 |
| 3.2.2.1. <i>S. pneumoniae</i> FtsE successfully extracted by SMALP nanodiscs possibly in its membrane anchored state for the very first time. | 126 |
| 3.2.2.2. <i>S. pneumoniae</i> FtsX with different N-terminal start sites extracted and purified successfully in SMALP nanodisc..... | 128 |
| 3.2.2.3. <i>S. pneumoniae</i> FtsA co-purified with low amount <i>E. coli</i> FtsX in SMALP nanodisc..... | 131 |
| 3.2.2.4. Successful extraction and purification of PcsB using SMALP nanodisc indicates a possible presence of lipid binding site in PcsB structure..... | 133 |
| 3.3. DISCUSSION: <i>S. pneumoniae</i> FtsE, FtsX, FtsA and PcsB are functionally active in a heterologous system while interacting with host lipid and divisome proteins..... | 135 |

CHAPTER 4. Heterologous expression and *in-vitro* characterisation of FtsEX complex138

4.1. INTRODUCTION.....138

4.2. RESULTS.....141

4.2.1. Overexpression of *S. pneumoniae ftsEX* operon (with 5'-end Strep tag and 3'-end His-tagged) in *E. coli Lemo21(DE3)::cam^R* cells..... 141

4.2.1.1. Large-scale overexpression, SMALP extraction and purification screens for SpFtsE and SpFtsX from overlapping *SpftsEX* operon in *E. coli Lemo21(DE3)::cam^R* 142

4.2.1.1.1. SMALP successfully extracted SpFtsEX, but high salt concentration in extraction and purification buffers possibly reduced the yield of strep-tagged SpFtsE 142

4.2.1.1.2. Auto-induction media, Nickel-IMAC resin and low salt concentration (NaCl 150 mM) in buffers for SMALP extraction and purification have improved the yield of both Strep-SpFtsE and SpFtsX-His10 proteins 144

4.2.1.1.3. SMALP coextracted and copurified *E. coli AcrB* along with successful purification of SpFtsEX as complex using low-salt concentration buffers..... 147

4.2.1.1.4. DDM extraction did not improve Strep-tagged or untagged SpFtsE expression in *E. coli Lemo21(DE3)::cam^R* cells 152

4.2.2. Overexpression of *S. pneumoniae ftsE* and *ftsX* either from overlapping operon or separate gene fragments, in *E. coli BL21(DE3)ΔacrB::kan^R* strain 154

4.2.2.1. Small-scale overexpression of overlapping *SpftsEX* (with 5'-end strep and 3'-end his tag) in *E. coli BL21(DE3)ΔacrB::kan^R* 154

4.2.2.2. Large-scale SMALP extraction of SpFtsE and SpFtsX from membrane fraction of *E. coli BL21(DE3)ΔacrB::kan^R* stain 156

4.2.2.3. An attempt to co-express and copurify SpFtsE and SpFtsX using multicloning plasmid *pETDuet* system 158

4.2.2.4. Successful reconstitution of SMALP extracted SpFtsE and SpFtsX from separate plasmids and expressions 159

4.2.2.5. Reconstitution of SpFtsEX in SMALP indicates their possible natural preference is to form a heterodimeric complex 161

| | |
|---|-----|
| 4.2.2.6. Comparison of extraction and purification process using SMALP and detergent | 163 |
| 4.2.3. A modification in the translation initiation site of <i>pETDuet</i> plasmid improved the yield and ratio of SpFtsE and SpFtsX from overlapping <i>his6-SpftsEX-his10</i> operon, in <i>E. coli BL21(DE3)ΔacrB::kan^R</i> | 167 |
| 4.2.3.1. SMALP successfully coextracted and co-purified <i>S. pneumoniae</i> FtsEX complex with high purity and good yield | 167 |
| 4.2.3.2. Heterologous expression of <i>S. pneumoniae ftsEX</i> overlapping operon in <i>E. coli</i> produced elongated and concatenated cells..... | 171 |
| 4.2.4. SpFtsEX complex in SMALP is functional in <i>in-vitro</i> assays.... | 172 |
| 4.2.4.1. ATP binding assay with SpFtsEX complex in SMALP nanodisc.... | 172 |
| 4.2.4.2. ATP hydrolysis assay with SpFtsEX in SMALP nanodisc | 174 |
| 4.2.5. A comparison of particle distributions of SpFtsEX that purified by reconstitution and Co-EEP methods, using negative stain electron microscopy | 175 |
| 4.3. DISCUSSION: <i>S. pneumoniae</i> FtsEX is co-ordinately expressed as a functional protein complex and has a phenotypic effect on <i>E. coli</i> when heterologously expressed | 177 |

CHAPTER 5. An investigation into the association of *S. pneumoniae* FtsEX with other divisome proteins FtsA, FtsZ and PcsB

| | |
|---|------------|
| 5.1. INTRODUCTION..... | 183 |
| 5.2. RESULTS..... | 188 |
| 5.2.1. An investigation into the association between FtsA and FtsEX complex | 188 |
| 5.2.1.1. Heterologous co-expression of SpFtsEX and SpFtsA elongates <i>E. coli</i> cells and shows aberrant phenotypes | 188 |
| 5.2.1.2. SpFtsA forms a tripartite complex with SpFtsEX, which extracted and purified successfully using SMALP nanodisc | 189 |
| 5.2.1.3. FtsA interacts with FtsX but not with FtsE | 190 |

| | | |
|----------|--|-----|
| 5.2.2. | The complex between FtsEX and PcsB play a significant role PG remodelling and separation | 194 |
| 5.2.2.1. | Co-expression of SpFtsEX and PcsB rescue <i>E. coli</i> cells from cell division defect..... | 194 |
| 5.2.2.2. | SpFtsEX and PcsB complex successfully extracted and purified using SMALP nanodisc | 195 |
| 5.2.2.3. | Expression of SpFtsEX or its co-expression with PcsB helps <i>E. coli ftsEX</i> knock-out mutant (MR10) strain growing in low-salt media..... | 199 |
| 5.2.3. | Purified SMALP complexes of FtsEX-FtsA and FtsEX-PcsB can bind and hydrolyse ATP..... | 201 |
| 5.3. | Building up a larger macromolecular divisome complex with FtsZ, FtsA, FtsEX, and PcsB..... | 204 |
| 5.3.1. | PcsB fails to rescue <i>E. coli</i> cells from severe cell division defect when SpFtsA co-expressed with SpFtsEX..... | 204 |
| 5.3.2. | A combined effect of FtsZ and PcsB counterbalance the phenotypic abnormalities of SpFtsEX-SpFtsA complex | 205 |
| 5.3.3. | A macromolecular cell divisome complex can be successfully purified in SMALP nanodisc by co-expressing SpFtsEX, SpFtsAZ and PcsB | 207 |
| 5.4. | DISCUSSION: PcsB forms functional complex with FtsEX and rescue cells from concatenation and aberrant cell division that observed with co-expression of SpFtsEX-SpFtsA complex | 210 |

CHAPTER 6. General discussion and future perspectives215

| | | |
|------|---|-----|
| 6.1. | The global concern with β -lactam and other antibiotic resistance | 215 |
| 6.2. | <i>S. pneumoniae</i> PBPs and β -lactam resistance..... | 217 |
| 6.3. | Targeting divisome complexes could restrict bacterial infections | 218 |

| | |
|--|------------|
| 6.4. Technical challenges and achievements associated with isolation of divisome protein complexes | 219 |
| 6.5. Key achievements and findings from this study | 221 |
| 6.6. Future investigations and experiments | 223 |
| 6.7. Concluding remarks | 226 |
| BIBLIOGRAPHY AND REFERENCES | 227 |
| APPENDIX | 260 |
| Appendix A1 | 260 |
| Initial biophysical and structural analysis of FtsEX, FtsEX-FtsA and FtsEX-PcsB complexes | 260 |
| Appendix A2. | 265 |
| Small-scale heterologous overexpression studies with <i>S. pneumoniae ftsEX</i> in <i>E. coli Lemo21(DE3)::cam^R</i> cells | 265 |
| Appendix A3 | 273 |

List of Figures

| | |
|--|-----|
| Figure 1.1. Bidirectional chromosome replication and segregation. | 2 |
| Figure 1.2. Bacterial Cytokinesis | 3 |
| Figure 1.3. Gram-positive and Gram-negative compartmentation of bacterial cell envelop. | 5 |
| Figure 1.4. <i>E. coli</i> elongasome and divisome assembly. | 9 |
| Figure 1.5. <i>E. coli</i> Z-ring positioning by Min system and NO. | 12 |
| Figure 1.6. <i>E. coli</i> divisome assembly and activation..... | 17 |
| Figure 1.7. <i>S. pneumoniae</i> Z-ring positioning and its assembly..... | 22 |
| Figure 1.8. Schematic representation of the <i>S. pneumoniae</i> elongasome and divisome complexes..... | 24 |
| Figure 1.9. Vegetative and asymmetric cell cycle of <i>B. subtilis</i> | 34 |
| Figure 1.10. Z-ring positioning by Min system and nucleoid occlusion (NO) in <i>B. subtilis</i> | 44 |
| Figure 1.11. Nucleoid occlusion protein factors Noc and SlmA in <i>B. subtilis</i> and <i>E. coli</i> respectively. | 46 |
| Figure 1.12. A proposed mechanism of Nucleoid occlusion protein, Noc in positioning Z-ring at mid-cell in <i>B. subtilis</i> | 47 |
| Figure 1.13. <i>B. subtilis</i> divisome assembly..... | 50 |
| Figure 1.14. Regulatory network of Sigma factors during of <i>B. subtilis</i> sporulation | 60 |
| Figure 1.15. The <i>B. subtilis</i> Endospore..... | 61 |
| Figure 1.16. Classic targets for antibiotics..... | 65 |
| Figure 1.17. Separate ligand interaction of FtsEX and its in three separate models. | 70 |
| Figure 1.18. SMALP and other extraction tools for membrane protein. | 73 |
| Figure 1.19. Schematic representation of FtsEX oriented complex in SMALP... .. | 75 |
| Figure 3.1. Heterologous expression of <i>S. pneumoniae</i> divisome proteins. | 125 |
| Figure 3.2. Purification of SpFtsE-His6 in SMALP nanodisc..... | 127 |
| Figure 3.3. Overlap region in sequence of <i>S. pneumoniae</i> ftsEX operon | 128 |

| | |
|---|-----|
| Figure 3.4. SpFtsX in SMALP nanodiscs and its cross-interaction with host divisome. | 130 |
| Figure 3.5. Purification of SpFtsA using SMALP. | 132 |
| Figure 3.6. PcsB successfully purified using SMALP. | 134 |
| Figure 4.1. Purification of SMALP extracted Strep-SpFtsE and SpFtsX-His ₁₀ in high salt (500 mM NaCl) buffers. | 143 |
| Figure 4.2. Comparison of IMAC resins (Ni-NTA and Co-Talon) in purification SMALP extracted SpFtsEX. | 145 |
| Figure 4.3. Comparison of growth media, induction methods and IMAC resins for purification of SMALP extracted SpFtsEX. | 146 |
| Figure 4.4. Purification of SMALP extracted SpFtsEX from <i>E. coli Lemo21(DE3)::cam^R</i> cells. | 148 |
| Figure 4.5. Identification of purified SpFtsEX from <i>E. coli Lemo21(DE3)::cam^R</i> cells. | 149 |
| Figure 4.6. LC-MS/MS analysis with bands (27, 38 and 46 kDa) excised from SDS-PAGE. | 151 |
| Figure 4.7. LC-MS/MS analysis with band (114 kDa) excised from SDS-PAGE. | 152 |
| Figure 4.8. Purification of DDM extracted SpFtsEX where SpFtsE was either untagged or Strep-tagged and SpFtsX was His-tagged C-terminally. | 153 |
| Figure 4.9. Small-scale overexpression of untagged or Strep-tagged SpFtsE and SpFtsX-His ₁₀ from overlapping SpftsEX operon in <i>BL21(DE3)ΔacrB::kan^R</i> cells. | 155 |
| Figure 4.10. SMALP extraction and purification of Strep-FtsSpEX-His ₁₀ from <i>E. coli BL21(DE3)ΔacrB::kan^R</i> cell membrane. | 157 |
| Figure 4.11. Multicloning duet system failed to co-express and copurify SpFtsEX as equimolar complex in SMALP but alternate reconstitution of purified SpFtsE and SpFtsX successfully reconstituted SpFtsEX in SMALP nanodisc. | 160 |
| Figure 4.12. Successful reconstitution of SpFtsEX in SMALP indicates their possible natural preference to form a heterodimeric complex. | 162 |
| Figure 4.13. Negative stain EM micrograph of reconstituted SpFtsEX in SMALP shows aggregated particles without Triton-X-100 treatment. | 164 |

| | |
|--|-----|
| Figure 4.14. Screening reconstitution of SpFtsEX in SMALP. | 166 |
| Figure 4.15. SpFtsEX successfully purified as complex in SMALP nanodisc... | 168 |
| Figure 4.16. LC-MS/MS analysis of SpFtsEX-SMALP band on Native PAGE. | 169 |
| Figure 4.17. LC-MS/MS analysis of SpFtsEX-SMALP on SDS-PAGE PAGE. | 170 |
| Figure 4.18. Empty vector did not express any His-tagged proteins. | 170 |
| Figure 4.19. Heterologous expression of SpFtsEX in <i>E. coli</i> cells is showing a phenotypic effect. | 171 |
| Figure 4.20. ATP-binding assays with purified SpFtsEX in SMALP. | 173 |
| Figure 4.21. ATP-hydrolysing assay with purified SpFtsEX in SMALP. | 174 |
| Figure 4.22. Negative stain EM micrographs of purified SpFtsEX using SMALP, DDM and SMALP-Tx100. | 176 |
| Figure 5.1. Schematic diagram of FtsEX, PcsB FtsA and FtsZ in context. | 185 |
| Figure 5.2. PcsB interacts with FtsEX extracellular loops for its activation. | 186 |
| Figure 5.3. Heterologous co-expression of SpFtsEX and SpFtsA in <i>E. coli</i> cells. | 189 |
| Figure 5.4. Purification of tripartite complex of SpFtsEX-SpFtsA in SMALP.. | 190 |
| Figure 5.5. SpFtsX interacts with SpFtsA, but not SpFtsE. | 192 |
| Figure 5.6. Identification of SpFtsE through LC-MS/MS. | 192 |
| Figure 5.7. Identification of SpFtsX and SpFtsA through LC-MS/MS. | 193 |
| Figure 5.8. Heterologous co-expression of SpFtsEX and PcsB in <i>E. coli</i> cells.. | 195 |
| Figure 5.9. Purification of SpFtsEX-PcsB complex using SMALP. | 196 |
| Figure 5.10. Identification of SpFtsE, SpFtsX and PcsB in a complex. | 197 |
| Figure 5.11. Purification of SpFtsEX and PcsB as complex using DDM. | 198 |
| Figure 5.12. SpFtsEX compensate the loss of function of <i>E. coli</i> Δ <i>f</i> <i>tsEX</i> mutant (MR10) in no salt LB media. | 200 |
| Figure 5.13. In-vitro functional assays with purified SpFtsEX-SpFtsA and SpFtsEX-PcsB complexes in SMALP. | 202 |
| Figure 5.14. Effects of co-expression of macromolecular complexes in combination. | 206 |
| Figure 5.15. Successful purification of macromolecular complex, consists of SpFtsEX, SpFtsA and PcsB, in SMALP nanodisc. | 209 |

List of Appendix Figures

| | |
|--|-----|
| Figure A 1. AUC plots for SpFtsEX and SpFtsEX-PcsB complexes in SMALP.. | 261 |
| Figure A 2. Negative Stain EM and DLS with SMALP-SpFtsEX. | 262 |
| Figure A 3. Negative Stain EM with SpFtsEX-SpFtsA and SpFtsEX-PcsB | 263 |
| Figure A 4. Cryo-EM with SpFtsEX, SpFtsEX-SpFtsA and SpFtsEX-PcsB | 263 |
| Figure A 5. DLS and preliminary Cryo-EM screening with SMALP-SpFtsEX-PcsB complex. | 264 |
| Figure A 6. Small-scale overexpression of Strep-SpFtsE and SpFtsX-His10 from overlapping <i>SpftsEX</i> operon in <i>Lemo21(DE3)::cam^R</i> cells..... | 267 |
| Figure A 7. Genetic organisation of <i>E. coli ftsYEX</i> operon. | 268 |
| Figure A 8. Genetic organisation of <i>S. pneumoniae ftsEX</i> operon..... | 269 |
| Figure A 9. Second purification of Strep-SpFtsEX-His ₁₀ using Streptactin resin. | 269 |
| Figure A 10. SEC chromatogram of Strep-SpFtsEX-His ₁₀ complex that extracted and purified using DDM. | 270 |
| Figure A 11. SDS-PAGE analysis of purified (IMAC and SEC) Strep-SpFtsE and SpFtsX-His ₁₀ complex that heated at 95 ° C. | 270 |
| Figure A 12. Protein markers run on SEC column. | 271 |
| Figure A 13. Individual expressions and purifications of SpFtsE-His6, SpFtsX-His10 and untagged-SpFtsA. | 271 |
| Figure A 14. Genetic organization of <i>S. pneumoniae ftsAZ</i> operon..... | 272 |

List of Tables

| | |
|---|-----|
| Table 1.1. List of <i>S. pneumoniae</i> proteins involved in cell elongation and division. | 25 |
| Table 1.2. Possible MreB interacting proteins identified as candidate components of the elongasome. | 39 |
| Table 1.3. Proteins of the <i>B. subtilis</i> divisome and its regulators. | 53 |
| Table 2.1. List of Medias and their compositions. | 76 |
| Table 2.2. List of buffers..... | 77 |
| Table 2.3. List of bacterial strains..... | 81 |
| Table 2.4. List of plasmids and constructs..... | 82 |
| Table 2.5. List of Primers..... | 86 |
| Table 2.6. PCR components of Phusion® HF kit and their final concentration... | 96 |
| Table 2.7. Phusion® HF PCR thermocycler conditions | 96 |
| Table 2.8. Reactants used in colony PCR | 101 |
| Table 2.9. Thermocycler conditions used in colony PCR..... | 101 |
| Table 2.10. Concentration of antibiotics used in cell culture..... | 109 |

Acknowledgements

I would like to take this opportunity to show my very special gratitude to my primary supervisor Professor David Roper and co-supervisor Dr Corinne Smith for their continuous support and guidance throughout this PhD project. Particularly, I like to tribute any outcome of this project to Professor David Roper for his excellent supervision. My very special thanks to him for accommodating me in his laboratory at the University of Warwick (UK), giving me the opportunity to work on this project under his excellent supervision, for his immense patience, very friendly behaviour, for all trust and encouragements. I thoroughly enjoyed all our science discussions and particularly his Golf lessons. Working with him and in his lab has been a great experience for me. Here, I also like to thank Professor Cristopher Dawson and Dr Adrian Lloyd for all their advice about this project.

My special gratitude to the Medical Research Council (MRC, UK) and the Warwick Medical School (University of Warwick, UK) for their continuous support and for funding this PhD project. I like to say thanks to all MRC-DTP management committee members and particularly I like to say a very special thanks to the MRC-DTP IBR director Professor Jonathan Millar for his all advice about this project, about presenting my work and my career. Also, my special thanks to the Doctoral Training Programmes Officer: Sally Blakeman for providing all administrative support and for all personal advice. I like to thank my PhD advisory panel (Professor Mohan Balasubramanian and Professor Steve Royle) for all valuable advice about this project. I like to acknowledge the Proteomic facility (SLS, University of Warwick) for providing protein mass spectroscopy service and the School of Life Sciences (University of Warwick, UK) for providing lab space and other facilities.

I would like to thank Dr Alvin Teo for showing me the SMALP extraction procedure; Dr Avinash Punekar, Dr Christopher Thoroughgood, Dr Anna York, Carmina Micelli, Katie Smart, Kathryn Maskew, Dr Cathy Rowland, Dr Ricky Cain, Julie Todd and Anita Catherwood for their kind cooperation, all help in learning several lab techniques and for their advice regarding many experiments. In

this regard, I also like to thank Liam Riley and Dr Sarah Smith who trained me and advised me in analysing Cryo-EM related data. A special thanks to Dr Alister Crow for his all guidance and valuable advice to progress this project.

I would like to acknowledge Dr Saskia Bakker (University of Warwick, UK) and Dr Cristos Savva (University of Leicester, UK) for all training and helping in Electron Microscopy; Mr. Ian Hands-Portman (University of Warwick, UK) for all guidance and training in Light Microscopy. I would like to thank Dr Pooja Sridhar (University of Birmingham, UK) for setting up and running AUC with my protein samples and Dr Sarah Lee (University of Birmingham, UK) for guiding and training on AUC data analysis. I like to acknowledge Dr. Naomi Pollock for her guidance in executing and analyzing DLS experiments.

Finally, I like to show my great respect, love and my special thanks to my parents for their love, strong principle and education about life. I like to thank my first teacher: my mother (Sipra Naskar) and to my father (Nikhilesh Naskar) for all discussions about Science, Career, Sports, Music and about life. Both my parents have always been my great source of inspiration. I like to thank my sister (Sayanti Naskar) for her love, for giving me continuous encouragement to progress in life and career; and giving me all assurance about looking after my parents in my absence in India. I like to thank my parents-in-law (Shishir Kanti Chowdhury and Suchitra Chowdhury) for their kind support and continuous encouragement to do well in my career and stay healthy. I like to thank my brother- and sister-law (Sumit Chowdhury and Satabdi Roy Chowdhury) and all my cousins for their love and all encouragement. Last but not the least, my very special thanks to my wife (Chandra Naskar Chowdhury) for tolerating my long working hours in the lab including many weekends and for giving me all support and encouragement to overcome all ups-and-downs and serious financial crisis during this PhD programme. My special apology for working in the lab during many bank holidays. Without the great support from my family and in-laws, I could not have finished this project. Achieving this PhD degree was the dream of my parents and I dedicate this degree especially to my parents, and to my family and in-laws.

Declaration

I hereby declare that I personally have carried out the work submitted in this thesis under the supervision of Professor David Roper and Dr Corinne Smith at the Warwick Medical School, University of Warwick, UK. Where training, supervision or work has been contributed to by other individuals it is specifically stated in the text or in the acknowledgement.

No part of this work has previously been submitted to be considered for a degree or qualification. All sources of information are specifically acknowledged in the form of references.

Abstract

Bacterial cell division is orchestrated by the divisome complex of proteins necessary for new peptidoglycan (PG) synthesis and PG remodeling during septum formation and cell separation. These proteins have homologues in both Gram-positive and Gram-negative species highlighting their fundamental biological role. The complex between FtsE and FtsX is recruited to the divisome at an early stage in mid-cell division and is required in assembling further downstream divisome proteins as well as in regulating divisome activity. Specifically, it provides a membrane anchor for an extracellular hydrolase that is required for hydrolysis of PG of old cell wall material and to enable separation of daughter cells during division.

In our heterologous expression study, we observed aberrant cell division defects in *Escherichia coli* (Ec) cell when subject to expression of the *Streptococcus pneumoniae* (Sp) FtsEX mimicking the phenotype of existing antibiotics. This phenotype can be rescued co-overexpressing SpFtsEX with its cognate peptidoglycan hydrolase; PcsB that hydrolyses *Escherichia coli* PG required for PG remodeling during cell separation. In this study, we have demonstrated *Streptococcus pneumoniae* FtsEX-FtsA and FtsEX-PcsB complexes can be isolated *in-vitro* using nanodiscs styrene-maleic-acid-lipid-particles (SMALP), preserving their membrane lipid environment. The protein-protein interaction studies indicate SpFtsX but not SpFtsE, interacts with the essential divisome protein SpFtsA, and PcsB successfully docks with FtsEX in the SMALP disk. Negative stain electron microscopy images and initial high resolution cryo-EM trials with these complexes indicates these tools could be prerequisite for investigating mechanistic insight about their structural-functional relationship and for further inhibitor screens for these complexes.

List of Abbreviations

| | |
|-----------------------------|---|
| °C | Degrees Celsius |
| 3D | Three-dimension |
| ADP | Adenosine Diphosphate |
| AIM | Auto-induction media |
| Amp | Current |
| APS | Ammonium per sulphate |
| ATP | Adenosine Triphosphate |
| AU | Absorbance Unit |
| <i>B. subtilis</i> | <i>Bacillus subtilis</i> |
| BCA | Bicinchoninic acid |
| bp | Base pair |
| <i>C. crescentus</i> | <i>Caulobacter crescentus</i> |
| CC | Coiled-coiled |
| CCTD | C-terminal domain |
| CHAP | Cysteine and histidine-dependent aminohydrolases/peptidases |
| CM | Colour marker |
| CMC | Critical Micelle Concentration |
| Co-EEP | Co-expression, co-extraction and co-purification |
| CT | C-terminus or Carboxy-terminus |
| CV | Column volume |
| DDM | n-Dodecyl-D-maltopyranoside |
| DMSO | Dimethyl Sulfoxide |
| DNA | Deoxyribonucleic acid |
| DNAse | Deoxyribonuclease I, from bovine pancreas |
| DTT | Dithiothreitol |
| E | Elute |
| <i>E. coli</i> or <i>Ec</i> | <i>Escherichia coli</i> |
| EDTA | Ethylenediaminetetraacetic acid |
| E _{FT} | Flow-through of concentrated elute |
| EM | Electron microscope |

| | |
|------------------------|--|
| EzrA | Extra Z-ring A |
| FisB | Fission protein B |
| FIW | Final imidazole wash |
| FT | Flow-through |
| Fts | Filamentous temperature sensitive |
| G | Gram |
| GlcNAc | N-acetyl glucosamine |
| GTase | Glycosyltransferase |
| HCl | Hydrochloric Acid |
| HCl | Hydrochloric Acid |
| HEPES | N-(2-hydroxyethyl) piperazine-N'-(3-ethanesulfonic acid) |
| HETIS | Highly efficient translation initiation site |
| HF | High fidelity |
| HRP | Horseradish peroxidase |
| HSS | High-speed-supernatant |
| IMAC | Immobilised Metal Affinity Chromatography |
| IMF | Insoluble membrane fraction |
| IN | Inner membrane |
| IPTG | Isopropyl-D-thiogalactopyranoside |
| kb | Kilobase |
| KCl | Potassium Chloride |
| kDa | Kilodalton |
| KO | Knock-out |
| kpsi | Kilopound per square inch |
| LB | Lysogeny broth (Luria-Bertani bacteria growth media) |
| LC-MS | Liquid chromatography mass spectrometry |
| LMW | Low molecular weight |
| LocZ | Localising of midcell of Z |
| LTA | Long anionic teichoic acid (LTA) |
| <i>M. tuberculosis</i> | <i>Mycobacterium tuberculosis</i> |
| MAP | Membrane associated protein |
| MapZ | Midcell-anchored protein Z |

| | |
|----------------------|--|
| mAU | Milli absorbance unit |
| MCS | Multiple cloning site |
| MD | Microdomain |
| MES | 2-morpholinoethane sulphonic acid |
| MF | Membrane fraction |
| mg | Milligram |
| MGT | Monofunctional glycosyltransferase |
| mL | Millilitre |
| mm | Millimetre |
| mM | Millimolar |
| MOPS | 3-(N-morpholino) propanesulfonic acid |
| MP | Membrane protein |
| Mre | Murine region e |
| mRNA | Messenger ribonucleic acid |
| MRSA | Methicillin-resistant <i>Staphylococcus aureus</i> |
| MTS | Membrane targeting sequence |
| MurNAc | N-acetyl muramic acid |
| NaCl | Sodium Chloride |
| NAD ⁺ | Nicotinamide adenine dinucleotide (Oxidised) |
| NADH | Nicotinamide adenine dinucleotide (Reduced) |
| NADPH | Nicotinamide adenine dinucleotide phosphate (Reduced) |
| Native-PAGE | Poly-acrylamide gel electrophoresis under native condition |
| ng | Nanogram |
| nm | Nanometre |
| NO | Nucleotide Occlusion |
| NT | N-terminus or Amino-terminus |
| OD600nm | Optical density at 600 nm |
| OM | Outer membrane |
| OMP | Outer membrane protein |
| oriC | Origin of replication |
| <i>P. aeruginosa</i> | <i>Pseudomonas aeruginosa</i> |
| PBP | Penicillin Binding Protein |

| | |
|----------------------|---|
| PBS | Phosphate-buffered saline |
| PCR | Polymerase Chain Reaction |
| PEG | Polyethylene glycol |
| PEP | Phosphoenol pyruvate |
| PG | Peptidoglycan |
| pH | Log ₁₀ [H ⁺] |
| RBS | Ribosome binding site |
| rcf | Relative centrifugal force |
| rpm | Revolutions per minute |
| <i>S. aureus</i> | <i>Staphylococcus aureus</i> |
| <i>S. pneumoniae</i> | <i>Streptococcus pneumoniae</i> |
| SAP | Shrimp alkaline phosphatase |
| SDS | Sodium Dodecyl Sulphate |
| SDS-PAGE | Sodium dodecyl sulphate poly-acrylamide gel electrophoresis |
| sec | Second |
| SEDS | Shape, elongation, division and sporulation |
| SMA | Styrene-Maleic Acid |
| SMALP | Styrene-Maleic Acid Lipid Particle |
| SOC | Super optimal broth with Catabolite repression |
| SPOR | Sporulation-related repeat |
| Spp. | Species |
| StkP | Serine/threonine protein kinase |
| Strep-L | Strep ladder |
| TA | Teichoic acid |
| TAE | Tris-acetate-Ethylenediaminetetraacetic acid |
| TBS | Tris Buffered Saline |
| Ter | Terminal region of chromosome |
| TFA | Trifluoroacetic acid |
| TM | Transmembrane |
| TPase | Transpeptidase |
| Tris | tris (hydroxymethyl) aminomethane |
| Tx-100 | Triton-X-100 (Reduced) |

| | |
|-----|---------------------------|
| UA | Uranyl acetate |
| V | Volt |
| v/v | volume to volume ratio |
| W | Wash |
| w/v | weight to volume ratio |
| WHO | World Health Organisation |
| WTA | Wall teichoic acid |
| μg | Microgram |
| μL | Microlitre |
| μm | Micrometre |
| μM | Micromolar |

CHAPTER 1. Towards bacterial cell division mechanisms in the quest for finding new antibiotic targets

Cell division is an extraordinary mechanism and an evolutionary successful survival strategy adopted and used by all forms of life. Unlike eukaryote cells where generally two types of cell division strategy have been observed, which are asexual (mitosis) and sexual (meiosis), prokaryotes depend only on asexual division or binary fission. Bacteria are one of the greatest surviving prokaryotic domains that have survived under extremely adverse conditions throughout the entire history of evolution of life on the Earth and have evolved a very tightly regulated cell division mechanism in order to reproduce efficiently and rapidly. The understanding of the division mechanism is very significant, not only to understand the evolutionary relationships to the eukaryotic cell division processes, but also to potentially combat any pathogenic bacteria that are resistant to current natural or synthetic antibiotics and may cause epidemics and/or pandemics in future. Bacteria divide and give rise to two daughter cells in a binary fission manner which mainly composed of two distinct events - chromosomal segregation and cytokinesis (Lutkenhaus, 1997).

Replication and segregation of the chromosome is a fundamental biological process by which different species share and transfer their genetic information from one progeny to another. This is possibly, the most important factor for all species to ensure their successful progeny. The fitness of the progeny depends on how tightly their chromosome replication and segregation events are regulated by their specific transcription factors and other macromolecular protein complexes, in order to ensure a complete transfer of an undamaged replica of a complete genome. Bacteria contain a single circular chromosome that starts duplicating from origin of replication (*oriC*; at 0°), then the replication fork continues bi-directionally until it reaches the terminal region (*Ter*; 180°) of the chromosome (**Figure 1.1**). Meanwhile, the newly formed sister chromatids start segregating from each other

and translocate away from each other. The *Ter* region plays a crucial role as cell cycle check point and ensures successful division of two daughter cells. Following successful replication and segregation of genetic material, the cell gets ready for the next big significant event that is, the cytokinesis (Adams, Wu, and Errington, 2014).

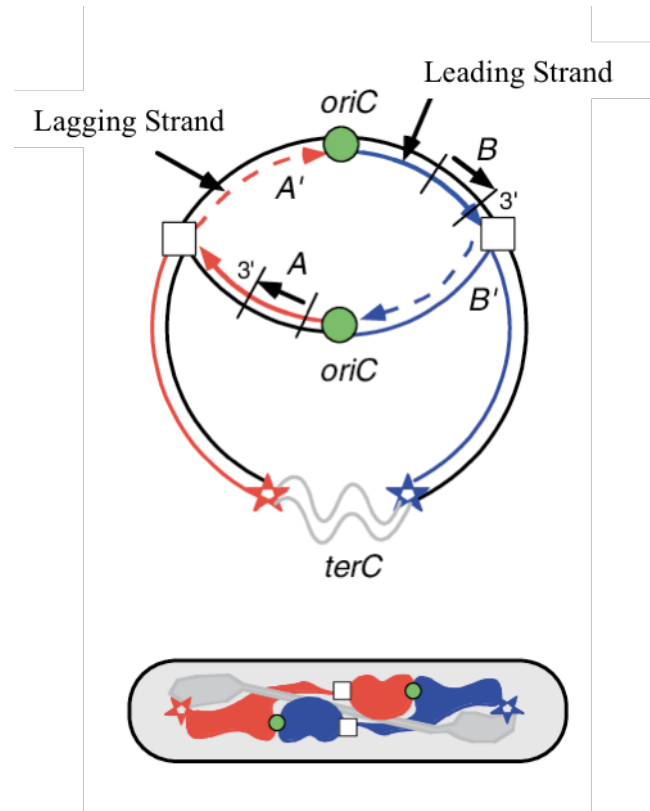


Figure 1.1. Bidirectional chromosome replication and segregation.

Top: Bidirectional replication starts from *oriC* results in two replicons (red and blue) with opposite replication polarity and direction marked by arrows at genes "A" and "B". Square white boxes represent replisomes. The terminal region of the chromosome represented as *terC*. **Bottom:** A schematic representation of leading and lagging (blue and red, respectively) strands as well as unreplicated regions (grey) of DNA in an *E. coli* cell.

Figure adopted and modified from Woldringh and Nanninga (2006).

The cytokinesis process involves three major mechanisms to complete the whole division cycle: elongation, Z-ring positioning and division. The elongation mechanisms which help cell grow rapidly to double its size approximately, this step is followed by Z-ring positioning and septum formation, and finally cell wall separation that is conducted by divisome mechanisms. While elongation helps daughter cells to gain required cell wall with a normal size and volume, the Z-ring

regulator guides the Z-assembly at the midcell where the division helps progenitor cell to divide into two new daughter cells (**Figure 1.2**). Any distortion or mutation to any essential proteins involving in these mechanisms cause morphological changes to the bacterial cell, which may lead to cell death (Reshes et al., 2008). This phenomenon stimulates a large part of microbiologists to explore and understand the structural and functional relationship of specific protein molecules or macromolecular complexes that are involved in the cell division process.

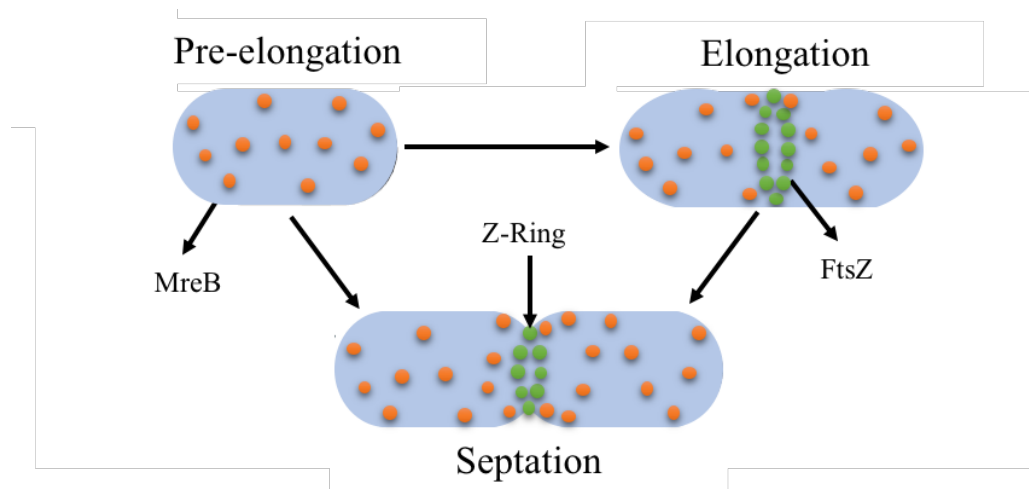


Figure 1.2. Bacterial Cytokinesis

Bacterial cytokinesis starts with cell elongation that mediated by MreB then follow the FtsZ mediated septation and final daughter cell separation.

In this introductory chapter, we have briefly described major cell division processes and mechanisms involved in *Escherichia coli* (*E. coli*), *Streptococcus pneumoniae* (*S. pneumoniae*) as well as in *Bacillus subtilis* (*B. subtilis*). Understanding the similarities in cell division mechanisms in the rod-shaped bacteria *E. coli* and *B. subtilis* helps us to categories rod-shaped specific protein complexes that are involved along with their vast protein network in coordinated cell division events. By contrast, a knowledge surrounding *S. pneumoniae* cell division and its similarities and dissimilarities with above two bacterial species, allow us to identify or categorize Gram-positive specific cell division mechanism and/or diversity from rod-shaped cell division. Knowledge of cell division protein complexes from these three diverse bacterial species and their roles in cell division in a spatio-temporal manner, is fundamental in microbiology, and relevant to this study.

1.1. Bacterial cell envelopes and their differential organization in Gram-positive and Gram-negative bacteria

The bacterial cell envelope plays a very crucial role to protect the cytoplasmic environment including genetic components, from the surrounding adverse environment and helps maintain the shape and size of the cell. Interestingly, throughout the bacterial domains, two major types of cell envelope organizations have been classically observed. These two types can be distinguished by a century old staining method, that was developed by Cristian Gram in 1884, and is named as Gram's staining (Gram and Friedlaender, 1884). Since its discovery, this is the most widespread used method to categorize bacteria as either Gram negative that do not retain Cristian's stain; or as Gram positive that retain the stain. The basic reason for this retention of Gram stain is the differences in the structural organization of different compartments of bacterial envelope between above two categories (**Figure 1.3**) (Silhavy, Kahne, and Walker, 2010). Most Gram-negative bacteria has three major compartments, these are: the cytoplasmic or inner membrane (IM); the periplasm that consist of thin peptidoglycan (murein) layer; and the outer membrane (OM) (**Figure 1.3**). By contrast, Gram-positive bacteria lacks the OM and has thicker peptidoglycan (PG) layer (**Figure 1.3**) as well as additional structure including polysaccharides (e.g. Teichoic acids) or in some cases additional protein layers (e.g. S-layer). This OM is a vital layer for most Gram-negative bacteria and provides an additional protective barrier and compartmentation for the bacterial cell. This extra layer also provides an additional support and stability to inner membrane of Gram-negative bacteria to survive in very harsh conditions, at the same time this OM is also a barrier for most antibiotics. While the OM of Gram-negative bacteria provides a protecting layer and support to IM, this group of bacteria has been evolved with a relatively thin layer of PG at the periplasmic space compared to Gram-positive species. Peptidoglycan is a polymer of long chains of linear glycan stands that are cross-linked by short pentapeptide side chains to form a three-dimensional (3D) mesh. The glycan stands are composed of repeated alternating units of disaccharide sugars, N-acetyl

glucosamine (GlcNAc) and N-acetyl muramic acid (MurNAc) (Vollmer, Blanot, and de Pedro, 2008).

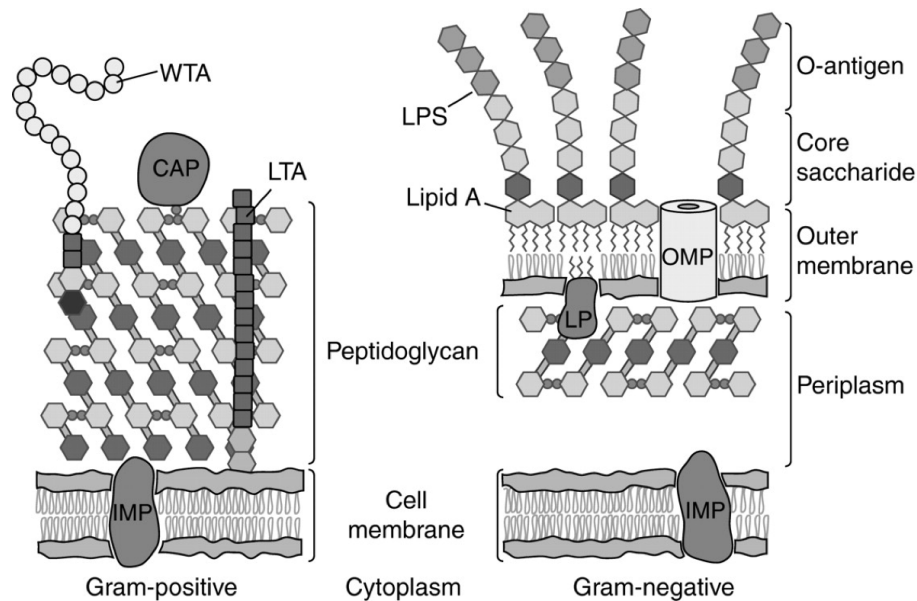


Figure 1.3. Gram-positive and Gram-negative compartmentation of bacterial cell envelop.

Schematic representation of cell envelopes from Gram-positive and Gram-negative bacteria. IMP, integral membrane protein; LP, lipoprotein; LPS, lipopolysaccharide; LTA, lipoteichoic acid; OMP, outer membrane protein; WTA, wall teichoic acid. CAP, covalently attached protein.

Figure adopted from Silhavy et al. (2010)

The Gram-positive bacteria can also survive in very adverse conditions comparable to Gram-negative bacteria, but surprisingly this group of bacteria have developed a different strategy to support its IM and internal cytoplasmic environmental pressure. They evolved with very thick layers of peptidoglycan that is supported by long anionic teichoic acid (TA) polymers. This polymer is composed of glycerol phosphate, glucosyl phosphate, or ribitol phosphate repeats (Silhavy et al., 2010). The Gram-positive periplasm is largely composed of two types of TA polymers, these are categorized as: wall teichoic acid (WTA) and lipoteichoic acid (LTA). The WTA is attached to PG covalently, whereas LTA is attached to lipid heads at the IM or plasma membrane (**Figure 1.3**) (Neuhaus and Baddiley, 2003; Silhavy et al., 2010). In addition to PG (in both types of bacteria) and TA (in Gram-positive), the cell wall of both types of bacteria is also the attachment point for many proteins that are anchored to membrane. (Dramsi et al., 2008; Scott and Barnett, 2006; Silhavy et al., 2010).

1.2. Cell division in the *E. coli*, a model for Gram-negative and rod-shaped bacteria

E. coli is a Gram-negative rod-shaped bacterium, which contain a thin layer of PG in the periplasm. The rod shape is mainly maintained by synthesis of PG during cell elongation, whereas the invagination of cell wall and formation of septum during cell division are largely depends on septal PG synthesis. These two processes are initially thought to function in a mutually exclusive way by recruiting discrete set of protein complexes specific to their respective loci, at two different phases of a cell cycle (Lleo, Canepari, and Satta, 1990). However, recent reports in the literature indicate some functions of these complexes are interdependent and overlaps each other to some extent, consequently a cell growth has been observed during septum maturation (van der Ploeg et al., 2013). These two distinct complexes are known as elongasome complexes (den Blaauwen et al., 2008; Holtje, 1998; Typas et al., 2011) and divisome complexes (Alexeeva, et al., 2010; Di Lallo, et al., 2003; Goehring and Beckwith, 2005; Holtje, 1998; Karimova, Dautin, and Ladant, 2005; Maggi et al., 2008; M. Vicente, 2006), respectively.

1.2.1. *E. coli* elongation complexes, their assembly and roles during cell elongation

In *E. coli* cells, the peripheral PG synthesis and thus lateral cell wall synthesis is coordinated and achieved by the macromolecular elongasome complexes (**Figure 1.4**) that comprised of Mre (murine region e) proteins such as MreB, MreC, MreD; bi-functional class A and mono-functional class B penicillin binding proteins (PBPs) such as PBP1a and PBP2 respectively; and SEDS (for Shape, elongation, division and sporulation) such as RodA and RodZ (den Blaauwen et al., 2008; Typas et al., 2011; Typas and Sourjik, 2015). The Mre proteins are specifically involved in elongation and mutation; deletion of the *mre* genes, prevented lateral growth and transformed rod-shaped *E. coli* to a spherical shape (Wachi et al., 1987).

The elongation of the cell is initiated with formation of bacterial cytoskeleton filament-like double protofilaments that are organized anti-parallelly, made of actin-like protein MreB (van den Ent, Amos, and Lowe, 2001; van den Ent et al., 2014). The MreB molecules polymerise to form these doublet protofilaments in ATP-dependent manner and tethered tightly to IM through its amino-terminal (N-terminal) domain (Esue et al., 2005; Esue, Wirtz, and Tseng, 2006; Salje et al., 2011; Typas and Sourjik, 2015; van den Ent et al., 2014). This tight tethering helps MreB to provide strong scaffolds for further essential additional structural subunits MreC and MreD at the early stage of elongasome assembly (**Figure 1.4**), and genes of which are apparently located in the same operon as MreB (Kruse, Bork-Jensen, and Gerdes, 2005; van den Ent et al., 2014; van den Ent et al., 2006). MreC is an early structural subunit acting as central hub for recruitment of further proteins like MreD and selected penicillin binding proteins (PBPs) such as PBP2 and PBP1a, which act as monofunctional and bifunctional peptidoglycan synthases respectively which are required to synthesize peripheral PG leading to a lateral increase in cell wall and size. PBP2 has monofunctional transpeptidase (TPase) activity, whereas PBP1a has bifunctional ability and shows both transpeptidase (TPase) and glycosyltransferase (GTase) activities (Banzhaf et al., 2012; Goffin and Ghuyesen, 1998; Yin et al., 2015). Inactivation of the class B PBP2 results in cell elongation inhibition and the formation of spherical cells similar to *mre* mutants, indicates its active role during elongation (Vinella et al., 1993). The activity of class A PBP1a in *E. coli* and a number of other eubacteria, is controlled by an outer-membrane co-factor protein LpoB (Paradis-Bleau et al., 2010; Yin et al., 2015). These PG synthases are mainly responsible for peripheral PG synthesis and thus the cell wall (Kruse et al., 2005; Leaver and Errington, 2005). Among other components of the elongasome, the SEDS protein RodA has been found to form a complex with PBP2. The role of RodA is to polymerise the PG precursor Lipid II in a glycan strand and thus provides a substrate for the transpeptidase activity of PBP2. The transmembrane protein, RodZ is an elongasome complex protein with a single membrane spanning α -helix (Gerdes, 2009; Shiomi, Sakai, and Niki, 2008). The RodZ has been reported as conditionally essential in *E. coli* and shown to interact with PBP2, possibly by its periplasmic domain (Bendezu and de Boer, 2008), in

addition to its reported direct interaction with cytoplasmic domain of MreB (van den Ent et al., 2010). The RodZ and MreB proteins have also been found to be genetically dependent on each other for normal growth (Shiomi et al., 2013; van den Ent et al., 2014). Together all these findings suggest that the RodZ is responsible for localizing and stabilizing MreB in the elongasome, and thus to maintaining proper cell shape (Bendezu and de Boer, 2008; Gerdes, 2009; Yoshii, Niki, and Shiomi, 2019). Recently RodZ has also been shown to interact with FtsZ through its N-terminal cytoplasmic domain, this implying that this interaction is important for RodZ to localise in the divisome site, and so as its close association with MreB (Yoshii et al., 2019). Because, in absence of MreB, the RodZ could not localize to the division site (Yoshii et al., 2019). The same study (Yoshii et al., 2019) also showed that in addition to RodZ, the FtsZ has been directly involved in localizing MreB to the division site, which previously noted in several studies (Vats and Rothfield, 2007; Vats, Shih, and Rothfield, 2009). Moreover, this finding supports the study by (Fenton and Gerdes, 2013) where they showed a specific mutation in *mreB* interrupted an interaction between MreB and FtsZ, which consequently elongated cell size. All these findings strongly suggest that MreB associates with RodZ and that both directly interact with FtsZ at the division site. This provides a significant event to link cell elongation to division process (Fenton and Gerdes, 2013; Yoshii et al., 2019). Similarly, a reported direct interaction between another elongasome complex PBP2 with a divisome complex PBP3 at the division site (van der Ploeg et al., 2013), indicate another functional collaboration between elongasome and divisome complexes. Inactivation of these elongasome complexes, evidently caused static growth by restricting *E. coli* cells to divide, which subsequently deformed cells to abnormal spherical size and reduced viability (Bendezu and de Boer, 2008; Vinella et al., 1993; Wachi et al., 1987).

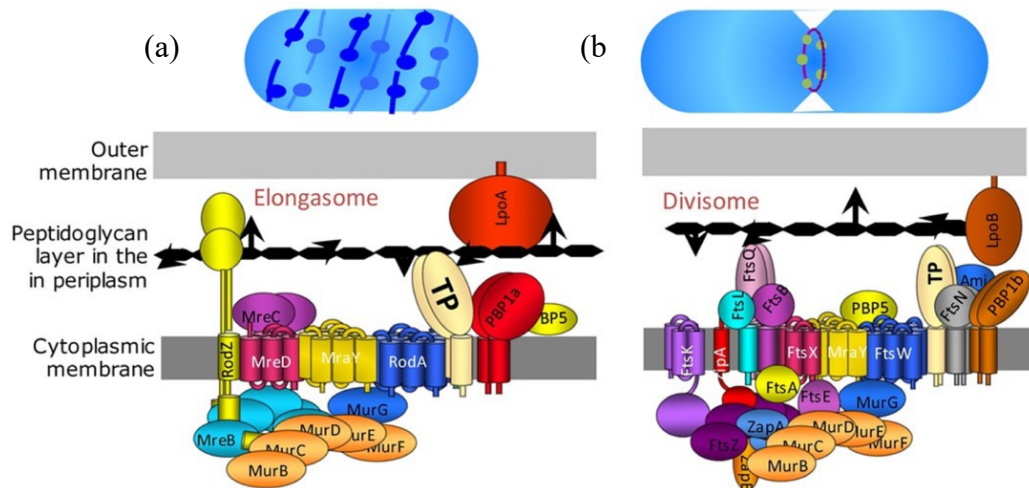


Figure 1.4. *E. coli* elongasome and divisome assembly.

Two sets of protein complexes are involved in a bacterial cell cycle – elongasome and divisome complex. Elongasome complexes (a), consist of RodZ, MreB along with other membrane proteins MreC, MreD, help regulating the peptidoglycan synthases (PBP1A and PBP2) and maintaining cell shape during elongation and promote lateral growth. Whereas, divisome complexes (b), start assembling at the midcell recruiting FtsZ as very first protein, followed by FtsA, ZipA, FtsE, FtsX, FtsK, FtsQ, FtsB, FtsL, FtsW, PBP3 (FtsI) and FtsN in almost sequential order, and helps synthesizing new peptidoglycan during cell division. FtsEX, arrive and assemble at Z-ring around early to midcell cycle stage but its roles in further divisome assembling and regulating divisome activity, are still under investigation. However, FtsE suspected to transduce signal and initiate PG hydrolysis by activating amidases (e.g. EnvC) and complete separation of the septum. Other divisome associates are PBPs, Tol-Pal complex and amidase enzymes. Figure adopted from Hugonnet et al. (2016)

1.2.2. *E. coli* Z-ring positioning and its regulators

One of the key events of bacterial cytokinesis is the formation of Z-ring (Bi and Lutkenhaus, 1991). It is named after a bacterial cytoskeletal GTPase protein FtsZ that is a bacterial homologue of the eukaryotic tubulin protein (Nogales et al., 1998). Unlike tubulin which assemble 13 protofilaments to form a microtubule in eukaryotic cells, the polymerization of FtsZ gives rise to single protofilament (Du et al., 2018). Cytokinesis is instigated by assembling FtsZ molecules at the midcell. This midcell assembly of FtsZ is triggered by GTP-dependent polymerization of FtsZ monomers (de Boer, Crossley, and Rothfield, 1992) followed by a consequent switch from a closed to open conformation of the protein in a GTP-dependent manner. GTP binding and hydrolysis has been proposed to directs its rapid

assembly and disassembly mechanism, associated with treadmilling activity that has been coupled to septum formation (Du et al., 2018; Wagstaff et al., 2017; Yang et al., 2017). Therefore, tight regulation and correct position of this Z-ring at the midcell is crucial. In *E. coli* and many other rod-shaped bacteria, this is mainly regulated by two negative regulatory systems known as Min system (Min) and nucleoid occlusion (NO). While the Min system prevents the formation of Z-ring near poles (Hale, Meinhardt, and de Boer, 2001; Raskin and de Boer, 1999), the NO protein factors inhibits Z-ring assembly over the nucleoid (Bernhardt and de Boer, 2005). Regulators from these two systems and few other negative and positive regulators, all together ensures correct positioning of Z-ring only at midcell (Hajduk et al., 2019; Randich and Brun, 2015).

1.2.2.1. The Min system in *E. coli*

The term Min system derived from minicell that is much smaller than a normal bacteria cell and is devoid of a nucleoid, and thus minicells fails to divide but remain metabolically active for several hours. The first such *E. coli* minicell was identified by Adler (Adler et al., 1967) and subsequently similar minicells were also observed in several other bacterial species (Reeve et al., 1973). Major proteins that were identified in the minicell formation, are broadly categorised as Min proteins. Minicells were thought to results of asymmetric cell division due to abnormal septum formation near poles in those min mutants (de Boer, Crossley, and Rothfield, 1989), which later correlated with aberrant z-ring formation near poles (Shih and Zheng, 2013). The *E. coli* Min system is mainly composed of four known proteins – MinC, MinD, MinE and MinJ, and together these proteins are largely responsible for prevention of Z-ring formation at the nucleoid-free polar regions of cells (de Boer et al., 1989; Rowlett and Margolin, 2015; Shih and Zheng, 2013) (**Figure 1.5**). The MinC protein is the key molecule behind this inhibition. First a Par-like ATPase known as MinD, attaches to plasma membrane as dimer using its C-terminal membrane targeting sequence (MTS) (Szeto et al., 2002), binds MinC (de Boer, Crossley, Hand, and Rothfield, 1991; Zonglin Hu and Lutkenhaus, 2003) and recruits it to the plasma membrane near the cell poles. Alternate dimers of MinC-MinD copolymers have structural similarities to eukaryotic septins (Conti,

Viola, and Camberg, 2015; Ghosal et al., 2014). This similarity may indicate that they have similar roles to septins which act as membrane scaffolds like other cytoskeletal proteins and assemble larger complexes. Additionally, septins create a diffusion barrier for subcellular compartmentalization of components (Errington and Wu, 2017; Ghosal et al., 2014). Concurrent with MinC-MinD copolymers formation, the MinE protein moves to the cell poles by diffusion, forming a ring like structure and interacting with MinD dimers. This interaction detaches the MinCD complexes from the plasma membrane (Raskin and de Boer, 1997; Rowlett and Margolin, 2015) (**Figure 1.5**). The dynamics of MinE molecules oscillate with the detached MinCD complex from one pole to other (Z. Hu and Lutkenhaus, 1999; Zonglin Hu and Lutkenhaus, 2003; Raskin and de Boer, 1997) and creates a gradient of MinCD complex at cell poles, which in turn inhibits FtsZ polymerisation via MinC and prevent aberrant Z-rings formation at cell poles (**Figure 1.5**). *E. coli* cells that lacking MinE showed lethal filamentous phenotype as a result of uniform distribution of MinCD complex across the plasma membrane and thus failure to assemble Z-ring throughout cell length (de Boer et al., 1989; Rowlett and Margolin, 2015).

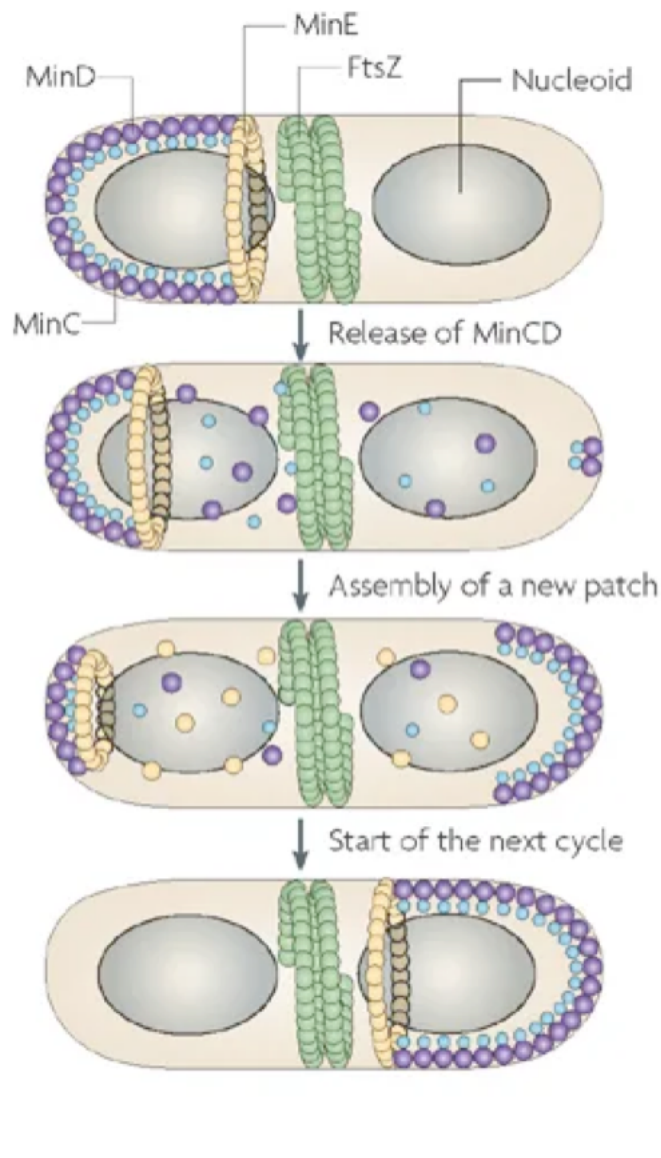


Figure 1.5. *E. coli* Z-ring positioning by Min system and NO.

In *Escherichia coli*, the Z-ring assembly is mainly controlled by nucleoid occlusion (performed by *SlmA*) and the Min system that operated by *MinE* which oscillate *MinCD* and prevents Z-ring formation at the poles.

Figure adopted from Thanbichler and Shapiro (2008).

1.2.2.2. The Nucleoid Occlusion system in *E. coli*

The “nucleoid occlusion” term was first coined by Cook et al (Cook, de Boer, and Rothfield, 1989) based on an assumption that the bacterial chromosome/DNA itself was possibly inhibiting the Z-ring from assembling over the nucleoid and dividing the cell over intact or incompletely segregated chromosomes (Cook et al., 1989; Mulder and Woldringh, 1989; Woldringh et al., 1990). However, instead of DNA

itself, a protein was identified to perform a similar role as NO, known as SlmA (Bernhardt and de Boer, 2005; Errington and Wu, 2017). The protein was identified from a screen for mutants that acted in a synthetically lethal manner with defective Min system (*slm* mutants), hence the name SlmA (Bernhardt and de Boer, 2005). In the same screen, SlmA allele was found to have all the possible characteristics to consider SlmA as protein factor for NO. It has been characterised as a member of TetR DNA binding protein family (Bernhardt and de Boer, 2005) and has between 24 and 52 specific DNA binding sites, known as SlmA binding sites (SBS) distributed all over the chromosome with the exception of chromosome terminus (Ter region) (Adams, Wu, and Errington, 2015; Cho et al., 2011; Tonthat et al., 2011) (**Figure 1.5**). This observation is particularly interesting because the same Ter region/Ter macrodomain (MD) has been found to have association with Z-ring via the Ter linkage that composed of three proteins, MatP (a Ter MD organising protein), ZapB and ZapA (Z-ring associated proteins) (Bailey et al., 2014; Buss et al., 2015) as described later in section 1.2.3. The same Ter region does not leave the midcell until the constriction starts (Espeli et al., 2012). Together these events indicate the Ter linkage and SlmA mediated NO, acts as cell cycle checkpoints to prevent any catastrophic disaster. The SlmA acts as a NO protein factor by directly interacting conserved C-terminal domain (CCTD) of FtsZ, which antagonise the FtsZ protofilament formation and thus blocks the Z-ring assembly (Bernhardt and de Boer, 2005; Cho et al., 2011; Du and Lutkenhaus, 2014; Schumacher and Zeng, 2016). However, the exact mechanism of this antagonistic behaviour is still not clear. This SlmA inhibition has been found to strengthened by binding the SBSs on nucleoid (Adams et al., 2015; Cho and Bernhardt, 2013; Tonthat et al., 2011). Overall, this SlmA mediated NO prevents Z-ring assembly over nucleoid until the major chromosome segregation process is complete and ready for cytokinesis; this allows FtsZ to be assembled either at the nucleoid free regions likely at poles or midcell. However, the Min system prevents FtsZ assembly near poles, which leave the midcell loci as the only suitable position to form a Z-ring (Adams et al., 2014; Bernhardt and de Boer, 2005; Cho and Bernhardt, 2013; Hajduk et al., 2019; Wu and Errington, 2004).

1.2.3. *E. coli* divisome complexes, their assembly and roles during septation and cell separation

E. coli cell division starts with invagination of cell wall and formation of Septum at midcell. This process involves formation of septal PG (sPG) synthesis that is guided, activated and achieved by divisome complexes which are spanned across three compartments of the bacteria cell envelop (de Boer, 2010; Du and Lutkenhaus, 2017; Lutkenhaus, Pichoff, and Du, 2012; Tsang and Bernhardt, 2015a). This remarkable event is orchestrated by more than 30 different proteins have been reported to be involved directly or indirectly in divisome assembly and/or associated with one or more submodules of divisome network (B. Liu, Persons, Lee, and de Boer, 2015). Initially most these proteins and their genes in *E. coli* that were found to be involved in cell division, were categorised as *fts* (filamentous temperature sensitive) genes and thus Fts proteins. The reason behind such name is elongated or filamentous growth of *fts* mutant *E. coli* at non-permissive temperature over 37 °C, usually observed at 42 °C (Bi and Lutkenhaus, 1991; Rowlett and Margolin, 2015). Among all these Fts proteins and their associated cell division proteins, at least a dozen has been identified as essential or conditionally essential in *E. coli*. These proteins are, in the hierarchical order of their recruitment to the divisome assembly: FtsZ, FtsA, ZipA, FtsK, FtsE, FtsX, FtsQ, FtsB, FtsL, FtsW, PBP3 (FtsI) and FtsN (**Figure 1.6**). These proteins are highly conserved across bacterial species and in *E. coli* these proteins together form the core divisome network (Aarsman et al., 2005; de Boer, 2010; Du and Lutkenhaus, 2017; Egan and Vollmer, 2013; Gamba et al., 2009; Goehring, Gueiros-Filho, and Beckwith, 2005; Huang, Durand-Heredia, and Janakiraman, 2013; Lutkenhaus et al., 2012). Proteins associated in this network accomplish crucial jobs, such as formation of cytoskeletal Z-ring to provide scaffold to other divisome proteins to assemble such as FtsZ, FtsA (Bi and Lutkenhaus, 1991; Pichoff and Lutkenhaus, 2005); some of which involves in chromosome segregation process such as FtsK (Stouf, Meile, and Cornet, 2013); some to septal PG synthesis such as FtsW and PBP3 (PBP3: also known as FtsI) (Fraipont et al., 2011; Mohammadi et al., 2011) and others in PG remodelling and final separation of daughter cell by hydrolysing old PG such as FtsEX, EnvC, NlpD, AmiA, AmiB

and AmiC (Du et al., 2019; Du, Pichoff, and Lutkenhaus, 2016). These processes functionally interdependent and associated complexes are interlinked and complete the whole divisome assembly in two clearly distinguishable phases.

In the first phase (**Figure 1.6.a**), the Z-ring is nucleated by a GTP-dependent polymerization of FtsZ monomers at the midcell loci (Bi and Lutkenhaus, 1991; Fu et al., 2010; Lowe and Amos, 1998), where actin-like proteins FtsA (Szwedziak et al., 2012) and a Z-interacting protein (ZipA) both has been reported to tether FtsZ filaments to cell inner membrane (Bi and Lutkenhaus, 1991). FtsA binds directly to conserved C-terminal domain (CCTD) of FtsZ and tether the FtsZ protofilaments to inner side of cytoplasmic membrane using the conserved membrane targeting amphipathic C-terminal helix of FtsA (Pichoff and Lutkenhaus, 2005). ZipA also targets the FtsZ CCTD, has been predicted to compete with FtsA for binding to FtsZ (Krupka et al., 2018; Mosyak et al., 2000) and protecting the Z-ring from ClpXP mediated degradation during divisome assembly (Hernandez-Rocamora et al., 2012; Krupka et al., 2018; Pazos, Natale, and Vicente, 2013). However, the mechanism by which ZipA is tethering the Z-ring to inner the membrane, is not clear. FtsA and ZipA both has been reported as essential in *E. coli*, and recently has shown to interact with each other directly (Vega and Margolin, 2019). These two proteins have been suggested to have somewhat overlapping roles in tethering the FtsZ protofilaments to the cytoplasmic side of the membrane and assembling further divisome assemblies (Krupka et al., 2018; Pichoff and Lutkenhaus, 2002). However, a gain of function FtsA mutant (FtsA*), has shown to complete cell division successfully in the absence of ZipA (Geissler, Elraheb, and Margolin, 2003). This gain of function with *ftsA** mutant shows a reduced oligomerized state for the FtsA* protein, which indicates the gain of function in *ftsA** mutant may be related to a deficiency in polymerization of this mutant form of FtsA. ZipA has been hypothesized to regulate the same function as FtsA*, in wild type *E. coli* (Pichoff et al., 2012). Apart from above two essential membrane associated proteins, some non-essential FtsZ-associated-proteins such as ZapA, ZapB, ZapC, ZapD and ZapE, also has been reported to have ability to crosslink FtsZ and these are necessary to stabilize the Z-ring at the early stage of divisome assembly

(Dajkovic et al., 2010; Dewachter et al., 2018; Durand-Heredia et al., 2012; Durand-Heredia et al., 2011; Ebersbach et al., 2008; Gueiros-Filho and Losick, 2002; Hale et al., 2011; Marteyn et al., 2014; Pacheco-Gomez et al., 2013; Small et al., 2007). In addition, association of ZapA and ZapB to the Z-ring interlinks FtsZ protofilaments to chromosome terminus (Ter) macrodomain (MD) via a direct interaction between ZapB and MatP (Espeli et al., 2012). This multiprotein association known as Ter linkage that may provide vital information about the link between cell division and chromosome segregation process (Bailey et al., 2014; Buss et al., 2015; Buss et al., 2017; Du and Lutkenhaus, 2017; Espeli et al., 2012; Mercier et al., 2008). During midcell division stage, an ATP-binding-cassette-transporter (ABC-transporter) like protein complex, FtsEX is recruited to divisome (Schmidt et al., 2004) via an interaction between FtsE and FtsZ (Corbin et al., 2007). In *E. coli*, the FtsEX has been reported as conditionally essential (Reddy, 2007).

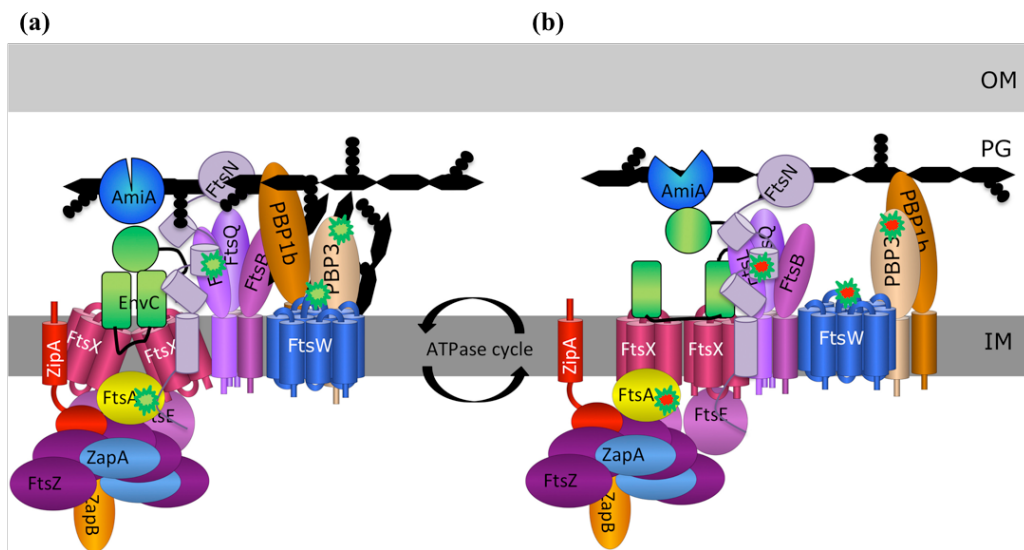


Figure 1.6. *E. coli* divisome assembly and activation.

The *E. coli* divisome organises and activates in two phases: **(a)** the early phase driven by FtsZ, FtsA, ZipA, and ZapB (in this figure), which helps anchoring the Z-ring to the membrane and scaffold other downstream protein at divisome. FtsEX arrives early to midcell division stage and subsequently recruit further downstream proteins and assemble the PG synthesis machineries in the second phase of divisome assembly **(b)**, when the FtsN links the early and late proteins via an interaction with FtsA and stabilize the FtsW-FtsI (PBP3) complex as well as the FtsQLB complex. These macromolecular interactions trigger the cell wall synthesis. This activation is represented by both Green and Red starbursts which indicate activated state **(b)**; whereas the Green only starbursts represents the pre-activation state of FtsA, FtsN, FtsW and FtsI/PBP3. While these molecules are involved in sPG synthesis process the FtsEX mediated ATP hydrolysis triggers amidase/PG hydrolase activity (represented by AmiA in this figure, other amidases are not shown in this figure) which in turn enable daughter cell separation. The figure is representative of hypothesised model and does not represent their stoichiometries.

Figure adopted from den Blaauwen, Hamoen, and Levin (2017).

In the second phase (**Figure 1.6.b**), the *E. coli* FtsEX has been hypothesised to assemble further essential downstream division proteins to the divisome (Du and Lutkenhaus, 2017). This function makes FtsEX a required divisome protein under certain physiological condition such in low osmolarity (Reddy, 2007; Schmidt et al., 2004). Recruitment of the late cell division proteins starts with an essential divisome component FtsK that acts as a DNA-translocase (Begg, Dewar, and Donachie, 1995) and links the DNA segregation process to cell division (Liu, Draper, and Donachie, 1998; Massey et al., 2006). There is also a direct interaction

between FtsX and FtsQ (Karimova et al., 2005) which is necessary to allow the FtsQ, FtsL and FtsB complex to associate with the Z-ring as a complex (FtsQLB) and are involved in sPG synthesis and class A PBP regulation (Buddelmeijer and Beckwith, 2004; van den Berg van Saparoea et al., 2013). Similarly, the recruitment of another complex between FtsW and FtsI (PBP3) also drives the sPG synthesis (Yang et al., 2017). However, its location to Z-ring and further activity is controlled by FtsQLB complex (Tsang and Bernhardt, 2015b). The FtsW protein has been recently characterized as a protein from the SEDS family and reported to have PG glycosyltransferase (GTase) activity whereas, the other partner FtsI (PBP3) is known for its D-D-transpeptidase activity (Meeske et al., 2016; Taguchi et al., 2019). Simultaneously, a class A penicillin-binding-protein, PBP1b that is non-essential division protein in *E. coli* and has been known for its bi-functional activity (that is both TPase and GTase), reinforce the sPG synthesis capacity along with FtsW-FtsI complex (Taguchi et al., 2019). Additionally, the presence of PBP1b at both peripheral cell wall and septum suggests its dual role in both peripheral as well as septal PG synthesis during elongation and division respectively (Bertsche et al., 2006). The presence of PBP1b at the septum is dependent on FtsI (PBP3) but not its activity (Bertsche et al., 2006). Apart from FtsW, the FtsI also has been suggested to interact with FtsA (Corbin, Geissler, Sadasivam, and Margolin, 2004), FtsQ (Piette et al., 2004) and the final core essential divisome protein FtsN (Wissel and Weiss, 2004). The FtsN has PG binding property via its periplasmic sporulation-related repeat (SPOR) domain (Gerding et al., 2009; Ursinus et al., 2004). FtsN is the last protein to be recruited at the divisome in the late cell division stage (Addinall, Cao, and Lutkenhaus, 1997) possibly through an interaction between FtsI and FtsN. The interaction was further confirmed through *in-vivo* chemical cross-linking study (Bertsche et al., 2006; Muller et al., 2007). However, a small sub-population of FtsN protein molecules are observed to localize at the midcell septum by FtsA at early stage (Weiss et al., 1999), which has been presumed to establish a positive feedback loop to initiate sPG synthesis in a SPOR-independent manner (Busiek et al., 2012).

Following recruitment of FtsN to the divisome, this bitopic protein (Dai, Xu, and Lutkenhaus, 1996) signals to its proposed cytoplasmic partner FtsA linking activity in the periplasm to cytoplasm across the cytoplasmic membrane. This interaction is mediated between the cytoplasmic domain of FtsN (FtsN_{Cyto}) and 1c subdomain of FtsA (Pichoff, Du, and Lutkenhaus, 2018) confirms the completion of divisome assembly in order to initiate constriction (den Blaauwen and Luirink, 2019; Du et al., 2016; Gerding et al., 2009; Weiss, 2015) and final cell separation. The invagination of cell wall at the constriction site initiated through an interaction of Tol/Pal complex (Gerding et al., 2007). Whereas, the sPG remodelling mediated by membrane bound FtsEX complex that recruits EnvC which in coordination with NlpD regulates the septal PG hydrolases (AmiA, AmiB and AmiC) (Peters, Dinh, and Bernhardt, 2011; Uehara et al., 2010; Yang et al., 2017). These PG hydrolases promote hydrolysis of old sPG and separation of septum (Bernhardt and de Boer, 2003; Heidrich et al., 2001; Peters et al., 2011; Uehara et al., 2010; Yang et al., 2017) to enable division.

1.3. Cell division in the *S. pneumoniae*, a model for Gram-positive and oval-shaped cocci bacteria

S. pneumoniae is an ovoid cocci (ovococci bacteria) and thus has an entirely different morphology compared to rod shaped *B. subtilis* or *E. coli*. However, like these rod-shaped bacterial, *S. pneumoniae* also possess two distinct sets of complexes – the elongasome and divisome, by which they initiate cell expansion/elongation and cell division, respectively (Massidda, Novakova, and Vollmer, 2013; Perez et al., 2019). Strikingly, a clear distinction between these two mechanisms and particularly the peripheral PG synthesis using conventional elongasome complexes has not been detected in most spherical cocci, and are suspected to have mechanisms that is only involved in septal PG synthesis (Lleo et al., 1990). Pioneering experiment by Higgins and Shockman (Higgins and Shockman, 1970; Higgins and Shockman, 1976) proposed a model of independent, simultaneous septal and peripheral PG mechanisms during cell division. The model is still valid and well accepted among recent researchers. According to this model, the septal PG synthesis leads over peripheral PG synthesis and the cell cycle starts with formation of a septal ring replacing the old equatorial ring at the midcell of the progenitor cell. The newly formed septal ring assembles all divisome proteins, simultaneously cytoskeletal proteins give rise to another two nascent rings that gradually moves away from the septum following peripheral PG synthesis using elongasome complexes. However, the septal PG synthesis components do not move away from divisome site and continue septal PG synthesis (**Figure 1.7**), while hydrolase enzymes hydrolyse matured sPG and separate daughter cells following a signal from their cognate cytoplasmic membrane partners (Higgins and Shockman, 1970; Perez et al., 2019).

1.3.1. Locating division site and Z-ring positing in *S. pneumoniae*

In comparison to rod-shaped model such as *E. coli* and *B. subtilis*, little is known about midcell Z-ring positioning mechanisms and its regulators in oval-shaped bacteria like *S. pneumoniae*. Ovococci do not generally have an MreB gene which has been linked to Rod shape but do have MreCD which are required for

elongasome function. More widely, *S. pneumoniae* has a fundamentally different mechanism to organise and position its Z-ring at the septum, due to lack of any nucleoid occlusion (NO) and Min systems found in rod-shaped bacteria (Daniela Fadda et al., 2007; Pinho, Kjos, and Veening, 2013). According to current models, the similar mechanism in *S. pneumoniae* is mediated through MapZ (Midcell-anchored protein Z) that was previously annotated as LocZ (Localising at midcell of FtsZ) (Fleurie et al., 2014; Holeckova et al., 2014). MapZ mutants are viable but shows severe morphogenetic defects and create minicells (Holeckova et al., 2014), which are typical signs of defects in divisome mechanisms related to Z-ring at midcell or to its regulation. Similar defects in the Min system in *E. coli* give rise to minicells as previously discussed (Adler et al., 1967; de Boer et al., 1989; Shih and Zheng, 2013). MapZ is known to localise and assemble to a ring-like structure at the equator of the cell that mark the future cell division site, before assembling of the Z-ring (**Figure 1.7**) (Fleurie et al., 2014; Holeckova et al., 2014; Perez et al., 2019; Rowlett and Margolin, 2015). FtsZ directly binds to MapZ and follows the MapZ ring near the equator where FtsZ further assembles to Z-ring structure (Fleurie et al., 2014). MapZ is a bitopic membrane protein which binds PG through its extracellular C-terminal domain (Manuse et al., 2016), whereas the N-terminal cytoplasmic domain has been predicted to bind to FtsZ. Notably, MapZ also has been found to act as substrate for the conserved Ser/Thr protein kinase, StkP which is a master regulator for pneumococcal cell division and cell shape determination (Beilharz et al., 2012; Fleurie et al., 2012). However, the role of this phosphorylated form of MapZ in the Z-ring assembly and constrict is not critical according to recent data (Perez et al., 2019). During cell elongation, MapZ at equator forms three ring-like structures, while the main ring start assembling the Z-ring and form septum (**Figure 1.7**), the other two MapZ rings split from the main ring and move away with the elongasome fork that localise the rings at the new equator of two daughter cells, this in turn also mark the future division site for next cycle. Meanwhile the main MapZ-ring at the septum stays at the construction site until the complete constriction is achieved (**Figure 1.7**) (Garcia et al., 2016).

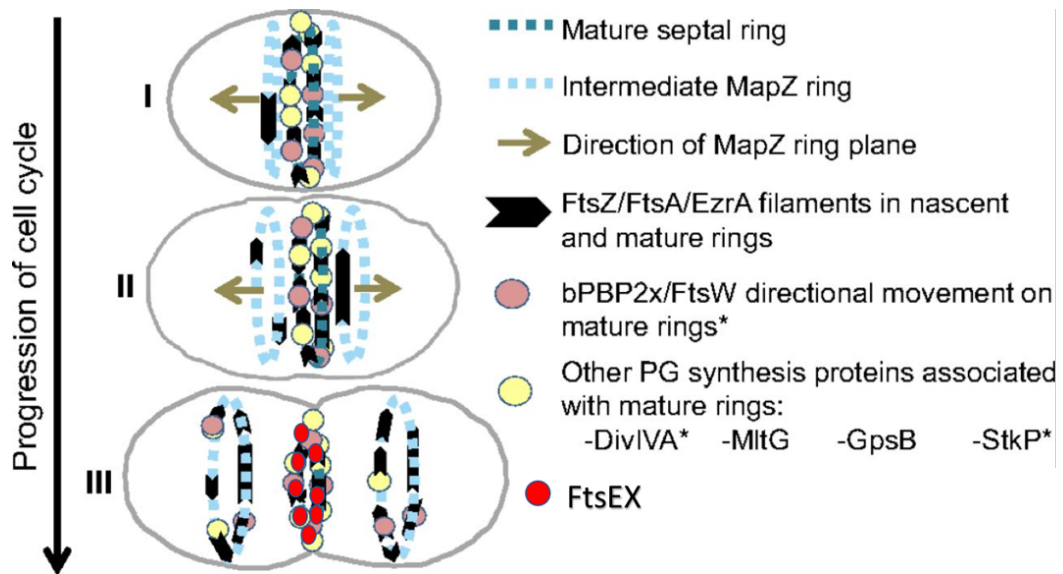


Figure 1.7. *S. pneumoniae* Z-ring positioning and its assembly.

The above diagram summarises the movement dynamics of divisome proteins that includes *FtsZ*, *FtsA*, *EzrA*, class B PBP2x (*bPBP2x*), *FtsW*, and other regulators of PG synthesis during elongation and division in *S. pneumoniae* cells. The cell division and dynamics is simplified in three major steps. In early stage (I) of division the equator becomes the loci for new septum for progenitor cell. This directed by MapZ and *FtsZ* accompany at the new septum location where other divisome proteins assemble to form a bigger macromolecular divisome complex. At new septum MapZ splits into three and two of them moves in opposite direction towards equators in the developing daughter cells. Next a protofilament bundle consists of *FtsZ* and its membrane anchor associates such as *FtsA* and *EzrA* follows the MapZ rings, which guides them to new equatorial rings in the daughter cells (II-III). Migration of these bundles to the equators of newly formed daughter cells direct the future site for *FtsZ* to nucleate and assemble the Z-ring at the equator region. Interestingly, while this *FtsZ*/*FtsA*/*EzrA* bundles moves to MapZ guided equatorial rings the PG synthesis machinery comprised of *FtsW*, *bPBP2x* does not leave the septum. Same also has been predicted for PG separation machinery and its regulators such as *FtsEX*. This suggest their these late divisome proteins and their associates are crucial and does not leave septum until completion of new septal PG synthesis and separation of old cell wall afterwards.

Figure adopted and modified from Perez et al.(2019).

1.3.2. *S. pneumoniae* elongation complexes, their assembly and roles during cell elongation

Like the *E. coli* complex, the *S. pneumoniae* elongasome complex includes several Mre proteins (MreC, MreD); class A PBPs (PBP1a) and class B PBPs (PBP2b); and proteins for SEDS (RodA, RodZ) (Philippe, Vernet, and Zapun, 2014; Zapun, Vernet, and Pinho, 2008) (**Table 1.1**) (**Figure 1.8**). However, *S. pneumoniae* lacks the rod-shape determinant protein MreB that is the first to nucleate the elongasome in *E. coli* (Typas and Sourjik, 2015; Wachi et al., 1987). The other two Mre proteins, MreC and MreD were shown to have essential roles in the elongation of *S. pneumoniae* strain that lacks PBP1a activity (Land and Winkler, 2011). The same research also suggested the bifunctional class A PBP1a that possess both GTase and TPase activity, is genetically associated to MreC and MreD proteins and has role in elongation. By contrast the role of class B PBP2b has been found essential in peripheral growth thus in elongation of *S. pneumoniae* cells (Berg et al., 2013; Perez et al., 2019) and its predicted TPase activity has been confirmed in an *in-vitro* experiment (Zapun et al., 2013). Among SEDS group of proteins, RodA was found essential in global gene inactivation studies (Song et al., 2005; Thanassi et al., 2002) and regarded as having a role in regulating elongation (Land and Winkler, 2011) by formation of an elongasome complex with PBP2b (analogous to the RodA-PBP2 complex in *E. coli*). RodZ has been identified in *S. pneumoniae* and has been suggested to have role in assembling MreC and MreD proteins in the elongasome (Alyahya et al., 2009; Massidda et al., 2013; Philippe et al., 2014).

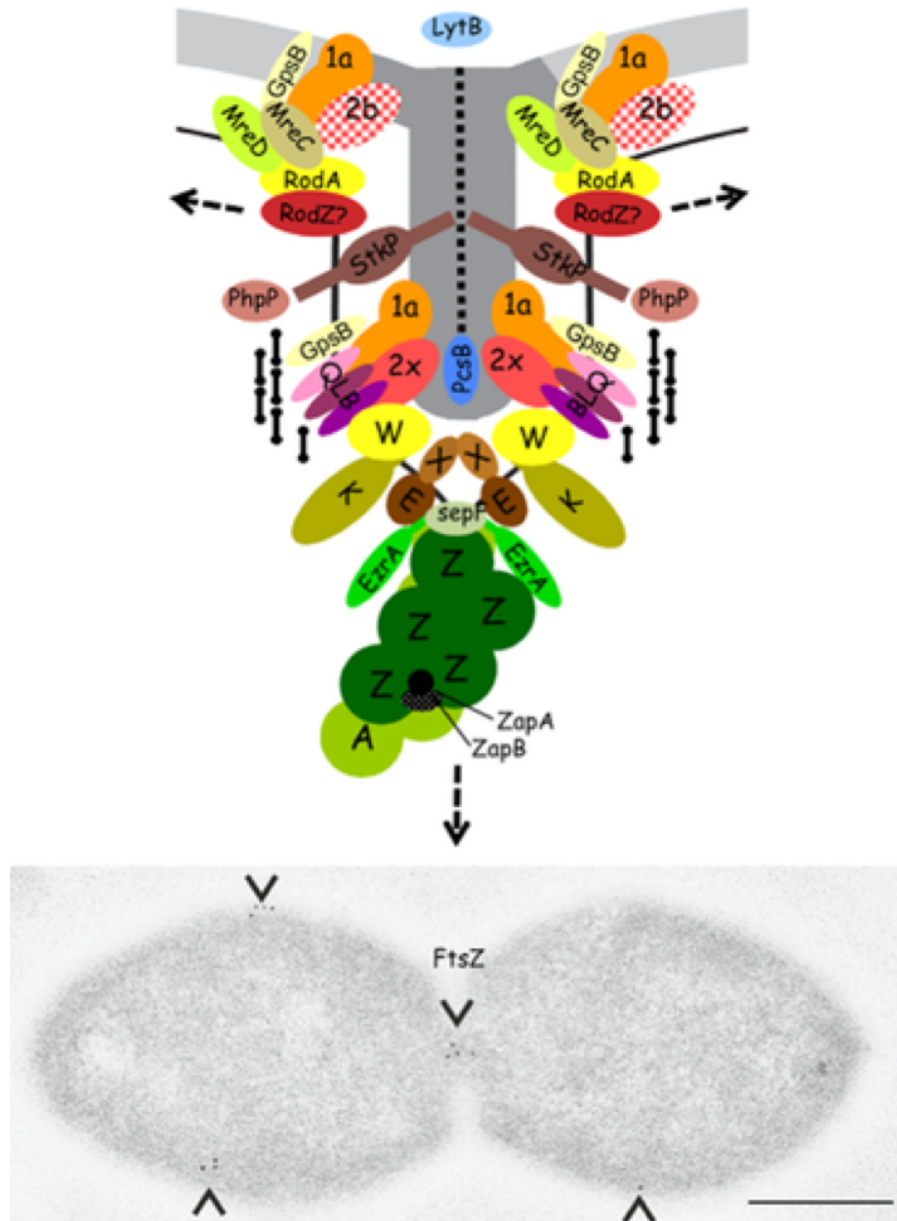


Figure 1.8. Schematic representation of the *S. pneumoniae* elongasome and divisome complexes.

Septal peptidoglycan (PG) synthesis at the midcell is orchestrated by coordinated assembly and activity of wider network of proteins complexes, involved in cell elongation and division in *S. pneumoniae*. The mature or old PG layer is represented as black dotted line, whereas the new septal wall is represented as dark grey and the peripheral wall as light grey. All Fts proteins are represented by their single letter or number-letter after their group name (Fts) and for PBPs (e.g. FtsZ and PBP2x represented as Z and 2x respectively). DivIVA represented as black bars around septum. See the main text for details of their assembly and interactions. The EM image below shows the localization of FtsZ using immunogold labelling (as observed as black dots at midcell and equators indicated by an arrow), in *S. pneumoniae* ovococci cells (image courtesy: O. Massidda; Scale bar = 0.25 μm). Figure adopted from Massidda et al. (2013).

Table 1.1. List of *S. pneumoniae* proteins involved in cell elongation and division.

| Protein | ^a Essen. | ^b Loc. | Comment/Function | ^c Protein–protein interactions (Sp) | References |
|-----------------|---------------------|-------------------|---|---|--|
| Divisome | | | | | |
| FtsZ | E | Septa | Tubulin structural homologue; GTPase; First protein in cell division; Z-ring formation at midcell | @FtsA, ZapA, FtsK, FtsB, FtsL, FtsW | (Lara et al., 2005; Maggi et al., 2008; Morlot, Zapun, Dideberg, and Vernet, 2003) |
| FtsA | E | Septa | Actin-structural homologue; Tethers FtsZ to membrane and stabilizes the Z-ring | @FtsZ, ZapA, PBP2x, FtsK, FtsL | (Lara et al., 2005; Maggi et al., 2008) |
| ZapA | NE | nd | Z-ring positive regulator | @ZapA, FtsZ, FtsA, FtsK, FtsQ, FtsB, FtsL, FtsW | (Maggi et al., 2008) |
| ZapB | NE | nd | Z-ring positive regulator | nd | |
| SepF (YlmF) | NE | nd | Z-ring positive regulator | nd | (D. Fadda et al., 2003) |
| EzrA | E | nd | Z-ring negative regulator | nd | |
| FtsE | E | Septa | ABC transporter with FtsX; required for PcsB localization and activation | FtsX | (Sham et al., 2011) |
| FtsX | E | Septa | ABC transporter with FtsE; required for PcsB localization and activation | FtsE, PcsB | (Sham et al., 2011) |

| | | | | | |
|------------------|----|-------|---|---|--|
| FtsK (SpoIII) | NE | Septa | Chromosome segregation and cell division | @FtsZ, ZapA, FtsQ, FtsL, FtsA | |
| FtsQ (DivIB) | CE | Septa | Unknown; possible role in septal PG synthesis. | @ZapA, FtsK, FtsB, FtsL, FtsW, FtsZ | (Le Gouellec et al., 2008; Maggi et al., 2008; Masson et al., 2009; Noirclerc-Savoie et al., 2005) |
| FtsB (DivIC) | E | Septa | Unknown; possible role in septal PG synthesis. | @ZapA, FtsK, FtsQ, FtsL, FtsW, FtsZ | (Le Gouellec et al., 2008; Maggi et al., 2008; Masson et al., 2009; Noirclerc-Savoie et al., 2005) |
| FtsL | E | Septa | Unknown; possible role in septal PG synthesis. | @ZapA, FtsK, FtsQ, FtsB, FtsW, FtsZ, FtsA, FtsI (PBP2x), PBP1a | (Le Gouellec et al., 2008; Maggi et al., 2008; Masson et al., 2009; Noirclerc-Savoie et al., 2005) |
| FtsW | nd | Septa | Lipid II flippase; septal PG synthesis | ZapA, FtsQ, FtsL, FtsZ, FtsK | (Maggi et al., 2008; Morlot, Noirclerc-Savoie, Zapun, Dideberg, and Vernet, 2004) |
| PBP2x (FtsI) | E | Septa | PG transpeptidase; septal PG synthesis | @FtsA, FtsL | (Kell et al., 1993; Maggi et al., 2008; Morlot et al., 2004; Zapun et al., 2008) |
| PBP1a | NE | Septa | PG glycosyltransferase/transpeptidase; peripheral and septal PG synthesis | FtsL | (Kell et al., 1993; Maggi et al., 2008; Morlot et al., 2004; Zapun et al., 2008) |

| | | | | | |
|--------|----|--------------------|---|--|--|
| GpsB | NE | nd | Unknown; hypothetical role in peripheral and septal PG synthesis | nd | (Massidda, Anderluzzi, Friedli, and Feger, 1998) |
| DivIVA | NE | Septa and poles | Unknown; required for completion of cell division and pole maturation | @FtsZ, FtsA, ZapA, EzrA, FtsK, FtsL, FtsB, FtsQ, FtsW, PcsB, LytB | (D. Fadda et al., 2003; Daniela Fadda et al., 2007) |
| PcsB | CE | Septa and/or poles | PG hydrolase; PG remodelling and cell separation | Found to interact FtsX, and also suspected to interact DivIVA for septum localisation. | (Daniela Fadda et al., 2007; Giefing et al., 2008; Giefing-Kroll et al., 2011; Ng et al., 2003; Sham et al., 2011) |
| LytB | NE | Poles | PG hydrolase; cell separation | Possibly DivIVA | (De Las Rivas, García, López, and García, 2002; Daniela Fadda et al., 2007) |

Elongasome

| | | | | | |
|------|----|-------|---|----|--------------------------|
| MreC | CE | Septa | Unknown; possible role in peripheral PG synthesis | nd | (Land and Winkler, 2011) |
| MreD | CE | Septa | Unknown; possible role in peripheral PG synthesis | nd | (Land and Winkler, 2011) |
| RodZ | nd | nd | Unknown; possible role in peripheral PG synthesis | nd | |

| | | | | | |
|-------|----|-------|---|------------------------|--|
| RodA | nd | nd | Lipid II flippase; peripheral PG synthesis | nd | |
| PBP2b | E | Septa | PG transpeptidase; peripheral PG synthesis? | FtsZ, FtsA, FtsB, FtsL | (Kell et al., 1993; Maggi et al., 2008; Morlot et al., 2004; Zapun et al., 2008) |
| PBP1a | NE | Septa | PG glycosyltransferase/transpeptidase; peripheral and septal PG synthesis | FtsL | (Kell et al., 1993; Morlot et al., 2004; Zapun et al., 2008) |
| GpsB | NE | nd | Unknown; hypothetical role in peripheral and septal PG synthesis | nd | (Massidda et al., 1998) |

Signalling/control

| | | | | | |
|-------------|----|--------------|--|----|--|
| StkP | NE | Septa | Serine/threonine kinase; control of cell division | nd | (Beilharz et al., 2012; Fleurie et al., 2012; Giefing et al., 2010; Novakova et al., 2010) |
| PhpP | CE | Septa | Phosphatase; control of cell division | nd | (Agarwal et al., 2011; Osaki et al., 2009) |
| PBP3 (DacA) | NE | Cell surface | DD-carboxypeptidase; availability of pentetide substrates in PG | nd | (Barendt, Sham, and Winkler, 2011; Morlot et al., 2004) |
| DacB | NE | Cell surface | LD-carboxypeptidase; availability of tetrapeptide substrates in PG | nd | (Barendt et al., 2011) |

Uncharacterized

| | | | | | |
|-------|----|----|---------|----|---|
| Pmp23 | NE | nd | Unknown | nd | (Barendt et al., 2011; Pagliero et al., 2005) |
|-------|----|----|---------|----|---|

a Essentiality: CE, conditionally essential; E, essential; nd, not determined; NE, not essential; PG, peptidoglycan.

b Subcellular localization

c @Indicate polymerization and self-assembly

This table including all descriptions and references in the table is adopted and modified from Massidda et al. (2013)

1.3.3. *S. pneumoniae* divisome complexes, their assembly and roles during septation and cell separation

In *S. pneumoniae*, divisome complexes are assembled on the septal ring that localizes at the equator of the progenitor cell. The *S. pneumoniae* divisome is composed of similar groups of proteins (**Table 1.1**) that have been observed in *E. coli* divisome. The essential core *S. pneumoniae* divisome network includes cytoskeleton proteins (FtsZ and FtsA), several Z-ring associated proteins (ZapA, ZapB), some Z-ring and cell wall regulatory proteins EzrA and GpsB, an ATPase FtsE and its transmembrane partner FtsX, a series of Fts bitopic proteins (DivIB/FtsQ, DivIC/FtsB, FtsL, FtsW) and associated PG synthases (PBP2x, PBP1a), hydrolase proteins (PcsB) and an additional cell division protein DivIVA (Massidda et al., 2013). In exception to other divisome proteins the last two proteins (PcsB and DivIVA) are found to be present in both divisome and poles at the same time (Daniela Fadda et al., 2007; Miguel Vicente and García-Ovalle, 2007). Among all rod-model essential divisome proteins, ZipA and FtsN are not present in *S. pneumoniae* and among non-essential proteins ZapC and ZapD are also absent in *S. pneumoniae*. Whereas the presence of FtsK in *S. pneumoniae* has not been found with any essential role in divisome assembly and cell viability (Maggi et al., 2008) except its suggested interaction with FtsZ, ZapA, DivIB and FtsL (Maggi et al., 2008).

In *S. pneumoniae*, the divisome (**Figure 1.8**) is assembled in two major phases. Like *E. coli*, it starts with migration of FtsZ molecules to the equator. This migration recently has been shown to be guided by MapZ (Perez et al., 2019). A GTP dependent polymerization of FtsZ forms protofilaments which are tethered to the membrane by FtsA and stabilized by EzrA (Lara et al., 2005; Morlot et al., 2003; Perez et al., 2019). The EzrA protein acts as a positive regulator of Z-ring formation, and the ZapA and ZapB proteins were found to act as somewhat negative regulators of division (Massidda et al., 2013). In contrast, another Z-ring associated protein SepF (YlmF) has been identified as a positive stabilizer and conditionally essential in *S. pneumoniae*, inactivation of which is observed with cell division defects and elongated cells (D. Fadda et al., 2003; Massidda et al., 1998). During the early-mid cell division stage, similar to *E. coli* divisome assembly, the rest of the *S. pneumoniae* divisome proteins assemble into a Z-ring in a predicted similar order as in *E. coli* – FtsE, FtsX, DivIB (FtsQ), DivIC (FtsB), FtsL, FtsW, PBP2x and PBP1a (Morlot et al., 2004; Morlot et al., 2003; Noirclerc-Savoie et al., 2005). PBP2x and another essential cell synthesis regulator; GpsB, has been suggested to mediate septal PG synthesis and subsequent septum ring closure (Land et al., 2013). Selective inhibition of the class B, PBP2x by methicillin is reported to block septal PG synthesis. Similarly, depletion of GpsB shows morphological consequences that include elongated cell phenotypes with no septum PG closure and subsequent cell lysis (Fleurie et al., 2014; Land et al., 2013). Additionally, the cell division protein DivIVA that is also suspected to interact with FtsZ and has a possible role in localizing PcsB, assembles to the Z-ring (Beilharz et al., 2012; Daniela Fadda et al., 2007). However, the localization and recruitment of these proteins to the Z-ring in an absolute spatio-temporal order, is not clear at this point. Amongst the above assembly, the FtsE and FtsX proteins, are found to be essential in *S. pneumoniae*, since deletion of either gene is not tolerated. Together they form a functional complex that has been predicted to be a component required for hydrolysis of PG specifically via an interaction between the FtsX membrane protein and PcsB which is a PG hydrolase (Sham et al., 2011) and is discussed further below.

By comparison, very little is known about *S. pneumoniae* FtsK beyond its participation in an overall interaction network with other Fts proteins (Maggi et al., 2008). Similar to *E. coli*, the next three essential bitopic proteins FtsQ (DivIB), FtsB (DivIC) and FtsL, form a tripartite complex and have been shown to have similar function as of their *E. coli* counterparts (Buddelmeijer and Beckwith, 2004; Masson et al., 2009; Noirclerc-Savoie et al., 2005). At the late cell division stage, another essential divisome protein FtsW along with its cognate class B PBP2x (Perez et al., 2019) recruits to septal ring through a suggested interaction with FtsQ (DivIB) and FtsL (Maggi et al., 2008; Morlot et al., 2004). A global gene silencing studies, conducted by Thanassi et al., 2002 and Song et al., 2005, confirm essentiality of most above described divisome proteins.

In final second phase, completion of divisome assembly sends signals to two machineries through unknown mechanisms. These are sPG synthesis and old PG hydrolysis (**Figure 1.8**). The first one has been predicted to mediated through an interaction between FtsW and PBPs. However, like *E. coli*, the interaction between FtsW and several common PBPs have only recently been explored including coupled movement dynamics of FtsW and PBP2x along the matured septa, which evident a spatio-temporal and presumed functional interaction between FtsW and PBP2x (Perez et al., 2019). The same research also demonstrated the movement dynamics of predicted FtsW-PBP2x complex is independent of FtsZ treadmilling and observed restricted to only septal rings where movement of DivIVA also has been localized, other cell division regulators including GpsB, MltG and StkP mostly remain at the septa with varying movement between septal and equatorial rings (Perez et al., 2019). This evidence of colocalization of FtsW and class B PBP2x throughout the *S. pneumoniae* cell division, coupled with recent biochemical evidence of absolute co-dependence of FtsW on its cognate class B PBP2x for their respective GTase and TPase activity during PG synthesis (Taguchi et al., 2019), links their interaction in *S. pneumoniae* model.

The other set of machinery that is strongly implicated as necessary following divisome assembly, is related to PG hydrolysis. This process has been hypothesized

to be conducted through an interaction between FtsEX and PcsB (Bajaj et al., 2016; Sham et al., 2013). The activity of PcsB has been predicted to dependent on an ATP hydrolysis event at the cytoplasmic subunit (FtsE) of FtsEX complex (Bajaj et al., 2016; Sham et al., 2011; Sham et al., 2013). Additionally, another identified PG hydrolase LytB (endo- β -N-acetylglucosaminidase) also found to act and hydrolyse PG at the end of cell division but suspected to act much later than PcsB (De Las Rivas et al., 2002; Garcia et al., 1999), together these PG hydrolases results in separation of daughter cells. Recently, the conserved cell shape regulatory protein, and serine-threonine kinase, StkP has been shown coordinate the constriction mechanism to separation presumably via phosphoregulation of required divisome proteins (Zucchini et al., 2018).

1.4. Cell division in *Bacillus subtilis*, a model for Gram-positive and rod-shaped bacteria

Bacillus subtilis is a Gram-positive, rod-shaped, aerobic and endospore-forming bacteria that has been studied and best characterized among all Gram-positive bacteria. The most interesting feature of this bacteria is endospore or spore formation, which makes this model suitable for studying symmetric and asymmetric cell division using the same model (**Figure 1.9**), as well as shed light on mechanisms by which certain bacteria like *B. subtilis* has evolved a sophisticated survival strategy to save their genetic information/material during the unfavourable or harsh condition (Errington, 2003). *B. subtilis* is non-pathogenic bacteria and secretes a large number of commercially valuable hydrolase enzymes that includes several amylase and proteases, into its surrounding environment and thus directly into growth media. This extraordinary ability of *B. subtilis* has been commercially exploited by many biotechnology companies and created industrial interest for studying its cell cycles (Errington and Wu, 2017). Therefore, the *B. subtilis* has gained significant scientific interest in order to understand the two different types of cell cycle, namely vegetative or normal cycle and endospore or spore development cycle.

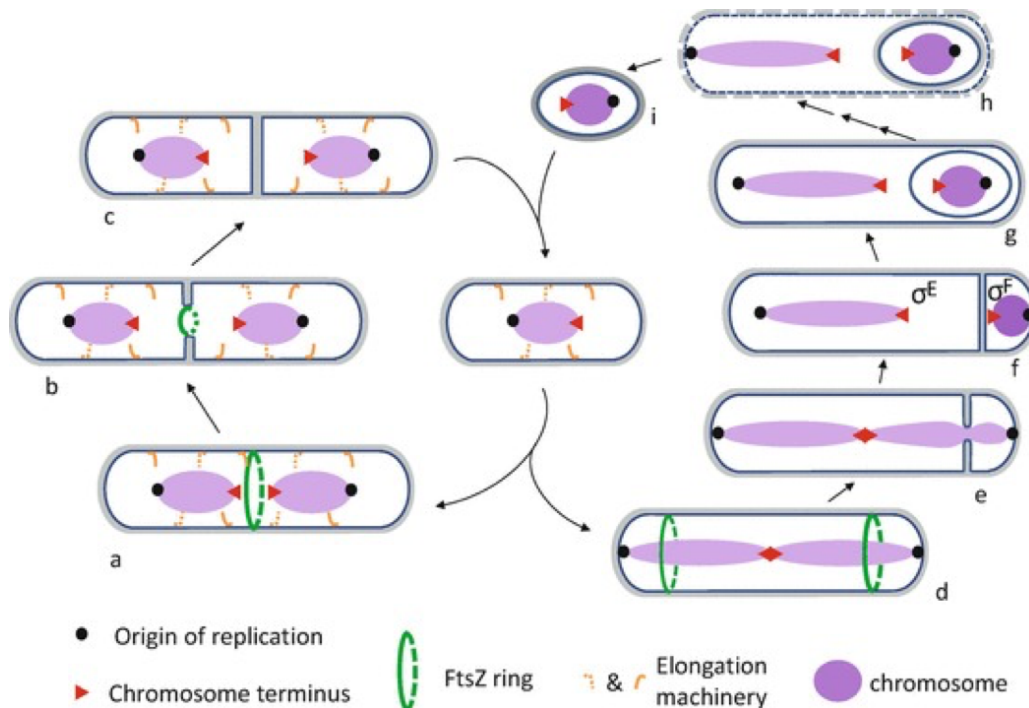


Figure 1.9. Vegetative and asymmetric cell cycle of *B. subtilis*.

The vegetative cell cycle is shown in the left cycle and the asymmetric cell cycle in the right. The cell in the centre (middle of two cycle) represents the new-born cell. The growth and elongation of the peripheral cell wall is controlled by the elongation complexes (orange curved lines). The Z-ring (green) assembles at the mid cell following segregation of chromosomes (a) and constricts down to centre of the cell as the septal PG synthesis continue (b and c). Once new cell wall formed at the midcell the Z-ring get dissolved from the septum and septation of two daughter cells follows (c), which generate single cells (centre). Under starvation or non-favourable harsh conditions *B. subtilis* cells switch to spore development cycle (right half). The cycle initiates with a conformational change at the sister chromatids, which leads to formation of axial chromosome separation and assembling of FtsZ at near polar regions (d). However only one of them operates a septum formation near pole (e). This leads to asymmetric separation and formation of endospore using a complex network of sigma transcription factors (e-i) as described in the main text.

Figure adopted from Errington and Wu (2017)

1.4.1. Vegetative cell cycle of *B. subtilis*

During the vegetative cell cycle, the *B. subtilis* progenitor cell also divides through the completion of two major events – chromosome segregation and cytokinesis, which occurs simultaneously (Hajduk, Rodrigues, and Harry, 2016). Like *E. coli*, *B. subtilis* also use three distinct sets of types of machinery to complete the cytokinesis process in a binary fission manner. Initially, the cycles start with

chromosome segregation and followed by three steps of cytokinesis – elongation, positioning of Z-ring at the midcell division site for symmetric cell division and finally cell division and separation of daughter cells (**Figure 1.9**). Similar to *E. coli* cell division, three major steps of cytokinesis are observed overlapping, and have similar sets of protein complexes to accomplish each step (Errington and Wu, 2017): the cell elongation is accomplished by the elongasome complexes; the Z-positioning mostly by Min and NO system; and the cell division by divisome complexes. Although *E. coli* and *B. subtilis* are both rod-shaped and have remarkable similarities in their set of above complexes, there are some notable differences between these Gram-negative and Gram-positive bacterial species respectively that deserve some discussion.

1.4.1.1. *B. subtilis* elongasome complexes, their assembly and roles during cell elongation

Like other rod-shaped bacteria, *B. subtilis* also has very sophisticated mechanism in determining and maintaining its rod-shape. Although *B. subtilis* is Gram-positive bacteria with a relatively thick PG layer and lacks an outer membrane layer just like *S. pneumoniae*, it still possesses a rod-shape morphology like *E. coli*. Maintaining rod-shape is a challenging physiological function and an actin-like protein MreB has been found in common among bacterial species with rod-shape (Errington and Wu, 2017). *B. subtilis* has three paralogues of MreB compared to one in *E. coli*. While the chromosome position of the *mreB* gene is located upstream of *mreC* and *mreD* genes in common with most other rod-shaped bacteria, the other paralogues *mbl* (MreB-like) and *mreBH* (MreB homologue) are located in some distant region of the chromosome (Abhayawardhane and Stewart, 1995; Errington and Wu, 2017; Levin et al., 1992; Varley and Stewart, 1992).

Individual mutants of *mreB*, *mbl* and *mreBH* genes have shown specific characteristic phenotypes with varied cell morphology such as swelled diameter, highly twisted bulged cells, and thin cells with diameter shorter than normal (particularly in low Mg^{2+} media / condition) respectively (Defeu Soufo and Graumann, 2006; Errington and Wu, 2017; Jones, Carballido-Lopez, and Errington,

2001; Kawai, Asai, and Errington, 2009). However, these mutations did not have any fatal effect on cell viability except in the case of triple null mutation. Any suspected loss of function due to inactivation of any one or two of these paralogues has been complemented by overexpressing the remaining functional paralogues of MreB (Errington and Wu, 2017; Kawai, Asai and Errington, 2009). These three MreB paralogues form helical filaments and localize near the cell periphery in close proximity of inner cytoplasmic membrane (Jones et al., 2001). Later, in a series of microscopic studies, scientists observed a circumferential movement of these MreB paralogues (Carballido-Lopez et al., 2006; Dominguez-Escobar et al., 2011; Garner et al., 2011), and the event has been associated with the PG synthesis process (Olshausen et al., 2013; Reimold, Defeu Soufo, Dempwolff, and Graumann, 2013). These three paralogues form the major platform for the other elongasome complexes to arrive and assemble. Like most bacterial species, the *B. subtilis* elongasome is composed of MreC, MreD (Leaver and Errington, 2005); bi-functional class A and mono-functional class B penicillin binding proteins (PBPs) such as PBP1 and PBP2A respectively; some SEDS group of proteins such RodA and RodZ (Dominguez-Escobar et al., 2011; Emami et al., 2017; Muchova, Chromikova, and Barak, 2013). In addition, some proteins which are involved in TA synthesis and cell wall assembly such as TagA, TagB, TagF, TagG, TagH, TagO (Formstone et al., 2008), TagT and TagU (Kawai et al., 2011), which have been suspected to have interaction with elongation complexes particularly MreB paralogues (Errington and Wu, 2017); cell wall hydrolases such as LytE and CwlO (Dominguez-Cuevas et al., 2013) (**Table 1.2**).

In contrast to *E. coli*, the *B. subtilis* MreB does not interact directly with MreC and instead the other MreB paralogue, Mbl interacts MreB to form short helices, which then interacts with MreC and is recruited to the elongasome (Defeu Soufo and Graumann, 2006). Following recruitment of MreC and MreD to the elongasome, MreB paralogues have been bound to associate cell wall synthesis and modifying complexes such as PG synthases and cell wall hydrolases to the elongasome in order to govern cell wall synthesis during elongation and particularly in helical pattern. Among the three, the MreB has been found to interact directly with PBP1 (Kawai,

Daniel, and Errington, 2009), which helps maintaining normal cell wall synthesis. However, other associations between Mre proteins and PG synthases are suspected as indirect (Margolin, 2009). In contrast to *E. coli* MreB, the *B. subtilis* MreB is thought to regulate the action of group of proteins that involved in TA synthesis at the cell wall, through an association of complex network that includes MreBCD and Tag proteins, as mentioned before (Formstone et al., 2008).

In addition to the above, the two autolysins LytE and CwlO that act as cell wall hydrolases, has been found to interact directly with MreBH and Mbl respectively (Carballido-Lopez et al., 2006; Dominguez-Cuevas et al., 2013). These interactions with MreB paralogues, assemble both cell wall hydrolases to the elongasome at the later stage, and control their functions for cell wall remodelling in a rod-shape manner. Tight regulation of these autolysins in cell wall modification is crucial step to achieve normal cell morphogenesis during cell elongation (Carballido-Lopez et al., 2006; Dominguez-Cuevas et al., 2013). However, little is known about the MreBH and Mbl specific mechanisms in regulating these autolytic endopeptidases in cell wall turnover or remodelling. Bisicchia et al. (Bisicchia et al., 2007) reported these two autolytic endopeptidases have an overlapping essential role in cell elongation. Whereas Dominguez-Cuevas et al. (Dominguez-Cuevas et al., 2013) demonstrated that these autolysins have differential roles in cell elongation. The activity of autolysin CwlO has been found to regulated by an ABC-transporter like protein FtsEX protein complex (Dominguez-Cuevas et al., 2013; Meisner et al., 2013) in a similar manner to that hypothesized in other bacteria such as in *S. pneumoniae* and *E. coli* (Sham et al., 2011; Yang et al., 2011). Surprisingly, the role of this FtsEX complex has been found to associated with divisome machineries and hypothesized to regulate cell wall hydrolases during cell division and septum separation in *S. pneumoniae* and *E. coli*. In contrast, in *B. subtilis* its function has been exclusively observed during cell elongation process (Dominguez-Cuevas et al., 2013; Sham et al., 2011; Yang et al., 2011). Recently, two uncharacterized proteins SweD and SweC are found to form a multimeric complex with FtsEX in the cell membrane and act as essential co-factors of FtsEX function to regulate CwlO activity in *B. subtilis* (Brunet, Wang, and Rudner, 2019). Whilst

a major difference of *B. subtilis* FtsEX with other two models (*E. coli* and *S. pneumoniae*) is its regulation in different phase of cell division, similarities can be noticed in the interactions of Mre proteins with other elongation and division proteins, particularly between *E. coli* and *B. subtilis*. The cytoskeletal, morphogenic *B. subtilis* Mre proteins were found to have direct interaction with both SEDS group of proteins RodA and RodZ (Dominguez-Escobar et al., 2011). RodA recently has been reported to have role in PG synthesis by its suspected monofunctional GTase activity (Dominguez-Escobar et al., 2011; Emami et al., 2017). Whereas, RodZ has been found to interact all three paralogues of Mre (MreB, Mbl and MreBH) as well as MreD, which form a large complex network with cell wall synthesis machinery and helps determining and maintaining normal rod-cell shape phenotype (Muchova et al., 2013). Very recently, RodZ also has been shown to interact the one of the Min system proteins, MinJ and has been predicted to influence the Min system in order to localizing the Z-ring and the septum correctly at the midcell and not elsewhere in the cell (Muchova et al., 2017).

Table 1.2. Possible MreB interacting proteins identified as candidate components of the elongasome.

| Protein^a | MW (kDa) | Loc^b | Comment | Key References |
|----------------------------|---------------------|------------------------|---|--|
| MreC | 32 | I/E | Cell shape function. Encoded by gene immediately downstream from <i>mreB</i> | (Dominguez-Escobar et al., 2011; Garner et al., 2011; Kawai, Daniel, et al., 2009; Leaver and Errington, 2005) |
| MreD | 19 | I | Cell shape function. Encoded by gene immediately downstream from <i>mreBC</i> | (Dominguez-Escobar et al., 2011; Garner et al., 2011; Kawai, Daniel, et al., 2009; Leaver and Errington, 2005; Muchova et al., 2013) |
| RodZ | 23 | I/C | Required for normal cell shape | (Dominguez-Escobar et al., 2011; Muchova et al., 2013) |
| CwlO | 50 | E | Autolytic enzyme, regulated by FtsEX | (Dominguez-Cuevas et al., 2013) |
| LytE | 37 | E | Autolytic enzyme. Export of LytE has been suspected to regulated by MreBH | (Carballido-Lopez et al., 2006) |
| FtsE | 25 | C | ABC-transporter (ATP-binding protein). With FtsX regulates CwlO. Suspected to be controlled specifically by Mbl | (Dominguez-Cuevas et al., 2013) |
| FtsX | 32 | I | ABC-transporter (membrane protein). With FtsE regulates CwlO. Suspected to be controlled specifically by Mbl | (Dominguez-Cuevas et al., 2013) |
| PBP 1 | 99 | E | Major bifunctional PBP. Important for both cell elongation and division | (Kawai, Asai and Errington, 2009; Kawai, Daniel, et al., 2009; van den Ent et al., 2006) |

| | | | | |
|--------|----|---|---|---|
| PBP 2A | 79 | E | Major TPase with specific role in elongation. Partially redundant to PBP H | (Dominguez-Escobar et al., 2011; Garner et al., 2011; Kawai, Asai and Errington, 2009; Kawai, Daniel, et al., 2009; van den Ent et al., 2006) |
| PBP 2B | 79 | E | Major TPase with specific role in division | (Kawai, Daniel, et al., 2009; van den Ent et al., 2006) |
| PBP 2C | 79 | E | Bifunctional PBP with unknown function | (Kawai, Daniel, et al., 2009; van den Ent et al., 2006) |
| PBP 2D | 71 | E | Transpeptidase with unknown function | (Kawai, Daniel, et al., 2009; van den Ent et al., 2006) |
| PBP 3 | 74 | E | Accessory TPase that can rescue cell division in the absence of PBP 2B activity | (Kawai, Daniel, et al., 2009) |
| PBP 4 | 70 | E | Bifunctional PBP with unknown function | (Kawai, Asai and Errington, 2009; Kawai, Daniel, et al., 2009) |
| PBP H | 76 | E | Major TPase with specific role in elongation. Partially redundant to PBP 2A | (Dominguez-Escobar et al., 2011; Kawai, Daniel, et al., 2009; van den Ent et al., 2006) |
| PBP I | 65 | E | TPase of unknown function. | (Kawai, Daniel, et al., 2009; van den Ent et al., 2006) |
| RodA | 43 | I | PG synthesis. Possible monofunctional GTase | (Dominguez-Escobar et al., 2011; Emami et al., 2017; Meeske et al., 2016) |
| DapI | 41 | C | N-acetyl-diaminopimelate deacetylase. PG synthesis | (Rueff et al., 2014) |
| TagA | 29 | C | Teichoic acid synthesis. UDP-N-acetyl-D-mannosamine transferase | (Formstone et al., 2008) |

| | | | | |
|-------|----|---|--|---|
| TagB | 44 | C | Teichoic acid synthesis. Putative CDP-glycerol:glycerol phosphate glycerophosphotransferase | (Formstone et al., 2008) |
| TagF | 87 | C | Teichoic acid synthesis. CDP-glycerol:polyglycerol phosphate glycerophosphotransferase | (Formstone et al., 2008) |
| TagG | 32 | I | ABC transporter for teichoic acid translocation (permease) | (Formstone et al., 2008) |
| TagH | 59 | C | ABC transporter for teichoic acid translocation (ATP-binding protein) | (Formstone et al., 2008) |
| TagO | 39 | C | Teichoic acid synthesis. Undecaprenyl-phosphate-GlcNAc-1-phosphate transferase | (Formstone et al., 2008) |
| TagT | 35 | E | Transfer of anionic cell wall polymers from lipid-linked precursors to peptidoglycan | (Formstone et al., 2008) |
| TagU | 34 | E | Transfer of anionic cell wall polymers from lipid-linked precursors to peptidoglycan | (Kawai et al., 2011) |
| YvcK | 34 | C | Required for normal localization of PBP 1 | (Foulquier, Pompeo, Bernadac, Espinosa, and Galinier, 2011) |
| GpsB | 11 | C | Regulation of PBP 1 localization, especially its switch between elongation and division sites. | (Claessen et al., 2008) |
| EF-Tu | 43 | C | Translation elongation factor | (Defeu Soufo et al., 2015) |

a In addition to the above, Kawai et al. (2011) identified many additional MreB-associated proteins by pull-down mass spectrometry.

b Loc (Location): *I* - integral membrane; *E* – extracellular; *C* – cytoplasmic.

This table including all descriptions and references in the table is adopted and modified from Errington and Wu (2017).

1.4.1.2. *B. subtilis* Z-ring positioning and its regulators

Despite the fact that they are both Gram-positive bacteria, *S. pneumoniae* and *B. subtilis* differ in respect of the Min and nucleoid occlusion (NO) system, in that *B. subtilis* has these systems to position its Z-ring and the septum correctly at the midcell of its rod-shaped cell. In this context, *B. subtilis* vegetative cell division model shows remarkable similarities with *E. coli* model, except their regulation and dynamics.

1.4.1.2.1. The Min system in *B. subtilis*

In *B. subtilis*, the Min system positions the Z-ring at the septa mainly by preventing FtsZ polymerization at cell poles or elsewhere in the cell, except midcell as previously discussed. Like *E. coli*, the *B. subtilis* Min system is also known to be composed of four proteins. These are MinC, MinD, DivIVA and MinJ (**Figure 1.10**) (Muchova et al., 2017; Rowlett and Margolin, 2015). The clear distinction between *E. coli* and *B. subtilis* Min system is the DivIVA protein that is absent in *E. coli* model system, instead contain another Min variant, MinE (Raskin and de Boer, 1997). In this context, it is interesting to note that the DivIVA protein has very high affinity for sharp negative curvatures in the plasma membrane, which directs this protein towards cell poles and the developing septum (Eswaramoorthy et al., 2011; Lenarcic et al., 2009; Muchova et al., 2017; Ramamurthi and Losick, 2009; Rowlett and Margolin, 2015). Whereas MinE forms a ring and oscillates one pole to opposite while detaches MinDC complex from the plasma membrane. These differential dynamics of the two protein is a major difference between and *E. coli* and *B. subtilis*. Moreover, the exclusive structural feature of DivIVA to sense negative curvature, possibly has a great implication in those bacteria that has evolved both vegetative as well as endospore forming cell cycles. Rationally it has been presumed that this is not possible in the presence of MinE since in *E. coli* it has been reported to interacts with MinD and oscillates the MinDC complex from one pole to another as described in section 1.2.2.1. above. This pole-to-pole oscillation and short transition period over the midcell is a major disadvantage for FtsZ assembly at poles or near poles, which has been commonly observed during spore forming cell cycle and described below (Rowlett and Margolin, 2015). In

case of vegetative cell division in *B. subtilis*, following high trafficking of DivIVA molecules at cell poles and towards newly forming septum, the MinJ moves to same locations through its direct interaction with DivIVA molecules (Bramkamp et al., 2008; Marston and Errington, 1999; Marston, Thomaides, Edwards, Sharpe, and Errington, 1998; Patrick and Kearns, 2008). During this polar-specific shift, MinJ acts as an adaptor protein which connects both DivIVA and MinD and increases the population of MinD proteins at DivIVA directed poles (Szeto et al., 2002). The MinD protein anchors itself to plasma membrane of poles through its C-terminal helix (Szeto et al., 2002), while it also interacts MinC and recruits it to the same polar locations. This recruitment of MinC inhibits FtsZ assembly through their direct interaction in the same place (Bramkamp et al., 2008; Dajkovic, Lan, Sun, Wirtz, and Lutkenhaus, 2008; de Boer et al., 1991; Patrick and Kearns, 2008). This subcellular DivIVA oriented static-gradient deposition of Min proteins at the poles, stops FtsZ polymerization and subsequent Z-ring formation at, or near to the poles. Surprisingly, the similar deposition of Min proteins at septum, do not dissociate the Z-ring that has already initiated or formed, instead these proteins prevents formations of further multiple Z-rings at septum and ensures development of only one division site (van Baarle and Bramkamp, 2010). Recently, RodJ has been found to localize this Min system to midcell via an interaction with MinJ (Muchova et al., 2017).

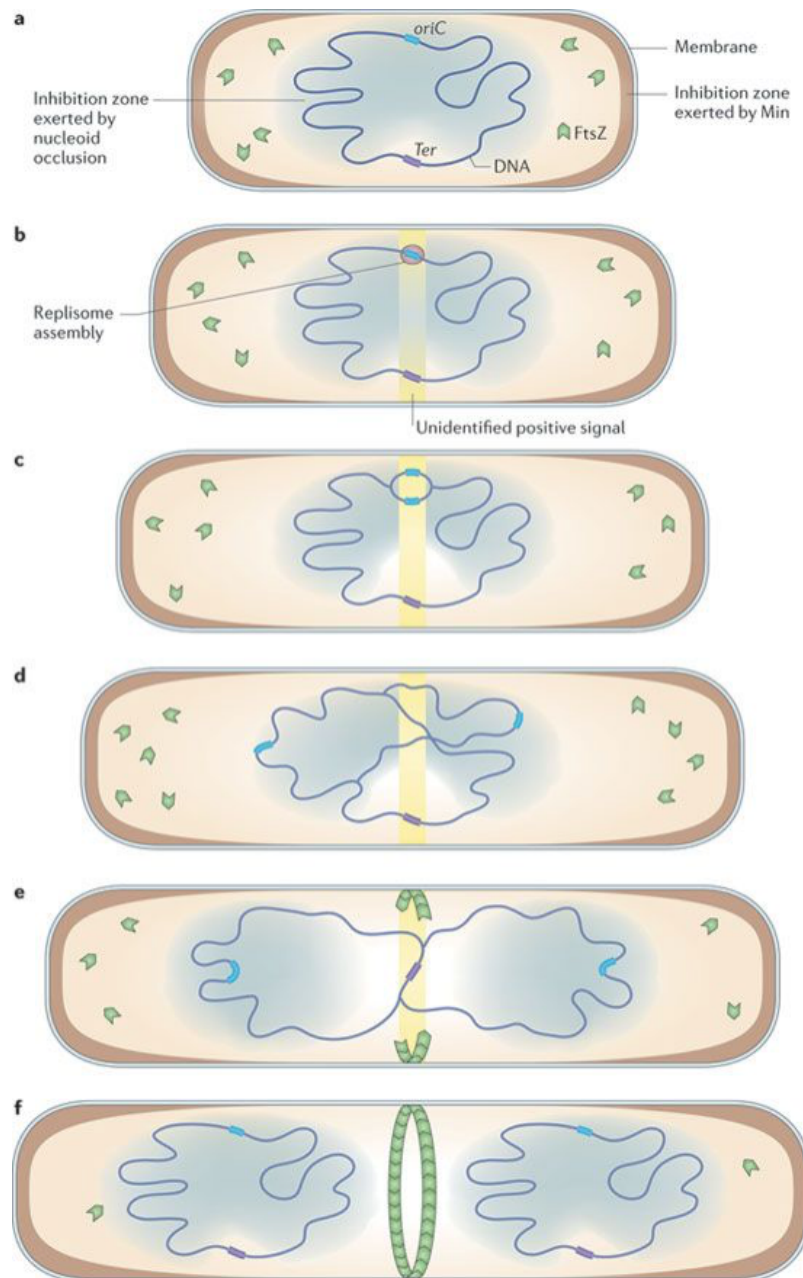


Figure 1.10. Z-ring positioning by Min system and nucleoid occlusion (NO) in *B. subtilis*.

In *B. subtilis*, the formation of Z-ring at the midcell over undivided nucleoid is prevented by the nucleoid occlusion. This occlusion executed by the nucleoid occlusion protein, Noc at midcell until chromosome segregation is complete. While the Min proteins prevent formation of Z-ring at poles or near poles (a-d). Once the replication machinery completes the chromosome segregation from oriC to near Ter region, it leaves a narrow free zone at the midcell for FtsZ to assemble (e-f).

Figure adapted from Wu and Errington (2011)

1.4.1.2.2. The Nucleoid Occlusion (NO) system in *B. subtilis*

B. subtilis NO system has a similar major role as described for *E. coli*, which prevents Z-ring assembly over nucleoid. The *B. subtilis* NO protein factor Noc was discovered around the same time as the *E. coli* NO protein factor SlmA. Despite this protein being NO protein factor and having a similar function as SlmA, the *B. subtilis* Noc is not related to SlmA, rather these two proteins are members of two different families of DNA-binding proteins, namely ParB and TetR respectively (Adams et al., 2014; Bernhardt and de Boer, 2005; Wu and Errington, 2004). The Noc also has a different mode of action in preventing FtsZ assembly over Nucleoid, compared to its *E. coli* counterpart SlmA. However, similar to other NO protein factors from different bacteria, Noc possess similar structural and functional characteristics such as - it possesses similar DNA binding motif (helix-turn-helix) that is typical for tight binding of DNA; it showed synthetic lethal cell division phenotype such as overexpression of Noc had a mild inhibitory effect on cell division, whereas Noc mutants failed to prevent abnormal Z-ring formation and thus formed septum over nucleoid, which produced guillotined nucleoid (Bernhardt and de Boer, 2005; Errington and Wu, 2017; Wu and Errington, 2004). Like SlmA, the Noc also has been found to bind very specific DNA binding sites, known as Noc binding sites (NBS) contain a signature 14 bp palindromic consensus sequence. So far, about 70 of such NBS have been identified, which ubiquitously distributed all over the chromosome except the terminal region (*Ter*) (**Figure 1.11**) (Adams et al., 2015; Errington and Wu, 2017; Wu et al., 2009).

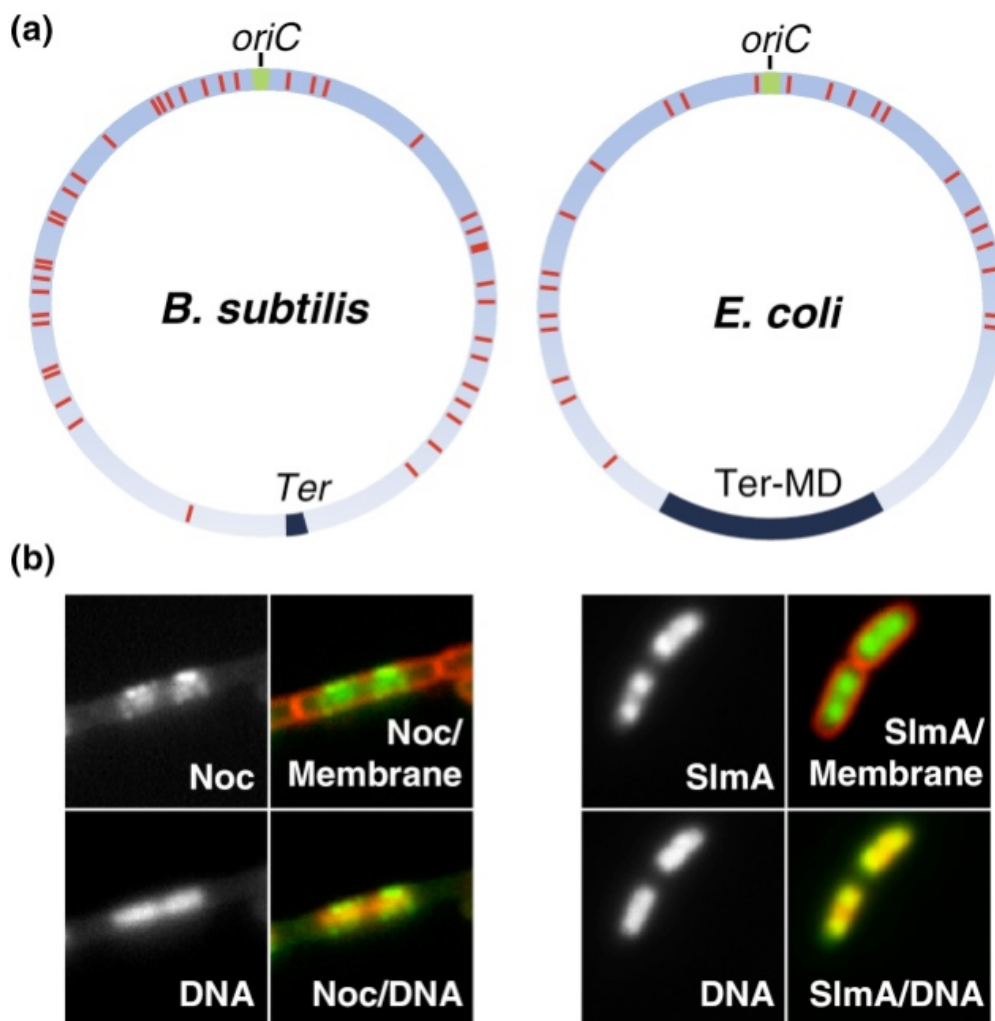


Figure 1.11. Nucleoid occlusion protein factors *Noc* and *SlmA* in *B. subtilis* and *E. coli* respectively.

Noc and *SlmA* binding sites at the *B. subtilis* and *E. coli* chromosome respectively (a); Localisation of *Noc* and *SlmA* over their respective nucleoids.

Figures adopted from Adams et al.(2014)

Noc has been hypothesized to regulate *FtsZ* assembly by a direct interaction as has been found between *E. coli* *SlmA* and *FtsZ*. However, no such direct evidence has been reported as yet, except for evidence where deletion or overexpression of *Noc* caused defective Z-ring formation and effected cell division as mentioned above (Wu and Errington, 2004). *Noc* has been presumed to prevent Z-ring formation over nucleoid by assembling *Noc* proteins around its NBS where it also attaches the plasma membrane, which in turns restricts *FtsZ* assembly to its surrounding NBS regions (Adams et al., 2015; Errington and Wu, 2017) (Figure 1.12). Very recently,

another sporulation related ParB-like protein Spo0J has been identified to have similar role as Noc to prevent Z-ring over nucleoid (Hajduk et al., 2019).

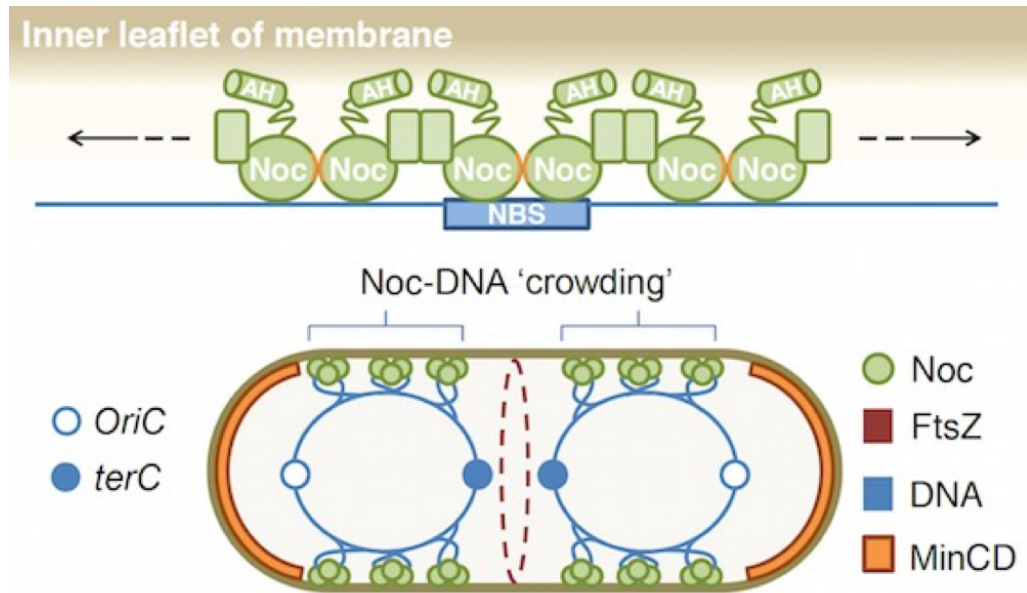


Figure 1.12. A proposed mechanism of Nucleoid occlusion protein, Noc in positioning Z-ring at mid-cell in *B. subtilis*.

The model hypothesises that the membrane attachment of Noc protein (via an N-terminal amphipathic helix) while binding to DNA bring the chromosome close the plasma membrane and block formation of Z-ring in close proximity. Whereas, the membrane attachment of MinCD complex blocks attachment of Z-ring assembly at the plasma membrane near pole regions. Figure adopted from Adams et al. (2015)

1.4.1.2.3. EzrA, is one of the major regulators of Z-ring positioning in *B. subtilis*

With the exception of the Min and NO system, *B. subtilis* has common divisome regulators systems to other Gram-positive bacteria like *S. pneumoniae*. One of such regulators, is EzrA protein. Although there is low primary sequence conservation across species, the EzrA proteins from a variety of species share common features including an N-terminal membrane anchor which leads into three to five coiled-coil motifs and lastly a patch of highly conserved residues in the C-terminus, termed as the QNR motif which has been shown to be essential for EzrA function in *B. subtilis* (Adams et al., 2014; Haeusser et al., 2007). EzrA is very common across Gram-

positive bacteria and shows two distinct arrangement of subcellular localization. In *B. subtilis*, EzrA has been observed to be distributed uniformly across the cell membrane before the cell division event, but once the division proceeds the concentration of EzrA molecules shift more towards midcell and coordinate the Z-ring at the septum (Levin, Kurtser, and Grossman, 1999). Moreover, depletion of EzrA in *B. subtilis*, showed additional Z-ring accumulation at the cell poles along with the one at midcell. This suggest one of the main roles of EzrA is to prevent any abnormal Z-ring assembly at the cell poles (Levin et al., 1999) in favour of the midcell. In *B. subtilis*, EzrA was found to anchor in the cytoplasmic side of the membrane possibly through its N-terminal transmembrane domain while rest predicted coiled-coil domains the QNR region trails in cytoplasm (Haeusser et al., 2007). However, mutants in the QNR motif did not lose their ability to prevent FtsZ assembly at cell poles as well as when assayed *in-vitro* (Haeusser et al., 2007). Similar *in-vitro* assays and further domain specific analysis confirmed an interaction between EzrA and FtsZ and suggested the first two coiled-coils domains are necessary to prevent the FtsZ assembly at cell poles, however the direct or indirect mechanism behind this event has not been understood clearly (Land, Luo, and Levin, 2014). Additionally, the EzrA protein has been found to interact with several other division proteins including FtsA, GpsB and PBPs at the divisome site (Claessen et al., 2008; Egan et al., 2017). This clearly indicates the role of EzrA is not just limited to correct positioning of Z-ring at the midcell, rather it has much more complex regulatory roles to wider divisome protein network associated with several division machineries (Claessen et al., 2008; Gamba et al., 2015; Muchova et al., 2017).

1.4.1.3. *B. subtilis* divisome complexes, their assembly and roles during septation and cell separation

Similar to other rod-shaped bacteria *E. coli*, cell division in *B. subtilis* is commenced by the formation of a Z-ring and assembly of a multiprotein complex, the divisome. As described before, one of the key and essential elements of this divisome is FtsZ protein and more precisely its GTP-dependent manner of polymerisation to form the Z-ring at the midcell. The *B. subtilis* divisome is not

exceptional and the Z-ring made of FtsZ protofilaments have been observed at midcell during vegetative cell division (Levin and Losick, 1996; Wang and Lutkenhaus, 1993). Like Gram-positive *S. pneumoniae*, the essential core *B. subtilis* divisome network includes cytoskeleton proteins such as FtsZ and FtsA (Beall, Lowe, and Lutkenhaus, 1988; Beall and Lutkenhaus, 1991; Feucht et al., 2001; Jensen, Thompson, and Harry, 2005; Wang and Lutkenhaus, 1993); Z-ring associated protein ZapA (Gueiros-Filho and Losick, 2002); some Z-ring and cell wall regulatory proteins EzrA and GpsB (Claessen et al., 2008; Haeusser et al., 2004; Levin et al., 1999; Tavares et al., 2008); a series of Fts bitopic membrane proteins such as DivIB/FtsQ (Beall and Lutkenhaus, 1989; Katis and Wake, 1999), DivIC/FtsB (Katis, Harry, and Wake, 1997), FtsL (Daniel and Errington, 2000; Daniel et al., 1998), FtsW (Lu, Takeuchi, and Sato, 2007) and associated PG synthase PBP2b (Yanouri et al., 1993) and an additional cell division protein DivIVA (Edwards and Errington, 1997) (**Table 1.3**) (**Figure 1.13**). Apart from these a synthetically lethal FtsZ-interacting protein SepF also found necessary for the proper function of Z-ring and mutant of this was shown to affect at the septum constriction (Hamoen et al., 2006).

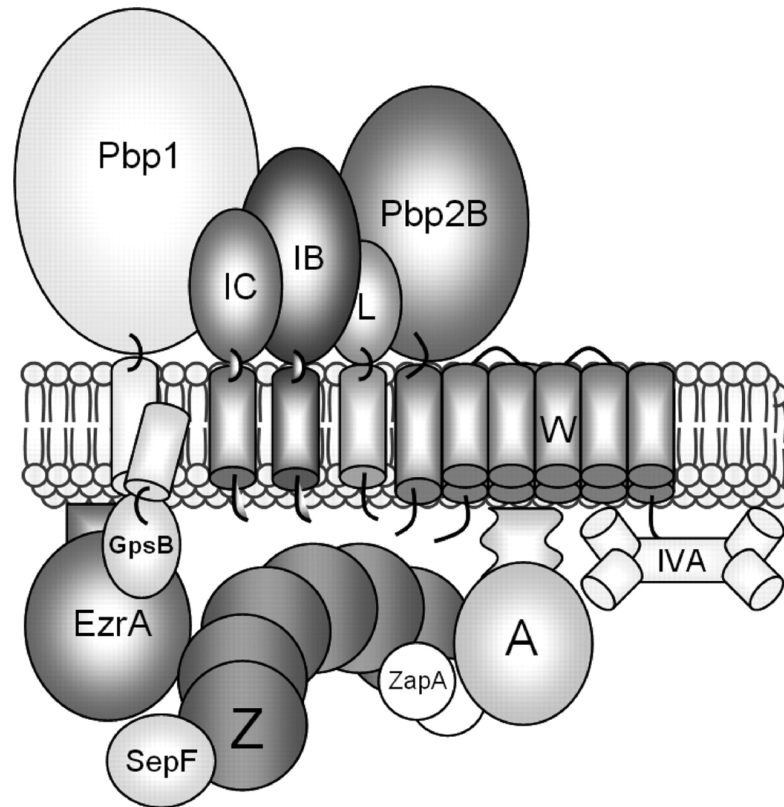


Figure 1.13. *B. subtilis* divisome assembly.

Schematic representation of divisome assembly with known proteins in B. subtilis. Z: FtsZ; A: FtsA; IC: DivIC; IB: DivIB; L: FtsL; W: FtsW; IVA: DivIVA. Remaining proteins in the picture represents proteins as per their abbreviation.

Figure adopted from Gamba et al. (2009)

Rod shaped *B. subtilis* and *E. coli* both have comparable divisome components except that the latter is equipped with additional components which are particularly involved in PG hydrolysis and outer membrane invagination process. However, the most fascinating difference between the two divisomes is how they assemble and are regulated (Errington, 2003; Hamoen et al., 2006). In this context *B. subtilis* has many similarities with the divisome of its Gram-positive counterpart *S. pneumoniae* though they too have differences in essentiality of some divisome components like FtsA, and with components involved in PG hydrolysis machinery such as FtsEX. Unlike *E. coli* and *S. pneumoniae*, *B. subtilis* Z-ring assembly does not depend on other divisome proteins including FtsA and other core divisome proteins. Depletion of core divisome proteins such as FtsA, DivIC, FtsL or PBP2b does not affect FtsZ polymerization but some mutants failed to assemble the whole

divisome recruiting other divisome proteins at the septum (Errington, 2003). This indicated the *B. subtilis* divisome most probably does not follow the simple sequential linear hierarchical assembly, as can be observed in *E. coli*. Instead *B. subtilis* has evolved a cooperative network to assemble the whole divisome.

In *B. subtilis*, following the formation of Z-ring, the FtsA appears at the midcell Z-ring at an early stage and tethers the Z-ring to the cytoplasmic membrane (Jensen et al., 2005). The ratio of these two molecules at the Z-ring was proposed to be critical for cell division to occur (Dai and Lutkenhaus, 1992; Dewar, Begg, and Donachie, 1992; Lara et al., 2005). FtsA has been reported essential in *E. coli*, *S. pneumoniae* (Lutkenhaus and Donachie, 1979) and *C. crescentus* (Sackett, Kelly, and Brun, 1998), depletion of FtsA was not tolerated in the above bacterial species. However, the same deletion in *B. subtilis* was tolerated albeit with severe growth impairment, low viability, and formation of spores (Beal and Lutkenhaus, 1992; Lara et al., 2005). Interestingly, SepF has been found to bypass the requirement of FtsA in *B. subtilis*, suggest a similar role in tethering and stabilizing the Z-ring (Gamba et al., 2009; Hamoen et al., 2006; Ishikawa et al., 2006). Deletion of SepF caused reduced cell division frequency and abnormal morphology but has no effect on Z-ring assembly (Hamoen et al., 2006). The same protein also reported as synthetically lethal with EzrA (Hamoen et al., 2006). As discussed, EzrA plays an important role in positioning the Z-ring to the midcell septum as described above (1.4.1.2.3.). Interestingly, despite having similarities in unusual structural topology between EzrA and ZipA (that is essential to *E. coli*), they are not related in sequence or belongs to same protein family. Another important cell division regulatory protein in *B. subtilis*, the GpsB is involved in regulating both elongasome and divisome machineries. It is a DivIVA-related protein and interact with one of the major PG synthases PBP1 during elongation and shuttle it between elongation and divisome complexes during the cell cycle progression (Claessen et al., 2008). GpsB has been found synthetically lethal in combination with *ftsA* mutation and synthetically sick in combination with *ezrA* mutation (Claessen et al., 2008; Errington and Wu, 2017; Tavares et al., 2008). Once Z-ring tethered to the inner wall of cytoplasmic membrane the ZapA directly interact FtsZ

and start endorsing further Z-ring assembly (Gueiros-Filho and Losick, 2002) upon which other late cell division divisome proteins FtsL, DivIB (FtsQ), DivIC (FtsB), and all PG synthesis machinery consists of FtsW and PBP2b. All these are mainly bitopic membrane proteins and interact both cytoplasmic and extra-cytoplasmic partners, which transverse the signals between cytoplasmic and extra-cytoplasmic events. These divisome proteins are thought to interact and assemble to larger complex through complex network that is still elusive, except DivIC (FtsB) has been found to interact FtsL directly (Daniel et al., 2006). These proteins are predicted to play similar roles as described in *E. coli* and *S. pneumoniae* models above. Perhaps one of notable differences between *E. coli* and *B. subtilis* divisome is the absence of DNA translocase protein FtsK. Instead, *B. subtilis* employ two cytoplasmic DNA translocase proteins SpoIIIE and SftA, to perform the dimer resolution for successful chromosome segregation and move the segregated monomeric chromosome away from each other (Kaimer, Gonzalez-Pastor, and Graumann, 2009; Kaimer, Schenk, and Graumann, 2011). Lacking both these proteins had more severe consequences and showed chromosome segregation defect than their individual depletion, which suggest their coordinated function in chromosome segregation and translocation to daughter cells (de Sousa Borges, 2017; Kaimer et al., 2009; Kaimer et al., 2011) . In this context, it is also important to note that the *B. subtilis* strain lacking all four major class A PBPs are still viable with normal phenotype and cable of synthesizing PG. This indicates *B. subtilis* class B PBPs possibly play a major role in PG synthesis (McPherson and Popham, 2003). Therefore, a well-known sPG synthesis machinery composed of FtsW and PBP2b is very significant in *B. subtilis* cell division, and its regulation has been found to directly coupled with FtsZ treadmilling, the action which colocalize both FtsW and PBP2b at septum thus regulate their synthases activity (Bisson-Filho et al., 2017; Taguchi et al., 2019).

Table 1.3. Proteins of the *B. subtilis* divisome and its regulators.

| Protein | MW (kDa) | Loc^a | Comments | Key references |
|----------------|---------------------|------------------------|--|--|
| FtsZ | 40 | C | Tubulin-like protein. Assembles into protofilaments and higher order structures to generate the “Z ring” at the division site. Recruits other divisome proteins to the ring. | (Beall et al., 1988; Beall and Lutkenhaus, 1991; Wang and Lutkenhaus, 1993) |
| FtsA | 48 | C | Actin / HSP70 superfamily ATPase. Dimerises and can form higher order structures. C-terminal amphipathic helix promotes membrane association. Direct interaction with FtsZ, which contributes to membrane association of the Z ring. | (Beall et al., 1988; Feucht et al., 2001; Ishikawa et al., 2006; Jensen et al., 2005) |
| SepF | 17 | C | Forms regular 50 nm diameter rings in vitro and interacts directly with FtsZ in vitro, promoting FtsZ bundling. Membrane targeting domain contributes to membrane association of the Z ring. | (Gundogdu et al., 2011; Hamoen et al., 2006) |
| ZapA | 9 | C | Widely conserved protein that promotes Z ring formation by direct interaction with FtsZ. | (Gueiros-Filho and Losick, 2002) |
| EzrA | 65 | C | N-terminal transmembrane anchor. Cytosolic domain has a spectrin-like fold. Interacts with FtsZ, contributing to membrane association of the Z ring. Additional role in cell elongation via interactions with PBP 2B and GpsB. | (Claessen et al., 2008; Cleverley et al., 2014; Haeusser et al., 2004; Levin et al., 1999) |
| GpsB | 11 | C | DivIVA-related protein involved in both cell elongation and cell division. Interacts with the major PG synthase, PBP 1, and thought to be involved in shuttling of this protein between elongation and division complexes. | (Claessen et al., 2008; Tavares et al., 2008) |

Synthetic lethal in combination with *ftsA* mutation. Synthetic “sick” in combination with *ezrA*. *EzrA*-*SepF* interaction probably important for shuttling.

| | | | | |
|-------|----|---|---|---|
| FtsL | 13 | E | Bitopic membrane protein with short extracytoplasmic coiled-coil-like domain. Target of several cell division regulatory mechanisms. Unstable protein subject to degradation by a regulated intramembrane proteolysis (RIP) process involving YluC protease. Stability also regulated by interactions with DivIC and DivIB. | (Bramkamp et al., 2006; Daniel and Errington, 2000; Daniel et al., 1998; Daniel et al., 2006; Yoshikazu Kawai and Ogasawara, 2006; Sievers and Errington, 2000a, 2000b) |
| DivIB | 30 | E | Bitopic membrane protein with large extracellular domain. Structural data from other organisms suggests two domains, one of which resembles the POTRA domain often involved in protein interactions. Complex pattern of interactions with FtsL and DivIC. Homologue called FtsQ in <i>E. coli</i> . | (Beall and Lutkenhaus, 1989; Daniel and Errington, 2000; Daniel et al., 2006; Katis and Wake, 1999; Katis, Wake, and Harry, 2000) |
| DivIC | 15 | E | Bitopic membrane protein with short extracytoplasmic coiled-coil-like domain. Interacts with FtsL and DivIB. Likely homologue confusingly called FtsB in <i>E. coli</i> . | (Daniel and Errington, 2000; Katis et al., 1997; Katis and Wake, 1999; Katis et al., 2000; Robson et al., 2002; Sievers and Errington, 2000b) |
| FtsW | 44 | I | Integral membrane protein closely related to RodA involved in cell elongation. | (Lu et al., 2007) |

| | | | | |
|--------|----|-------|---|---|
| Pbp2B | 79 | E | Penicillin binding protein. Monofunctional (class B) transpeptidase specifically required for cell division. | (Daniel and Errington, 2000; Daniel, Williams, and Errington, 1996; Yanouri et al., 1993) |
| DivIVA | 19 | C | Coiled coil protein with weak similarity to eukaryotic tropomyosins. Targeted to division sites and cell poles at least in part by sensing membrane curvature. Membrane interaction through conserved N-terminal domain containing essential tryptophan residue. Involved in a range of cell pole associated functions in Gram positive bacteria. | (Cha and Stewart, 1997; Edwards and Errington, 1997; Hamoen and Errington, 2003; Lenarcic et al., 2009; Ramamurthi and Losick, 2009; van Baarle and Bramkamp, 2010) |
| MinC | 25 | C | Widely conserved division inhibitor acting on FtsZ and possibly other steps in division. | (Gregory, Becker, and Pogliano, 2008; Levin et al., 1992; Marston and Errington, 1999; Reeve et al., 1973) |
| MinD | 29 | C | Widely conserved indirect division inhibitor that works by spatial regulation of MinC protein. Poorly characterised additional role in chromosome segregation during sporulation. | (Levin et al., 1992; Marston and Errington, 1999; Reeve et al., 1973) |
| MinJ | 44 | I / C | PDZ-domain protein targeted to cell poles by interaction with DivIVA (at least). Required for correct spatial localization of the MinCD complex and thus the regulation of cell division. | (Bramkamp et al., 2008; Patrick and Kearns, 2008; van Baarle and Bramkamp, 2010) |
| Noc | 33 | C | Site-specific DNA binding protein. Inhibitor of division. Major factor effecting nucleoid occlusion. | (Adams et al., 2015; Wu and Errington, 2004; Wu et al., 2009) |

| | | | | |
|--------|----|-----|--|--|
| WhiA | 36 | C | Enigmatic nucleoid associated factor. whiA mutation causes severe filamentation when combined with zapA, ezrA or various regulatory proteins of cell division. | (Surdova et al., 2013) |
| SpoIIE | 92 | C/I | Bifunctional sporulation-specific protein. C-terminal kinase domain regulates prespore-specific gene expression. C-terminal domain required for efficient switch in cell division position from mid cell to sub-polar position, probably via a direct interaction with FtsZ. | (Arigoni et al., 1995; Bradshaw and Losick, 2015; Carniol et al., 2005; Feucht et al., 2001; Lucet et al, 2000; Wu, Feucht, and Errington, 1998) |
| MciZ | 4 | C | Mother cell-specific inhibitor of FtsZ assembly. Captures FtsZ protofilaments at the “minus” end. | (Bisson-Filho et al., 2017; Handler, Lim, and Losick, 2008) |
| RefZ | 24 | C | Site-specific DNA-binding protein that contributes to precise relative positioning of chromosome and asymmetric division site during sporulation. | (Miller et al., 2016; Wagner-Herman et al., 2012) |

Loc^a (Localisation): C: cytosolic; I integral membrane; E: extracytoplasmic.

This table including all descriptions and references in the table is adopted and modified from Errington and Wu (2017)

1.4.2. Asymmetric cell cycle and sporulation of *B. subtilis*

B. subtilis is mainly a soil dwelling bacterium and sporulation in *B. subtilis* is largely triggered by nutrient stress or harsh surrounding environmental conditions. The *B. subtilis* endospore is one of the toughest spores compared to those from actinomycetes or other spore-forming bacteria such as *Clostridium spp.* and myxobacteria. Like most spore forming bacteria, *B. subtilis* cell also employ an altered and unusual mechanism that drives the cell towards an asymmetric cell division and ends with formation of endospore following chromosome segregation. The asymmetric cell division creates two obvious different size cells which are genetically identical. One is a much smaller cell, named as Prespore or Forespore, and the other larger cell named as Mother or Sporangium. Following this asymmetric division, the mother cell shows an altruistic behaviour and engulf the prespore. However, this altruistic behaviour has unusual outcome that actually helps the prespore gaining extra protective layers or coats over cellular membrane. This is a highly coordinated complex developmental process by which prespore enter into a dormant endospore state and mother cell trigger a programmed cell lysis (Tan and Ramamurthi, 2014). Formation of dormant endospore is a remarkable adaptation and strategy to protect its genome until access to favourable growth condition. The protective layers are extremely resistant to very harsh condition such temperature as high as 100 °C, several chemical solvents, detergents, several hydrolytic enzymes (Errington, 2003; Nicholson et al., 2000). As a result, endospores become extremely resilient to harsh conditions as well as in food/nutrient deprivation and can survive for years (Errington, 2003; Errington and Wu, 2017).

1.4.2.1. Formation of *B. subtilis* endospore

There are several mechanisms and steps that are involved in successful of sporulation. An early observation of endospore formation explored various morphological landmarks during the sporulation, which are still considered as classical representation of different stages of development (Tan and Ramamurthi, 2014). However, these stages are not a representation of a linear or sequential

mechanism. Instead, recent progress in this field suggests some of these stages possibly overlap. Details of each stage and its regulators are reviewed in detail in Tan and Ramamurthi, 2014. Here we present a brief overview of the sporulation process (**Figure 1.9**).

At the very initial stage of chromosome replication (stage 0), cell alters vegetative growth pathway to asymmetric division under nutrient stress condition. This alteration is controlled by a master transcription factor Spo0A that also govern the biofilm formation process (Hamon and Lazazzera, 2001). Spo0A is activated by five histidine-kinase sensors consisting KinA, KinB, KinC, KinD and KinE. These kinases respond to several environmental and nutritional stresses (LeDeaux, Yu, and Grossman, 1995) and send a signal to transcription factor regulators via phosphorylation (McKenney and Eichenberger, 2012). This phosphorylation helps Spo0A to regulate gene expressions in a wide span that includes gene responsible for asymmetric cell division and activation of RNA polymerase subunits sigma factors σ^E and σ^F , which are related to mother and prespore respectively (Kennedy, Reader, and Swierczynski, 1994). A higher level of Spo0A phosphorylation is associated to Spore formation cycle while a lower level of phosphorylation related to Biofilm formation (Tan and Ramamurthi, 2014). Interestingly, the interaction between FtsEX-CwlO in *B. subtilis* has been proposed to regulate the function of phosphorelay cascade located at the upstream of *spo0A* and possibly helps maintaining a high level of phosphorylated Spo0A to initiate sporulation (Garti-Levi et al., 2008; Meisner et al., 2013)

In stage I, the chromosome starts condensing, replicating and anchors the origin of replication at the cell poles. A protein known as RacA is responsible for such anchoring. RacA binds to GC-rich inverted repeats at surrounding regions of the origin of replication (*oriC*) and localizes to cell poles through an interaction between RacA and DivIVA, where the latter is a cell pole or negative membrane curvature sensing protein in *B. subtilis* (Ben-Yehuda et al., 2005; Ben-Yehuda, Rudner, and Losick, 2003).

In stage II, the transition from symmetric medial septation to asymmetric septation takes place. This transition is mostly regulated by two major factors. These factors are production and localization of a DNA translocase SpoIIE protein and an overproduction of FtsZ. The former protein has been predicted to have role in translocating and condensing a large part of chromosome into small forespore; additionally, the same protein under transcriptional control of Spo0A, also administers the spiral movement of FtsZ away from midcell, towards cell poles (Levin and Losick, 1996; Tan and Ramamurthi, 2014). Following this asymmetric septation, the forespore/prespore specific sigma factor σ^F becomes activated. However, the mechanism of this activation is not understood and it is presumed that the activation is related to the presence of SpoIIE which preferentially localises to forespore/prespore side (Guberman et al., 2008). Hence, the SpoIIE has been identified as an essential element in *B. subtilis* sporulating septum and helps in activating σ^F . Very recently, Muchova et al. (Muchova et al., 2017) has shown that the SpoIIE interacts with RodZ and plays active roles in *B. subtilis* vegetative cell elongation, by regulation of PG synthesis machinery and Z-ring positioning regulators (MinJ) (Muchova et al., 2013; Muchova et al., 2017). Simultaneously, the other mother cell-related sigma factor σ^E also becomes activated through a complex mechanism that involves other DNA translocases SpoIIGA and SpoIIR (Pedrido et al., 2013).

In Stage III, which is associated with engulfment of the forespore, the process is initiated via a PG degradation machinery consisting of SpoIID, SpoIIM and SpoIIP. Together these proteins start thinning the extracytoplasmic space by partial degradation of PG layers, whilst new synthesis of PG successively helps in movement of membrane and action of engulfment (Meyer et al., 2010; Tocheva et al., 2013). Following engulfment, the inner membrane of the forespore gets sealed by a proposed ratchet like mechanism mediated through a tight interaction of two proteins from each cell at the intermembrane space. These proteins are, mother cell-specific SpoIIAH and forespore specific SpoIIQ (Broder and Pogliano, 2006). In a subsequent step, the mother cell detaches its membrane by a process known as membrane fission. The FisB that has been identified specifically in the mother cell,

helps in membrane fission by promoting membrane remodelling presumably by interacting cardiolipin at the membrane with leading edges, which disrupt both leading edges and thus membrane fission (Doan et al., 2013; Tan and Ramamurthi, 2014). At the end of engulfment, localization and action of SpoIIAH and FisB (controlled by σ^E) and SpoIIQ (controlled by σ^F) at intermembrane space ensures a complete of compartmentalization of two cells, which activate another sigma factor σ^G . This sigma factor is specific to forespore and it is under transcriptional control of σ^F . The latter does not activate σ^G until and unless the forespore is compartmentalized. Because actions of σ^G are solely related to the further development of endospore, and nothing to mother cell. Activation of σ^G also induces activation last sigma factor σ^K in the mother cell. Hereafter, activation of σ^G and σ^K downregulate and replace their predecessors σ^E and σ^F in mother and forespore cell respectively (Fimlaid and Shen, 2015) (**Figure 1.14**).

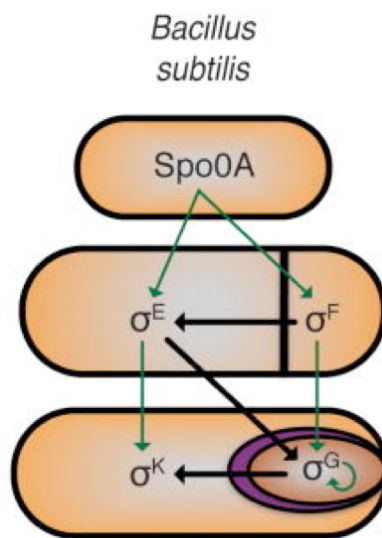


Figure 1.14. Regulatory network of Sigma factors during of *B. subtilis* sporulation

See main text for details. Figure adopted from Fimlaid and Shen (2015)

In the next two stages (IV and V) the forespore assembles two distinct shells around its inner cell membrane. The inner shell, known as the cortex and the outer is known as the coat (**Figure 1.15**). The cortex comprised of a special type of PG (Henriques and Moran, 2007) and the coat is composed of as many as 70 different proteins (McKenney, Driks, and Eichenberger, 2013). The coat formation on the

outer surface of forespore organized by mother cell-specific proteins SpoVM and SpoIVA, which identify the forespore membrane surface following its positive membrane curvature (Ramamurthi and Losick, 2009). Synthesis of cortex PG follows the similar mechanism as vegetative cell wall PG synthesis, and SpoVB and SpoVE both have been suspected to play similar roles as the Lipid II flippase. SpoVB and SpoVE were identified as sporulation specific homologues of *E. coli* MurJ and FtsW, which showed flippase activity *in-vivo* and *in-vitro* analysis respectively (Mohammadi et al., 2011; Sham et al., 2014). Last two stages are dedicated to endospore maturation and mother cell lysis through a programmed cell death pathway which releases the mature endospore in the outer environment (Tan and Ramamurthi, 2014).

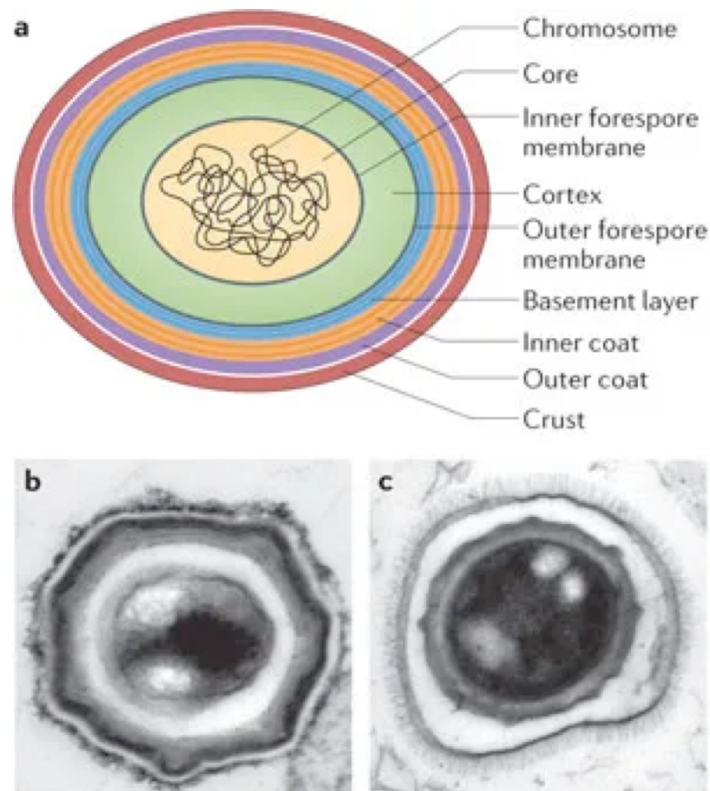


Figure 1.15. The *B. subtilis* Endospore.

Cartoon of a typical *Bacillus subtilis* spore showing multiple layers of the spore (a). The transmission electron micrograph (TEM) below the cartoon images, shows thin section of a *B. subtilis* spore (stained with ruthenium red) (b) and a thin section of a *Bacillus anthracis* spore (stained with osmium tetroxide) (c).

Figure adopted from McKenney et al. (2013)

1.4.2.2. Germination of *B. subtilis* endospore

Cells in the endospore form, stay dormant and metabolically inactive for extremely long periods of time, and the germination this endospore is possibly triggered by access to nutrients that favourable vegetative growth (Setlow and Johnson, 2007) (**Figure 1.9**). The germination process is still largely unknown. It is proposed to start with sensing specific nutrients or germinants such as L-alanine, D-glucose, D-fructose and potassium ions (AGFK) as identified with *B. subtilis* model (Pelczar et al., 2007). These nutrients bind to specific inner membrane receptors of endospore, known as germination receptor (GRs). In *B. subtilis*, three such GRs are identified which are GerA, GerB and GerK. Binding of specific nutrients to these receptors rerelease certain chemical signal to subsequent germination steps which eventually hydrolyse of cortex (Wang et al., 2011). In another study, release of Ca^{2+} with dipicolinic acid (CaDPA) during germination of *B. subtilis* with alteration in germination related proteins SpoVA and GerD, indicated CaDPA possibly play an important role to trigger subsequent germination steps. Some chemical agents such as cationic surfactant dodecylamine has also found to trigger germination that is independent of any GRs and GerD mediated pathway (Wang et al., 2011). Hydrolysis of cortex following CaDPA mediated germination and cortex hydrolases, influence expansion of core and further hydration and (Wang et al., 2011).

1.5. *Streptococcus pneumoniae* as pathogen and organism specific issues in AMR

Streptococcus pneumoniae (*S. pneumoniae*) is an ovoid-shaped, Gram-positive anaerobe. It is a highly adapting non-motile, non-spore forming pathogen. Recently, the World Health Organisation (WHO) has listed *S. pneumoniae* as a priority pathogen requiring new antibiotic development to combat antibiotic resistant strains, along with *Escherichia coli*, *Pseudomonas aeruginosa*, *Staphylococcus aureus* (Massidda et al., 2013; O'Brien et al., 2009). *S. pneumoniae* is responsible for many deadly diseases including meningitis, sinusitis and otitis, sepsis, osteomyelitis and brain abscess (Shak, Vidal, and Klugman, 2013), which estimated to cause almost 1.6 million deaths per year world-wide (Massidda et al., 2013). This pathogen mostly attacks children younger than 5 years old and adults 65 years or older (O'Brien et al., 2009). As a Gram-positive species, the cell wall of *S. pneumoniae* is composed of thick layers of peptidoglycan and teichoic acid, which provide tight integrity to rigid PG layers at the cell wall. With the discovery of penicillin, the mortality rate to many bacterial pathogens sharply decreased during 1940's, however the mortality rate gradually increased since the first report of penicillin resistance and chloramphenicol resistance in pneumococci in 1967 (Hansman and Bullen, 1967) followed by major outbreaks of pneumococcal disease in South-Africa in during 1970's (Appelbaum et al., 1977; Jacobs et al., 1978). A serious spreading of these resistant strains and several other clinical isolates become tolerant to many commonly prescribed antibiotics, worsening human healthcare worldwide, particularly in underdeveloped countries (Sham et al., 2012), and when coupled with immune-compromised and HIV individuals (Klugman, 2011; Massidda et al., 2013). This alarming rise in resistant pneumococcal pathogens and an increase in death tolls in pneumococcal disease caused by these pathogens, call for immediate urgency to step in and make all efforts to explore new targets to develop new vaccines and/or new classes of antibiotics (Massidda et al., 2013; Sham et al., 2012).

1.6. The divisome as a target for new antibiotics.

Anti-microbial resistance is a process whereby microbes evolve targeted mechanisms and associated proteins in order to be able to resist the action of that natural antimicrobials or antibiotic drugs. Since the discovery of penicillin and other antibiotics, human and animal healthcare has been with modern drugs which able to treat serious bacterial infections. However, excessive use, and misuse of these antibiotics provides a selection pressure on microbes to develop natural resistance mechanism faster than ever before. This situation has led AMR to be acknowledged as an international crisis and O'Neill's report (2016) has predicted there will be 10 million deaths due to AMR by 2050, which would be more than the deaths due to any other deadly disease including cancer (O'Neil, 2016). The same report pointed out and described several serious concerns related to emergence of multi-drug resistant superbugs, which urge for the immediate action for exploring novel antibacterial target compounds.

Current classic targets for most clinically approved main classes antibiotics, are being involved in cell wall biosynthesis, protein synthesis, DNA/RNA replication mechanisms and folate coenzyme biosynthesis (**Figure 1.16**) (Sass and Brotz-Oesterhelt, 2013; Walsh, 2003). Among other possible mechanisms the isoprenoid biosynthesis pathway and cell surface receptors (particularly for Gram-positive bacteria) have gained significant interest for finding new targets. However, in recent years more research focusing into the mechanisms involved in bacterial cell division which is intimately involved with cell wall biosynthesis. Particularly, divisome proteins are gaining more acceptance as ideal candidates for potential drug targets, because a vast majority of these proteins are essential in cell division and conserved across bacterial species. Additionally, a vast majority of them are absent in eukaryotic cells, which possibly suggests if any antibiotic is made targeting these proteins, the side-effects of drug toxicity would possibly be minimal in human or other animals. Therefore, any natural or synthetic inhibitors to these divisome proteins could possibly lead to discovery of a new class of antibiotic.

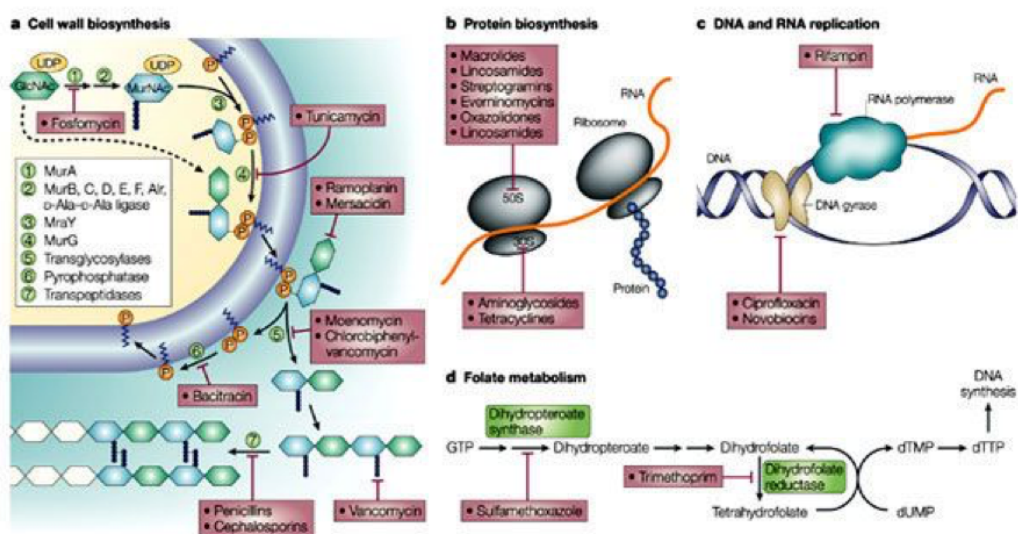


Figure 1.16. Classic targets for antibiotics.

Cell-wall biosynthesis includes the intracellular steps of PG biosynthesis. Many existing β -lactam group of antibiotics targets the PG synthesis enzymes (a); Protein biosynthesis includes bacterial ribosomes which are the prime targets of many current antibiotics (b); Another class of antibiotics targets the components of DNA and RNA replication machineries and prevents transcription (c). Few other classes target the components of Folate metabolism pathways that involves in synthesising thymine, an essential element of DNA (d).

Figure adopted and modified from Walsh (2003)

From an existing antimicrobial database, many antibiotics are known including those which directly target peptidoglycan biosynthesis including beta(β)-lactams, glycopeptides and other natural product inhibitors of lipid II. However, many of these classes of antibiotics are becoming ineffective and useless due to development of resistance against these antibiotics by bacteria, such resistance against β -lactams and urgent need for alternate new targets, are discussed in Chapter 6. Whilst these are not formally acknowledged as inhibitors of cell division, a recent understanding of the interplay of the cell division proteins (e.g. FtsZ, FtsA, RodA, FtsW etc.) with cell wall biosynthesis may need to be revised in respect of the interaction of these with proteins required for peptidoglycan biosynthesis. For example, with reference to *E. coli* nomenclature, the FtsW-PBP3 complex (Wang et al., 1998; Yang et al., 2017) is now widely acknowledged as a major core of the divisome along with PBP1b (Bertsche et al., 2006). In addition, the RodA-PBP2 complex is the core of the “machine” responsible for cell elongation. Inspection of the affinities of most

clinically used β -lactams shows that they preferentially target either PBP3 or PBP2 and therefore the cell division or cell elongation processes they are responsible for, is necessary to investigate in detail. With respect to the divisome, these proteins are clearly closely linked with other proteins that are more traditionally associated with cell division including FtsQLB and FtsEX, which have roles in operating macromolecular machineries involved in sPG synthesis and sPG hydrolysis, respectively (see section 1.2.3.). Among all known divisome proteins FtsZ has been examined most as a possible target of existing or new classes of antibiotics. Several natural or synthetic FtsZ inhibitors have already been tested or are under investigation in order to examine their efficacy and potentiality to be successful in clinical trials. Details of those inhibitors and their mode of actions have been reviewed in many articles (den Blaauwen, Andreu, and Monasterio, 2014; Sass and Brotz-Oesterhelt, 2013). Most of these inhibitors have been found to target the GTP-dependent polymerization of FtsZ directly or indirectly through binding its associates, and in other cases via some unknown mechanism (den Blaauwen et al., 2014). Benzamide compounds have been shown to compete for the GTP pocket allosterically, which transform the FtsZ monomers to open state and stimulate the FtsZ polymerization and resulted in nucleation of multiple Z-rings assembly with its associate divisome protein complexes in *in-vivo* experiments with *Staphylococcus aureus*, but lack of divisome activity ultimately led to complete blockage of cell separation and thus further block of cell division (den Blaauwen et al., 2014; Errington and Wu, 2017; Haydon et al., 2008).

Apart from the above mentioned FtsZ polymerization process, the tethering mechanism of FtsZ via FtsA and/or ZipA interactions are in focus for developing natural or synthetic inhibitors. FtsA and ZipA interact FtsZ through its conserved C-terminal domain (Hernandez-Rocamora et al., 2012; Krupka et al., 2018; Mosyak et al., 2000). However, variability in their site of interaction across bacterial species and absence of ZipA in many bacteria and specially in Gram-positive bacteria, make this complex selective for its inhibitor screening and future application (den Blaauwen et al., 2014). Considering ATPase activities and related molecules are important for many biological functions and so for several cell division

mechanisms, this group of proteins involving in cell division, could be potential target for antibiotics. Accordingly, small molecules or peptides that targets the ATP dependent proteins in bacterial cell division or related cell wall synthesis could be potential inhibitors. The caveat to this approach is of course the ability of any such candidate drug/inhibitor molecule to enter the cell and interact with its target. Whilst nucleotide binding site drugs are well established as cancer drugs in mammalian cells, targeting kinases involved in cell signalling for example, equivalent drugs in bacterial chemotherapy are less common. Whilst coumarin based drugs (e.g. Novobiocin) target the ATPase site of bacterial topoisomerases including DNA gyrase (Maxwell, 1993) resistance to these drugs is often generated by site specific mutation.

An alternative, but related approach is provided by degradation of the Z-ring following septation by an ATP-dependent protease activity of ClpXP, is under scrutiny for potential new class of antibiotics. ClpX recognize and unfold the FtsZ C-terminal flexible domain to ClpP which in turn degrade the FtsZ polymers and therefore dissolve the ring (Alexopoulos, Guarne, and Ortega, 2012; Camberg, Hoskins, and Wickner, 2009, 2011). A class known as cyclic acyldepsipeptides or ADEP, has been found to form complex with ClpP and induce its proteolytic activity independently without cognate ClpX (M. E. Lee, Baker, and Sauer, 2010). This activity promotes random degradation of FtsZ, which appeared to cause abnormal filamentous cell phenotype with the loss of Z-ring following ADEP treatment, and reduced viability in *B. subtilis* (den Blaauwen et al., 2014; Sass et al., 2011).

Another possible target for antibiotic development is represented by the ATP-binding-cassette-transporter (ABC-transporter); FtsEX which has been found to play vital role initially with divisome assembly and later in regulating PG hydrolase activity in *E. coli* (Du and Lutkenhaus, 2017); similar role in *S. pneumoniae* (Sham et al., 2011) and in regulating CwlO from elongasome complex (Dominguez-Cuevas et al., 2013; Meisner et al., 2013). The details of this are discussed in next section and throughout this thesis. Apart from these ATPases, bitopic membrane

proteins including the tripartite complex of FtsQLB and as mentioned above, the FtsW or RodA could potentially be a very good candidates for existing or new classes of antibiotics since their inhibition or disruption of function has clear consequence for cellular function. (Bisson-Filho et al., 2017; Perez et al., 2019; Taguchi et al., 2019). Inhibitors to any of these proteins could potentially block the signal transduction between cytoplasmic and extracytoplasmic molecular events, and subsequent loss of PG synthesis could elicit a cell division block. It is entirely possible that the antibacterial effects of beta-lactam drugs are in part a result of the decoupling effect on overall cell division and cell wall biosynthesis rather than a direct inhibition of cell wall crosslinking as has been previously proposed.

1.7. An ABC-transporter and hydrolase complex could potentially be a good target for novel antibiotics.

In most bacteria, like in *E. coli*, FtsE and FtsX recruited at the divisome around early-to-mid cell division stage following assembling of cytoskeleton proteins and associates. FtsE has been found to join FtsX via an interaction with FtsZ (Corbin et al., 2007), where FtsA has been reported to interact with FtsX (Du et al., 2016), these interactions have been hypothesized to play important role in assembling further downstream divisome proteins (Du et al., 2016). In *E. coli*, FtsEX is not essential and mutants of FtsEX are viable except in low osmotic condition (Reddy, 2007) but this is not the case in other organisms. It has been proposed that FtsE and FtsX form a complex that resembles an ABC-transporter complexes (Greene et al., 2018; Schmidt et al., 2004), where FtsE has been shown to act as ATPase by binding and hydrolysing ATP (Bajaj et al., 2016), and FtsX found to act as transmembrane subunit of predicted ABP-transporter (Bajaj et al., 2016; Du et al., 2019; Gill and Salmond, 1987; Schmidt et al., 2004). Specifically, however, FtsEX is categorised as protein complex belong to Type VII family of ABC superfamily (Du et al., 2019; Greene et al., 2018). This group is known for transducing signals, instead of transporting any molecule as is the paradigm for classically ABC transporter proteins. FtsEX has been predicted to operate as a transducer of signals via a cytoplasmic ATP-hydrolysis event (as a consequence of divisome activity in the cytoplasmic side of the membrane) to peripheral associate(s). Accordingly, in *E. coli* it has been predicted to control amidase activity through a direct interaction with EnvC in order to initiate PG hydrolysis (**Figure 1.17a**). Similarly, a *S. pneumoniae* amidase PcsB has been reported to interact directly with extracellular domains of FtsX (**Figure 1.17.b**) in order to serve the same purpose of sPG hydrolysis (Sham et al., 2011; Sham et al., 2013). In *B. subtilis* this hydrolase is CwlO which becomes activated in a similar fashion by coordination with associated co-factors SweC and SweD (**Figure 1.17.c**) (Brunet et al., 2019; Meisner et al., 2013). Recently, similar association and coordination also has been shown in non-pathogenic Corynebacterineae *C. glutamicum*, where FtsEX resides in a multimeric complex composed of SetA, SetB and RipC and operate the PG hydrolysis (Lim et

al., 2019). Among pathogenic Corynebacterineae, in *M. tuberculosis*, a protease (RipC) has been found to be activated by the extracellular domain of FtsX (Mavrici et al., 2014). All these reports commonly indicate an important role of FtsEX is to dock a PG hydrolase machinery directly (e.g. PcsB in *S. pneumoniae*), or indirectly via its extra regulator (e.g. EnvC in *E. coli*), in order to operate PG hydrolysis process at the extracellular space following ATPase activity of FtsE at the cytoplasmic side of the plasma membrane. These two events are coupled by an interaction of FtsX with its extracellular / periplasmic partner, which ultimately control the PG hydrolase and subsequent separation of septum. Therefore, inhibiting the action of FtsEX or its interactors in divisome (in *E. coli*, *S. pneumoniae* etc.) or in elongasome (like in *B. subtilis*), we could arrest the PG hydrolysis event during cell division and thus elicit a bacteriostatic effect which may lead to subsequent bacteriolytic events.

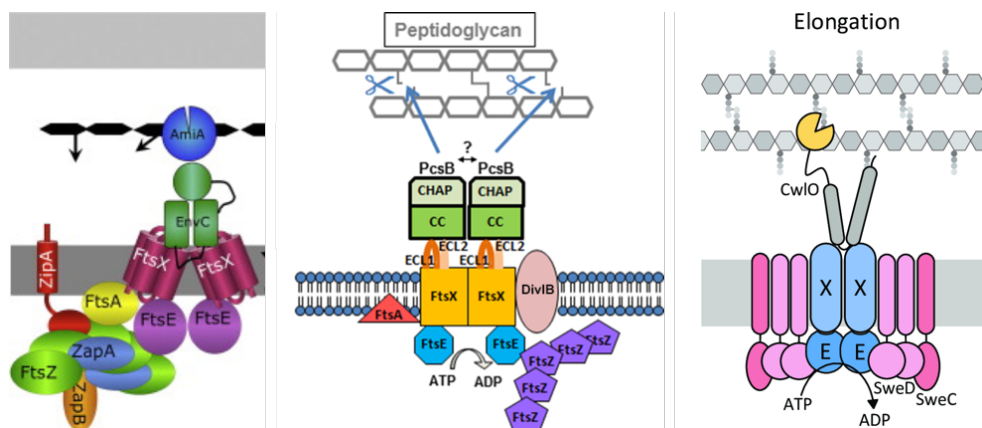


Figure 1.17. Separate ligand interaction of FtsEX and its in three separate models.

Mechanism are explained in the main text (section 1.7.) and in chapter 4 and 5. Figures adopted and edited from den Blaauwen et al. (2014) (a); Bajaj et al. (2016) (b); Brunet et al. (2019) (c).

Interestingly, apart from vegetative symmetric cell division, the FtsEX also has been reported to involve in initiating sporulation in *B. subtilis* (Garti-Levi et al., 2008). Under nutrient-stress condition, an FtsE depleted mutant and thus lacking functional FtsEX, has shown to delay the entry into sporulation, however this condition can be suppressed by activating the sporulation specific master regulator Spo0A or its histidine-kinases phosphorelay cascade (KinA, KinB and KinC) that are located upstream of Spo0A (Garti-Levi et al., 2008). This experiment indicated

a role of FtsEX, particularly the ATPase activity of the FtsE, in playing a key role in regulating specific/selective phosphorylation of selective kinases that trigger the Spo0A phosphorylation (Spo0A ~P) mediated sporulation, under stressed environmental conditions. Further to this finding, Meisner et al. (Meisner et al., 2013) reported similar delays in sporulating and morphogenesis changes in FtsEX and CwlO depleted cells. Considering their associate roles in similar PG-hydrolysis pathway, FtsEX has been suggested to promote sporulation by regulating CwlO activity. Recently, CwlO has been suggested to interact KinB/KinD to regulate the Spo0A mediated biofilm formation pathway in rhizobacterium *Bacillus velezensis* (Li et al., 2018). Together all these findings indicate the FtsEX interaction to its hydrolase partner, varies across bacterial species and so does the associated functions that include triggering PG-hydrolase activity as well as in triggering other cellular processes including sporulation or biofilm formation. This features and differential roles in different bacteria and in different conditions, make FtsEX-hydrolase complex an interesting target to deals infection and make selective antibiotics against this molecular machine.

Recently, a series of studies, aiming to find potential inhibitors for the above molecular machine and its fine mechanism, explored the action of certain chemokines which could potentially prevent the function of FtsEX-hydrolase machine (Crawford et al., 2019). In *Bacillus anthracis*, the human chemokine CXCL10 has been shown to interact with FtsX and disrupt the integrity of the PG at the cell wall and eventually arrest cell division (Crawford et al., 2011; Margulieux et al., 2016). However, while these reports are very encouraging, it is necessary to examine the details of the mechanisms involved and investigate if similar actions in other bacterial species could be harnessed. Nonetheless, this is just the beginning, and to investigate detail mechanism of any potential inhibitors to FtsEX and its associates, requires a complete structural detail of this complex and its interaction to its associates as to nail down the molecular mechanism involving the hydrolase activity and to screen natural or synthetic inhibitors of this macromolecular complex.

1.8. Challenges in studying membrane lipid bound divisome proteins and new tools to address these challenges

Divisome proteins are mostly either membrane proteins (MP) or membrane associated proteins (MAP). However, purification and structural analysis of membrane proteins, is extremely challenging because of their low abundance in cell membrane (less than 2% of all cell protein) and their hydrophobic nature and lipid association. These limitations restrict the production of MPs in large quantity suitable for *in-vitro* biochemical and biophysical characterization (White, 2015). Membrane proteins, by the very nature, are insoluble in aqueous buffers and therefore, detergent solubilization is necessary for extracting and solubilizing MPs. However, the use of detergents strip and replace the surrounding native lipid environment in which the MP is located. The interaction with the surrounding lipid environment is an important consideration when analysing the function or activity of any MP or MAP especially when such proteins are found in a protein complex. To understand a particular mechanism that involves a large macromolecular association, it is absolutely crucial to examine the structural-functional relationship of these proteins in such a macromolecular complex. Since most divisome proteins form complexes at or within the membrane, crystallization of such complexes for high resolution X-ray crystallography based structural elucidation can be extremely difficult due low abundance of the proteins in question. Recent developments in Cryo-electron microscopy offers almost similar high-resolution structural information as crystallography with an additional dynamic flexibility but require much lower amounts of sample for data collection. This resolution-revolution and advancements in the field of Cryo-EM as well as in developing new tools for MPs or MAPs, is encouraging more scientists to study structural-functional relationship of MPs in a macromolecular complex form rather than individual or partial domain analysis.

In this context, detergent micelle forms of MPs (**Figure 1.18.a**) as a consequence of detergent extraction may not be suitable for structural and biochemical study as

it may also disrupt the protein-lipid interactions that are necessary for function. Therefore, detergent-free methods may be more suitable in studying complexes and could be a novel strategy to purify complexes and, examine their structural association and functions. Several detergent-free tools and methods are now available (Dorr et al., 2016) and gaining popularity among structural biologists (Figure 1.18. b, c, d).

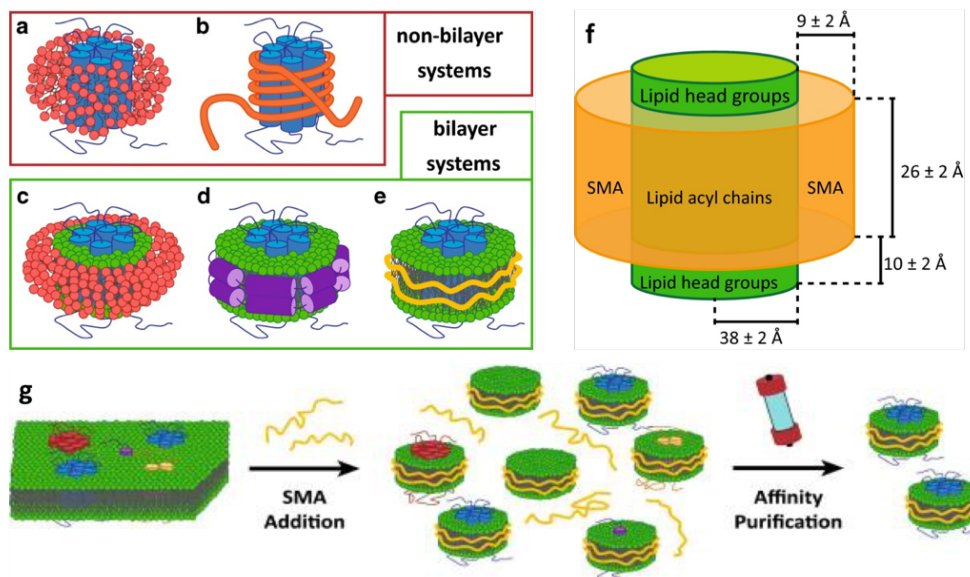


Figure 1.18. SMALP and other extraction tools for membrane protein.

The protein is colored blue and lipids in bilayers are in green. a. Protein in detergent (red) micelle. b. Protein bound in amphipol (orange). c. Protein in bicelle (detergent in red). d. Protein in nanodisc (purple). e. Protein extracted in nanodisc and stabilized by SMA (yellow). f. Dimensions of styrene–maleic acid/lipid particles (SMALPs) consisting of DMPC lipids and a SMA copolymer with a styrene–maleic acid (Jamshad et al., 2015). g. Extraction of membrane proteins encapsulated within native lipid environment by SMA. SMA interacts with lipid-bilayer and leads to formation of native lipid nanodiscs containing different MPs and other lipid material or just lipid material.

Figures adopted and modified from Dorr et al. (2016)

Recently one such detergent-free tool that composed of styrene–maleic acid (SMA) copolymers, provides just such a tool to scientists with an interest in examining MPs or MAPs (Figure 1.18.e). In principle, the SMA molecule in association of phospholipid tails of lipid particles, start self-assembling and form a disk-like structure, known as SMA-lipid particles (SMALP), while extracting those bilayer-

lipid chunks along with MPs (**Figure 1.18.g**) (Dorr et al., 2016; Lee et al., 2016). SMALPs self-assemble into a disk of around 10 nm diameter and capture membrane proteins with surrounding membrane lipids and allows their extraction into an aqueous environment (**Figure 1.18.f**). The SMALP procedure has been successfully used in different purification methods such as IMAC (Immobilized Metal Affinity Chromatography) with His-tag/Ni²⁺-NTA coupling (Gulati et al., 2014; Lee et al., 2016) as well as specific antibodies binding (Gulati et al., 2014). SMALPs has been reported to extract and successfully purify many MPs and MAPs across many biological organisms from bacteria (Dorr et al., 2014; Lee et al., 2016) to human cells (Jamshad et al., 2015) with satisfied yields and greater stability than detergent extracted MPs. Therefore, for studies with membrane proteins or membrane associated proteins, SMALP extraction method would be an ideal choice to extract the complex within its less dynamic lipid environment. Using this novel tool and extraction strategy may not only provide greater stability to the protein complex but may also offer flexibility in designing experiments for biophysical characterization and further structural examination with this complex. The Dafforn group (University of Birmingham, UK) have been successful visualized SMALP encapsulated membrane proteins with negative stain EM and this now includes key bacterial divisome components (Lee and Pollock, 2016; Alvin C. K. Teo et al., 2019).

1.9. AIMS and OBJECTIVES: Studying a macromolecular complex involves FtsAZ, FtsEX and PcsB complex in membrane lipid bound SMALP nanodisc

In order to understand a dynamic molecular mechanism, it is absolutely imperative to study the structural-functional relationships of a macromolecular complex as mentioned in previous section. I therefore sort to study the association of FtsE and FtsX as a complex in its own right, along with those proteins known to bind to the FtsEX complex from *S. pneumoniae* in which the function of FtsEX is known to be essential; and in which there is a direct association with the PG hydrolase PcsB. Previous attempts to purify either the individual FtsE or FtsX proteins or a complex of the two using detergent based methods had resulted in limited success (Sham et al., 2011; Sham et al., 2013). The colocalization and overlap of the two genes in the chromosome of many bacterial species is suggestive of a necessity for the two proteins to be co-expressed to enable complex formation and guided our strategy. We also devised a study that uses the SMALP approach (**Figure 1.19**) to extract these proteins in association with membrane lipids to assess if these lipids might have a function on protein-protein interactions required for such studies.

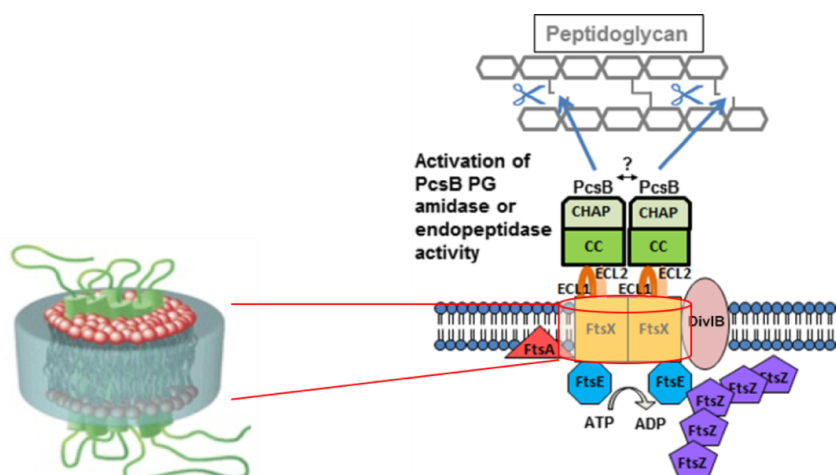


Figure 1.19. Schematic representation of FtsEX oriented complex in SMALP.

Figure adapted and modified from Bajaj et al. (2016) and Dorr et al. (2016)

CHAPTER 2. Materials and Methods

2.1. Materials

2.1.1. Media of bacterial culture

All media for culturing *E. coli* strains are listed in **Table 2.1**. All media were autoclaved immediately after preparation. For selective media both LB agar plates (LBA) and LB or AIM were supplemented with appropriate antibiotics and with concentration as mentioned in **Table 2.10**.

Table 2.1. List of Medias and their compositions.

| Name | Composition | Reference |
|----------------------------|---|---|
| LB Broth | 10 g Tryptone, 10 g Sodium Chloride (NaCl), 5 g Yeast Extract, made up to 1 L with double-distilled water and autoclaved. Supplied by the communal media preparation facility at School of Lifesciences (SLS, University of Warwick, UK). | ("LB (Luria-Bertani) liquid medium," 2006). |
| SOC | 20 g Tryptone, 0.5 g Sodium Chloride (NaCl), 5 g Yeast Extract, 0.2 g Potassium Chloride (KCl), 3.6 g Glucose and 1 g Magnesium Chloride and made up to 1 L with double-distilled water and autoclaved. Supplied by the communal media preparation facility (at SLS, University of Warwick, UK). | (Hanahan, 1983). |
| Auto-induction media (AIM) | 16 g Tryptone, 10 g Yeast Extract, 3.3 g Ammonium Sulphate (NH ₄) ₂ SO ₄ , 6.8 g Potassium Dihydrogen Phosphate (KH ₂ PO ₄), 7.1 g Disodium Hydrogen Phosphate (Na ₂ HPO ₄), 0.5 g Glucose, 2 g Lactose, 0.15 g Magnesium Sulphate, 0.03g Trace Elements, made up to 1L water and autoclaved. | Formedium (UK); Catalogue: AIM2YT0210 |

| | | |
|--------------------|---|---|
| LB0N | 10 g Tryptone (Sigma-Aldrich), 5 g Yeast Extract (Sigma-Aldrich), prepared to 1 L with double-distilled water and autoclaved. | (Bhandari and Gowrishankar, 1997; Reddy, 2007) |
| LB0N ₅₀ | 5 g Tryptone (Sigma-Aldrich), 2.5 g Yeast Extract (Sigma-Aldrich), prepared to 1 L in water and autoclaved | |
| LBA | 40 g Agar mixed with 1 L LB and autoclaved. | (Lennox, 1955) Supplied by the communal media preparation facility (at SLS, University of Warwick, UK) |

2.1.2. Buffers and solutions

All buffers and solutions used in this study are listed in **Table 2.2**. All chemicals bought from commercial companies were analytical grade. All buffers and solutions were made in the lab using MilliQ pure water and were filtered wherever applicable.

Table 2.2. List of buffers

| Name | Composition |
|---|---|
| Buffers used for competent cells | |
| TFB1 | 30 mM potassium acetate (Fluorochem), 10 mM CaCl ₂ (Sigma-Aldrich), 50 mM MnCl ₂ (Sigma-Aldrich), 100 mM RbCl (Sigma-Aldrich) and 15% glycerol (v/v) (Fisher Scientific). |
| TFB2 | 10 mM MOPS (Sigma-Aldrich), pH 6.5, 75 mM CaCl ₂ (Sigma-Aldrich), 10 mM RbCl (Sigma-Aldrich) and 15% glycerol (v/v) (Fisher Scientific). |

| General Buffers | |
|--|---|
| TAE | 40 mM Tris acetate (GoldBio), 1 mM EDTA (Fisher Scientific). |
| Native protein sample buffer (5X NPSB) | 310 mM Tris-HCl (Sigma-Aldrich) (pH 6.8), 0.05% Bromophenol Blue (w/v) (Tocris Bioscience), 50% Glycerol (v/v) (Fisher Scientific). |
| Reducing sample buffer (4XRSB) | 4 x LDS (Lithium Dodecyl Sulphate) sample buffer (NuPAGE, Invitrogen). |
| Native-PAGE running buffer (10x) | 250 mM Tris-HCl (Sigma-Aldrich), 1.92 M glycine (Sigma-Aldrich). |
| SDS-PAGE running buffer (10x) | 250 mM Tris-HCl (Sigma-Aldrich), 1.92 M glycine (Sigma-Aldrich), 1% SDS (w/v) (Sigma-Aldrich). |
| TBS | 50 mM Tris-HCl (Sigma-Aldrich), pH 7.6; 150 mM Sodium Chloride (NaCl) (Fisher Scientific). |
| TBS/T | 50 mM Tris-HCl (Sigma-Aldrich), pH 7.6; 150 mM Sodium Chloride (NaCl) (Fisher Scientific) and Tween20 (0.01%; v/v) (Sigma-Aldrich). |
| Cell lysis buffer | 20 mM HEPES (Sigma-Aldrich), 137 mM Potassium Chloride (KCl) (Sigma-Aldrich) and 5% Glycerol (v/v) (Fisher Scientific). pH 8 |
| Purification of SMALP-proteins | |
| SMALP extraction buffer | 50 mM HEPES, 500 mM Potassium Chloride (KCl) (Sigma-Aldrich) and 5% Glycerol (v/v) (Fisher Scientific), pH 8 |
| IMAC stock buffer | 50 mM HEPES (Sigma-Aldrich), 500 mM Potassium Chloride (KCl) (Sigma-Aldrich), 5% Glycerol (v/v) (Fisher Scientific) and Imidazole (1 M) (Sigma-Aldrich), pH 8 |

| | |
|--|---|
| IMAC wash buffer: W10 | 50 mM HEPES (Sigma-Aldrich), 500 mM Potassium Chloride (KCl) (Sigma-Aldrich), 5% Glycerol (v/v) (Fisher Scientific) and Imidazole (10 mM) (Sigma-Aldrich), pH 8 |
| IMAC wash buffer: W20 | 50 mM HEPES (Sigma-Aldrich), 500 mM Potassium Chloride (KCl) (Sigma-Aldrich), 5% Glycerol (v/v) (Fisher Scientific) and Imidazole (20 mM) (Sigma-Aldrich), pH 8 |
| IMAC wash buffer: W50 | 50 mM HEPES (Sigma-Aldrich), 500 mM Potassium Chloride (KCl) (Sigma-Aldrich), 5% Glycerol (v/v) (Fisher Scientific) and Imidazole (50 mM) (Sigma-Aldrich), pH 8 |
| IMAC Elute buffer: E | 50 mM HEPES (Sigma-Aldrich), 500 mM Potassium Chloride (KCl) (Sigma-Aldrich), 5% Glycerol (v/v) (Fisher Scientific), Imidazole (500 mM) (Sigma-Aldrich), pH 8 |
| SEC buffer | 25 mM HEPES (Sigma-Aldrich) and 150 mM Sodium Chloride (NaCl) (Fisher Scientific), pH 8 |
| <p>Purification of DDM-proteins (Sources of materials are same as mentioned above, unless otherwise stated)</p> | |
| DDM-Extraction buffer | 50 mM HEPES, 500 mM Potassium Chloride (KCl), 5% Glycerol (v/v), 1% DDM (w/v) pH 8 |
| DDM-IMAC stock buffer | 50 mM HEPES, 500 mM Potassium Chloride (KCl), 5% Glycerol (v/v) and Imidazole (1 M), pH 8 |
| DDM-IMAC wash buffer: DDM-W10 | 50 mM HEPES, 500 mM Potassium Chloride (KCl), 5% Glycerol (v/v), Imidazole (10 mM), 0.05% DDM (w/v), pH 8 |
| DDM-IMAC wash buffer: DDM-W20 | 50 mM HEPES, 500 mM Potassium Chloride (KCl), 5% Glycerol (v/v), Imidazole (20 mM), 0.05% DDM (w/v), pH 8 |

| | |
|---|---|
| DDM-IMAC wash buffer: DDM-W50 | 50 mM HEPES, 500 mM Potassium Chloride (KCl), 5% Glycerol (v/v), Imidazole (50 mM), 0.05% DDM (w/v), pH 8 |
| DDM IMAC Elute buffer: DDM-E | 50 mM HEPES, 500 mM Potassium Chloride (KCl) and 5% Glycerol (v/v), Imidazole (500 mM), 0.05% DDM (w/v), pH 8 |
| DDM-SEC buffer | 25 mM HEPES, 150 mM Sodium Chloride (NaCl), 0.02% DDM (w/v), pH 8 |
| <p>In-gel digestion buffers for mass-spectrometry (All materials and buffers are supplied by the Proteomic Facility at SLS, University of Warwick, UK)</p> | |
| Destain/Wash solution | 50% Ethanol (v/v), 50 mM Ammonium Bicarbonate (ABC). |
| Dehydrate solution | 100% Ethanol (v/v). |
| Reduction/Alkylation buffer (TCEP + CCA) | 10 mM Tris-(2-Carboxyethyl) Phosphine Hydrochloride (TCEP), 50 mM 2-Chloroacetamide (CAA). |
| Trypsin digestion solution | 2.5 ng/uL Trypsin in 50 mM ABC. |
| Peptide extraction buffer | 25% Acetonitrile (ACN) (v/v) and 5% Formic Acid (FA) (v/v) |
| Peptide resuspension buffer | 2% Acetonitrile (ACN) (v/v) and 0.1% Trifluoroacetic acid (TFA) (v/v). |

2.1.3. Bacterial strains

All *E. coli* bacterial strains used in this study are listed in **Table 2.3**. Among these the Top10 and NEB5 α strains were used for routine cloning and mini-preparation purpose. Whereas the Lemo21(DE3) and BL21(DE3) and their variants, mainly *BL21(DE3) Δ acrB::kan^R* were used for expressing and purifying protein(s) of

interest. All bacterial strains in appropriate buffer with 25% (v/v) glycerol were flash frozen in liquid nitrogen (Liq. N₂) before stored in – 80 ° C freezer.

Table 2.3. List of bacterial strains

| Strain | Genotype | Source |
|----------------------------------|--|---|
| Experimental <i>E. coli</i> | | |
| Top10 | Δ(ara-leu) 7697 araD139 fhuA ΔlacX74 galK16 galE15 e14- φ80dlacZΔM15 recA1 relA1 endA1 nupG rpsL (StrR) rph spoT1 Δ(mrr-hsdRMS-mcrBC) | Grant <i>et al.</i> , (1990); ThermoFisher (Invitrogen) |
| NEB5α | F' proA ⁺ B ⁺ lacI ^q Δ(lacZ)M15 zzzf::Tn10 (Tet ^R)/ fhuA2Δ(argF-lacZ)U169 phoA glnV44 Φ80Δ(lacZ)M15 gyrA96 recA1 relA1 endA1 thi-1 hsdR17 | NEB |
| BL21(DE3)ΔacrB::kan ^R | fhuA2 [lon] ompT gal (λ DE3) [dcm] ΔhsdS λ DE3 = λ sBamHIo ΔEcoRI-B int::(lacI::PlacUV5::T7 gene1) i21 Δnin5 ΔacrB KanR | (Baba <i>et al.</i> , 2006; Drew <i>et al.</i> , 2008; Studier and Moffatt, 1986) |
| Lemo21(DE3)::cam ^R | huA2 [lon] ompT gal (λ DE3) [dcm] ΔhsdS/ pLemo(CamR) λ DE3 = λ sBamHIo ΔEcoRI-B int::(lacI::PlacUV5::T7 gene1) i21 Δnin5 pLemo = pACYC184-PrhaBAD-lysY | NEB |

2.1.4. Plasmids used for cloning, mutagenesis and expression

All plasmid constructs that were used in this study for cloning, protein expression and mutagenesis, are listed in **Table 2.4**.

Table 2.4. List of plasmids and constructs

| Recombinant construct | Expressed <i>S. pneumoniae</i> gene | Tag(s) and description | Plasmid used for expression study | Source of plasmid backbone | Origin of replication | Antibiotic resistance marker | Source of recombinant construct |
|--|--|---|-----------------------------------|----------------------------|-----------------------|------------------------------|---------------------------------|
| <i>pET-52b(+)-strep-SpftsEX-his10</i> | <i>ftsEX</i> | The <i>ftsE</i> is strep tagged N-terminally and <i>ftsX</i> is histidine (6) tagged C-terminally | <i>pET-52b(+)</i> | Novagen (71554) | pBR322 | Ampicillin | In this study |
| <i>pET-52b(+)-SpftsEX-his10</i> | <i>ftsEX</i> | The <i>ftsE</i> is untagged and <i>ftsX</i> is histidine (6) tagged C-terminally | <i>pET-52b(+)</i> | Novagen (71554) | pBR322 | Ampicillin | In this study |
| <i>pETDuet1-His6-SpftsE(MCS1)-SpftsX-his10(MCS2)</i> | <i>ftsE</i> and <i>ftsX</i> from MCS1 and MCS2 respectively. | The <i>ftsE</i> is strep tagged N-terminally and <i>ftsX</i> is histidine (6) tagged C-terminally | <i>pETDuet1</i> | Novagen (71146) | pBR322 | Ampicillin | In this study |
| <i>pET-22b(+)-SpftsE-His6</i> | <i>ftsE</i> | The <i>ftsE</i> is histidine (6) tagged C-terminally | <i>pET-22b(+)</i> | Novagen (69744) | pBR322 | Ampicillin | In this study |
| <i>pETDuet1-SpftsE-his6</i> | <i>ftsE</i> | The <i>ftsE</i> is histidine (6) tagged C-terminally | <i>pETDuet1</i> | Novagen (71146) | pBR322 | Ampicillin | In this study |
| <i>pETDuet1-SpftsXval-his10</i> | <i>ftsX</i> with start codon valine (Val); translation start as VSLP | The <i>ftsX</i> is histidine (10) tagged C-terminally (amplified from <i>pET-52b(+)-strep-SpftsEX-his10</i>) | <i>pETDuet1</i> | Novagen, UK (71146) | pBR322 | Ampicillin | In this study |

| Recombinant construct | Expressed <i>S. pneumoniae</i> gene | Tag(s) and description | Plasmid used for cloning and expression study | Source of plasmid backbone | Origin of replication | Antibiotic resistance marker | Source of recombinant construct |
|--------------------------------|-------------------------------------|---|---|----------------------------|-----------------------|------------------------------|---------------------------------|
| <i>pETDuet1-SpftsX-His10</i> | <i>ftsX</i> | The <i>ftsX</i> is histidine (10) tagged C-terminally (amplified from pET-52b(+)-strep-SpftsEX-his10) | <i>pETDuet1</i> | Novagen (71146) | pBR322 | Ampicillin | In this study |
| <i>pETDuet1-His6-SpFtsA</i> | <i>ftsA</i> | The <i>ftsA</i> is histidine (6) tagged N-terminally | <i>pETDuet1</i> | Novagen (71146) | pBR322 | Ampicillin | In this study |
| <i>pACYCDuet1-SpFtsA</i> | <i>ftsA</i> | The <i>ftsA</i> is untagged | <i>pACYC-Duet1</i> | Novagen (71147) | P15A | Chloramphenicol | In this study |
| <i>pACYCDuet1-his6-SpftsAZ</i> | <i>ftsAZ</i> complete operon | The <i>ftsA</i> is histidine (6) tagged N-terminally and <i>ftsZ</i> is untagged. | <i>pACYC-Duet1</i> | Novagen (71147) | P15A | Chloramphenicol | In this study |
| <i>pETDuetHETIS</i> | Empty Vector | The <i>pETDuet1</i> plasmid is modified at upstream of multiple cloning site-1 by introducing a highly efficient translation initiation site (HETIS) that contain a strong ribosome binding site. | <i>pETDuet1</i> | Novagen (71146) | pBR322 | Ampicillin | In this study |

| Recombinant construct | Expressed <i>S. pneumoniae</i> gene | Tag(s) and description | Plasmid used for cloning and expression study | Source of plasmid backbone | Origin of replication | Antibiotic resistance marker | Source of recombinant construct |
|--|-------------------------------------|--|---|--|------------------------------|------------------------------|---------------------------------|
| <i>pCDFDuetHETIS</i> | Empty Vector | The <i>pCDFDuet1</i> plasmid is modified at upstream of first multiple cloning site-1 by introducing a HETIS sequence. | <i>pCDFDuet1</i> | Novagen (71340) | CloDF13-derived CDF replicon | streptomycin /spectinomycin | In this study |
| <i>pACYCDuetHETIS</i> | Empty Vector | The <i>pACYCDuet1</i> plasmid is modified at upstream of first multiple cloning site-1 by introducing a HETIS sequence. | <i>pACYCDuet1</i> | Novagen (71147) | P15A | Chloramphenicol | In this study |
| <i>pACYCDuetHETIS-His6-SpFtsA</i> | <i>ftsA</i> | The <i>ftsA</i> is histidine (6) tagged N-terminally; a HETIS sequence is included at upstream of MCS-1. | <i>pACYCDuetHETIS</i> | Modified plasmid backbone. | P15A | Chloramphenicol | In this study |
| <i>pETDuetHETIS-his6-SpftsEX-his10</i> | <i>ftsEX</i> complete operon | The overlapping operon of <i>ftsEX</i> is cloned into <i>pETDuetHETIS</i> . The <i>ftsE</i> is histidine (6) tagged N-terminally and <i>ftsX</i> is histidine (10) tagged C-terminally; a HETIS sequence is included at upstream of MCS-1. | <i>pETDuetHETIS</i> | Original plasmid backbone was modified in this study | pBR322 | Ampicillin | In this study |

| Recombinant construct | Expressed <i>S. pneumoniae</i> gene | Tag(s) and description | Plasmid used for cloning and expression study | Source of plasmid backbone | Origin of replication | Antibiotic resistance marker | Source of recombinant construct |
|-------------------------------------|--|---|---|--|------------------------------|------------------------------|---------------------------------|
| <i>pCDFDuetHETIS-pelB-pcsB-his6</i> | <i>pcsB</i> or <i>gsp-781</i> (in R6 strain) | The <i>pcsB</i> is histidine (6) tagged C-terminally; a HETIS sequence is included at upstream of MCS-1.. | <i>pHETIS-CDFDuet2</i> | Original plasmid backbone was modified in this study | CloDF13-derived CDF replicon | streptomycin /spectinomycin | In this study |
| <i>pACYCDuetHETIS-his6-SpftsAZ</i> | <i>ftsAZ</i> complete operon | The <i>ftsAZ</i> complete operon is cloned into <i>pACYCDuetHETIS</i> vector. The <i>ftsA</i> is histidine (6) tagged N-terminally and <i>ftsZ</i> is untagged. The plasmid containing a HETIS sequence at upstream of MCS-1. | <i>pACYCDuetHETIS</i> | Original plasmid backbone was modified in this study | P15A | Chloramphenicol | In this study |

2.1.5. Primers/Oligonucleotides

All primers or oligomers that used in this study, were synthesised by Integrated DNA Technology (IDT); are listed in **Table 2.5**.

Table 2.5. List of Primers

| Number | Name | SEQUENCE |
|--|--|--|
| Preparing pETDuet1-His₆-SpftsE(MCS1)-SpftsX-his₁₀(MCS2) | | |
| 75542642 | Insert1_SpFtsE-6xHis_MCS1.FOR | TTTAAGAAGGAGATATACATATGT CAATTATTGAAATGAGAGATGT |
| 75542643 | Insert1_SpFtsE-6xHis_MCS1.REV | ACTTAAGCATCAGTGGTGGTGGTG GTGGTGC |
| 75542644 | Insert2_SpFtsX-10xHis.FOR | TTAAGAAGGAGAGTATGGATACG ATGATTAGTAGATTTTT |
| 75542645 | pET-Duet_MCS1_SpFtsX.REV | GTATCCATACTCTCCTTCTTAAAGT TAAACAAAATTATTTCTAGAGGGG AATTG |
| 75542646 | DuetDOWN1 Primer | GATTATGCGGCCGTGTACAA |
| 75542647 | DuetUP2 Primer | TTGTACACGGCCGCATAATC |
| 75542648 | Insert2_SpFtsX- 10xHis_MCS2.FOR | TAGTTAAGTATAAGAAGGAGAGT ATGGATACGATGATTAGTAGATTT TT |
| 75542649 | Insert2_SpFtsX- 10xHis_MCS2.FOR (2) | TATAAGAAGGAGAGTATGGATAC GATGATTAGTAGATTTTT |
| 75542650 | Insert2_SpFtsX- 10xHis_MCS2.REV | GTGGCAGCAGCCTAGGTTAATTAG TGGTGGTG |
| 75542651 | Insert2_SpFtsX- 10xHis_MCS2.REV (2) | CCTAGGTTAATTAGTGGTGGTGAT GGTGA |
| 75542652 | Vec1_pET- Duet_Mcs1_SpFtsE.FOR | CACCACTGATGCTTAAGTCGAACA GAAAGTAATCGTATT |
| 75542653 | Vec1_pET- Duet_Mcs1_SpFtsE.REV | GACATATGTATATCTCCTTCTTAA AGTTAAACAAAATTATTTCTAGAG GGG |
| 75542654 | Vec2_pET-Duet_MCS2_SpFtsX- His.FOR | CCACCACTAATTAACCTAGGCTGC TGCCACC |

| | | |
|---|-----------------------------------|---|
| 75542655 | Vec2_pET-Duet_MCS2_SpFtsX-His.REV | CATCGTATCCATACTCTCCTTCTTA TACTTAACTAATATACTAAGAT |
| Preparing pETDuet1-His₆-SpftsE | | |
| 75542656 | Insert1_6xHis-SpFtsE.FOR | TCCGAATTCGATGTCAATTATTGA AATGAGAGATGTCTGTTAAAAAATA CG |
| 75542657 | Insert1_6xHis-SpFtsE.REV | CTAGGTTAATTAATCATCGTATCC ATACTCTCCTTTTGATT |
| 75542658 | Vec_pET-Duet_6xHis-SpFtsE.REV | TAATTGACATCGAATTCGGATCCT GGCTGTG |
| 75542659 | Vec_pET-Duet_6xHis-SpFtsE.FOR | GGATACGATGATTAATTAACCTAG GCTGCTGCCACC |
| Sequencing Primers | | |
| 75542660 | pET Upstream Primer | ATGCGTCCGGCGTAGA |
| 75542661 | T7 Terminator Primer | GCTAGTTATTGCTCAGCGG |
| 75904097 | ACYCDuetUP1 Primer | GGATCTCGACGCTCTCCCT |
| Preparing pACYCDuet1-SpftsA (untagged-SpFtsA) | | |
| 75904098 | Ins_SpFtsA_(pACYC-DUET).FOR | GAGATATACCATGGCTAGAGAAG GCTTTTTTTACAGG |
| 75904099 | Ins_SpFtsA_(pACYC-DUET).REV | CGACTTAAGCATTATTCGTCAAAC ATGCTTCCGATCAAG |
| 75904100 | Vec_pACYC-DUET(SpFtsA).FOR | TGACGAATAATGCTTAAGTCGAAC AGAAAGTAATCGTATTG |
| 75904101 | Vec_pACYC-DUET(SpFtsA).REV | TCTCTAGCCATGGTATATCTCCTTA TTAAAGTTAAACAAAATTATTCT ACAGG |
| Preparing pACYCDuet1-his₆-SpftsAZ | | |
| 75904102 | Ins_SpFtsAZ_(pACYC-Duet1).FOR | GAGATATACCATGGCTAGAGAAG GCTTTTTTTACAGG |
| 75904103 | Ins_SpFtsAZ_(pACYC-Duet1).REV | CGACTTAAGCATTAAACGATTTTTG AAAAATGGAGGTGTATCCAATTCA |
| 75904104 | Vec_pACYC-Duet1(SpFtsAZ).FOR | AAATCGTTAATGCTTAAGTCGAAC AGAAAGTAATCGTATTGTACAC |

| | | |
|---|-------------------------------|--|
| 75904105 | Vec_pACYC-Duet1(SpFtsAZ).REV | TCTCTAGCCATGGTATATCTCCTTA TTAAAGTTAAACAAAATTATTTCT ACAGG |
| Preparing pACYCDuet1-his₆-SpftsA | | |
| 76762514 | Ins_6xHis-SpFtsA(pDuet).FOR | CAGCCAGGATATGGCTAGAGAAG GCTTTTTTACAGGT |
| 76762515 | Ins_6xHis-SpFtsA(pDuet).REV | CGACTTAAGCATTATTCGTCAAAC ATGC |
| 76762516 | Vec_pET-Duet1(6H-SpFtsA).FOR | TGACGAATAATGCTTAAGTCGAAC AGAAAGTAATCGTATTG |
| 76762517 | Vec_pET-Duet1(6H-SpFtsA).REV | CTCTAGCCATATCCTGGCTGTGGT GATGAT |
| Preparing variants of pETDuet1-SpftsX_{val}-his₁₀ that start FtsX translation from Val residue (MAVS) | | |
| 76762518 | Ins_SpFtsX-Thr-10H.FOR | GATATACATATGGCCGTGTCGTTT GTGACGAAT |
| 76762519 | Ins_SpFtsX-Thr-10H.REV | GACTTAAGCATTAGTGGTGGTGAT GGTGATGATGG |
| 76762520 | Vec_pET-Duet2(SpFtsX-10H).FOR | CCACCACTAATGCTTAAGTCGAAC AGAAAGTAAT |
| 76762521 | Vec_pET-Duet2(SpFtsX-10H).REV | ACGACACGGCCATATGTATATCTC CTTCTTAAAGTTAAACAAAATTAT TTCTAGAG |
| Preparing variants of pETDuet1-SpftsX-his₁₀ that start FtsX translation from Val residue (VSLP) | | |
| 76787825 | Ins_SpFtsX(V)-Thr-10H.FOR | AGATATACATGTGTCATTGCCATT GAAAATGGCC |
| 76787826 | Ins_SpFtsX(V)-Thr-10H.REV | GACTTAAGCATTAGTGGTGGTGAT GGTGATGATGG |
| 76787827 | pET-Duet2(SpFtsX_Val).FOR | CCACCACTAATGCTTAAGTCGAAC AGAAAGTAAT |
| 76787828 | pET-Duet2(SpFtsX_Val).REV | GGCAATGACACATGTATATCTCCT TCTTAAAGTTAAAC |
| | | |

| Modifying pETDuet1-His₆-SpFtsA to pACYCDuetHETIS-His₆-SpFtsA | | |
|--|-----------------------------------|---|
| 77478128 | Ins_6H-SpFtsA(pDuet2).FOR | AGATATACATATGGGCAGCAGCCA TCACCATCA |
| 77478129 | Vec_pDuet2-SpFtsE_(6H-SpFtsA).FOR | TGACGAATAATGCTTAAGTCGAAC AGAAAGTAATCGTATT |
| 77478130 | Vec_pDuet2-SpFtsE_(6H-SpFtsA).REV | TGCTGCCCATATGTATATCTCCTTC TTAAAGTTAAACAAAATTATTCT AGAGGGG |
| 76762515 | Ins_6H-SpFtsA(pDuet2).REV | CGACTTAAGCATTATTCGTCAAAC ATGC |
| Modifying pETDuet1-His₆-SpFtsAZ to pACYCDuetHETIS-His₆-SpFtsAZ | | |
| 77478131 | Ins_HETIS_(pACYC).FOR | CGCTCTCCCTGGATCGAGATCGAT CTCGATCCC |
| 77478132 | Vec_HETIS_(pACYC).REV | ATCTCGATCCAGGGAGAGCGTCGA GATCC |
| 77478133 | Middle-Primer_SpFtsA-Z.FOR | TTTGACGAATAAAGAGGAAAAAT AAATTATGACATTTTCATTTGA |
| 77478134 | Middle-Primer_SpFtsA-Z.REV | TTATTTTTCCTCTTTATTCGTCAA CATGCTCCGATCAAGC |
| Adding NT-PelB and CT-His₆ site to SpPcsB using pET-22b(+)-PelB | | |
| 77478135 | Ins_SpPcsB_(pET22_PelB).FOR | GGCGATGGCCATGAAGAAAAAAA TCTTAGCGTCACTTTTATTAAGTAC AG |
| 77478136 | Ins_SpPcsB_(pET22_PelB).REV | GGTGCTCGAGATCTGCATAAATAT ATGTAACAAAACCTTCAGAAGT |
| 77478137 | Vec_pET22b_PelB_(SpPcsB).FOR | TTATGCAGATCTCGAGCACCACCA CCACCA |
| 77478138 | Vec_pET22b_PelB_(SpPcsB).REV | TTTTCTTCATGGCCATCGCCGGCT |
| Creating pETDuetHETIS-his₆-SpftsEX-his₁₀ (by Inserting PelB-PcsB-His₆ into pACYCDuetHETIS) | | |
| 77538109 | Ins_HETISp22_(pCDFDuet1).FOR | ATTAGGAAATCGAGATCTCGATCC CGC |
| 77538110 | Ins_HETISp22_(pCDFDuet1).REV | TTAAGCATTAGTGGTGGTGGTGGT GGTGC |

| | | |
|--|--------------------------------------|--|
| 77538111 | Vec_pCDFDuet1_(HETISp22).FOR | CCACCACCACTAATGCTTAAGTCG AACAGAAAGTAATCGTATTGTACA C |
| 77538112 | Vec_pCDFDuet1_(HETISp22).REV | CGAGATCTCGATTCCTAATGCAG GAGTCGCA |
| Creating pETDuetHETIS-his₆-SpftsEX-his₁₀ (by inserting SpFtsEX-His₁₀ [from pET-52b(+)] into pETDuetHETIS-NT-His₆) | | |
| 77538113 | Ins_SpFtsEX-10H_(pDuet2-NT-6H).FOR | CAGCCAGGATATGTCAATTATTGA AATGAGAGATGTCGTTAAAAAATA CG |
| 77538114 | Ins_SpFtsEX-10H_(pDuet2-NT-6H).REV | TGGGGAATTGTTAGTGGTGGTGAT GGTGATGATGGTGG |
| 77538115 | Vec_pDuet2-NT-6H_(SpFtsEX-10H).FOR | CCACCACTAACAATTCCCCATCTT AGTATATTAGTTAAGTATAAGAAG GAGA |
| 77538116 | Vec_pDuet2-NT-6H_(SpFtsEX-10H).REV | TAATTGACATATCCTGGCTGTGGT GATGA |
| Amplifying CXCL10 whole gBlock in pET-22b(+) | | |
| 77538117 | Ins_CXCL10w-HRV3C-6H_(pET22b).FOR | GGAGATATACATATGAATCAAACCT GCCATTCTGATTTGCT |
| 77538118 | Ins_CXCL10w-HRV3C-6H_(pET22b).REV | CAGCCGGATCTTAGTGGTGGTGGT GGTGGTGC |
| 77538119 | Vec_pET22b_(CXCL10w-HRV3C-6H).FOR | CCACCACTAAGATCCGGCTGCTAA CAA |
| 77538120 | Vec_pET22b_(CXCL10w-HRV3C-6H).REV | CAGTTTGATTCATATGTATATCTCC TTCTTAAAGTTAAACAAAATTATT TCTAGAGGG |
| Amplifying CXCL10val active block in pET-22b(+) | | |
| 77538121 | Ins_CXCL10v-HRV3C-6xHis.FOR | GAGATATACATGTACCTCTCTCTA GAACTGTACGCTG |
| 77538122 | Vec_pET22b_(CXCL10v-HRV3C-6xHis).REV | AGAGAGAGGTACATGTATATCTCC TTCTTAAAGTTAAACAAAATTATT TCTAGAGGG |

| | | |
|--|--|---|
| 77538118 | Ins_CXCL10w-HRV3C-6H_(pET22b).REV | CAGCCGGATCTTAGTGGTGGTGGTGGTGGTGC |
| 77538119 | Vec_pET22b_(CXCL10w-HRV3C-6H).FOR | CCACCACTAAGATCCGGCTGCTAA CAA |
| Amplifying CTT-CXCL10 active block in pET-22b(+) | | |
| 77538123 | Ins_CTTcxcl10-HRV3C-6xHis_(pET22b).REV | CAGCCGGATCCAGACATCTCTTCT CACCCCTTCTTTTT |
| 77538124 | Vec_pET22b_(CTTcxcl10-HRV3C-6xHis).FOR | GAGATGTCTGGATCCGGCTGCTAA CAAAGCC |
| 77538121 | Ins_CXCL10v-HRV3C-6xHis.FOR | GAGATATACATGTACCTCTCTCTA GAACTGTACGCTG |
| 77538122 | Vec_pET22b_(CXCL10v-HRV3C-6xHis).REV | AGAGAGAGGTACATGTATATCTCC TTCTTAAAGTTAAACAAAATTATT TCTAGAGGG |
| Sequencing Primers for pACYCDuet2_6xHis-SpFtsAZ | | |
| | SpFtsA_Mid_Seq-primer.FOR1 | TGAATTACGGGGAAGCCTATCCGC |
| | SpFtsA_Mid_Seq-primer.REV1 | TCCGTCACTTCGACTGCTTCTAC |
| | SpFtsZ_Mid_Seq-primer.FOR1 | TGATTGAGGCAGAAGAGGCTTCAC |
| | SpFtsZ_Mid_Seq-primer.REV1 | AGTGTCTACATGCTCACGAAGTTG |
| Sequencing Primers for pDuet2_6xHis-SpFtsEX-10xHis | | |
| | SpFtsE_Mid_Seq-primer.REV | ATGGCAATGACACGGTGGC |
| | SpFtsXm_Seq-primer.FOR | ATGGCCGTGTCGTTTCGTG |
| | SpFtsX_Seq_Mid-primer.FOR | ATGGCGGTGCCAATACAGAAAG |
| Sequencing Primers for pCDF-Duet2_PelB-PcsB-6xHis | | |
| | PcsB_Seq_Mid-primer.FOR | GGCTGATGATGCTCAAGCATTGAC |
| | PcsB_Seq_Mid-primer.REV | CGAGCCTCTGCCTCAGCTG |
| Q5SDM primers for deleting of signal-peptide (WT) from PcsB | | |
| | Q5SDM_PelB-PcsB(Del_SigPep).FOR | GAAACGACTGATGACAAAATTGCT GCTCAAG |
| | Q5SDM_PelB-PcsB(Del_SigPep).REV | GGCCATCGCCGGCTGG |

| SDM for SpFtsE(K43Q, D164A, E165A)-FtsX | | |
|--|------------------------------------|---|
| 222705897 | Q5SDM_SpFtsE(K43Q)X.FOR | GAGCAGGGCAGTCAACTTTTATTC G |
| 222705898 | Q5SDM_SpFtsE(K43Q)X.REV | CTGAAGGTCCTACGATGTAAG |
| 222705899 | Q5SDM_SpFtsE(D164A)X.FOR | GATAGCTGCTGAGCCAACAGGAA ATCTGGATC |
| 222705900 | Q5SDM_SpFtsE(D164A/E165A)X. REV | AATACTTTGGGATTATTTACAATT GCACGCG |
| 222705901 | Q5SDM_SpFtsE(E165A)X.FOR | GATAGCTGATGCGCCAACAGGAA ATCTGGATC |
| SDM for PcsB(C292A, del-CT6His) | | |
| 222705902 | Q5SDM_PcsB(C292A).FOR | CAATTGGAGAAGCTACATGGGGA GTAAAAACATTGGCAC |
| 222705903 | Q5SDM_PcsB(C292A).REV | GATAACTTGAAGCGTTTGTACTGT ATGTTG |
| 222705904 | Q5SDM_PcsB(Del-CT6His).FOR | TAATGCTTAAGTCGAACAGAAAGT AATCGTATTGTACAC |
| 222705905 | Q5SDM_PcsB(Del-CT6His).REV | ATCTGCATAAATATATGTAACAAA ACCTTCAGAAG |

2.2. Microbiology methods

2.2.1. Preparation of competent cells

Competent cells were made in order to transform the same cell lines with foreign plasmids that contain our gene(s) or fragment of gene(s) of interest. *E. coli* competent cells were made with cell lines are TOP10, NEB5 α , *Lemo21(DE3)::cam^R*, *BL21(DE3) Δ acrB::kan^R*. Among these the TOP10 and NEB cells have no known antibiotic resistance and used for the purpose of cloning plasmids. Whereas the other two *E. coli* cell lines *Lemo21(DE3)::cam^R* and *BL21(DE3) Δ acrB::kan^R*, as indicated in their name, are resistant to Chloramphenicol and Kanamycin respectively and are used for protein expression. Further, the last *E. coli* cell line was modified by transforming to *BL21(DE3) Δ acrB::kan^R-SpftsE-his₆*, *BL21(DE3) Δ acrB::kan^R-X-his₁₀*, *BL21(DE3) Δ acrB::kan^R-pETDuetHETIS-his₆-SpftsEX-his₁₀*, which containing expression plasmids for *SpftsE*, *SpftsX* and *SpftsEX* (complete operon) with histidine tags either N- or C-terminal end. Details are mentioned in the **Table 2.4**. Competent cells are prepared by chemical treatment using a modified protocol originally proposed by Hanahan (1985). A single colony of original cell lines or transformed cell lines as mentioned above, is picked from a LB agar plate and inoculated in 2.5 mL LB media. The broth incubated overnight at 37 °C with continuous shaking at 180 RPM. The entire 2.5 mL overnight LB broth then inoculated into 1 L LB media adding 20 mM MgSO₄ for good growth and incubated at 37 °C until the optical density at 600 nm (OD_{600nm}) reached between 0.4 and 0.6. Once the required OD_{600nm} achieved, the cells were pelleted by centrifuging at 4500 x g for 5 - 10 minutes at 4 °C, and supernatant was discarded. The pelleted cells resuspended gently in 100 mL (0.4 volume of original culture) ice cold TFB1 buffer for 5 – 10 minutes on ice (and preferably in a cold room). Cells were pelleted again by centrifuging at 4500 x g at 4 °C for 5 - 10 minutes and supernatant discarded. Pelleted cells then resuspended in 10 mL (0.04 volume of original culture) ice-cold TFB2 buffer and incubated for 45 – 60 minutes on ice (and preferably in a cold room) with intermittent gentle mixing few times. After about 45 minutes cells were

aliquoted into 100 μ L or 200 μ L in 0.5 mL or 1.5 mL Eppendorf tube and were flash frozen using liquid nitrogen (Liq. N₂) before storing them in -80° C.

2.2.2. Preparation of agarose plates with selective antibiotic(s)

LBA plates were prepared using LBA as mentioned in Table 2.1 and supplemented with appropriate antibiotics with concentration as mentioned in Table 2.10. These LBA plates were used for growing and culturing bacteria that resistant to specific antibiotic(s) used in the same LBA plate.

2.2.3. Synchronization of bacterial culture

Cells were synchronised as below before growing under required condition for phenotypic studies. A single colony of transformed cells were inoculated and grown in 5 mL – 10 mL Luria broth cultures and incubated overnight (OD_{600nm} is generally about 2 approximately). Then 1 mL of the overnight culture was mixed and inculcated with fresh 1 mL of fresh LB media and the OD_{600nm} diluted down to 1. At this point, 1.8 mL of the same inoculum was mixed with 0.2 mL concentrated stock solution (10x) of DL-serine hydroxamate to a final concentration of 1 mg/ml in order to induce the stringent response (Ferullo, Cooper, Moore, and Lovett, 2009). Following further incubation for 90 minutes, this culture (growth restricted and thus the $OD_{600nm} \sim 1$) were washed twice using LB media by gently pelleting cells (by centrifuging at 4500 x g for 5 - 10 minutes at 4° C) and discarding the supernatant each time. Washed cells were resuspended in fresh 1 mL LB media to concentrate the OD_{600nm} up to 2 (approximately) and the entire culture (1 mL) was mixed with 9 mL fresh AIM media (the final $OD_{600nm} \sim 0.2$) with appropriate antibiotic at 100-fold. This release the cells from stringent response and allow further synchronous growth.

2.3. Molecular biology methods

2.3.1. Gene cloning techniques

2.3.1.1. Polymerase chain reaction (PCR)

All genes are amplified by using appropriate forward and reverse primers in polymerase chain reaction (PCR) following manufacturers protocol either for Phusion or Q5 polymerase (NEB, UK). Like other DNA polymerases, these polymerases possess 5' → 3' polymerase activity, but additionally it also possesses 3' → 5' exonuclease activity as claimed by NEB (UK). Therefore, above two were selected particularly for their 3' → 5' exonuclease proof-reading activity which ensures high fidelity (HF) by spotting and fixing a mismatch with very high accuracy. The same activity also enables the Phusion polymerase to remove any 3' overhanging nucleotides and produce PCR products with blunt ends (NEB, UK). Amplified PCR products (genes of interest) were used as inserts for cloning into plasmids. Components and composition of a standard PCR was as below (**Table 2.6**, as recommended in manufacturer's protocol. DMSO was added in most amplifications in order to prevent any secondary structure formation in oligonucleotides. Primers were designed manually and synthesized by IDT, UK. All PCR cycles were standardized (**Table 2.7**) and based up on the program that recommended by the manufacturer for respective polymerase.

Table 2.6. PCR components of Phusion® HF kit and their final concentration.

| PCR Mix | Volume (µl) | Final Concentrations |
|---|---------------|----------------------|
| 5 x Phusion® HF buffer (NEB, UK) | 10 | 1x |
| 10 mM dNTPs | 1 | 200 µM |
| 10 µM forward primer | 2.5 | 0.5 µM |
| 10 µM reverse primer | 2.5 | 0.5 µM |
| Template DNA (~ 50 ng/µl) | 0.25 - 1 | < 250 ng |
| Phusion® DNA polymerase (NEB, UK) 2000 U/mL | 0.5 | 1 U / 50 µL |
| dd H2O | made up to 50 | |

Table 2.7. Phusion® HF PCR thermocycler conditions

| Step | Temperature (° C) | Time (seconds) | Number of cycles |
|-----------------------------|-------------------|----------------|------------------|
| Initial Denaturation | 98 | 30 | 1 |
| Denaturation | 98 | 10 | 35 |
| Primer Annealing | 55, 60, 64, 68 | 30 | |
| Elongation | 72 | 30 sec / kbps | |
| Final Extension | 72 | 600 | 1 |
| Hold | 4 | - | - |

2.3.1.2. Restriction enzyme digestion of DNA

Restriction enzyme digestion of DNA (Plasmid and/or PCR products) was performed by appropriate enzymes and their corresponding HF buffers (like CutSmart buffer 4X; NEB UK), both supplied by New England Biolab (NEB, UK). The typical DNA digestions were performed in 20 μ l to 50 μ l final reaction volumes, containing a standard amount of quick purified (QIAquick, QIAGEN) PCR products or plasmid DNA (approximately 1000 ng), restriction enzyme digestion buffer (final concentration 1x) and 1 to 5 unit of restriction enzyme. Double digestions were performed using suitable and compatible pair of restriction enzymes (that possess at least 75% activity in the same buffer) concurrently in the appropriate reaction buffer. All digestions were performed in microcentrifuge tubes and incubated at 37 ° C for one hour to overnight as per manufacturer recommendation. The size digested products were confirmed by agarose gel electrophoresis and appropriate bands of digested products(s) were extracted from the gel using gel extraction kit (QIAGEN, UK).

2.3.1.3. Dephosphorylation of linearized plasmid DNA to prevent its re-ligation

Dephosphorylation of plasmid DNA was performed by recombinant shrimp alkaline phosphatase (rSAP) (NEB, UK) to restrict prevent any self-ligation of plasmid DNA. Re-ligation of plasmid DNA after restriction digestion is a possibility with restriction digestion with single enzyme and in cases where double digestions produce similar complementary sites or blunt ends. Hence, dephosphorylation at the ends prevents the ends to re-ligation. In a typical dephosphorylation step, 1 uL of rSAP was added to the reaction buffer (50 μ L) that is generally compatible (particularly HF CutSmart buffer; NEB UK) for dephosphorylation reaction, and incubated another 30 minutes at 37 ° C. Once complete the reaction was stopped inactivating the rSAP enzyme and other restriction enzymes in the solution by heating the mixture at 65 ° C for 10 minutes.

2.3.1.4. DpnI digestion of template plasmid DNA

In some instances, the DpnI treatment was performed to digest and remove any traces of plasmid DNA template that isolated from *E. coli*, before proceeding to the ligation step. Commonly used *E. coli* K12 strains such as DH5-alpha or its derivatives such as NEB5 α competent lab strain contain Dam methylase which methylate the adenine of Dam specific site GATC as a self-defence mechanism (NEB). The same site is apparently overlap with the recognition site for the DpnI enzyme which only cuts the same site when it is methylated (NEB). Therefore, plasmid templates isolated from Dcm⁺ strain methylate the DpnI site which can be digested by the DpnI, but the PCR products are not methylated, hence are not affected by the DpnI activity. To remove the template plasmid DNA, reactions with DpnI were performed similarly as rSAP, by adding 1 μ L to the digestion mixture and incubated at 37 ° C for 60 minutes following inactivation at 80 ° C for 20 minutes.

2.3.1.5. Agarose gel electrophoresis

All digested DNA fragments, amplified PCR products were separated by agarose gel electrophoresis. Standard 0.8 % (w/v) agarose gel was prepared mixing appropriate weight of agarose into TAE buffer (**Table 2.2**). The mixture was supplemented with very little amount 1/10000 dilution of a stock of 10mg/ml of Ethidium Bromide (EtBr; final concentration was less than 0.5 μ g/mL). DNA fragments were mixed with 6x DNA loading dye (NEB, UK) (final concentration 1x) before loading DNA fragments into gel wells. The same TAE buffer as used for preparing agarose gels, was also used in the tanks during electrophoresis and migration of DNA fragments towards positively charged electrode. Electrophoresis was performed under constant voltage at 110 V for about 35 minutes or until the dye front reaches the far end of the gel. Following electrophoresis, separated and EtBr stained DNA fragments in the gel were visualized by exposing the gel on a UV-transilluminator and photographed the same using installed camera and thermal printer.

2.3.1.6. Cleaning PCR product

Occasionally, PCR products and restriction enzymes digested products were quickly purified through small DNA binding column (Qiagen QIAquick) to remove enzymes and other chemicals in the above samples. The quick clean steps were performed following manufacturer's protocol (Qiagen QIAquick).

2.3.1.7. Extraction and purification of amplified PCR product

In order to ligate correct size DNA fragments of inserts (gene of interest) and fragments of vectors, the PCR products and/or digested products were separated on agarose gel electrophoresis and bands with appropriate size were excised from the gel and chopped into small pieces using fresh razor for each band. Chopped gel slices for insert and vector were collected in separate tubes and DNA fragments were recovered/purified from the gel by using QIAquick Gel Extraction kit (Qiagen, UK) and following its protocol. Finally, DNA fragments were eluted either in fresh RNase/DNase free double distilled water (ddH₂O) or in 30 µL prewarmed (37 °C) eluted buffer supplied in the same kit.

2.3.1.8. Ligation

Ligations were performed using inserts and vectors (3:1 molar ratio) that purified by gel extraction kit. The typical ligation reaction was performed with 50 ng of linearized vector, about 3 times more inserts (150 ng), 20 units of T4 DNA ligase (NEB, UK), supplied compatible ligase buffer (final concentration 1x; NEB, UK) and ddH₂O to volume up to 20 µL - 30 µL. Generally, three sets of ligations were set up as follows - with vector, insert and T4 DNA ligase (VIT); vector ligation control (VLC; vector, T4 DNA ligase, no inserts); and vector control (VC: only vector, no inserts and no T4 DNA ligase). All assays were incubated over night at 10 °C to 16 °C. Following incubation ligation mixtures were immediately used to transform *E. coli* competent cells as mentioned below or stored in – 20 °C freezer to use in future transformation.

2.3.1.9. Transformation in *E. coli*

The *E. coli* competent cell lines TOP10, NEB5 α , *Lemo21(DE3)::cam^R*, *BL21(DE3) Δ acrB::kan^R* and others as mentioned in section 2.2.1. , were used for transformation. These cryo-preserved cells (stored at – 80 °C) were first thawed on ice and then 5 μ L of ligation mixtures (2.3.1.8.) or 2 μ L purified plasmid construct was added to 50 μ L aliquot of cells for each transformation. The mixtures were incubated for 30 minutes on ice with intermittent gentle tapping to mix evenly before the treatment of heat shock, where ice chilled cells in the tube were incubated straightaway into a water bath at 42 °C for 45 seconds, followed by immediate 2 minutes incubation on ice. Further, these heat-shocked transformed cells were incubated in 500 μ L of SOC media at 37 °C with continuous shaking (180 RPM) for an hour. Once complete, 100 μ L of cells from each transformation were plated on to LBA plates with appropriate dilution of antibiotics and incubated at 37 °C overnight, but not more than 16 hours in case of single construct transformation with one or two antibiotic(s) selection. However, the final incubation time for the transformants with two or three plasmids and with multiple antibiotics selection, was varied and lengthened.

2.3.1.10. Colony screening by PCR

Successful transformants with appropriate antibiotic(s) selection were picked to verify the correct ligation of inserts by colony PCR using primers specific for the T7 promoter and T7 terminator regions in pET-based plasmids (**Table 2.5**). Isolated colonies were picked by with sterile pipette tips and copied to fresh LBA plate with respective antibiotic(s). The same tips were used in a PCR assay by mixing any remaining bacterial colonies into respective PCR master mix in a 96-well PCR plates. The master mix contains following components as shown in the **Table 2.8**, and the reactions were conducted following a thermocycler's program at **Table 2.9**. Following the colony PCR, the products were separated by running 0.8% (w/v) agarose gel electrophoresis and visualized by staining with EtBr, where lanes with correct insert size were indicative of positive colonies with successful ligation.

Table 2.8. Reactants used in colony PCR

| Components | Volume (µL) |
|--|--------------------|
| 10 x PCR reaction buffer (Invitrogen, UK) | 2.00 |
| 50 mM MgCl ₂ (Invitrogen, UK) | 0.60 |
| 10 uM T7 promoter / other forward primer (Table 2.5) | 1.00 |
| 10 uM T7 terminator/ other reverse primer (Table 2.5) | 1.00 |
| 10 mM dNTPs | 0.40 |
| DMSO (3%; v/v) | 0.60 |
| 100 U Taq polymerase (Invitrogen, UK) | 0.25 |
| dd H ₂ O | Volume up to 20 |

Table 2.9. Thermocycler conditions used in colony PCR

| Step | Temperature (° C) | Time (Secs) | Cycles |
|-----------------------------|------------------------------|------------------------|---------------|
| Initial Denaturation | 95 | 300 | 1 |
| Denaturation | 95 | 30 | 35 |
| Primer Annealing | 55 | 30 | |
| Elongation | 72 | 60 sec / kbps | |
| Final Extension | 72 | 300 | 1 |
| Hold | 4 | - | - |

2.3.1.11. Isolation of plasmid DNA and minipreparation

A single colony of successful transformants containing plasmid DNA either with positive gene insert or just empty vector backbone (in case of vector mini preparation) was inoculated in LB and grown overnight at 37 °C with appropriate antibiotics(s). Cells from about 5 mL culture were pelleted and plasmids from these cells were isolated in a minipreparation (50 µL) using GeneJET Plasmid Miniprep Kit (ThermoFisher, UK) following protocol as directed by the manufacturer. Concentrations of the plasmid minipreps were measured using a Nanodrop (ThermoFisher) machine and were stored at -20 °C.

2.3.1.12. Measurement of DNA concentration

Concentrations of DNA was determined by measuring the absorbances at A260 and A280 on a Nanodrop (ThermoFisher) machine, where their ratio estimated the purity of DNA. Generally, a ratio between 1.6 and 2.0 was considered as good purity of plasmid DNA.

2.3.1.13. Restriction enzyme mapping

All minipreps were quickly digested with insert specific restriction enzymes in order to confirm the presence of right amplicons into the MCS of the plasmid. This extra step is optional to screen further for positive insertions of the gene of interest before sending few of those plasmid constructs for detailed sequencing. To perform the restriction enzyme digestion 5 µL of purified minipreps were double digested with 0.5 µL of each restriction enzymes in a digestion buffer containing CutSmart buffer (final concentration 1x) (NEB, UK) and ddH₂O to volume up to 10 µL. The digestion mixture was incubated at 37°C for 1 hour or overnight and resulting fragments were visualized by 0.8% (w/v) agarose gel electrophoresis and ethidium bromide staining. Plasmid minipreps with successful restriction site mapping, were further selected for detailed sequencing of the plasmid construct.

2.3.1.14. DNA Sequencing

Positive plasmid constructs were sent to GATC Biotech (Germany) for detailed Sanger sequencing, particularly between T7-promoter and T7-terminator region by using T7p and T7t primers (see **Table 2.5**). Generally, 5 µL of plasmid DNA (80 – 100 ng/µl) was mixed with 5 µl of 5 µM primer, as directed by GATC-Biotech. Results were checked using sequence alignments programs provided by one of the following software Snapgene, Clustal Omega (EMBL-EBI) software / ApE plasmid editor (v2.0.49.10).

2.3.2. Plasmid construct assembly by Gibson cloning method

Gibson cloning method or Gibson assembly (Gibson et al., 2009) was used to assemble multiple inserts at the same time, it was also used as an alternate to classical method by using restriction enzyme digestion followed by ligation. All Gibson assembly cloning were achieved by using the NEBuilder® HiFi DNA Assembly Cloning Kit (NEB, UK) which provides a seamless cloning and flexibility of adding inserts independent of any restriction enzyme digestion site. All overlapping (about 20 bases) primers were designed and steps are followed as directed by the manufacturer protocol. The above kit supplies NEBuilder® HiFi DNA assembly master mix that contain a 5' → 3' exonuclease, DNA polymerase and ligase enzymes. In brief the overlapping PCR fragments are mixed with master mix (2x) in 1:1 ratio so that the final master mix ratio become (1x) in the reaction buffer. The reaction was incubated at 50 °C for 20 minutes to 60 minutes. During the incubation the 5' → 3' exonuclease activity creates a single stranded 3' overhang and expose the complementary sequences from two different fragments which then anneal at isothermal temperature at 50 °C, while the DNA polymerase extends the 3' end and fill in the gaps and ligase seals any nicks and ligate strands (NEB, UK). Rest transformation (2.3.1.9.), screening (2.3.1.10.), isolation (2.3.1.11.) and validation (2.3.1.14.) process were same as followed for classical gene cloning by restriction digestion and ligation, as mentioned above.

2.3.3. Plasmid construct mutagenesis

All plasmid mutagenesis that includes deletion, substitution and insertion was performed by using NEB Q5 mutagenesis kit (NEB, UK) which provide an exclusive KLD mix that contain kinase, ligase and DpnI enzymes. The primers for mutagenesis were made following manufacturer instruction for specific purpose (deletion, substitution and insertion) and PCRs were conducted by using either Q5 or Phusion DNA polymerase. Following PCR, the amplified fragments and the above KLD master mix (2x) were mixed in 1:1 ratio and incubated for 5 minutes. During this incubation the kinase phosphorylate the 5' ends of the amplified products and the ligase ligate the strands, these rapid actions seal the PCR fragments as circular plasmids, while the endonuclease activity of DpnI enzyme digest and degrade the template plasmid DNA (as mentioned in section 2.3.1.4.). Combining activity of these three enzymes ensures transformation of newly ligated PCR products, which further cloned into *E. coli* on selected antibiotic(s) plate (2.3.1.9.). Rest colony PCR screen (2.3.1.10.), isolation of plasmids (2.3.1.11.) and sequence/mutation validated (2.3.1.14.) by standard steps as mentioned in their respective sections above.

2.4. Protein expression, extraction and purification

2.4.1. Small-scale induction and membrane preparation

All small-scale studies were performed with fresh transformants. A single colony of the transformants was inoculated in 10 mL LB with appropriate antibiotic(s) and grown overnight at 37 °C. Next morning, generally the overnight culture was inoculated in fresh LB at 100-fold dilution. For small-scale studies, 1 mL of same overnight culture inoculated in 100 mL of fresh LB with or without desired L-rhamnose concentration and appropriate antibiotic(s). For experiments with L-rhamnose typically a series of dilutions (100 µM, 250 µM, 500 µM, 750 µM, 1000 µM, 2000 µM) are recommended and were tested in previous study (Naskar MSc report), but for this study transformed *E. coli* cultures were grown either presence of only 500 µM L-rhamnose or no L-rhamnose in the LB with proper antibiotic(s). These cultures (in 100 mL LB) were initially grown at 37 °C with continuous shaking at 180 rpm until OD_{600nm} reaches between 0.4, when the cultures were immediately moved to 20 °C. Subsequently, 400 µM Isopropyl β-D-1-thiogalactopyranoside (IPTG) was added to the culture media to induce transformed cells when the OD_{600nm} reaches between 0.5 and 0.6. Following an overnight induction, the cells were harvested next morning by centrifuging the entire cultures at 6000 rcf for 10 minutes at 4 °C and pelleting all cells at the bottom. After discarding the supernatants, dry weight of each pellet was measured and recorded. Cell pellets were resuspended in 10 mL cell lysis buffer (**Table 2.2**) with protease inhibitor cocktail (EDTA free; 1 tablet / 50 mL; Pierce, Thermo-scientific, UK) and PMSF (200 µM) using a continuous shaker for 20 to 30 minutes (until cells are completely resuspended) at low temperature (4 °C – 12 °C). Later these resuspended cells were lysed by passing the resuspension mix with one-drop antifoam 204 (Sigma, UK) through a one-shot cell disrupter at 30 psi (Constant Systems, UK). Lysed cells and its contents were then centrifuged at 20,000 rcf at 4°C for 20 minutes to pellet all cell debris and discard them. While supernatants were collected and were further ultra-centrifuged (UC) at 150,000 rcf for 1 hour at 4 °C to pellet membranes using Ti-70 rotor and Beckman-Coulter (USA) centrifuge

machine. The high-speed supernatants (HSS) were separated for future protein analysis. The membrane pellets were dried by decanting all liquids (or HSS) onto tissue and by air-drying for 4 to 5 minutes before resuspending in 1 mL TBS buffer with protease inhibitor cocktail (Pierce, Thermo-scientific, UK). Both, HSS and resuspended membrane solution were analysed immediately for protein expression or were stored at -20 °C for future analysis.

2.4.2. Large-scale induction and membrane preparation

Similar to small-scale studies, fresh transformants were used for large all large-scale studies. All transformed cell lines were grown aerobically in 100 mL Luria broth (LB) overnight (at 37 °C) before diluting the overnight cultures (OD_{600nm} is about 2) 10-folds into 900 mL 2YT autoinduction media (AIM, Formedium, UK) at 37 °C with appropriate antibiotics. This estimate starting OD_{600nm} of the overnight cultures in AIM were about 0.2. The cultures were incubated at 37 °C with continuous shaking at 180 rpm for about 1 hour, till the OD_{600nm} reaches between 0.4 and 0.6. At this point, cells in AIM were immediately transferred to 20 °C or 15 °C incubator and grown overnight with continuous shaking at 180 rpm. Cells for purification of protein of interest, were grown in up to 6 L volumes as required and harvested by centrifugation at 6,000 rcf for 10 mins at 4 °C. Harvested cells were washed and resuspended (at 4 – 5 ml per gram of cells) in cell lysis buffer (20 mM Tris-HCl/HEPES, pH – 8; 137 mM KCl; Glycerol 5% v/v) with PMSF (200 µM) and protease inhibitor cocktail (EDTA free, Pierce, Thermo-scientific, UK) as recommended by the manufacturer. Resuspended cells were lysed using cell disrupter in two passes at 30 kpsi and 25 kpsi (Constant Systems, UK), centrifuged at 12,000 rcf for 10 minutes at 4 °C to pellet and discard cell debris. Supernatant from the spin was collected and further ultra-centrifuged (UC) at 42000 rpm for 1 hour 15 minutes at 4 °C using Ti-45 rotor (Beckman Coulter, USA). High-speed supernatants (HSS) were collected and stored at -20 °C for further analysis. Membrane pellets were dried (tipped-off any liquid HSS) and following measuring the mass of the membrane pellets, these were either resuspended straightaway in SMALP extraction buffer (50 mM Tris-HCl/HEPES, 500 mM KCl,

5% v/v glycerol, pH 8) at 160 mg/mL concentration, or the dry membrane stored at -20 °C for future resuspension.

2.4.3. Extraction and purification of Membrane protein (MP) and/or membrane associated protein (MAP)

2.4.3.1. MP and/or MAP extraction using SMALP and purification using affinity (IMAC) and size-exclusion chromatography (SEC)

Membrane pellets were solubilized using 2.5% SMA (w/v) co-polymer in same extraction buffer as recommended by Lee et al. (Lee et al., 2016). In brief, the resuspended membranes (160 mg/mL) were further homogenized using hand-held glass homogenizer with 20 to 30 gentle strokes. The homogenized sample was then mixed with 5% (w/v) solution of SMA co-polymer (solubilised using SMALP extraction buffer) in 1:1 ratio. Thereby the final concentration of SMA become 2.5% (w/v) and final concentration of membrane become 80 mg/mL in the solubilisation/SMALP extraction buffer. This mixture was incubated for 3 hours at room temperature (RT) with gentle shaking on a roller, once the opaque sample become clear as a result of SMALP encapsulation of protein-lipid fragments, the sample was ultra-centrifuged at 42000 rpm for 1 hour 15 minutes at 4 °C using Ti-45 rotor, and high-speed soluble membrane fraction (in the supernatant) was collected and incubated with 1 or 2 ml Nickel-charged affinity resin (Ni-Nitrilotriacetic acid; Ni-NTA) overnight at 4 °C cold room on a rocker. SMALP-proteins bound to Ni²⁺-charged resins through recombinant histidine tags were purified through immobilized metal affinity chromatography (IMAC) (section 2.4.4.1.) where his-tagged proteins (extracted by SMALP) eluted with 500 mM imidazole Ni-NTA buffer (50 mM Tris-HCl/HEPES, 500 mM KCl, 5% v/v glycerol, pH 8) by flowing through the over-night incubation and washed the beads with varying imidazole wash buffers - W₁₀ (50mL), W₂₀ (50 ml) and W₅₀ (25 ml), which containing 10 mM, 20 mM and 50 mM imidazole respectively (**Table 2.2**) in succession. The high imidazole in the buffer with eluted protein(s), was removed

and exchanged to SEC buffer either by overnight dialysis using Snake skin dialysis tube (ThermoFisher, UK; MWCO 3.5 kDa) at 4 ° C; or by centrifuging the imidazole buffer through the Viva-spin 20 (Sartorius, UK) filter tubes (MWCO 10 - 50 kDa) and topping up with fresh SEC buffer every 15 minutes imidazole in the buffers diluted below 50 mM. During this buffer exchange the above filter tube prevents protein(s) (sizing above specified MWCO) to flow-through the filter tube but not the imidazole in the buffer, thereby proteins are collected in the filter tube and resuspended in the freshly added SEC buffers. Following buffer exchange, very little amount (0.06 - 0.08% v/v Triton-X-100 or about 3 - 4 CMC) of Triton-X-100 or DDM (3 - 4 CMC; used only during trials) was added to the sample containing SMALP-protein(s) and incubated for about 30 to 60 minutes before concentrated down to 500 µL in the same above filter tubes by centrifugation at 4500 rpm. The same concentrated samples (about 500 µL) collected in a microcentrifuge tubes and centrifuged at 13,500 rcf for 15 min to pellet any precipitate/aggregate before further separation and purification of the SMALP-protein using size exclusion chromatography (SEC; Superose 6 10/300 GL or Superdex 200 Increase 10/300 GL; GE Healthcare). Fractions were monitored using UV-spectra associated with the ACTA pure device.

Table 2.10. Concentration of antibiotics used in cell culture

| | | A | B | | | | |
|-----------------------|-----------------------------|-----------------------------|---------------------------------------|--------------------------------------|--------------------------------------|---------------------------------------|-----------------------|
| | Stock Conc. ^C | Final Conc. ^D | Kan | Chlor | Strep /Spect | Amp | |
| | mg/mL | µg/mL | µg /mL | µg /mL | µg /mL | µg /mL | |
| Amp (A) | 100 | 100 | A: 100; K: 25; C: 18; S: 25; | A: 100; C: 35; C: 0; K: 25; | A: 100; S: 25; C: 18; A: 0; | A: 100; A: 0; C: 35; C: 0; | Chlor (C) |
| Kan (K) | 50 | 50 | K: 50; K: 0; S: 50; S: 0; | K: 25; C: 18; S: 25; K: 0; | K: 25; S: 18; S: 0; A: 100; | K: 25; A: 100; S: 25; C: 18; | Strep /Spec (S) |
| Chlor (C) | 35 | 35 | C: 18; K: 25; A: 100; S: 25; | C: 35; C: 0; A: 100; K: 25; | C: 18; S: 25; A: 100; A: 0; | C: 35; A: 100; A: 0; C: 0; | Amp (A) |
| Strep /Spec (S) | 50 | 50 | S: 50; K: 50; K: 0; S: 0; | S: 25; C: 18; K: 25; K: 0; | S: 25; S: 0; K: 25; A: 100 | S: 25; A: 100; K: 25; C: 18; | Kan (K) |
| | | | Strep /Spec (S) | Kan (K) | Amp (A) | Chlor (C) | |

A: Concentration of antibiotics in culture media with cells containing single plasmid that provide resistance to single antibiotics.

B: Concentration of antibiotics in culture media with cells containing combination multiple plasmids that contribute resistance to multiple antibiotics.

C: Stock concentration of antibiotics; **D:** Final concentration of antibiotics

Amp (A): Ampicillin; **Kan (K):** Kanamycin; **Chlor (C):** Chloramphenicol; **Strep/Spec (S):** Streptomycin/Spectinomycin.

Combination of antibiotics are arranged clockwise starting from left. It follows as left–top–right–bottom manner (Initials represent antibiotics and numbers are concentrations in µg).

2.4.3.1.1. Reconstitution of SMALP extracted protein from separate inductions

Reconstitution of SMALP-proteins was performed by mixing two SMALP-protein samples that collected (elutes) following IMAC purification and incubating for 2 hours or overnight in a dialysis bag, while dialysis was performed at the same time to remove imidazole and exchanging to SEC buffer (without imidazole) (**Table 2.2**). Following reconstitution and dialysis, the non-reconstituted molecules were further separated on SEC column as mentioned in section (2.4.3.1.).

2.4.3.1.2. Co-expression, co-extraction and co-purification (Co-EEP) of SMALP-Proteins

When *E. coli* cells co-transformed with multiple plasmids (2-3 plasmids) each carrying genes of interest, distinct origin of replications and genes of antibiotic resistance, these cells co-expressed proteins of interest successfully under optimised condition as mentioned above (2.4.2.) except the concentration of multiple antibiotics. During the cell culture with multiple antibiotics specially with Kanamycin, Chloramphenicol and Streptomycin/Spectinomycin, these antibiotics were used half of their usual recommended concentration as used in most laboratory experiments and this project (**Table 2.10**). Co-expressed proteins if interacting with each other at membrane, these proteins were further co-extracted as complex using SMALP nanodisc (2.4.3.1.) and co-purified following same IMAC, buffer exchange and SEC procedure as mentioned in section (2.4.3.1.).

2.4.3.2. MP and/or MAP extraction using detergent and purification using IMAC and SEC

Detergent extraction of MP and MAP was performed by DDM detergent. Membrane pellets were resuspended and homogenized (see section 2.4.3.1.) in DDM extraction buffer (**Table 2.2**) but without DDM. It was not added in the buffer during homogenization in order to avoid formation of foams and bubbles. For DDM solubilisation, membranes were resuspended and homogenized at 200 - 300 mg/mL concentration. While 2% DDM (w/v) solution was prepared by

diluting 20% DDM (w/v) stock solution 10-fold into same extraction buffer as used for membrane homogenization. Once prepared, the two solutions, homogenized membrane resuspension and DDM (2%; w/v) solution were mixed at 1:1 ratio, and incubated for 1 hour at cold room or 4 °C. During DDM solubilisation the final concentration of membrane in the mixed solution become 100 – 150 mg/mL and the final concentration of DDM become 1% (w/v). Following incubation, the insoluble membrane fractions were pelleted by ultra-centrifuging the above mixed solution at 42000 rpm using Ti-45 rotor for 1 hour 15 minutes at 4 °C, and the high speed supernatants containing the solubilised MP or MAP in DDM micelle were collected and incubated with Ni-NTA beads (that washed and equilibrated in the same DDM extraction buffer), for 1 to 2 hours on a gentle rocker at 4 °C. The histidine tagged MPs or MAPs (in DDM micelle) bound to Ni-NTA beads were washed and eluted following similar steps as mentioned in section 2.4.3.1. and 2.4.4.1. using DDM IMAC buffers with varying strength of imidazole (**Table 2.2**). The dialysis and further purification by SEC were also performed as mentioned in section 2.4.3.1. except all buffers for the respective steps were containing very little amount of DDM (0.02%; w/v). DDM extracted MPs and MAPs are always stored at 4 °C or in cold room.

2.4.4. Protein purification techniques

2.4.4.1. Immobilised metal affinity chromatography (IMAC)

Initial purification of poly-histidine-tagged proteins were performed by immobilised metal affinity column/chromatography (IMAC). The method originally proposed and developed by Porath et al. (Porath, Carlsson, Olsson, and Belfrage, 1975; Porath and Olin, 1983) and since then the same principle has been routinely used in successful purification of histidine-tagged proteins. Poly-histidine domain containing imidazole rings, has strong natural affinity for positively charged cations particularly for divalent cations such as Ni²⁺ and Co²⁺. Therefore, these divalent cations when crosslinked to insoluble matrix (agarose beads), chelates poly-histidine tagged proteins and immobilize them to agarose beads, which in turn isolate poly-histidine tagged-protein(s) from the pool of proteins in a

sample. Later, the isolated fusion protein can be sequestered/dissociated from the metal divalent cation and thereby from agarose beads by either using imidazole gradient or changing pH or chelating using other metal ions. All these processes destabilize the metal chelation with the imidazole rings in the poly-histidine domain of fused proteins. Among known crosslinking resins or chelating ligands for above divalent cations to agarose beads, nitrilotriacetic acid (NTA), TALON and iminodiacetic acid (IDA) are very popular and routinely have been used for protein purification across the globe. In this project, we used Ni-NTA (ThermoFisher Scientific, UK) and Co-TALON (Clontech, UK) for purification of poly-histidine tagged proteins, whereas strep-tagged proteins were purified using Strep-Tactin® Superflow® (IBA life sciences, UK) following their protocol and using recommended buffers. In general, 2-4 mL of above resins or beads (50% w/v slurry) were collected into disposable columns and the storage buffers were flown-through by gravity-flow, which end-up with a column volume (CV) of about 1-2 mL. Next the columns were washed several times (10 CV) by flowing through sterile ddH₂O to remove any residual storage buffer, before equilibrating (10 CV) them with same extraction buffer as MPs or MAPs were extracted and incubating them 2 hours to overnight with the extracted MPs and MAPs at cold room (4 °C – 6 °C) on a gentle roller for continuous mixing. After incubation the protein extract with beads were flown through the disposable column. All his tagged-proteins were immobilized to beads filtered through the solution and the column beds were washed with wash buffers (**Table 2.2**) W₁₀ (50 mL), W₂₀ (25 mL) and W₅₀ (20 mL), which contain 10 mM, 20 mM and 50 mM imidazole in succession to remove any binding of non-specific proteins or histidine rich proteins. Finally, proteins were eluted in 8 – 10 mL elute buffer E (**Table 2.2**) containing 500 mM imidazole and 300 - 500 mM KCl, which immediately diluted to half (250 mM imidazole) by mixing SEC buffer contain no imidazole. Further, the imidazole was removed by exchanging the buffers to SEC buffer either through dialysis or centrifuging through Viva-spin 20 (Sartorius, UK) filter tubes (MWCO 10 - 50 kDa) as mentioned in section 2.4.3.1. The columns were further treated with 1 mM imidazole buffer to remove any traces of proteins, washed with 20 CV sterile water and 10 CV storage buffer containing 20% (v/v) ethanol. Finally, beads were stored

as 50% (w/v) slurry in same storage in 4 °C. Generally, fresh charged beads were used for protein purification that used for further analysis and characterisation. However, for trial runs the stored beads can be used for couple of times if same proteins are to be purified. Alternatively, beads were stripped off metal ions, cleaned and recharged again with metal ions in between different protein purifications following instructions as directed by the manufacturers.

2.4.4.2. Size-exclusion chromatography (SEC)

Size-exclusion chromatography was performed to separate any aggregated proteins (which are very common among MPs or MAPs) from the pool of protein complex of interest or to separate proteins that are not contributing to that SMALP-proteins complex. IMAC purified protein samples following removing imidazole and exchanging buffer (to SEC buffer), were concentrated down to recommended loading volume (for SEC column) by centrifuging protein filter tubes tube as mentioned above sections (2.4.4.1.) and further centrifuged at high-speed using bench-top centrifuge at 4 °C to remove any precipitates as mentioned (2.4.3.1.). Simultaneously, the SEC column either Superose 6 10/300 GL (GE Healthcare) or Superdex 200 Increase 10/300 GL (GE Healthcare) in filtered storage buffer (20% v/v Ethanol) were washed with sterile and filters water (4 CV) and equilibrated with 2 CV SEC buffer (**Table 2.2**). Once equilibrated and occasionally columns were calibrated running known low-to-high MW marker proteins as supplied in a kit (GE Healthcare) or simply by running BSA (10 - 16 mg/mL) through the SEC columns using selected SEC buffer as equilibrated. This calibration helps estimating the unknown size of the separated/purified protein(s) or protein complex. Samples were loaded onto column through a super-loop (for 0.5 mL or 1 mL). SECs with SMALP-proteins were performed in both RT and in cold cabinet (4 °C - 6 °C), whereas with detergent-protein micelles the SECs were always perform in cold cabinet. The column was installed to ACTA pure machine (GE Healthcare) and controlled by in-built software which allows to set up a program for each run. A complete elution of protein(s) was performed with 1.5 CV SEC buffer by passing through the column at a set flow speed of 0.5 to 0.75 mL/min, when the column and

system pressure as well as other features were set as per directions from manufacturer protocol. Resolution or separation of the protein(s) was monitored using in-built UV-traces at 280 nm, additionally 260 nm and 215 nm traces were also monitored for any indication of nucleotide binding or contamination and random short peptides respectively. Fractions were collected in a 96-well fraction collector plate through an automated fraction collection system. Once all fractions are collected proteins were stored immediately in cold room or fridge at 4 ° C for short-term and quick screen and analysis, later selected fractions were aliquoted in 20 – 50 µL in several microcentrifuges and were flash frozen in liquid nitrogen before stored in -80 ° C freezer for long term.

2.4.5. Protein measurement

Protein(s) concentration in the cell lysate or purified samples was determined either by Biorad reagent or BCA reagents (Bio-rad Ltd., UK) following manufacturer's protocol. Alternatively, for SEC purified samples the Nanodrop ND-1000 Spectrophotometer (Nanodrop Technologies) was used to determine the protein concentration by measuring the absorbance at 280 nm ($A_{280\text{nm}}$) and calculating the molecular weight and molar extinction coefficient. However, the latter technique only followed for the estimation of single protein concentration. For protein complex as mentioned above mostly Biorad reagent was used to measure the absorbance at 595 nm (A_{595}) and concentrations were calculated following a standard curve with BSA and considering the volume added to the mix.

2.4.6. Protein characterisation and analysis using biochemical and biophysical techniques

2.4.6.1. Native polyacrylamide gel electrophoresis (Native-PAGE) analysis

Proteins separated through IMAC and SEC column were collected in a 96-well fractions collector where each fraction volume was set to 500 μ L. Fractions under prominent peaks as observed in the chromatogram were screened using native-PAGE for analysing native size of protein(s) of interest and any sign of formation of complex or aggregated proteins. As the name indicates protein(s) or protein complex were not reduced or denatures or the native structure was not alerted during native-PAGE except applying current during electrophoresis. Before loading on to native gel, the purified protein(s) from SEC fractions or other IMAC purification steps, were mixed with non-reducing 1x native protein sample buffer (from concentrated 5xNPSB) (Table 2.2). For each native protein run either BSA or proteins markers (for calibrating SEC column) were run alongside to estimate the size of the separated protein(s). Native gels (8% - 10%; v/v) were either made manually or the Mini/Midi-protean Tris-Glycine (TGX) stain free pre-cast gels (Any kDa or 4-20%) (Bio-Rad, UK) were used to resolve native proteins using native gel running buffer (1x) under constant voltage of 80 V or 100 V until the dye reaches the bottom. Once complete the run, the gel with resolved native proteins were stained with Coomassie blue (Instant blue, Expedeon - ISB1L) stain for couple of hours before washed off extra unused stain by ddH₂O and visualized/images protein bands under white light. Running native protein run with SMALP-proteins have extra advantage over DDM/detergent-protein micelle, that is SMALP itself has negative charge which helps migrating its bound lipid disk and thus protein or protein complex. All native-PAGE was performed in the cold room at 4 - 6 ° C.

2.4.6.2. Sodium dodecyl sulphate polyacrylamide gel electrophoresis (SDS-PAGE)

Expressed proteins in small-scale studies and the purified SMALP proteins were reduced and separated on SDS-PAGE in order to check the purity of the purified samples and confirm the expression of proteins of interests based on their size. SDS-PAGE also an important step to analyse separated proteins further by mass-spectrometry, by Western blot and immunoassay to identity of the proteins of interest. Before loading protein samples onto PAGE, proteins from cell lysates were reduced by 0.1M DTT that added to sample buffer (1x) (diluted from 4x SB, Sigma, UK) and denatured by heating at ~ 95 ° C for 5 minutes. However, purified MPs or MAPs were not heated at 95 ° C but incubated with above reducing sample buffer (RSB; that contain DTT and 1xSB) at 37 ° C for about 20 to 30 minutes. For small-scale comparison studies, approximately 20 µg of total proteins were reduced and loaded on to 18-combs Midi-protean Tris-Glycine (TGX) stain free pre-cast gels (BioRad, UK). Whereas, for proteins from different steps of IMAC purifications and for screening SEC fractions for purified proteins, about 20 µL of proteins were mixed and incubated with 1x RSB as mentioned above and 25-30 µL of the same mixtures were loaded onto either manually made polyacrylamide gels (10% - 12%) or onto Mini/Midi-protean Tris-Glycine (TGX) stain free pre-cast gels (Any kDa or 4 - 20%) (BioRad, UK). For routine screening purposes gels were made manually following standard recipes for stacking gel and resolving/separating gel, as originally recommended by Laemmli (Laemmli, 1970). In all cases, the electrophoresis conducted using SDS-PAGE running buffer (1x) (**Table 2.2**) under constant 150 V until the protein marker(s) reached the bottom of the gel. The separated proteins on pre-cast gels were then either stained for Coomassie (instant blue; Expedeon - ISB1L) or directly transblotted to PVDF membrane and immunoassays. Coomassie stained gels were further washed couple of times with ddH₂O before imaging them using Bio-Rad imaging machine, the same also used to imaging stain-free precast gels.

2.4.6.3. Western blot (WB) and immunoassay

Following SDS-PAGE proteins were transblotted to a PVDF membrane using a Western blot kit (Bio-Rad, UK) and tagged (Strep- and/or His-tagged) proteins were immunoassayed (IA) using HRP conjugated primary antibodies against His-tag (1:500; Roche, UK). Before any of these this antibody assays, the PVDF membranes (that binds transferred proteins) were washed once with TBS and twice with TBS that containing 0.01% (v/v) Tween20 (TBS/T). All washes were performed for 10 minutes each. Washed PVDF membrane was incubated with blocking buffer containing BSA (4%; w/v) in TBS/T, to prevent any non-specific binding during antibody assay. The blocking was generally performed for overnight. Next, the blocking buffer was discarded and a biotin blocker (1:1000; IBA, UK) was added and incubated for 30 minutes at room temperature with gentle shaking. This biotin blocker (1:1000; IBA, UK) was optional and only used to block any endogenously synthesized biotinylated proteins, which may potentially bind anti-strep-tactin monoclonal (mAb) (IBA, UK) and show false positive results. Therefore, the same blocker was not necessarily used for assays using Anti-His₆-HRP antibody. During primary antibody assays, the mouse monoclonal Strep-Tactin®-HRP (IBA, UK) and mouse monoclonal Anti-His₆-Peroxidase (Roche, UK) were added to 10 – 20 ml blocking buffer (including biotin blocker 1:1000 where necessary) at 1:500 and 1:1000 ratio respectively. The primary antibody incubations were performed either on separate Western blots or on the same blot, for two hours, at room temperature with gentle shaking. Following primary antibody incubations, blots were washed 3 times with TBS/T, and 2 times with TBS buffer to wash off any unbound or non-specific binding of primary antibody. All washes were performed with gentle shaking for 15-20 minutes at room temperature. Protein(s) tagged with either Strep-tag or His-tag or both binds to HRP conjugated antibodies during immunoassays, were visualised using ECL (Enhanced Chemiluminescent) substrate from Clarity (Bio-rad, UK) following manufacturer's protocol, and capturing the image of the blot using a gel imager (GE healthcare, UK) by setting up varying exposures.

2.4.6.4. In-gel protein digestion and mass-spectrometry

Protein bands with desired size in the SDS-PAGE gel, were identified by degerming the peptide sequences in those bands of interest and comparing the exclusive unique peptides to primary sequence any particular protein. About 20 -50 μg of complex protein mixture was loaded on to each well of a gel and reduced or non-reduce protein mixtures were resolved up on SDS-PAGE and native-PAGE respectively. Following Coomassie staining and imaging/visualizing separated protein bands on the gels, the protein bands of interest that estimated close to correct size or completely unknown protein bands, were excised by fresh razor/scalpel. All selected bands were excised very carefully as tight as possible, so that there is no cross-contamination with other proteins in close proximity in the same lane or next in the gel. Gel slice containing our protein of interest or completely unknown protein, was sliced into cubes about 2-4 mm size and transferred into a 1.5 mL microcentrifuge tube. Coomassie stain of the protein was destained by 50 mM ammonium bicarbonate (ABC) solution with 50% (v/v) ethanol (**Table 2.2**) at room temperature or 55 ° C for 20 shaking on a bench top shaker at 650 rpm. This destaining step was repeated at least three times or until the gel bands were clear and every time the liquid in the tube replaced with fresh destain/wash solution. Next, gel slices in small cubes were dehydrated by incubating them in 100% ethanol solution at RT for 5 minutes on a shaker at 650 rpm, and protein in those gel cubes was reduced and alkylated by incubating with a solution (reduction/alkylation) containing 10 mM TCEP (reducing agent) and 40 mM CAA (see **Table 2.2**) for 5 minutes at 70 ° C with gentle vortex. After alkylation protein in the gel cubes were washed three times and dehydrated to remove all liquid as before using same solutions and conditions as mentioned above. Protein in the gel cubes then digested using Trypsin enzyme in solution (at 2.5 ng/ μL in 50 mM ABC) while rehydrating at the same time. Initially, a small volume of the Trypsin solution that was just enough to rehydrate the gel cubes, was added to the tube and incubated for 10 minutes at RT. So that most of the Trypsin can reach to the protein and digest efficiently. Later, the digestion mix (gel cubes with protein in the Trypsin solution) was topped-up to gel volume with fresh ABC solution (50 mM ABC) to avoid any dehydration during an overnight digestion at 37 ° C. Next day, peptides from

protein digestion, were extracted by adding 50 μL peptide extraction solution containing 25% (v/v) ACN and 5% (v/v) FA (**Table 2.2**) and incubating on a sonicating water bath for 5 to 10 minutes at RT before transferring the extracted solution to a fresh microcentrifuge tube. This extraction and sonication steps were repeated twice more by adding 50 μL peptide extraction solution to the gel cubes and collecting the extracted peptide (in solution) to the above fresh microcentrifuge tube. This way total about 150-200 μL of extracted solution with peptides was collected in the tube. Further the peptide concentration was increased by reducing the volume down to 20 μL using rotating speed-vacuum machine at 40-50 $^{\circ}\text{C}$. Finally, the peptides were resuspended in peptide resuspension solution containing 2% (v/v) ACN and 0.1% (v/v) TFA (**Table 2.2**) to a final volume of 50 μL before transferred the sample to special vial that is suitable for mass-spectrometer. The mass-spectrometry and data annotations were performed by the proteomics facility at University of Warwick (UK). Results were analysed using the Scaffold software.

2.4.6.5. ATP-binding assay

ATP binding assay was performed using an ATP fluorescent analogue BODIPYTM FL ATP- γ -S, (Adenosine 5'-O-(3-Thiotriphosphate), BODIPYTM FL Thioester, Sodium Salt) (A22184; ThermoFisher Scientific, UK). Purified protein samples were incubated with BODIPY-ATP- γ -S (5 μM) and MgCl_2 (5 mM) for an hour, while their respective control assays were performed either absence of MgCl_2 or absence of both BODIPY-ATP- γ -S and MgCl_2 . Following incubation all protein samples were separated upon non-reducing Native-PAGE and gels were imaged by exciting protein bands at 473 nm and filtered emission around 510 nm. Further the same gels were visualized under white light using Coomassie stain.

2.4.6.6. ATP-hydrolysis assay

ATP hydrolysis ability of the purified protein complexes was determined by a standard pyruvate kinase and lactate dehydrogenase coupled enzyme assay as described in previous studies (Bajaj et al., 2016; Orelle, Ayvaz, Everly, Klug, and Davidson, 2008). Each assay was performed with 1 to 5 μg of purified protein

complexes in total volume of 200 μ L HEPES (50 mM, pH 8.0) buffer that containing 1.5 mM ATP, 5 mM $MgCl_2$, 1 mM DTT, 50 mM KCl, 2 mM phosphoenolpyruvate (PEP), 0.3 mM NADH, pyruvate kinase 60 μ g/mL, lactate dehydrogenase 32 μ g/mL. The reduced absorbance for NADH at 340 nm, was an indicator of ATP-hydrolysis, recorded using spectrophotometer at 25 °C for 30 min. Where necessary samples were normalised or corrected against blank which do not contain any ATP.

2.4.6.7. Dynamic light scattering (DLS)

High-throughput, automated dynamic light-scattering of the SMALP-protein(s) were performed using DynaPro Plate Reader (Wyatt Technology) to check size distribution of the SMALP-protein disks and to screen good SEC fractions which are without any aggregated protein or particles, for further AUC, Negative staining EM and Cryo-EM analysis.

2.4.6.8. Analytical ultracentrifugation (AUC)

Analytical ultracentrifugation (AUC) with SMALP-protein samples were performed with a volume of 500 μ L and the OD ranging between 0.1 and 1.0. All samples were run parallelly with its blank containing the same buffer as SMALP-protein sample. All AUCs were performed at 30,000 RPM for 12 hours at 20 °C using a Beckman XL-I analytical ultracentrifuge with an AN-50Ti rotor. During the run absorbance at 280 nm (A_{280nm}) traces were recorded and data were processed and analysed using SEDFIT by fitting to the c(s) model and extracting data to excel.

2.5. Microscopy techniques

2.5.1. Visualizing cells using confocal airy-scan microscopy

Synchronised cells (as mentioned above in section 2.2.3.) were grown until OD_{600nm} reaches approximately 3, when 100 μ L of culture was spun on a bench-top centrifuge for 1 min at 8000 rpm. Cell pellet was washed by resuspending the pellet

in 100 mL PBS and re-centrifuging the pellet again at 8000 rpm. The washed pellet resuspended in 100 μ L PBS with FM4-64 (1:100; ThermoFisher, UK) and DAPI (4',6-diamidino-2-phenylindole; 1:100) and incubated for 5 minutes at 37 °C. Following incubation, 5-10 μ L of sample pipetted onto agarose pad in order to immobilize live bacteria cells and covered carefully using cover slips. Bacterial membrane was stained and visualised with lipophilic dye FM4-64 (excitation/emission maxima \sim 488/640 nm), while bacterial nucleus was stained using DAPI (excitation/emission \sim 405/450 nm). Images were captured as a Z-stack (2-3 μ m) of 20-25 optical slices (0.14 μ m) processed under airy scan program and projected based on maximum intensity calculation. Images with red fluorescent represent FM4-64 stain and blue represents DAPI stain.

2.5.2. Visualizing proteins using Negative staining and electron microscopy (EM)

Negative staining of the purified SMALP-protein (3 μ L at a concentration between 80 and 100 μ g/mL) was performed using uranyl-acetate stain (2%; w/v) on a glow-discharged EM grade continuous carbon grid and imaged using Jeol 2100 (200kV). Negative stained EM images were processed using EMAN2.2 programs.

2.5.3. Visualizing proteins using Cryo-EM

Grids (Quantifoil R1.2/1.3, UK) for cryo-electron microscopy (Cryo-EM) were glow-discharged (for 1 min) and coated with graphene oxide (GO) following standard protocol (1 min incubation with GO following 3 washes with double distilled water). Samples (3 μ L at a concentration between 40 and 80 μ g/mL) were incubated for 30 seconds on GO coated grids before blotted for 7-8 seconds and plunged-frozen into liquid-ethane using Leica EM GP - Automatic Plunge Freezer (Leica Microsystem, UK). Frozen grids with protein were transferred to an FEG transmission electron microscope Jeol 2200FS (200kV). Images were captured using an estimated dose of 16 electrons/ \AA^2 for 0.5 s exposures.

CHAPTER 3. Heterologous expression and purification of individual proteins involved with ABC-transporter and PG hydrolase complex

3.1. INTRODUCTION

Separation of cells into two daughter cells, is one of the critical steps in the bacterial cell division process. As described in chapter 1 (section 1.7.) there is considerable genetic and biochemical evidence that this process is coordinated by an ABC-transporter like protein complex FtsEX, in combination with the actin homologue FtsA and the PG hydrolase PcsB in Gram-positive *S. pneumoniae* bacteria. In order to study how these proteins assemble the PG separation machinery and coordinate the cell separation process, first we need to understand the effect on cell phenotype of their individual gene expression. Mutant and knock-out (KO) of many of *S. pneumoniae* divisome related genes including *ftsA*, *ftsE*, *ftsX* and *pcsB* have been examined in *S. pneumoniae* compatible knock-out strains and phenotypes have been reported before (Barendt et al., 2009; Mura et al., 2017; Sham et al., 2011; Sham et al., 2013). However, many of these strains are not suitable for overproduction of those divisome proteins to allow both *in-vivo* and *in-vitro* studies due to limitations of the available expression tools and system. Hence there is a need for a suitable heterologous expression system and it is necessary, particularly for the divisome proteins, to test for their cross-interaction with a heterologous divisome. In this study we observed for any phenotype due to heterologous expression of *S. pneumoniae* divisome proteins in an *E. coli* host strain. In the first instance, we chose to simply express each individual protein, access phenotypic character and develop *in-vitro* purification as vessels to further biochemical characterization. Expression constructs based on *E. coli* pETDuet, pACYCduet and pCDFDuet vectors were constructed bearing the genes for *S. pneumoniae* *ftsA*, *ftsE*,

ftsX and *pcsB* and thus allow later co-expression of these proteins in the same cell using compatible vectors backbones. This strategy will allow the examination of the interaction between the divisome proteins expressed and also to host proteins which may result in phenotypic observations within the host cell. Some heterologous expression systems are inevitable for large-scale purification and structural analysis of proteins from pathogenic bacterial species. Such was the case, in this study where an *E. coli* host strain was used to express and purify *S. pneumoniae* divisome proteins of interest in order to characterise them biochemically and biophysically, to study their interactions with other divisome proteins and to analyse their structures. In this chapter, heterologous expressions and *in-vitro* characterisation of individual components of an *S. pneumoniae* PG separation machine, are reported and discussed.

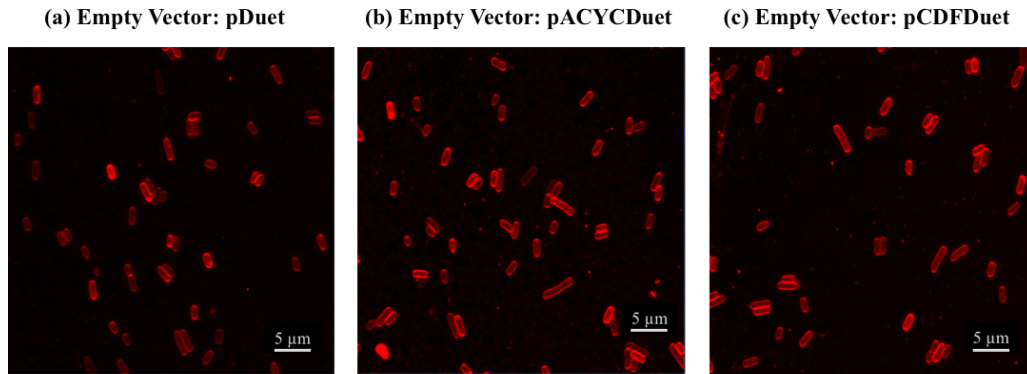
3.2. RESULTS

3.2.1. Heterologous expression of *Streptococcus pneumoniae* FtsE, FtsX, FtsA and PcsB has their distinct phenotypes

S. pneumoniae ftsE, *ftsX*, *ftsA* and *pcsB* genes were amplified and cloned into respective *pDuet* based modified expression plasmid vectors (see **Table 2.4**) and used to transform *E. coli BL21(DE3)ΔacrB::kan^R* strain (**Table 2.3**). In these initial experiments, cells were grown and auto-induced with overnight grow at 20°C to avoid excessive stress on the cells when expressing heterologous proteins. Growth and induction of cells containing the empty vectors produced cells of normal rod shape irrespective of the vector, producing normal rod-shaped cells below 5 μm. (**Figure 3.1a,b,c**). By contrast, cells transformed with expression constructs for *SpftsE*, *SpftsX* and *SpftsA* genes, showed elongated phenotypes compared to cells that have been transformed with empty vector plasmids *pDuet* or *pACYCDuet* (**Figure 3.1. a and b**), Most cells overexpressed with the *SpftsE*, *SpftsX* and *SpftsA* genes elongated over 5 μm and some grown over 25 μm (**Figure 3.1. d, e, and f**). In contrast however, cells transformed and induced with *pcsB* under the same

conditions, did not show similar elongated phenotype and had shapes and sizes comparable to the *pCDFDuet* empty vector phenotype (**Figure 3.1. c**). This strongly suggests the elongation in *E. coli* cells, is a consequence of overexpression of *SpftsE* or *SpFtsX* or *SpftsA* genes. The FM4-64 staining of live cell membranes that overexpressed with these three genes exclusively, shows patchy staining over the length of these cells (yellow arrows; **Figure 3.1. d, e and f**). This may indicate dense packing of lipids in those patchy staining locations. However, it is more abruptly distributed in *SpftsA* (**Figure 3.1. f**) overexpressed membrane compared to *SpftsE* and *SpftsX* (**Figure 3.1. d and e**). In contrast, cells with overexpressed *pcsB* shows uniformly distributed FM4-64 staining along the cell circumference with slight stronger staining at the polar regions, and exhibited minicell-like phenotype (**Figure 3.1. d, e and g**) with marginally smaller cells than normal or empty vector induced cells.

Expression of empty vectors (Controls)



Heterologous expression of *S. pneumoniae* FtsE, FtsX, FtsA and PcsB in *E. coli*

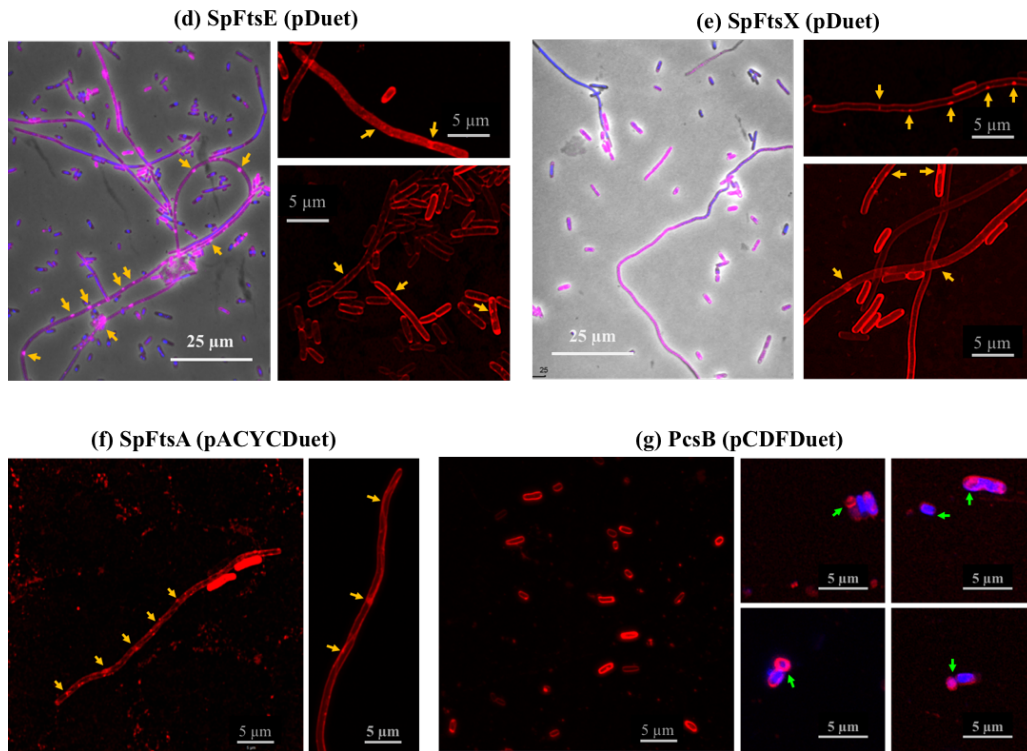


Figure 3.1. Heterologous expression of *S. pneumoniae* divisome proteins. FM4-64 (red) and DAPI (blue) stained *E. coli* cells at 100x magnification transformed with empty vector pETDuet (a), pACYCDuet (b) and pCDFDuet (c) plasmids compared to the same cell line harbouring their respective above expression constructs for SpFtsE (d), SpFtsX (e), SpFtsA (f) and PcsB (g). Merged phase contrast micrograph with FM4-64 and DAPI channels at 40x magnification shows the cell surface morphology of SpFtsE (d: left panel) and SpFtsX (e: left) overproduced cells; whereas 100x magnification micrographs with FM4-64 staining of SpFtsE (d: right panel; top and bottom), SpFtsX (e: right panel; top and bottom) and SpFtsA (f: left and right) shows patchy staining pattern (yellow arrows) in elongated cells. In contrast, PcsB overproduced cells with FM4-64 staining (g: left and right)

shows normal cells, but some were observed with minicell-type formation pointed with green arrows (g: top and bottom images of centre and left panel).

3.2.2. In-vitro characterisation of FtsE, FtsX, FtsA, PcsB in lipid bound SMALP nanodiscs.

3.2.2.1. *S. pneumoniae* FtsE successfully extracted by SMALP nanodiscs possibly in its membrane anchored state for the very first time.

S. pneumoniae *ftsE* with a polyhistidine (6xhistidine) tag (*SpftsE-his₆*) at the C-Terminal, was cloned into modified *pETDuetHETIS* vector (**Table 2.4**) and induced in *E. coli* *BL21(DE3)ΔacrB::kan^R* cells (**Table 2.3**). Overexpressed SpFtsE protein was successfully extracted using SMALPs from corresponding *E. coli* membrane preparations (2.4.2. and 2.4.3.1.). FtsE is the cytoplasmically located as a part of the FtsEX complex and has no discernible membrane anchoring region in its primary sequence. However as has been previously seen with membrane associated proteins (E.g. *E. coli* FtsA: Prof T Dafforn University of Birmingham) SMALP extraction is adept at enabling the purification of such membrane associated proteins and thus likely reflects the membrane associated state of FtsE and has implications of its ability to form a complex with SpFtsX in future reconstitution process with SMALP-SpFtsX. The size-exclusion chromatogram (**Figure 3.2. a**) shows possible presence of monomer, dimer and oligomeric forms of SpFtsE-His₆ in different fractions, which can be directly analysed for its structure organization using negative staining EM. One of such micrographs with SpFtsE-His₆ sample from peak corresponds to dimeric size, is shown in (**Figure 3.2. b**). This extraction for the very first time provides direct evidence of membrane anchoring/association of SpFtsE. Purity of SpFtsE-His₆ was determined with Coomassie stain in SDS-PAGE (**Figure 3.2. c**), the associated histidine-tag was detected with corresponding molecular weight (~ 27 kDa) band for SpFtsE-His₆ through western blot detection with an anti-His-HRP monoclonal antibody (**Figure 3.2. d**). The identity of the same band was independently confirmed through LC-MS/MS analysis and peptide sequencing (**Figure 5.6**).

3.2.2.2. *S. pneumoniae* FtsX with different N-terminal start sites extracted and purified successfully in SMALP nanodisc.

In Gram-negative bacterial strains, *ftsE* and *ftsX* genes are overlapping in an operon and are coordinately expressed with *ftsY* in an operon structure (Appendix **Figure A 7**). However, the coordination with *ftsY* is not retained in Gram-positive strains. The identity of the start codon for the *SpftsE* is easy to discern in such circumstances (Appendix **Figure A 8**). In contrast, *ftsX* has an overlapping N-terminal region (5' end of the gene) with C-terminal region (3' end of the gene) for *ftsE* in both Gram-positive and Gram-negative bacteria (Appendix **Figure A 7** and **Figure A 8**). This is strongly suggestive of coordinated expression and thus regulation of *ftsEX* expression. In case of *S. pneumoniae*, examination of the *ftsX* 5' region of the gene suggests that there are more than one possible methionine (ATG) translation start sites for *ftsX*. In addition, an alternate start codon GTG that code for a valine, could theoretically also initiate translation of *SpftsX*, in *S. pneumoniae* R6 strain (**Figure 3.3**). Initially, we cloned two variants of *SpftsX* with start sites V(M)LSP and MAVS (**Figure 3.3**) and C-terminal histidine (10) tag into *pETDuetHETIS* vector (**Table 2.4**).

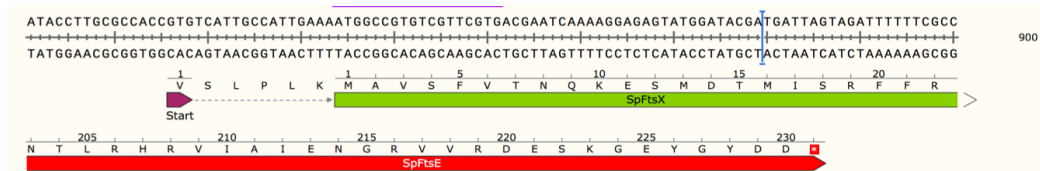


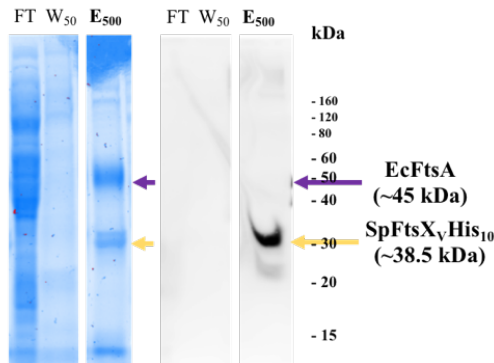
Figure 3.3. Overlap region in sequence of *S. pneumoniae* *ftsEX* operon
The overlap region of *SpftsEX* operon contains multiple start sites for *ftsX*.

Following transformation and induction in *E. coli* BL21(*DE3*) Δ *acrB::kan^R* cells, proteins were extracted using SMALP and purified through Ni-NTA IMAC. Analysis of these purified SpFtsX-His₁₀ protein variants on SDS-PAGE and stain-free gel images showed a band around 38 kDa (**Figure 3.4. a and b**) that also predicted from its amino acid sequence, confirmed by Western blot and immunoassay against His-tag (**Figure 3.4. a and b**). However, the start site with MAVS showed better expression for the same protein compared to V(M)LSP which showed another band in close proximity in Western blot when immunoassayed with monoclonal antibody against His-tag (**Figure 3.4. a and b**). This possibly

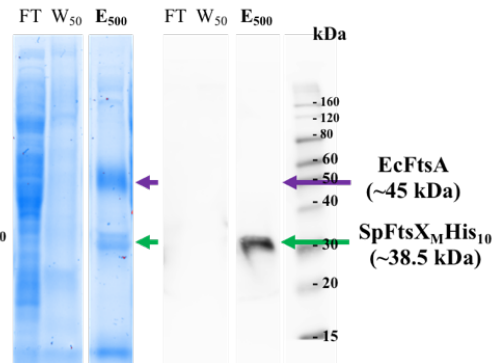
indicates, either degradation of some full length SpFtsX-His₁₀ or translation of another variant from later start site, in low quantity. However, the same band was not observed clearly in stain-free images, probably because of poor sensitivity of this technique to low abundance protein expression. In subsequent experiments, the SpFtsX construct with start site MAVS has been selected for additional purification through SEC following IMAC. The SEC profile indicated presence of different oligomeric form and/or other interactor proteins (**Figure 3.4. c**). Indeed, an additional band was observed at around 46 kDa (**Figure 3.4. e**), which was also noticed in stain-free images with purified both variants of SpFtsX after IMAC (**Figure 3.4. a and b**), later confirmed as *E. coli* FtsA by mass-spectrometry analysis (**Figure 4.17**). Western blot and immunoassay (IA) with monoclonal anti-His antibody (HRP conjugated) recognized the His-tag associated with SpFtsX for same 38 kDa band. However, the same antibody did not detect any other bands that spotted on SDS-PAGE (**Figure 3.4. e**). The detected 38 kDa band on SDS-PAGE and WB-IA, was confirmed as SpFtsX through LC/MS-MS exclusive unique peptide sequencing analysis in later experiments (**Figure 4.17** and **Figure 5.7**)

Although all SpFtsX variants (with start site VLSP and MAVS) translated the SpFtsX-His₁₀ with the predicted molecular weight on SDS-PAGE and were identified with its exclusive unique peptides and with about 50% sequence coverage by mass spectrometry, the latter analysis did not cover the very N-terminal peptide sequence. The N-terminal exclusive unique peptide (FFRHLFEALKSLK) that was found closest to start site of above variants, are about 25 and 19 amino acid far from above start site (VLSP and MAVS) respectively (**Figure 3.3**, **Figure 4.17** and **Figure 5.7**). While we failed to detect the N-terminal start site of SpFtsX protein from those variants through mass-spectrometry analysis, the protein with start site MAVS expressed slightly better and was selected for further experiments with individual or co-expression study. In support of this approach, the transmembrane protein SpFtsX that encapsulated with lipid environment, extracted and purified successfully using SMALP nanodisc. The same nanodiscs with SpFtsX can be visualized in negative stained EM images (**Figure 3.4. d**). The size of these monodispersed SMALP-SpFtsX-His₁₀ disks are ranges between 12 nm and 14 nm.

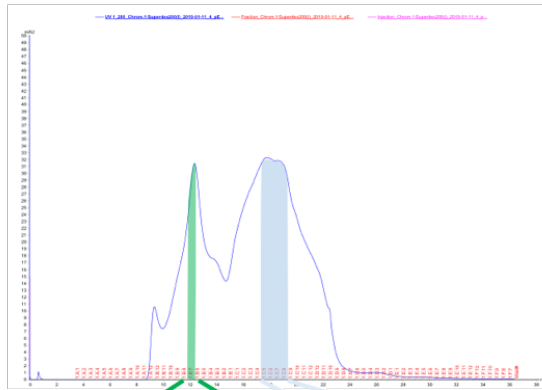
(a) SMALP extraction and purification of SpFtsX_V using Ni-NTA IMAC



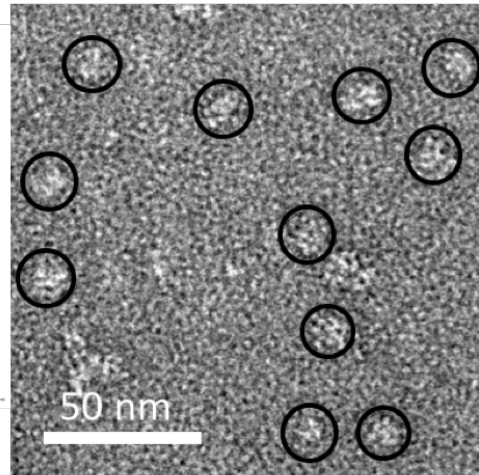
(b) SMALP extraction and purification of SpFtsX_M using Ni-NTA IMAC



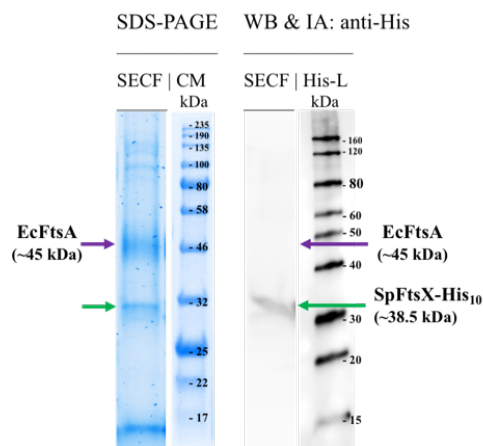
(c) Size exclusion chromatogram of SpFtsX_M in SMALP



(d) Negative stain EM of SpFtsX_M in SMALP nano-disk



(e) SDS-PAGE and WB-IA (mAb xHis) analysis with SEC fractions



(f) SDS-PAGE with lower molecular weight fractions

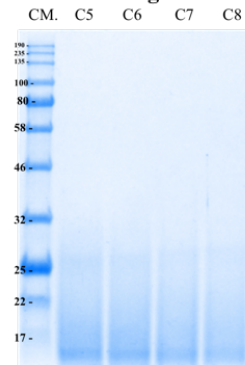


Figure 3.4. SpFtsX in SMALP nanodisks and its cross-interaction with host divisome.

Integral membrane protein SpFtsEX with two possible translation start site (a: SpFtsX_V and b: SpftsX_M) were purified and tested for its expression on

SDS-PAGE (stain-free gel pseudocoloured) and Western Blot-Immunoassay (WB-IA) using monoclonal anti-His antibody (mAbxHis) with HRP conjugated. Selected SpFtsX_M (Ni-NTA IMAC purified) when further purified through SEC, the chromatogram showed two distinct peaks (c). Sample from fractions marked with green area in SEC chromatogram (c) showed monodispersed disk like structures (black circled) that containing SpFtsX in SMALP, in negative stain (UA) EM micrographs (d). The existence of SpFtsX confirmed upon SDS-PAGE and WB-IA analysis using stain-free gel and monoclonal anti-His antibody respectively, where SpFtsX-His₁₀ (~ 38 kDa) surprising found co-purified with host *E. coli* FtsA (~ 45 kDa) (e). The fractions under light blue area in the SEC chromatogram (c) were also analysed upon SDS-PAGE that shows no prominent band for SpFtsX around its corresponding molecular weight, shows more low-molecular weight proteins or degraded proteins (f). FT: Flow-through; W₅₀: Wash with 50 mM imidazole wash buffer; E₅₀₀: Elute with 500 mM imidazole elute buffer; SECF: Size-exclusion chromatography fractions; CM: Coloured marker; His-L: Histidine-tagged ladder; Scale bar as mentioned in the image.

3.2.2.3. *S. pneumoniae* FtsA co-purified with low amount *E. coli* FtsX in SMALP nanodisc.

The eukaryote actin homologue, FtsA (van den Ent et al., 2001) is an essential cell division protein in *S. pneumoniae* (Mura et al., 2017) as well as many other bacterial species (absent in actinobacteria and cyanobacteria). The gene is located in the *dcw* cluster (Ayala, Garrido, De Pedro, and Vicente, 1994) where other cell division and cell wall biosynthesis genes are clustered together (Lara et al., 2005; Massidda et al., 1998; Pucci, Thanassi, Discotto, Kessler, and Dougherty, 1997; Tamames, Gonzalez-Moreno, Mingorance, Valencia, and Vicente, 2001). In *S. pneumoniae* the *ftsA* gene that adjoins *ftsZ*, is located only 16 bps upstream of the latter (Nikolaichik and Donachie, 2000) (Appendix **Figure A 14**). *SpftsA* tagged with 6 histidine residues at the N-terminal (*his*₆-*SpftsA*) was cloned into modified *pACYCDuetHETIS* vector (**Table 2.4**) and induced in *E. coli* BL21(DE3)Δ*acrB*::*kan*^R cells. The overexpression of *his*₆-*SpftsA* evidently showed a clear cell division phenotype *in-vivo* in *E. coli* cells (**Figure 3.1. f**). Since the FtsA protein is predicted as membrane associated protein in previous literature (Pichoff and Lutkenhaus, 2005), we attempted to extract and purify this membrane associated subpopulation within SMALP encapsulated lipid environment.

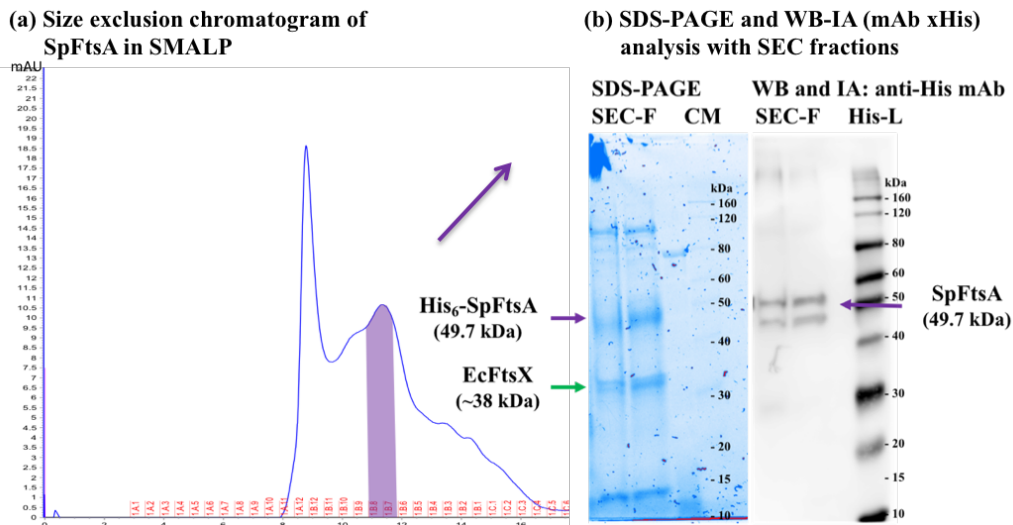


Figure 3.5. Purification of SpFtsA using SMALP.

SMALP extracted SpFtsA purified through Ni-NTA and SEC column showed a prominent peak followed by an near void volume (about 8 ml) peak (for aggregated proteins) in SEC chromatogram (a); selected fractions (marked in purple area in above chromatogram) when analysed on SDS-PAGE, SpFtsA (~49 kDa) that is His₆-tagged N-terminally, co-purified with traces of *E. coli* FtsX (~34 kDa) in the absence of cognate *S. pneumoniae* FtsX, as observed on SDS-PAGE (b: left) but on WB and Immunoassay (b: right) with monoclonal-anti His antibody (mAbxHis-HRP), only His-tagged SpFtsA is detected. The same Immunoblot also detected another close band that is His-tagged. SEC-F: Size exclusion chromatography fractions; CM: Coloured marker; His-L: Histidine-tagged ladder.

The His₆-SpFtsA protein was successfully extracted using SMALP and purified through Ni-NTA IMAC followed by SEC (2.4.3.1.). The chromatogram shows a typical shoulder peak (that is common SEC peak characteristic with SMALP extracted proteins) following a peak near the void volume about 8 ml on superdex 200 increase 10/300 GL (Figure 3.5. a). The SDS-PAGE and stain-free gel imaging of the fractions under marked (purple) peak area, detected the 49 kDa molecular weight band for His₆-SpFtsA (as predicted from amino acid sequence), which further identified by WB-IA (against His-tag) (Figure 3.5. b) and LC/MS-MS peptide sequencing. Notably, Western blotting detected another slightly lower molecular weight band that is His-tagged. The same band were not prominent in stain-free gel image (Figure 3.5. b) as also noticed before with low quantity protein band (see 3.2.2.2. above; Figure 3.4). This slightly lower band could be another

variant of His₆-FtsA that is truncated at the C-terminus. This double band expression also reported before when SpFtsA expressed heterologously in *E. coli* host (Krupka et al., 2014). Additionally, on the same SDS-PAGE analysis another band was detected around 38 kDa, which identified as *E. coli* FtsX through mass spectrometry, was not detected on the same immunoblot assayed with His-tag antibody indicating that this additional protein did not have a histidine tag (**Figure 3.5. b**).

3.2.2.4. Successful extraction and purification of PcsB using SMALP nanodisc indicates a possible presence of lipid binding site in PcsB structure.

PcsB has been reported be essential in the D39 and R6 *S. pneumoniae* strains (Barendt et al., 2009; Giefing-Kroll et al., 2011; Ng, Kazmierczak, and Winkler, 2004; Ng et al., 2003; Ng, Tsui, and Winkler, 2005) and plays a critical role in PG hydrolysis during cell separation process. Consistent with its essential role, the amino acid sequence of PcsB is highly conserved in all serotypes of *S. pneumoniae*, and the *pcsB* gene is the only essential member of the regulon controlled by the WalRK_{Spn} (VicRK) two-component system which detects and controls peptidoglycan homeostasis and stress (Sham et al., 2011). Functional activity including PG hydrolysis has not been demonstrated in *in-vitro* with full length PcsB in any experiment so far and is restricted to the isolated cysteine- and histidine-dependent aminohydrolases/peptidases (CHAP) domain (Bartual et al., 2014) highly suggestive that a conformational change is required in the full length protein in order to active this CHAP domain.

In this study we cloned a full length PcsB (including its signal peptide and single membrane spanning helix) that was tagged with a PelB periplasmic secretion signal and a polyhistidine residues (6xhistidine or *his₆*) at the N-terminal and C-terminal respectively, into a *pCDFDuetHETIS* vector (**Table 2.4**). Expression of the same construct has been found functional in *E. coli* BL21(DE3) Δ *acrB::kan^R* cells (**Figure**

3.1. f) and the full length PcsB from a membrane preparation of these cells was successfully extracted and purified using SMALP nanodisc and standard two steps purification (Ni-NTA IMAC and SEC) (2.4.3.1.). SEC chromatogram shows a clear peak following a peak between 10 ml and 12 ml (column volume is about 24 ml) following a peak near void volume (**Figure 3.6. a**). The purity of a 42 kDa band for PcsB was checked by SDS-PAGE and Coomassie staining, whereas the identity was confirmed through WB-IA and peptide sequencing (**Figure 3.6. b**). The successful extraction of full length PcsB using SMALP suggesting that PcsB in isolation may have some affinity for membrane phospholipids without cognate FtsEX, an observation that has previously not been seen.

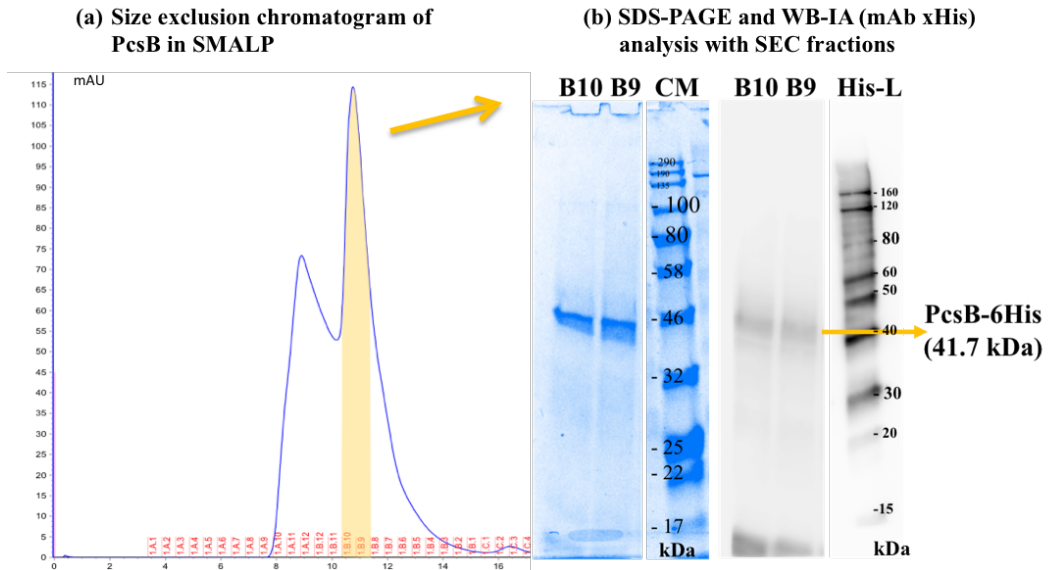


Figure 3.6. PcsB successfully purified using SMALP. SMALP extracted and purified PcsB protein from selected SEC fractions (**a**) shows good purity of PcsB as single band around 42 kDa on SDS-PAGE (**b: left**), the same band also detected on Western blot and immunoassay (WB-IA) (**b: right**). CM: Coloured marker; His-L: Histidine-tagged ladder.

3.3. DISCUSSION: *S. pneumoniae* FtsE, FtsX, FtsA and PcsB are functionally active in a heterologous system while interacting with host lipid and divisome proteins

A large-scale expression study with *S. pneumoniae* divisome proteins FtsA, FtsE, FtsX and PcsB and their structural and functional relationships in native cell lines, are still missing in the literature due to a lack of suitable compatible *S. pneumoniae* strains and expression systems. The study of the structure and function of pneumococcal cell divisome proteins not only allows better understanding of the cell division process and related anti-microbial resistance mechanisms of *S. pneumoniae*, but also provides new innovative strategies to combat this challenging pneumococcal pathogen and its related diseases. The functional and *in-vivo* interactions studies are generally performed by the existing and developing complementation/mutagenesis systems, which results in poor expression and low production of protein yields; and the yields have generally been found lowest in case of most membrane proteins and such as the case for most bacterial divisome proteins. This insufficient yield of proteins restricts the usage of these precious, low abundant membrane proteins for a series of *in-vitro* biochemical, biophysical characterisations and further structural/functional analysis. With the above limitations in pneumococcal expression systems, we need to depend on heterologous expression systems for large-scale protein production, high-yield purification and *in-vitro* characterisations of the purified proteins.

The *E. coli* expression system is one of the most convenient and cost-effective systems for heterologous protein expression and has been used for this study for *in-vitro* characterisation of SpFtsA, SpFtsE, SpFtsX and PcsB divisome proteins. However, the *E. coli* heterologous system does have limitations in expressing certain foreign genes and so as for *S. pneumoniae* genes, because of codon bias, post-translation modification, insolubility/inclusion body problem and protein toxicity. The last two often considered to cause toxicity to the host *E. coli* cell and consequently shows phenotypic change, slow growth rate and effects on viability of *E. coli* cells following expression of heterologous genes (Rosano and Ceccarelli,

2014). This is particularly interesting because it has been previously noted that mutating or effecting Fts proteins resulted in elongated or concatenated cells, static growths and cell division defect and in some cases cell death. This is in fact how “Fts” gene and their protein products were first identified as a result of phenotypic observations of cell growth in certain temperature sensitive mutations in selective genes (Hirota, Ryter, and Jacob, 1968). Whilst Fts genes are often those associated directly with cell division, other genes which produce an Fts phenotype are associated with other activities directly and manifest as cell division mutants due to downstream/polar effects, for example FtsH is a processive, ATP-dependent zinc metallopeptidase that play a dual role in regulating both cytoplasmic and membrane proteins and executes a quality control check of integral membrane proteins (Ito and Akiyama, 2005; Katz and Ron, 2008).

We therefore tested expression and overexpression of our targeted *S. pneumoniae* divisome proteins in *E. coli* heterologous expression system and examined phenotypic responses. While similar *in-vivo* overexpression experiments with above proteins using their respective compatible KO *S. pneumoniae* strains, shows gain of function and rescuing cell division defects, the overexpression of the same proteins alone in *E. coli* cells showed a dominant negative effect and elongated cells except PcsB. One of the reasons for this dominant effect could be due to rapid production of these homologue/analogue proteins that changes the stoichiometric ratio at the divisome.

In our study, we noticed a profound dominant negative effect for the overexpression of *SpftsE* and *SpftsA* genes. The overproduction of SpFtsE and SpFtsA alone has been found toxic to divisome as evident and reported before (Du et al., 2016;Krupka et al., 2014). This is most probably due to disruption in ABC signal transducing system involving with FtsX and amidase/hydrolase. Also, we cannot ignore the possible effects of cross communication between *S. pneumoniae* FtsE or FtsX or FtsA and *E. coli* divisome counterparts or other components, which indeed may disrupt the synchronization of the cell division process. By contrast, when PcsB alone was tested, there was no visible effect noticed in heterologously expressed *E. coli* host cells, they are observed with very little difference to a vector only control.

While *E. coli* cells with overexpression of heterologous *SpftsA*, *SpftsE*, *SpftsX* and *pcsB* genes were found to be viable (i.e. the expression of these genes did not kill the cells), and clearly causing elongated phenotypes in the case of *SpftsA*, *SpftsE*, *SpftsX*, the next big challenge was to extract the respective overproduced proteins and purify them within the host lipid context. This is something never attempted before and absolutely crucial to study these either membrane associated/bound (SpFtsE, SpFtsA and PcsB) or integral membrane protein (FtsX). This study is the very first to purify these four proteins successfully in a solubilised form, with surrounding host lipids in SMALP nanodisc, and with sufficiently high yields for biochemical, biophysical and structural/functional analysis. Previous attempts to express solubilise SpFtsE and SpFtsX using detergent solubilisation had only produced FtsX in a detergent solubilised form and FtsE, despite its largely cytoplasmic location, was entirely insoluble (Bajaj et al., 2016). Where SpFtsA and SpFtsX hypothesised as membrane associated and integral membrane protein respectively, successful SMALP extraction of these two proteins are logical. However, a successful extraction SMALP extraction and purification of SpFtsE and PcsB with their lipid surrounding, is interesting and indicating a membrane insertion site in their structure itself. The later has been hypothesized to dock on the transmembrane subunit (SpFtsX) of an ABC transporter like protein complex SpFtsEX (Rued et al., 2019; Sham et al., 2011) and a previous study found PcsB coiled-coiled (CC) domain binds to charged phospholipids preferentially phosphatidylethanolamine. However, in case of heterologous *E. coli* lipids, the purified individual CC(PcsB)-His and CHAP(PcsB)-His domains exhibited affinities for mixtures of both polar and total lipids from *E. coli* (Bajaj et al., 2016). Together with all these evidences along with the successful extraction PcsB in SMALP nanodisc through this study, suggests PcsB may not just depend on SpFtsX to dock, but to membrane lipid as well. A mechanism of how PcsB inserts to the membrane lipids and/or dock into FtsX as well as its modus operandi in PG hydrolysis using FtsEX ABC transporter like system, would be an interesting question to explore.

CHAPTER 4. Heterologous expression and *in-vitro* characterisation of FtsEX complex

4.1. INTRODUCTION

The protein complex FtsEX is one of a dozen necessary filamentous temperature sensitive (Fts) proteins that are part of active divisome in *E. coli* (Aarsman et al., 2005; Errington, Daniel, and Scheffers, 2003; Goehring and Beckwith, 2005; Nanninga, 1998; Weiss, 2004). Since the identification FtsE and FtsX as members of Fts group of proteins and the location of their genes in an overlapping operon along with *ftsY* (Gill, Hatfull, and Salmond, 1986), their roles and essentiality in cell division, have been not been clearly understood but are linked to certain environmental conditions including high osmotic strength (de Leeuw et al., 1999; Reddy, 2007; Schmidt et al., 2004; Taschner et al., 1988). FtsE and FtsX arrive at the divisome around early-to-mid cell cycle stage and form a complex that has recently been proposed to have roles in assembling other downstream Fts or cell division related proteins into divisome, as well as in regulating the divisome activity (Du et al., 2019; Du et al., 2016). Although these roles are critical, it is hypothesised to be regulated through an interaction between FtsA and FtsX (Du et al., 2019) as is investigated further in Chapter 5. As described in Chapter 1 (section 1.7.), these two proteins form an ABC-transporter like protein complex where FtsE contributes an ATP binding subunit and FtsX to transmembrane subunit (Schmidt et al., 2004). In *E. coli*, this complex was initially predicted to have a role in transportation of salts (de Leeuw et al., 1999), but later the speculation has been rejected (Reddy, 2007). Instead, a very significant role in anchoring amidase or PG hydrolase (EnvC in *E. coli* and PcsB in *S. pneumoniae*) and in regulating the PG hydrolysis event, has been emerged from recent research into the role of the FtsEX complex (Meisner et al., 2013; Sham et al., 2011; Sham et al., 2013; Yang et al., 2011). Their association is further examined in this study in Chapter 5.

In most Gram-negative bacteria like *E. coli*, the *ftsY* is located adjacent (generally few base pairs upstream) of the *ftsEX* gene cluster. Together it is also known as *ftsYEX* operon (Appendix **Figure A 7**). The FtsY acts as a receptor to signal recognition particle (SRP) that has been predicted to be involved in incorporation of FtsEX and other proteins appropriately into the plasma membrane (de Leeuw et al., 1999; Gill and Salmond, 1987, 1990). By contrast, in most Gram-positive bacteria like *S. pneumoniae* the same *ftsY* gene is not located at the same operon as *ftsEX* but in position more distant in the genome. While the evolutionary reason behind this difference between most Gram-positive and Gram-negative bacteria, is still unknown; it may be related to the absence of an outer membrane in Gram-positive bacteria. It is possible that the function of FtsY in relation to the SEC system (Kuhn, Koch, and Dalbey, 2017) for secretion of unfolded proteins across the cytoplasmic membrane into the extracellular space.

In this Chapter 4, we focused our study on *S. pneumoniae* FtsEX (SpFtsEX). While the FtsEX is conditionally essential in *E. coli* and many other rod-shaped bacteria (Du et al., 2019; Meisner et al., 2013; Reddy, 2007; Schmidt et al., 2004; Yang et al., 2011), the complex is utterly essential in *S. pneumoniae* (Sham et al., 2011). Deletion of either gene from the *S. pneumoniae ftsEX* cluster, is not tolerated and attenuation of FtsEX caused abnormal cell shape and growth inhibition (Sham et al., 2011; Sham et al., 2013). Like many other bacteria, in *S. pneumoniae* the *ftsE* and *ftsX* are not only located in same operon, but also overlap by several base pairs (bps) between them. Dependent on the true translation start site for FtsX, in *E. coli* there is an overlap of either 35 or 8 bps can be noticed between *EcftsE* and *EcftsX* (Appendix **Figure A 7**). Likewise, in *S. pneumoniae* the overlap is suspected to be of either 71 bps or 53 bps (Appendix **Figure A 8**). Until now, a full-length FtsEX from *E. coli* or *M. tuberculosis* or *S. pneumoniae*, has not been reported to purify as a complex, probably because overexpression in isolation of these two proteins in *E. coli* cells has been observed to have toxic effect (Bajaj et al., 2016; de Leeuw et al., 1999; Mir et al., 2015; Mir et al., 2006). Only one group report a successful attempt to purify *S. pneumoniae* FtsE and full-length FtsX in isolation, but not in form of a complex, also quantity of both proteins was problematic, particularly

SpFtsE (Bajaj et al., 2016). In our study, individual expression of these two proteins indicated similar toxic effects, where we observed elongated cells, but these cells were viable and grew normally at low temperature. The results from individual heterologous expression and purification of SpFtsE and SpFtsX, encouraged us to express the full length SpFtsEX as complex from the overlapping operon of *SpftsEX*. This work therefore extends previous observation of SpFtsE and SpFtsX isolation and characterization (Bajaj et al., 2016).

In this chapter, we tested the overexpression and feasibility to purify SpFtsEX as protein complex as encapsulated within *E. coli* host lipid environment by SMALP. This is particularly important in order to understand their interactions with other cell divisome proteins while surrounded within host membrane lipids. This purification strategy (SMALP encapsulation) may be advantageous to mimic the *in-vivo* membrane bound conditions for FtsEX which would allow us to analyse the behavior of the proteins complex using, in *in-vitro* experiments.

In order to achieve this, either the whole overlapping operon or individual genes from the same operon were cloned into expression vectors and expressed from them heterologously in *E. coli* cell lines. Expression conditions were optimised through small-scale studies before extracting and purifying this protein either as complex or individually in large scale. Both reconstitution (for individually purified protein) (2.4.3.1.1.) as well as co-expression, co-extraction and co-purification (Co-EEP) strategies (2.4.3.1.2.) were employed to purify SpFtsEX as complex with its surrounding host lipids and interacting proteins, in SMALP nanodiscs.

4.2. RESULTS

4.2.1. Overexpression of *S. pneumoniae* *ftsEX* operon (with 5'-end Strep tag and 3'-end His-tagged) in *E. coli* *Lemo21(DE3)::cam^R* cells

Initially, the *S. pneumoniae* *ftsEX* overlapping operon was cloned into a commercial expression vector *pET-52b(+)* that provides a *strep*-tag and *10-histidine* tag (*his₁₀*) at the 5'-end and 3'-end respectively (**Table 2.4**). The multiple cloning site (MCS) of *pET-52* was designed in such a way, so that the first open reading frame (ORF) should translate SpFtsE with N-terminal (NT) Strep-tag (Strep-SpFtsE) and the second overlapping ORF should translate SpFtsX with (CT) His₁₀-tag (SpFtsX-His₁₀) proteins. The expression of the construct was first tested and optimised in a small-scale study and later tested in a large-scale preparation using the same optimised condition.

The expression conditions for this construct was initially optimized in *E. coli* *Lemo21(DE3)::cam^R* strain in order to test if the *pLemo* system that could control T7 RNA polymerase (T7RNAP) activity by producing its natural inhibitor T7 Lysozyme Y (a T7RNAP repressor) under an efficient titratable rhamnose promoter (*P_{rhaBAD}*) (Wagner et al., 2008). Therefore, by varying the concentration of L-Rhamnose, it is possible to modulate the expression of T7RNAP inversely via T7LysY. This feature of the Lemo21 (DE3) competent cells provides an extra control to prevent any oversaturation and unwanted aggregation of the expressed protein from a transformed foreign construct. This also provides chloramphenicol resistance for further specific selection of transformed colonies. During these small-scale overexpression study, a concentration of L-rhamnose, IPTG induction temperature and length of induction were optimised (see section **Appendix A2**).

4.2.1.1. Large-scale overexpression, SMALP extraction and purification screens for SpFtsE and SpFtsX from overlapping *SpftsEX* operon in *E. coli Lemo21(DE3)::cam^R*

4.2.1.1.1. SMALP successfully extracted SpFtsEX, but high salt concentration in extraction and purification buffers possibly reduced the yield of strep-tagged SpFtsE

Large-scale overexpression study was performed using optimised conditions achieved from small-scale studies with *pET-52b(+)-strep-SpftsEX-his₁₀* constructs (**Table 2.4**) as mentioned in the small-scale studies (see **Appendix A2**). Initially, an overnight inoculum (10 mL) of a single colony of *Lemo21(DE3)::cam^R* competent cells (**Table 2.3**) that was freshly transformed with above constructs, were used to inoculate fresh 1 L culture volume. A total of 2 L or 4 L cultures were grown until OD_{600nm} reaches 0.4 at 37 °C. At this point cultures were moved to 20 °C incubator to reduce the temperature before an IPTG induction (0.4 mM) in between OD_{600nm} 0.5 and 0.6, and grown overnight at 20 °C. Next day, cells were harvested, and membrane was pelleted following protocol as mentioned in (2.4.2.). Proteins from the membrane were extracted using SMALPs and purified with His-tag/Ni-NTA in high salt (500 mM) NaCl buffer. The purity of elutes were checked using SDS-PAGE (**Figure 4.1.a**) and further expression of SpFtsE and SpFtsX were confirmed by western blot and immunoassays against their Strep- and His-tag respectively (**Figure 4.1. b and c**). However, an attempt of double purification using two-tags system (Ni-NTA IMAC for His-tag protein followed by affinity chromatography using Streptactin superflow resin for Strep-tag) was not successful in purifying Strep-SpFtsE (**Appendix Figure A 9**). The expression of purified Strep-SpFtsE after the first IMAC purification was not satisfying compared to purified SpFtsX-His₁₀ protein. The latter expressed and purified well from the membrane fraction and was consistent with the small-scale studies. Notably, the Strep-SpFtsE expression mostly found in the insoluble membrane fraction (IMF) than in eluted fractions (**Figure 4.1. a and b**), which indicates either improper

folding of the protein or an inefficient extraction and solubilisation of Strep-SpFtsE using SMALP.

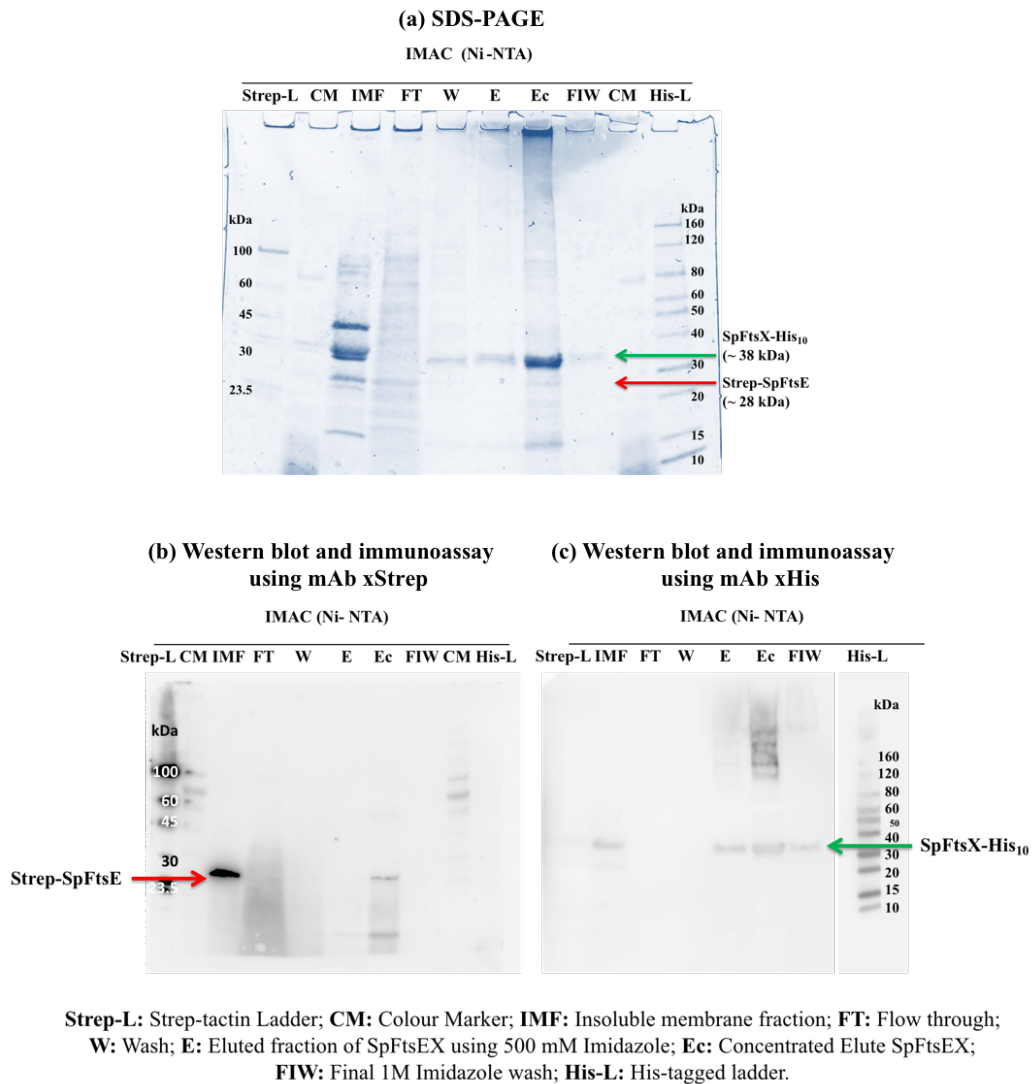


Figure 4.1. Purification of SMALP extracted Strep-SpFtsE and SpFtsX-His₁₀ in high salt (500 mM NaCl) buffers.

SDS-PAGE with samples from different stages of purification process following Coomassie staining of the gel clearly shows the successful purification SMALP extracted SpFtsX-His₁₀ (38 kDa) as well as a faint band for Strep-SpFtsE (28 kDa) in lanes for concentrated elute (Ec) (a). These two proteins were visualised on the Western blot at their corresponding molecular weight band sizes when immunoassayed using monoclonal antibodies against their respective Strep- or His-tag (b and c respectively). Strep-SpFtsE was observed in lanes for IMF and Ec, but most in IMF (b), whereas SpFtsX-His₁₀ was observed in lanes for IMF, E, Ec and FIW, with not much notable difference (c).

One possible reason for the inefficient SMALP extraction of the proteins in this scenario, could be the high salt concentration (500mM) used during SMALP extraction process and further purification steps. This may be affecting the binding of membrane-associated protein SpFtsE with SpFtsX (transmembrane protein). Therefore, in next few screens, in order to increase the yield of both purified proteins, different culture media, IMAC resins (Ni-NTA or Co-Talon) and salt concentration in buffers (that used for extraction and purification of this complex), were tested and optimised.

4.2.1.1.2. Auto-induction media, Nickel-IMAC resin and low salt concentration (NaCl 150 mM) in buffers for SMALP extraction and purification have improved the yield of both Strep-SpFtsE and SpFtsX-His10 proteins

In order to improve the purity and quantity of the SpFtsEX protein complex, firstly IMAC resins were examined. In general, the Co²⁺-resins are known for its higher specificity over Ni²⁺-resins. In an experiment, we tested the total yield and specificity of the purification using Ni-NTA and Co-Talon commercial IMAC beads/resins. These resins were used to purify the SMALP extracted SpFtsEX (in low salt buffers) that expressed in *E. coli Lemo21(DE3)::cam^R* cells grown in LB media and induced by IPTG. The result shows the Ni-NTA resins purified more SpFtsEX protein than Co-Talon. The Co-Talon resin appeared to produce a purer form of elute SpFtsX protein, and the SpFtsE protein band was not notable in the same lane when imaged the stain-free SDS-PAGE gel with all samples (**Figure 4.2**). Overall, the Co-talon showed higher specificity in purifying His-tagged (CT) SpFtsX but failed to purify Strep-tagged (NT) SpFtsE. In comparison, the Ni-NTA has purified both Strep-SpFtsE and SpFtsX-His₁₀ with higher quantity (**Figure 4.2**).

In another separate screening, the growth media and induction methods were reviewed in order to increase the yield of the FtsEX. The induction method using IPTG in LB media was compared with auto induction media (AIM) 2xYT (Formedium, UK) under same optimised growth condition. The AIM increased the

number of *E. coli* *Lemo21(DE3)::cam^R* cells that pelleted 3 - 4 times more cells (in dry weight, g) than cell pellet from LB media (with IPTG induced).

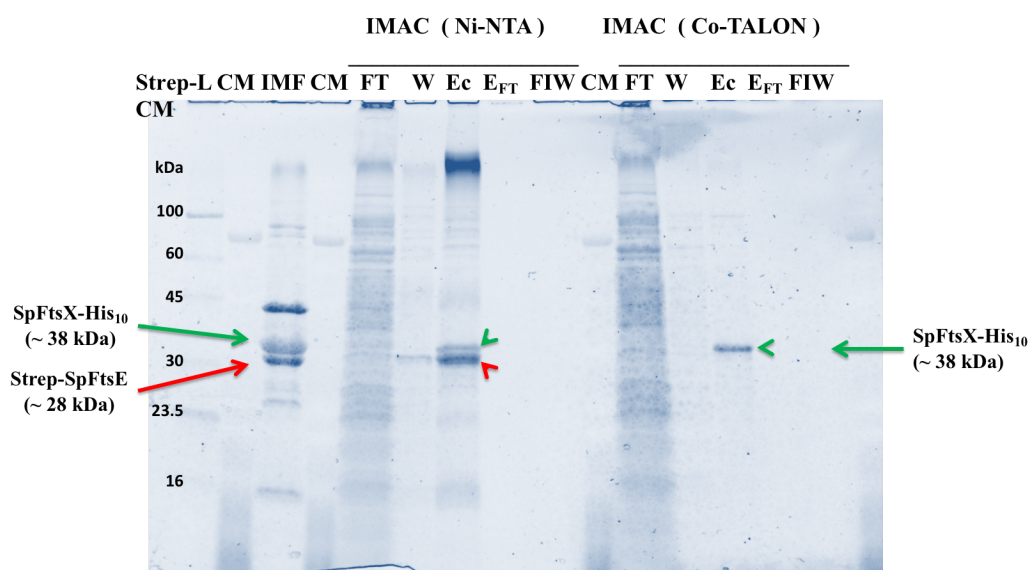


Figure 4.2. Comparison of IMAC resins (Ni-NTA and Co-Talon) in purification SMALP extracted SpFtsEX.

Stain-free image of SDS-PAGE with samples from IMAC (Ni-NTA and Co-Talon) purification using low-salt concentration buffers. Ni-NTA resins showed efficient purification of SpFtsEX as complex compared to Co-Talon. Strep-L: Strep ladder; CM: Colour marker; IMF: Insoluble membrane fraction; FT: Flow-through; W: Wash; Ec: Elute concentrated; FIW: Final imidazole wash; E_{FT}: Flow-through of concentrated elute.

Expressed proteins were extracted using SMALP in low salt concentration (150mM NaCl) buffer and purified using either His-tag/Ni-NTA or His-tag/Co-Talon IMAC followed by further purification using SEC (on Superose 6 10/300 GL). Ni-NTA resin showed marginally higher expression of both proteins Strep-SpFtsE and SpFtsX-His₁₀ from cells that induced in AIM compared to LB media (**Figure 4.3**). However, the same proteins were not found in fractions that eluted from Co-Talon columns (**Figure 4.3**). This could be due to low yield in the first instance when purified through Co-talons as noticed in previous occasion. When the Ni-NTA purified SEC fractions (from cells induced and grown in LB media as well as in AIM) were immunoassayed on separate Western blots using monoclonal HRP conjugated antibodies against Strep- and His-tag, the proteins Strep-SpFtsE and SpFtsX-His₁₀ were identified on their respective blots at their correct MW sizes (~ 27 kDa and ~ 38 kDa), respectively (**Figure 4.3. c and d**). The Western blot shows

better expression of both Strep-SpFtsE and SpFtsX-His₁₀ from cells that induced in AIM than in LB media, as also observed on SDS-PAGE (Figure 4.3. a and b).

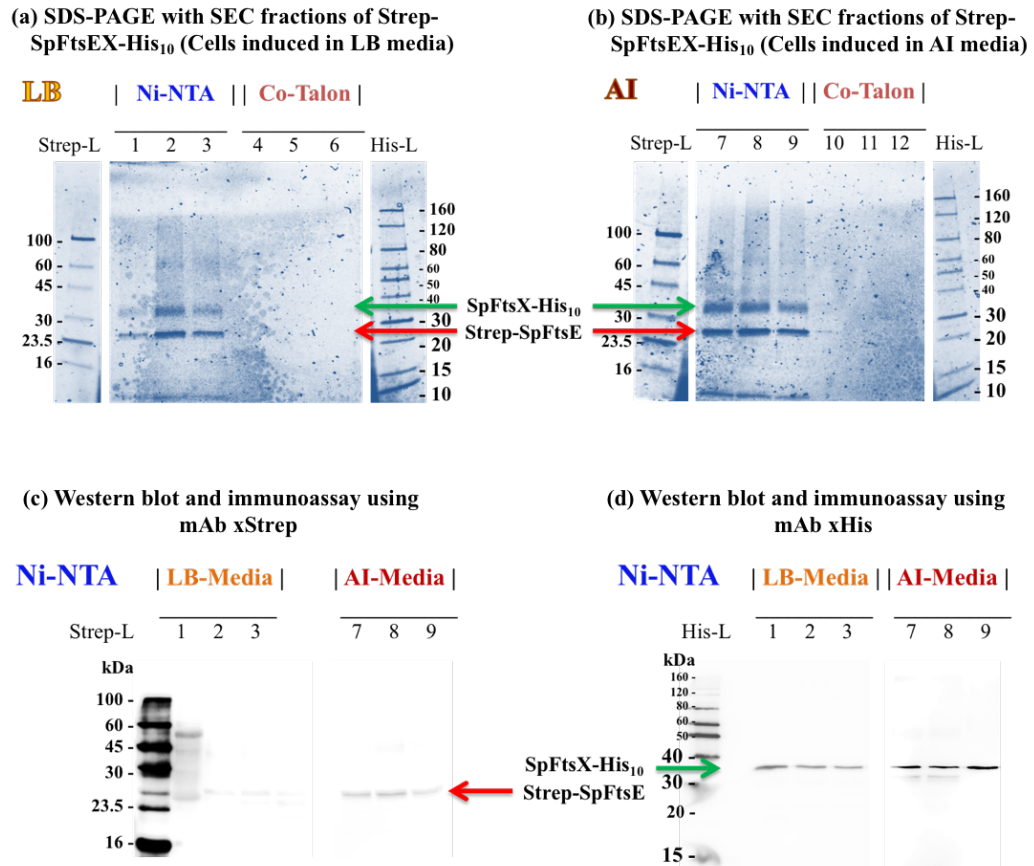


Figure 4.3. Comparison of growth media, induction methods and IMAC resins for purification of SMALP extracted SpFtsEX.

Stain-free SDS-PAGE images (a and b) shows better expression of both SpFtsE and SpFtsX proteins that induced in AI media (b) than LB media (a), and only observed well in lanes (a: 1-3 and b: 7-9) with samples initially purified through Ni-NTA resin, not Co-Talon resin. The same Ni-NTA samples when further analysed on Western blots using monoclonal HRP conjugated antibodies (mAb) against Strep-tag (c) and His-tag (d), the Strep-SpFtsE and SpFtsX-His₁₀ were identified on their respective blots. Consistent to SDS-PAGE, the expressions of both proteins are observed stronger in lanes for AIM than LB media, on Western blots.

Lanes 1-3: Proteins expressed in LB media and purified through Ni-NTA resin; **Lanes 4-6:** Proteins expressed in LB media and purified through Co-Talon resin; **Lanes 7-9:** Proteins expressed AI media and purified through Ni-NTA resin; **Lanes 10-12:** Proteins expressed AI media and purified through Ni-NTA resin. **LB:** Luria-Bertani media; **AIM:** Auto-induction media; **Strep-L:** Strep-tagged ladder; **His-L:** His-tagged ladder.

4.2.1.1.3. SMALP coextracted and copurified *E. coli* AcrB along with successful purification of SpFtsEX as complex using low-salt concentration buffers

An overnight inoculum (in 10 mL LB) of *E. coli* Lemo21(DE3)::*cam*^R cells that transformed with *pET-52b(+)-Strep-FtsEX-His₁₀* construct, was cultured and induced in large scale (as mentioned in 4.2.1.1.1. except addition of IPTG) using auto-induction (2xYT; Formedium, UK) media and optimised growth condition (20 °C; overnight). Since, potassium chloride (KCl) is more relevant to bacterial physiological salt content and reported to stimulate Mg⁺²-induced ATPase activity, a low concentration of KCl salt was used in all steps beginning from cell lysis (137 mM), SMALP extraction and solubilisation of membrane (150 mM), and was maintained at the same concentration throughout the IMAC (His-tag/Ni-NTA) as well as in following SEC (Superose 6 10/300 GL) purification. The SEC UV-trace showed multiple peaks with one highest peak near the void volume and few consecutive shoulder peaks that are very common with SMALP extracted proteins. Repeated experiments with SMALP samples showed very similar characteristic overlapping multiple peaks (**Figure 4.4.a**), instead of having distinct peaks for monomeric or dimeric forms of the purified protein(s). The latter trend generally common for soluble proteins or when extracted with detergents. Seemingly, when the same SpFtsEX was extracted using DDM and purified (IMAC using His-tag/Ni-NTA and SEC using Superose 6 10/300 GL) using same salt concentration (KCl; 150mM) in all buffers, the peaks started appearing much later (**Figure 4.8.b and Appendix Figure A 10**) that is indicating a smaller protein-detergent micelle compared to SMALP extracted proteins, which also surrounds lipid particles. Number of these lipid particles within the SMALP disk may vary, thus in sizes too. Indeed, multiple shoulder peaks in SEC chromatogram with UV280 curves indicates the fractions are a mixture of different sized particles, which can be observed in non-reduced native gels as well as in electron-micrograph of negatively stained (using 2 % uranyl-acetate) protein sample from SEC fraction (**Figure 4.4**).

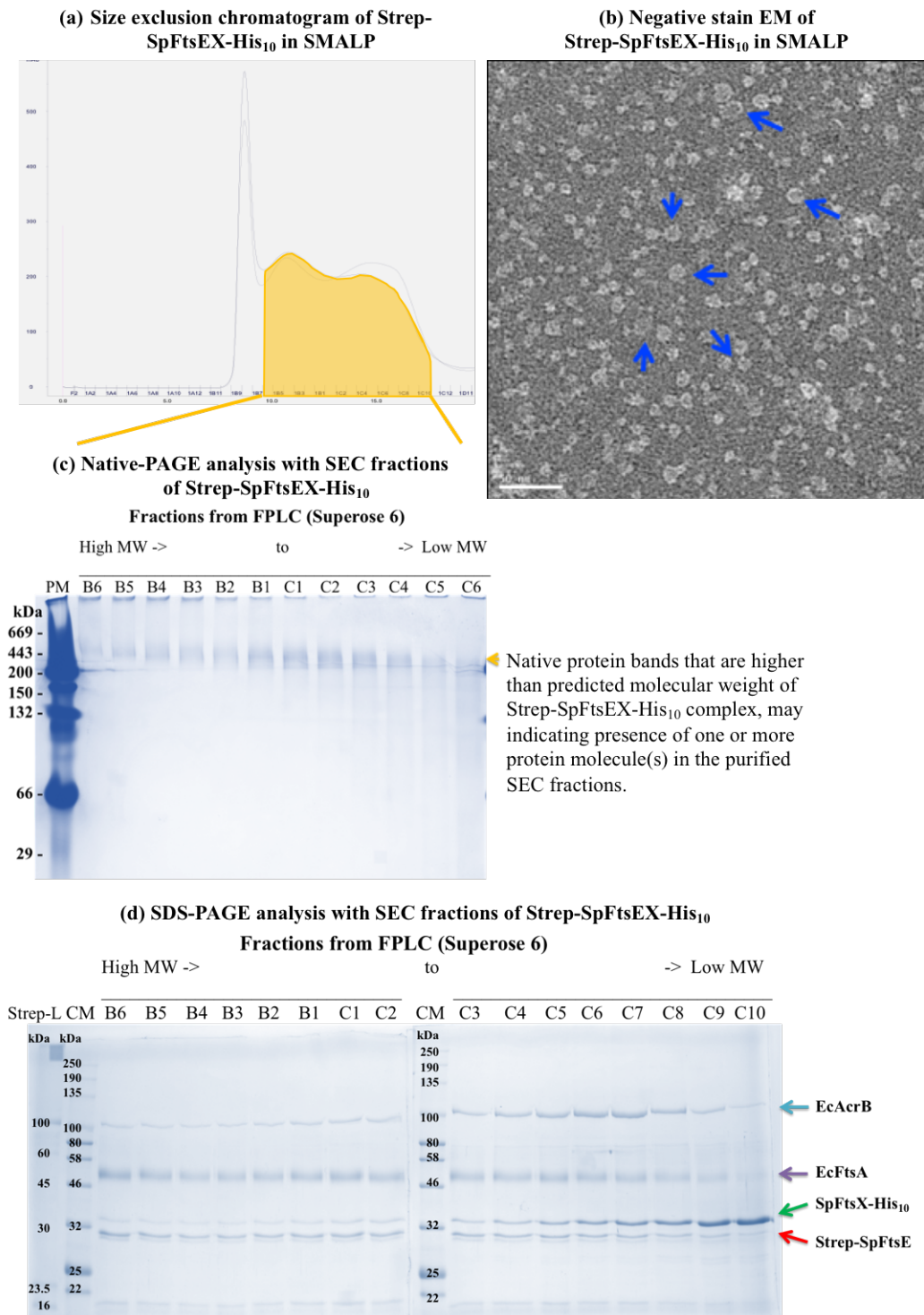


Figure 4.4. Purification of SMALP extracted SpFtsEX from *E. coli* Lemo21(DE3)::cam^R cells

SEC chromatogram shows shoulder peaks for SMALP extracted and IMAC purified SpFtsEX (a). Analysis of same fractions revealed the SMALP-SpFtsEX particles are not monodispersed on Negative stain EM micrograph (b). The Native-PAGE with fractions under yellow peak area shows the complex migrated to higher molecular weight than their respective individual molecular weight (c), suggesting formation of complex. The same SEC

fractions when reduced on SDS-PAGE, the Coomassie staining revealed bands for S. pneumoniae FtsE (~ 27 kDa) and FtsX (~ 38 kDa), along with othr two E. coli proteins FtsA (~ 46 kDa) and AcrB (~114 kDa).

SEC fractions of SMALP extracted and IMAC purified sample, when reduced at both 95 °C (Appendix **Figure A 11**) and 37 °C (**Figure 4.4.d**), both these conditions showed four prominent protein bands. However, some aggregation of proteins was noticed (above ~100 kDa band) in samples reduced at 95 °C for 5 minutes (Appendix **Figure A 11**). This aggregation could be a consequence of heating membrane proteins, which have high hydrophobic regions. This aggregation was not apparent when samples for SDS-PAGE were incubated with loading buffer at 37 °C for 30 minutes, and much clearer gel with four intense bands was observed (**Figure 4.4.d**). Two of these bands identified as Strep-SpFtsE (~28 kDa) and SpFtsX-His₁₀ (~ 38 kDa) when immunoassayed with primary antibodies (anti-Strep-HRP and anti-His-HRP, respectively) against their corresponding Strep- and His-tag respectively (**Figure 4.5**). However, their ratio varied in higher to lower molecular weight SEC fractions (Superose 6 10/300 GL), and only few fractions (C4, C5, C6) showed satisfactory ratio on Coomassie stained SDS-PAGE and Western blots.

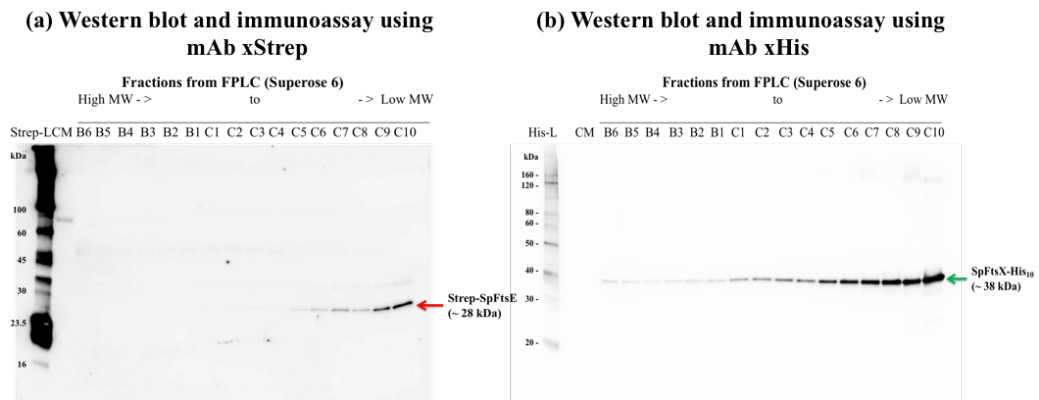


Figure 4.5. Identification of purified SpFtsEX from E. coli Lemo21(DE3)::cam^R cells.

Western blot and immunoassays with anti-Strep-HRP (a) anti-His-HRP (b).

Additional in-gel liquid-chromatography mass-spectroscopy (LC/MS) analysis with these two bands confirmed their identity with about 50% amino acid sequence

match for both proteins as well as identification of 9 and 31 exclusive unique peptides for SpFtsE and SpFtsX respectively (**Figure 4.6. a and b**). Unexpectedly, the same analysis with bands around 110 kDa, revealed an AcrB (~114 kDa) membrane protein contamination (60% amino acid sequence similarity and 85 exclusive unique peptides) (**Figure 4.7**). The other “fuzzy” band around 54 kDa evident a mixture of peptides from both SpFtsE and SpFtsX as well as exclusive unique peptides of *E. coli* FtsA (**Figure 4.6.c**). This mixture could be a consequence of partial denaturation and reduction of the same complex in buffer containing KCl that reacts with LDS (Lithium-Dodecyl-Sulphate) present in reducing sample buffer. The reaction can precipitate KDS (Potassium-Dodecyl-Sulphate) as insoluble salt, thus protein may lose sulphate anions and run as partially denatured product in SDS-PAGE.

(a) Band around 27 kDa: *S. pneumoniae* FtsE (SpFtsE)

Q8DQH4_STRR6 (100%), 25,797.3 Da
 ABC transporter ATP-binding protein & cell division protein OS=Streptococcus pneumoniae (strain ATCC BAA-255 / R6) GN=ftsE PE=4 SV=1
 9 exclusive unique peptides, 10 exclusive unique spectra, 10 total spectra, 113/230 amino acids (49% coverage)

| | | | | |
|--------------|------------|------------|------------|------------|
| MS I IEMRDVV | KKYDNGTTAL | RGVSVSVOPG | EFAYIVGPSG | AGKSTFIRSL |
| YREVKIDKGS | LSVAGFNLVK | IKKKDVPLLR | RSVGVVFODY | KLLPKKTVYE |
| NIAYAMEVIG | ENRRNIKRRV | MEVLDLVGLK | HKVRSFPNEL | SGGEOORIAI |
| ARAIVNNPKV | LIADPTGNL | DPDNSWEIMN | LLERINLQGT | TILMATHNSQ |
| IVNTLRHRVI | AIENGRVVRD | ESKGEYGYDD | | |

(b) Band around 38 kDa: *S. pneumoniae* FtsX (SpFtsX)

Q8DQH3_STRR6 (100%), 36,583.2 Da
 Cell division protein FtsX OS=Streptococcus pneumoniae (strain ATCC BAA-255 / R6) GN=ftsX PE=3 SV=1
 27 exclusive unique peptides, 54 exclusive unique spectra, 193 total spectra, 163/329 amino acids (50% coverage)

| | | | | |
|-------------|------------|-------------|-------------|-------------|
| MSLPLKMAVS | FVTNOKESMD | TMISRFFRHL | FEALKSLKRN | GWMTVAAVSS |
| VMITLTLVAI | FASVIFNTAK | LATDIENNVR | VVVYIRKDVE | DNSOTIEKEG |
| QTVTNNNDYHK | VYDSLKNMST | VKSVTFSSKE | EOYEKLT EIM | GDNWKIFEED |
| ANPLYDAYIV | EANAPNDVKT | IAEDAkkIEG | VSEVODGGAN | TERLFKCLASF |
| IRVWGLGIAA | LLIFIAAFLI | SNTIRITIIIS | RSREIOIMRL | VGAKNSYIRG |
| PFLLLEGAFIG | LLGAIAPSVL | VFIVYOIVYQ | SVNKS LVGQN | LSMISPD LFS |
| PLMIALLFVI | GVFIGSLGSG | ISMRRFLKI | | |

(c) Band around 50 kDa: Mix peptides of SpFtsE, SpFtsX and *E. coli* FtsA (EcFtsA)

Q8DQH4_STRR6 (100%), 25,797.3 Da
 ABC transporter ATP-binding protein & cell division protein OS=Streptococcus pneumoniae (strain ATCC BAA-255 / R6) GN=ftsE PE=4 SV=1
 4 exclusive unique peptides, 4 exclusive unique spectra, 5 total spectra, 48/230 amino acids (21% coverage)

| | | | | |
|--------------|------------|------------|------------|------------|
| MS I IEMRDVV | KKYDNGTTAL | RGVSVSVOPG | EFAYIVGPSG | AGKSTFIRSL |
| YREVKIDKGS | LSVAGFNLVK | IKKKDVPLLR | RSVGVVFODY | KLLPKKTVYE |
| NIAYAMEVIG | ENRRNIKRRV | MEVLDLVGLK | HKVRSFPNEL | SGGEOORIAI |
| ARAIVNNPKV | LIADPTGNL | DPDNSWEIMN | LLERINLQGT | TILMATHNSQ |
| IVNTLRHRVI | AIENGRVVRD | ESKGEYGYDD | | |

Q8DQH3_STRR6 (100%), 36,583.2 Da
 Cell division protein FtsX OS=Streptococcus pneumoniae (strain ATCC BAA-255 / R6) GN=ftsX PE=3 SV=1
 7 exclusive unique peptides, 9 exclusive unique spectra, 10 total spectra, 96/329 amino acids (29% coverage)

| | | | | |
|-------------|------------|-------------|-------------|-------------|
| MSLPLKMAVS | FVTNOKESMD | TMISRFFRHL | FEALKSLKRN | GWMTVAAVSS |
| VMITLTLVAI | FASVIFNTAK | LATDIENNVR | VVVYIRKDVE | DNSOTIEKEG |
| QTVTNNNDYHK | VYDSLKNMST | VKSVTFSSKE | EOYEKLT EIM | GDNWKIFEED |
| ANPLYDAYIV | EANAPNDVKT | IAEDAkkIEG | VSEVODGGAN | TERLFKCLASF |
| IRVWGLGIAA | LLIFIAAFLI | SNTIRITIIIS | RSREIOIMRL | VGAKNSYIRG |
| PFLLLEGAFIG | LLGAIAPSVL | VFIVYOIVYQ | SVNKS LVGQN | LSMISPD LFS |
| PLMIALLFVI | GVFIGSLGSG | ISMRRFLKI | | |

FTSA_ECOLI (100%), 45,328.8 Da
 Cell division protein FtsA OS=Escherichia coli (strain K12) GN=ftsA PE=1 SV=1
 3 exclusive unique peptides, 3 exclusive unique spectra, 3 total spectra, 25/420 amino acids (6% coverage)

| | | | | |
|------------|-------------|-------------|-------------|-------------|
| MIKATDRKLV | VGLEIGTAKV | AALVGEVLPD | GMVNIIGVGS | CPSR GMDKGG |
| VNDLESVVKC | VORAI DOAEL | MADCOISSVY | LALSGKHISC | ONEIGMVPIS |
| EEEVTOEDVE | NVVHTAKSVR | VRDEHRVLLHV | IPOEYAI DYO | EGIKNPVGLS |
| GVRMOAKVHL | ITCHNDMAKN | IVKAVERCGL | KVDQLIFAGL | ASSYSVLTED |
| ERELGVCVVD | IGGGTMDIAV | YTGGALRHTK | VIPYAGNVVT | SDIAYAFGTP |
| PSDAEAIKVR | HGCALGSIVG | KDESVEVPSV | GGRPPRS LOR | OTLAEVIEPR |
| YTELLNLVNE | EILLOLEKLR | OQGVKHH LAA | GIVLTGGAAO | IEGLAAC AOR |
| VFHTOVRIGA | PLNITGLTDY | AQEPYYSTAV | GLLHYGKESH | LNGEA EVEKR |
| VTASVGSWIK | RLNSWLRKEF | | | |

Figure 4.6. LC-MS/MS analysis with bands (27, 38 and 46 kDa) excised from SDS-PAGE.

Band around 114 kDa: *E. coli* AcrB (EcAcrB)

ACRB_ECOLI (100%), 113,576.1 Da
 Multidrug efflux pump subunit AcrB OS=Escherichia coli (strain K12) GN=acrB PE=1 SV=1
 85 exclusive unique peptides, 175 exclusive unique spectra, 339 total spectra, 629/1049 amino acids (60% cov)

| | | | | |
|-------------|-------------|-------------|------------|-------------|
| MPNFFIDRPI | FAWVIAIIM | LAGGLAILKL | PVAOYPTIAP | PAVTISASYP |
| GADAKTVDOT | VTOVLEONMN | GIDNLMYMSS | NSDSTGTVOI | TLTFESGTD |
| DIAOVQVONK | LOLAMP LLPO | EVOOOGVSVE | KSSSSFLMVV | GVINTDGMT |
| OEDISDYVAA | NMKDAISRST | GVGDVOLFSG | OYAMRIWMNP | NELNKFOLTP |
| VDVITAIKAO | NAOVAAGOLG | GTTPPVKGOOL | NASTIAOTRL | TSTEEFGKIL |
| LKVNODGSRV | LLRDVAKIEL | GGENYDIAE | FNGOPASGLG | IKLATGANAL |
| DAAAIRAEL | AKMEPFFPSG | LKIVVYDPTT | PFVKISIEHV | VKTLVEAIL |
| VFLVMYLFLO | NFRATLIPTI | AVPVVLLGTF | AVLAAFQFSI | NTLTMFGMVL |
| AIGLLVDDAI | VVVENVERVM | AEEGLPPKEA | TRKSMGOIQG | ALVGIAMVLS |
| AVFVPMAFFG | GSTGAIYROF | SITIVSAMAL | SVLVALILTP | ALCATMLKPI |
| AKGDHGEK | GFFGWFNRMF | EKSTHHYTDS | VGGILRSTGR | YLVLYLIIVV |
| GMAYLFVRLP | SSFLPDEDQG | VFMTMVOLPA | GATOERTOKV | LNEVTHYILT |
| KEKNNVESVF | AVNGFGFAGR | GONTGIAFVS | LKDWARDPGE | ENKVEAITMR |
| ATRAFISOIKD | AMVFAFNLPA | IVELGTATGF | DFELIDOAGL | GHEKLTQARN |
| OLLAEAAKHP | DMLTSVRPNG | LEDTPOFKID | IDOEKQALG | VSINDINTTL |
| GAAWGSSYVN | DFIDRGRVKK | VYVMSEAKYR | MLPDDIGDWY | VRAADGOMVP |
| FSAFSSSRWE | YGSPrLERYN | GLPSMEILGO | AAPGKSTGEA | MELMEOLASK |
| LPTGCVGYDWT | GMSYOERLSC | NOAPSLYAIS | LIVVFLCLAA | LYESWSIPFS |
| VMLVVP LGVI | GALLAATFRG | LTNDVYFOVG | LTTTIGLSAK | NAILVEFAK |
| DLMDKEGKGL | I EATLDAVRM | RLRPILMTSL | AFILGVMLPV | I STGAGSQAQ |
| NAVGTGVMGG | MVTATVLAIF | FVPVFFVVVR | RRFSRKNEDI | EHSHTVDHH |

Figure 4.7. LC-MS/MS analysis with band (114 kDa) excised from SDS-PAGE.

4.2.1.1.4. DDM extraction did not improve Strep-tagged or untagged SpFtsE expression in *E. coli* Lemo21(DE3)::cam^R cells

The existing plasmid *pET-52b(+)-strep-SpftsEX-his₁₀* (with N-terminal Strep-tag and C-terminal His-tag) was modified by removing the Strep-tag from N-terminal of FtsE (5'-end of *SpftsEX* operon). This resulting plasmid, *pET-52b(+)-SpftsEX-his₁₀* was made aiming to express an untagged SpFtsE and His-tagged (C-terminally) SpFtsX (Table 2.4). The purpose of this modification was to test whether an untagged version of SpFtsE might improve its yield and ratio when copurified with SpFtsX. In addition, this would provide further evidence for a functional complex between FtsE and FtsE since copurification of the complex by IMAC would be dependent entirely on the FtsX C-terminal his tag. Also, in order to avoid any AcrB contamination (AcrB is a common contaminant with IMAC purification from *E. coli*) (Veesler, Blangy, Cambillau, and Sciara, 2008), DDM detergent was used to extract overexpressed proteins from *E. coli* Lemo21(DE3)::cam^R cells. These cells were transformed with above two plasmids, were grown and induced at 20 °C overnight. Proteins were purified following DDM detergent extraction (2.4.3.2.), His-tag/Ni-NTA IMAC and further SEC using optimised KCl salt concentrations as mentioned in section 4.2.1.1.3. above. Purified proteins from both constructs, were reduced and separated on SDS-PAGE. Both plasmids were found overexpressed SpFtsX-His₁₀ protein very well as can be

observed on SDS-PAGE (**Figure 4.8.c**) and Western blot that immunoassayed using monoclonal anti-His antibody (**Figure 4.8.e**). In contrast, the yield of SpFtsE (untagged or Strep-tagged) after purification was not satisfactory and barely notable on stain-free SDS-PAGE gel (**Figure 4.8.c**) possibly due to less sensitivity of stain-free gels for low quantity protein.

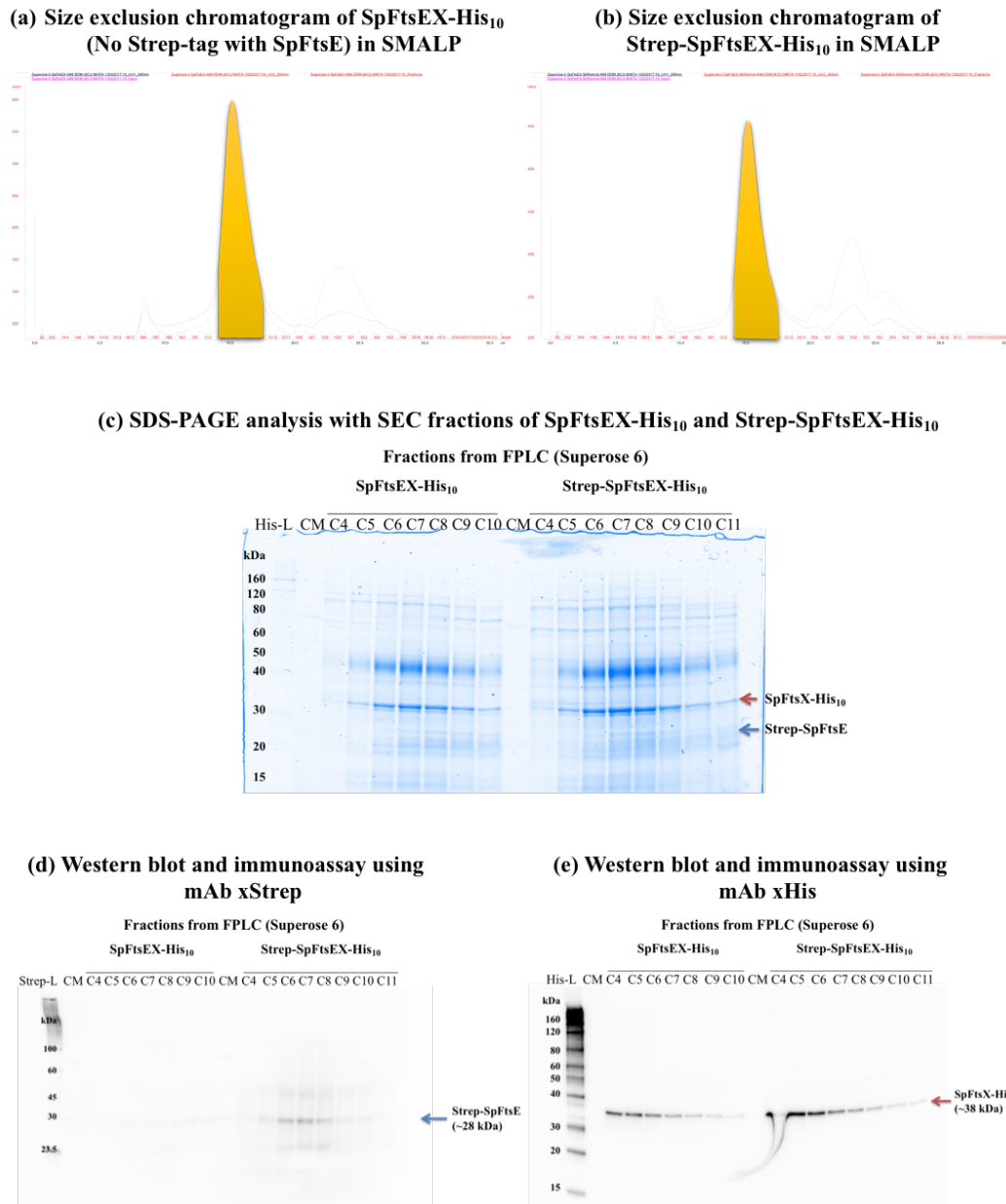


Figure 4.8. Purification of DDM extracted SpFtsEX where SpFtsE was either untagged or Strep-tagged and SpFtsX was His-tagged C-terminally. SEC chromatograms of SpFtsEX-His₁₀ that had untagged-SpFtsE (a) and Strep-tagged SpFtsE (N-terminally) (b). SDS-PAGE and Coomassie staining of SEC fractions of His-tag/Ni-NTA purified SpFtsEX-His₁₀ that was

untagged-SpFtsE (left) and Strep-tagged SpFtsE (right), extracted using DDM, reduced at 37 °C (c). The same samples when immunoassayed using monoclonal antibody against Strep-tag (d) and against His-tag (e) on separate Western blots, these antibodies correctly recognised Strep-SpFtsE but not untagged-SpFtsE (d) and SpFtsX-His₁₀ (e), respectively.

However, the Strep-tagged SpFtsE can be seen on the Western blot with same fractions when immunoassayed using monoclonal anti-Strep antibody (**Figure 4.8.d**). Overall the purity of the DDM extracted samples was not pure in comparison to the SMALP extracted samples and no significant improvement or difference in expression of SpFtsE or FtsX was observed between Strep-tagged and untagged SpFtsE constructs.

4.2.2. Overexpression of *S. pneumoniae ftsE* and *ftsX* either from overlapping operon or separate gene fragments, in *E. coli BL21(DE3)ΔacrB::kan^R* strain

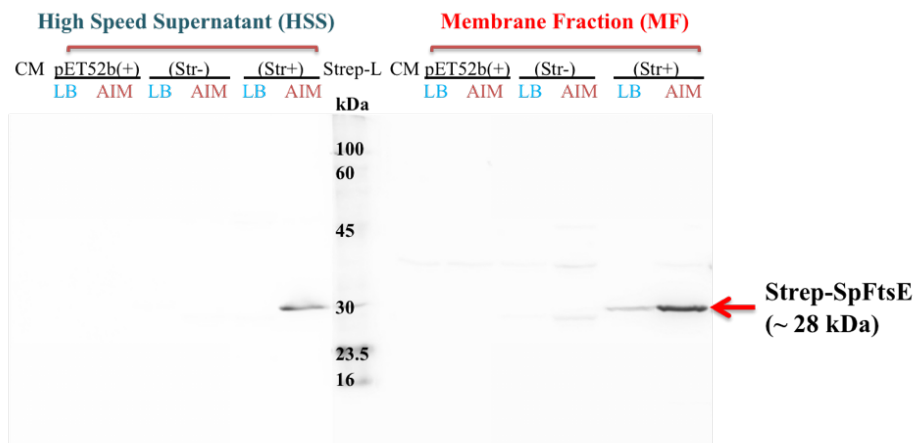
In previous experiment, when the *SpftsEX* overlapping operon was expressed in *E. coli Lemo21(DE3)::cam^R* cells and proteins were extracted from the membrane using SMALP, the complex coextracted and further copurified AcrB along with SpFtsE and SpFtsX. AcrB has been reported as very common contaminant with SMALP extraction of membrane proteins (Veesler et al., 2008). In order to avoid this contaminant, a modified *E. coli* strain with a deletion in the AcrB gene: *E. coli BL21(DE3)ΔAcrB* (**Table 2.3**) has been tested for further large scale SMALP extraction and purification of SpFtsE and SpFtsX from *E. coli* overexpression strains.

4.2.2.1. Small-scale overexpression of overlapping *SpftsEX* (with 5'-end strep and 3'-end his tag) in *E. coli BL21(DE3)ΔacrB::kan^R*

Before committing to any large scale protein production, the existing two plasmids *pET-52b(+)-strep-SpftsEX-his₁₀* (Strep+), *pET-52b(+)-SpftsEX-his₁₀* (Untagged-SpFtsE or Strep-) (**Table 2.4**) described previously were screened for their expression in comparison to empty vector *pET-52b(+)* control. *E. coli*

BL21(DE3)ΔAcrB cells were transformed with these three separate plasmids, and were grown and induced in either LB (IPTG induction) or auto-induction media (AIM) overnight at 20 °C. Membranes were prepared from harvested cells and resuspended in TBS buffer as previously described. Proteins from all these membrane fractions (MF) and their respective high-speed supernatants (HSS), were analysed on separate Western blots where immunoassays using monoclonal anti-Strep-HRP and monoclonal anti-His-HRP has identified and confirmed overexpression Strep-SpFtsE (**Figure 4.9.a**) and SpFtsX-His₁₀ (**Figure 4.9.b**) respectively in MF. The latter was not observed in HSS.

(a) Western blot and immunoassay using mAb xStrep



(b) Western blot and immunoassay using mAb xHis

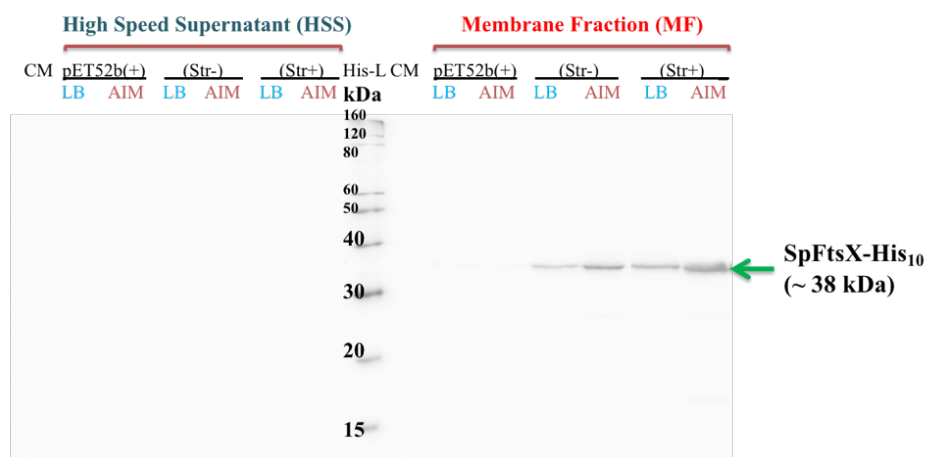


Figure 4.9. Small-scale overexpression of untagged or Strep-tagged *SpFtsE* and *SpFtsX-His₁₀* from overlapping *SpftsEX* operon in *BL21(DE3)ΔacrB::kan^R* cells.

Western blots of overexpressed untagged-SpFtsE, Strep-SpFtsE and SpFtsX-His₁₀ from membrane fraction (MF) and high-speed supernatant (HSS), were immunoassayed separately with mouse monoclonal (mAb) anti-Strep-HRP (a) and with mouse monoclonal (mAb) anti-His-HRP (b). These antibodies confirmed expression of Strep-SpFtsE and SpFtsX-His₁₀ respectively, in membrane fraction (MF) but not in high-speed supernatant (HSS) except in one case where cells induced in auto-induction media (AIM). Empty vector *pET-52b(+)* that was used as control, did not show any expression of above proteins. **Str-**: *pET-52b(+)-SpftsEX-his10*; **Str+**: *pET-52b(+)-strep-SpftsEX-his10*. **LB**: cultures grown in LB media, **AIM**: cultures grown in auto-induction media.

Strep-SpFtsE was only seen in the HSS from AIM that generally has been found to overproduce these proteins in higher quantities than LB. It should be noted that since untagged SpFtsE was used as control and monoclonal anti-Strep-HRP did not recognise any of these untagged SpFtsE from cells induced in LB or AIM in a western blott (**Figure 4.9.a**).

4.2.2.2. Large-scale SMALP extraction of SpFtsE and SpFtsX from membrane fraction of *E. coli BL21(DE3)ΔacrB::kan^R* strain

Large-scale overexpression of plasmid *pET-52b(+)-strep-SpftsEX-his10* was tested in *E. coli BL21(DE3)ΔacrB::kan^R* cells with the above plasmids using autoinduction media following steps as mentioned in the sections 4.2.1.1. and 4.2.1.1.3. above overnight, at 20 °C. SMALP extractions of expressed SpFtsEX protein complex was performed successfully without AcrB contamination that is evident in the SDS-PAGE with SEC fractions (**Figure 4.10.b**). The SEC chromatogram shows a broader peak instead multiple shoulder peaks (**Figure 4.10.a**). Western blot and separate immunoassays clearly verified expression of Strep-SpFtsE (**Figure 4.10.c**) and FtsX-His₁₀ (**Figure 4.10.d**) in the purified fractions. However, very low-level staining of Strep-FtsE on Coomassie stained SDS-PAGE was a major concern with this *pET-52b(+)-Strep-SpFtsEX-His10* construct. This construct was either overproducing more SpFtsX-His₁₀ compared to Strep-SpFtsE or the co-purification of Strep-FtsE using the His-tag associated with SpFtsX was not very efficient to maintain the correct stoichiometry of these proteins throughout the rigorous double purification process. Although the low salt

concentration used in all the extraction and purification buffers slightly improved the expression of Strep-SpFtsE but not at a level that judged to be satisfactory compared to the level of SpFtsX-His₁₀ expression.

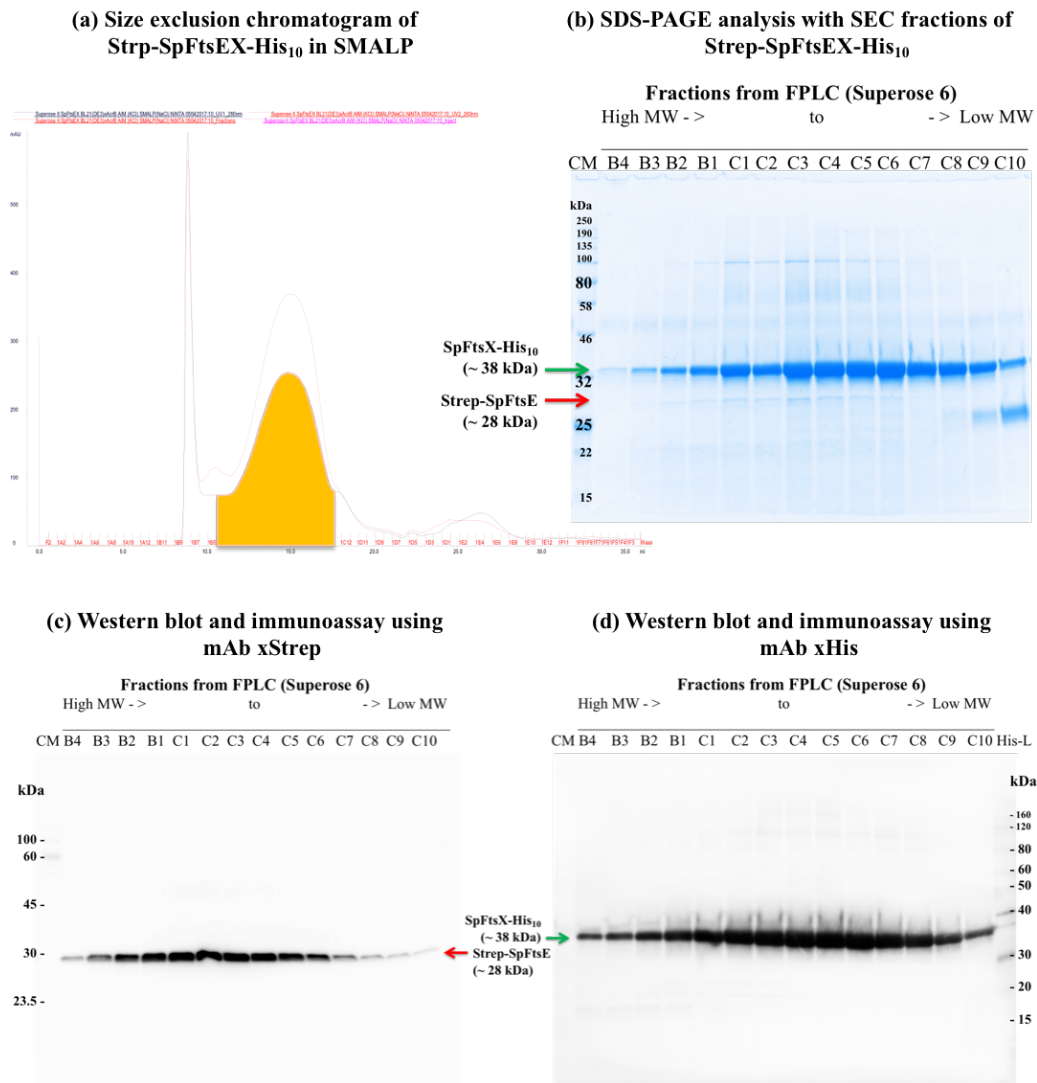


Figure 4.10. SMALP extraction and purification of Strep-FtsSpEX-His₁₀ from *E. coli* BL21(DE3) Δ acrB::kan^R cell membrane. SEC chromatograms of SMALP extracted Strep-SpFtsEX-His₁₀ (a). SDS-PAGE and Coomassie staining of SEC fractions of His-tag/Ni-NTA purified strep-SpFtsEX-His₁₀ that extracted using SMALP, reduced at 37 ° C (b). Immunoassays using monoclonal antibody against Strep-tag (c) and against His-tag (d) on separate Western blots, confirmed presence of Strep-SpFtsE (c) and SpFtsX-His₁₀ (d), respectively.

4.2.2.3. An attempt to co-express and copurify SpFtsE and SpFtsX using multicloning plasmid *pETDuet* system

Successive unsatisfactory expression and purification attempts for Strep-SpFtsE in large-scale studies, lead to a change in strategy from the expression plasmid from *pET-52b(+)* to *pETDuet1* based plasmid. Although both plasmids have an ampicillin resistance gene, the *pETDuet1* based plasmid allows the cloning for two genes as inserts into two tandem and separate multiple cloning sites (MCS1 and MCS2). These cloning sites have their distinct ribosome binding sites (RBS) before start sites but both MCSs regulates under *T7 promoter / lac operator* system associated further upstream of each MCS. In this duet system both *SpftsE* and *SpftsX* genes were tagged with *histidine* (6 and 10 repeated *his* residues respectively) at the 3'-end and inserted into MCS1 and MCS2 respectively. Using this duet plasmid *pETDuet1-SpftsE-his₆-SpftsX-his₁₀*, (**Table 2.4**) we wanted to test whether the expression of separate gene fragments for SpFtsE and SpFtsX, would improve the expression of both proteins. Accordingly, *E. coli* *BL21(DE3)ΔacrB::kan^R* cells that transformed with plasmid *pETDuet1-SpftsE-his₆-SpftsX-his₁₀*, induced overnight in AIM at 20 °C, as mentioned in sections **4.2.1.1.** and **4.2.1.1.3.**). However, an attempt to SMALP extraction and IMAC (His-tag/Ni-NTA) purify of SpFtsE-His₆ and SpFtsX-His₁₀ proteins using low salt concentrations (as described in section **4.2.1.1.3.** above), was contrasting. The duet construct *pETDuet1-SpftsE-his₆-SpftsX-his₁₀* expressed SpFtsE-His₆ very well but this contrasted with the SpFtsX-His₁₀ as observed on Coomassie stained SDS-PAGE gel with SMALP extracted and purified samples (**Figure 4.11.a**). On Western blots, both proteins were identified using monoclonal anti-His-HRP antibody against their associated C-terminal (CT) His-tags, but similar to SDS-PAGE, the enhanced chemiluminescent (ECL) image of the blot showed more SpFtsE-His₆ expression than SpFtsX-His₁₀ (**Figure 4.11.b**). This result is contrary to the conclusion from previous expression trials using *SpftsEX* overlapping operon in plasmid *pET-52b(+)-strep-SpftsEX-his₁₀*, where we noticed more SpFtsX-His₁₀ expression than SpFtsE-His₆. One reason for this low expression of *SpftsX-his₁₀* may be because of the insertion of the FtsX into the second MCS of *pETDuet* which

we note has a different spacer region sequence between the RBS and initiation codon than in the first MCS for pETDuet.

4.2.2.4. Successful reconstitution of SMALP extracted SpFtsE and SpFtsX from separate plasmids and expressions

Following a series of failed attempts to express and purify both SpFtsE and SpFtsX proteins separately with good quantity using SMALP or DDM, we planned to reconstitute these proteins together in SMALP nanodisc (2.4.3.1.1.). In previous attempts, we were successful to SMALP extract and purify either SpFtsE (4.2.2.3.) or SpFtsX (4.2.2.2.) but not both together. In this attempt, reconstitution of separately purified SpFtsE and SpFtsX was performed from two separate / parallel expressions of *E. coli* BL21(DE3) Δ *acrB::kan^R* cells transformed with plasmid *pET22b(+)-SpftsE-his₆ (amp^R)* and other with *pETDuet1-SpftsX-his₁₀ (amp^R)* inserted into MCS1 (Table 2.4). In large-scale trials, both transformed cells were grown and induced separately in AIM overnight at 20 °C, as mentioned in sections 4.2.1.1. and 4.2.1.1.3.). SMALP extraction and IMAC (His-tag/Ni-NTA) purification of both SpFtsE-His₆ and SpFtsX-His₁₀ were performed separately, which shows successful purification of both proteins (in isolation) in good quantity on SDS-PAGE (Figure 4.11.a) and on their respective Western blots (Figure 4.11.b) that immunoassayed using monoclonal anti-His-HRP antibody. Later, these two proteins were reconstituted by mixing and incubating post IMAC purified elutes of two proteins in a dialysis bag (MWCO 3 kDa), while at the same time imidazole was dialysed overnight. Reconstituted proteins in SMALP nanodiscs were further purified on SEC (Superdex 200 Increase 10/300 GL) in order to avoid any aggregation or non-reconstituted forms of purified proteins. SDS-PAGE with SEC fractions confirmed presence of both SpFtsE-His₆ (~ 27 kDa) and SpFtsX-His₁₀ (~ 38 kDa) in the same fractions (Figure 4.11.a). Western blot and immunoassay using above antibody identified the His-tags associated with SpFtsE and SpFtsX at their corresponding molecular weight bands on Western blot (Figure 4.11.b). This indicates a successful reconstitution of SpFtsE-His₆::SpFtsX-His₁₀ in SMALP nanodisc (SMALP-SpFtsEX).

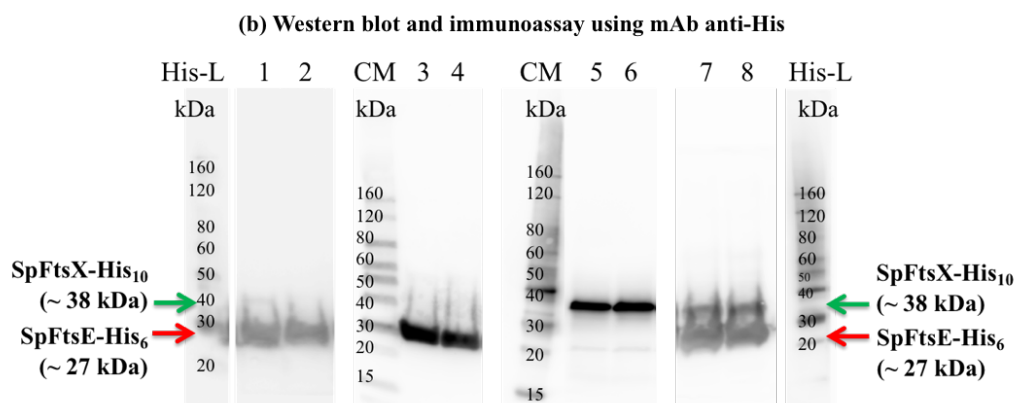
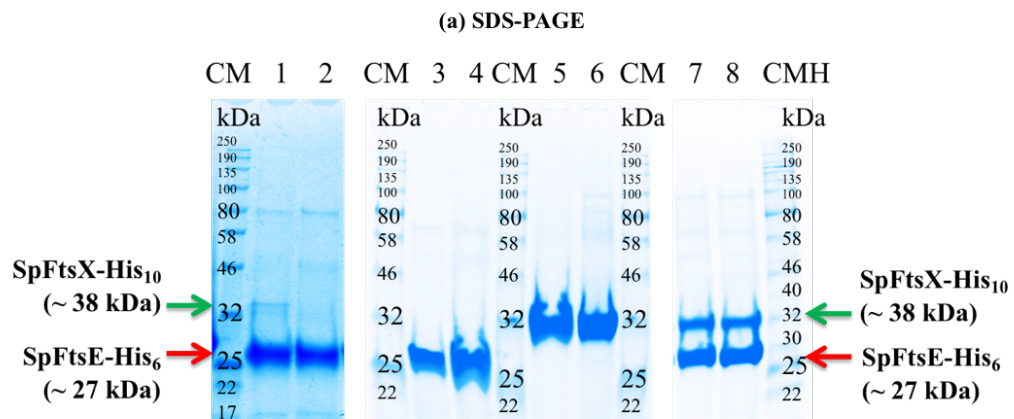


Figure 4.11. Multicloning duet system failed to co-express and copurify SpFtsEX as equimolar complex in SMALP but alternate reconstitution of purified SpFtsE and SpFtsX successfully reconstituted SpFtsEX in SMALP nanodisc.

(a) SDS-PAGE with SMALP extracted and SEC purified protein samples (reduced) that expressed inducing *pETDuet1-SpFtsE-His₆-SpftsX-His₁₀* (1 and 2), *pET22b(+)-SpFtsE-His₆* (3 and 4), *pETDuet1-SpFtsX-His₁₀* (5 and 6) and from post-IMAC reconstitution of SpFtsE-His₆ and SpFtsX-His₁₀ (7 and 8) using their respective individual *pETDuet1* plasmids. **(b)** Western blot and immunoassays with same samples using monoclonal anti-His-HRP antibody. CM: Colour markers; His-L: His-tagged ladder; CMH: A mixture of colour marker and His-tagged ladder.

4.2.2.5. Reconstitution of SpFtsEX in SMALP indicates their possible natural preference is to form a heterodimeric complex

Post-IMAC reconstitution of SMALP-SpFtsEX and further purification following SEC (as mentioned in above section 4.2.2.4.) exhibited an aggregated peak near void volume and an immediate shoulder peak (**Figure 4.12.a**) that generally shows equimolar fractions of SpFtsE and SpFtsX (**Figure 4.12. e and f**). However, the large peak near void volume was indicative of aggregated particles in number of fractions. In order to avoid these aggregated particles, a second SEC purification was performed concentrating fractions under shoulder peak (coloured area, **Figure 4.12.a**) and loading it on to same column (Superdex 200 Increase 10/300 GL) for purer sample. After double SEC purification a segregated broad peak was observed with highest concentration around 144 kDa MW (**Figure 4.12.b**) (according to SEC/GF calibration marker, Appendix **Figure A 12**), which is close to equivalent MW of possible heterodimer SpFtsEX complex. The Native-PAGE with same fractions also indicative of presence of similar molecular weight broad band around 150 kDa (**Figure 4.12.c**) which were when reduced and separated up on SDS-PAGE, the Coomassie stained gel shows much cleaner fractions with two clear bands (**Figure 4.12.e**) which identified as SpFtsE-His₆ (~ 27 kDa) and SpFtsX-His₁₀ (~ 38 kDa) on Western blot (WB) using immunoassay (IA) with anti-His-HRP (**Figure 4.12.f**). Both SDS-PAGE and WB-IA detected satisfactory stoichiometry between these two proteins in fractions under peak area, which never achieved in all previous trials. However, negative stain EM micrographs indicative of some fractions of aggregated particles (**Figure 4.12.d**).

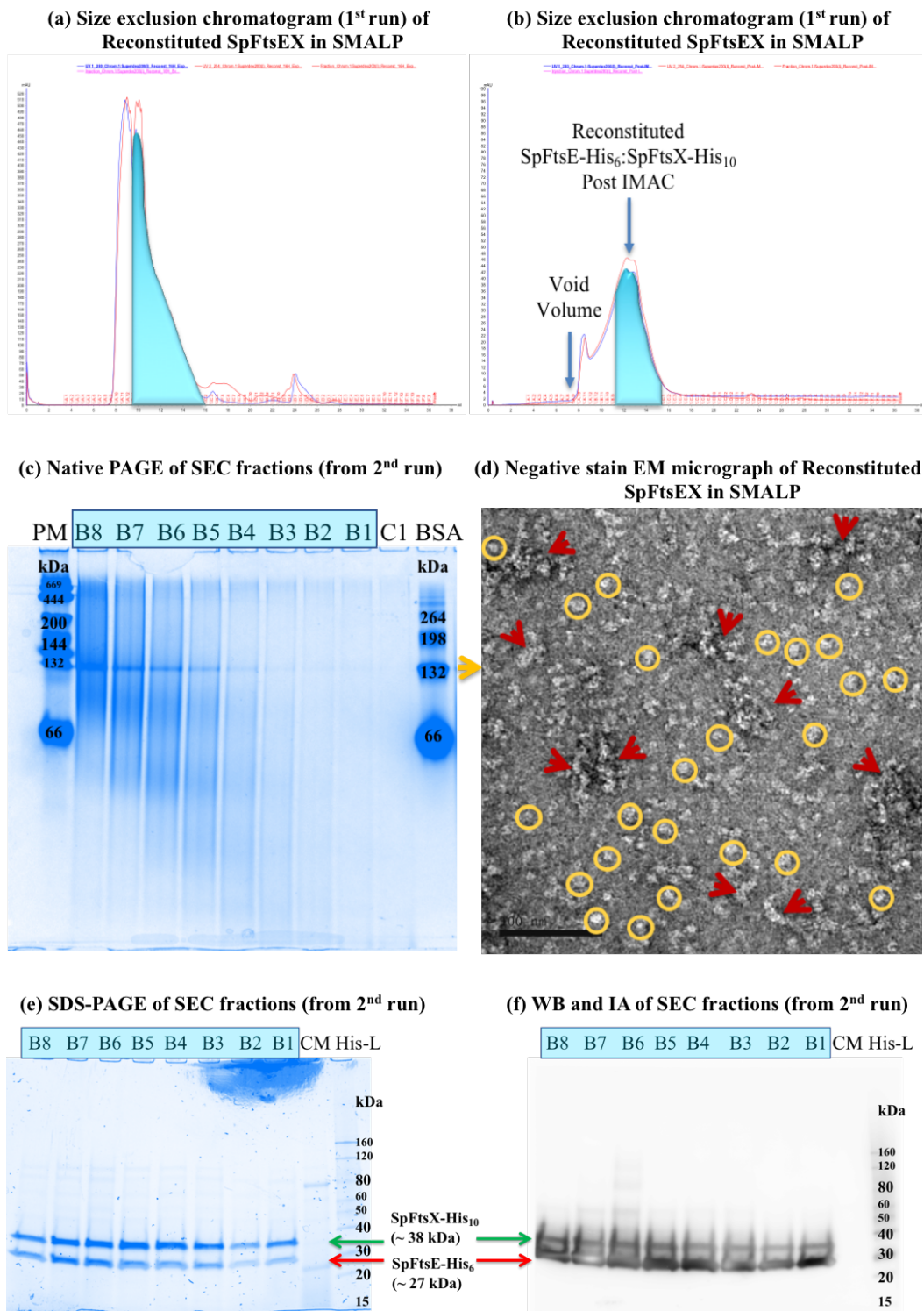


Figure 4.12. Successful reconstitution of SpFtsEX in SMALP indicates their possible natural preference to form a heterodimeric complex. First SEC chromatogram of post IMAC reconstituted SMALP-SpFtsEX (a) showed aggregation near void. Fractions under coloured area were re-purified through SEC (2nd run) (b) segregated reconstituted proteins from aggregated fractions. Native-PAGE indicates reconstitution of SpFtsEX in SMALP with possible heterodimeric conformation (c). Negative stain EM

micrograph of reconstituted SMALP-SpFtsEX shows disk like structures (yellow circles), however number of particles were spotted still aggregated (red arrows) (d). SDS-PAGE of SEC fractions under coloured (turquoise) area confirms presence of SpFtsE-His₆ and SpFtsX-His₁₀ (e) and WB and immunoassay with anti-His-HRP identified their associated His-tags at their corresponding molecular weight bands, in the same fractions (f). PM: Protein markers; BSA: Bovine serum albumin; B8-B1: high MW to Low MW; CM: Colour markers; His-L: His-tagged ladder; Scale bar: 50 nm.

4.2.2.6. Comparison of extraction and purification process using SMALP and detergent

Since, EM micrographs of negative stained (2% UA stained) particles indicated a significant portion of aggregated particles in the sample, a thorough screening was set up in order to achieve a segregated peak for monodispersed sample (with correct and similar size protein complex inside a SMALP disk) through size-exclusion chromatography (SEC) / gel filtration (GF). All screens were performed using HEPES based buffers at pH 8 because SMALP precipitate at a pH below 6.5 (Lee et al., 2016). Several additives such as DTT, L-Arginine and PEG200, and different salt concentrations (from 150mM to 500 mM) in buffers for extraction and different stages of purification, were tested during trials. Among these additives, DTT was used because although FtsE and FtsX has no cysteine residues, FtsE in particular is located at the cytoplasmic side of the membrane, which is reducing environment. Arginine was used simultaneously to stabilise the complex preventing any further intermolecular hydrophobic interaction or surface charge interaction and stop aggregation (Das et al., 2007). PEG200 has been reported to have a crowding effect and may help protein stay in its homogenous state (either as monomer or dimer but not in mixed stoichiometry). However, no significant improvements were noticed using any of these additives except the usage of different salt concentrations at different steps of extraction and purification process. Finally, a medium KCL salt concentration (300 mM) in SMALP extraction buffer, high salt concentration (KCl 500 mM) in IMAC buffer and low salt concentration (150-200 mM) in SEC purification buffer were optimised for further extraction and purification of

SpFtsEX. However, a vast portion of sample was still found aggregated on SEC chromatogram and on EM through negative stain (**Figure 4.13**).

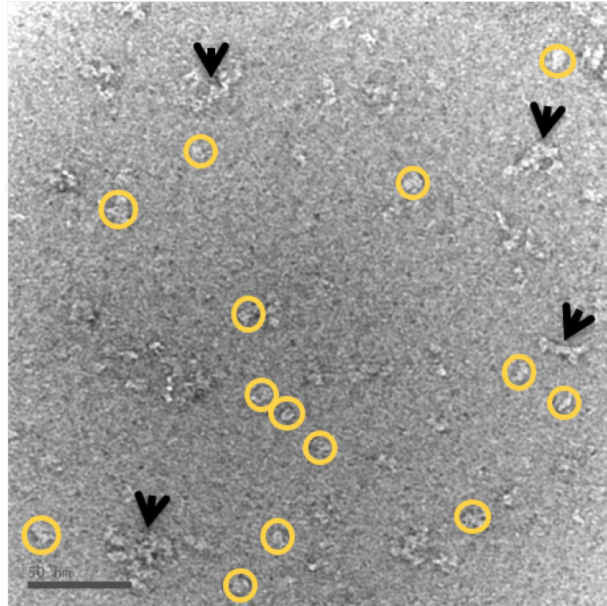


Figure 4.13. *Negative stain EM micrograph of reconstituted SpFtsEX in SMALP shows aggregated particles without Triton-X-100 treatment.*

To solve this issue, a new screen was performed where SMALP extracted and reconstituted samples were incubated with low CMC (3 - 4 CMC) of detergents (either TritonX-100-reduced or DDM) for about an hour, before gel filtration through SEC. The rationale for this was that since the FtsEX complex is a membrane protein complex it is likely to have an overall hydrophobic character and thus small amounts of biochemical detergents may help to overcome hydrophobic aggregation. Triton is a common additive to the stabilisation buffers used with many commercially supplied restriction enzyme and DNA modifying enzymes for example. This protocol dramatically reduced the initial aggregated peak on SEC chromatogram (**Figure 4.14. a and b**) and improved the quality and quantity of homogenous SMALP-protein disc. Hence, a new protocol was established for SMALP-FtsEX purification, where FtsE was extracted using low salt concentration buffer (with 150 mM KCl), since higher 500 mM salt concentration decreases the expression of FtsE from the complex as evident in previous trials (**4.2.1.1.3.** and **4.2.2.2.** above) and FtsX was extracted using higher salt concentration buffer (KCl 300 mM), later both purified through His-tag/Ni-NTA IMAC column separately

using IMAC buffer with high salt concentration (500 mM KCl). Reconstitution of purified SpFtsE-His₆ and SpFtsX-His₁₀ was performed in a dialysis overnight in a buffer without imidazole and glycerol, but with 150 mM NaCl and HEPES 50 mM pH 8, which is used as SEC/GF buffer at the final purification stage. Following dialysis, the reconstituted sample was incubated with different detergents (DDM and reduced Triton-X-100) and concentrated down to 250 µl before applying onto a SEC column.

Following above optimised conditions a comparison was made between SMALP, SMALP-detergent combination and detergent extracted proteins reconstitution and purification of SpFtsEX in **Figure 4.14**. In summary, the results show SMALP extraction definitely produce much purer reconstituted protein complex (SMALP-SpFtsEX) than DDM only extraction and reconstitution (DDM-SpFtsEX). Whereas SMALP extracted and reconstituted SpFtsEX followed by incubation with low CMC detergent either reduced Triton-X-100 (SMALP-Tx100-SpFtsEX) or DDM (SMALP-DDM-SpFtsEX), shows Triton-X-100 treatment/incubation before SEC increased the quantity and purity of the SMALP-SpFtsEX along with its other possible interacting protein. One such interacting protein has been observed around 46 kDa marker on Coomassie stained SDS-PAGE gels (**Figure 4.14. c, f, i and l**), which later has been identified as EcFtsA in LC/MS-MS analysis (**Figure 4.17**). It appears that the addition of detergent prevents SMALP disks to interlock or stick them together and aggregate. Something we noticed in previous occasions when proteins were extracted using SMALP and purified without any detergent on SEC. The new combination increased the yield of the protein complex SpFtsEX (**Figure 4.14. d, e, f**) by reducing aggregation and improved quality of the particle distribution (**Figure 4.22.d**).

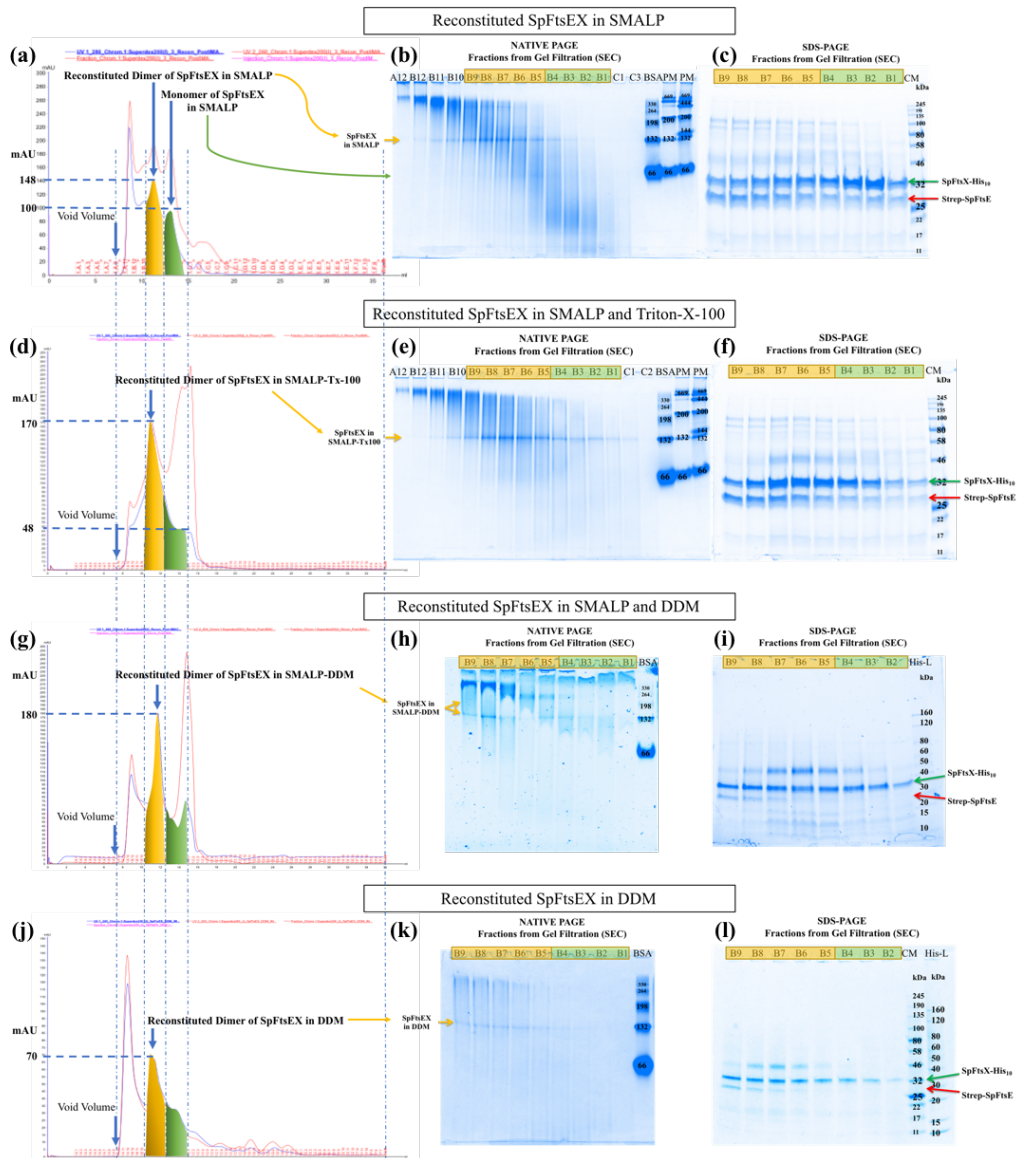


Figure 4.14. Screening reconstitution of SpFtsEX in SMALP.

Comparison of purity of reconstituted SpFtsEX that purified using SMALP extraction (a, b, c), SMALP extraction and Triton-X-100 incubation post reconstitution (d, e, f), SMALP extraction and DDM incubation post reconstitution (g, h, i) and DDM extraction (j, k, l). ACTA traces (a, d, g and j) are indicating SMALP and Triton-X-100 combination clearly reduced aggregation; Native-PAGEs (b, e, h and k) confirmed the same and showing much purer SpFtsEX fractions than other two methods; SDS-PAGEs (c, f, i and l) are showing mainly three major bands around 27 kDa, 36 kDa and 46 kDa. Equimolar proteins complex (SpFtsEX) noticed mostly in SMALP and SMALP-Tx-100 treated samples (c and f), but DDM treatment has disrupted the complex and reduced the yield of SpFtsE.

4.2.3. A modification in the translation initiation site of *pETDuet* plasmid improved the yield and ratio of SpFtsE and SpFtsX from overlapping *his₆-SpftsEX-his₁₀* operon, in *E. coli* *BL21(DE3)ΔacrB::kan^R*

Substantial improvement in expression and post-purification protein yields of individual SpFtsE and SpFtsX, following successful reconstruction and purification of SpFtsEX as a complex with good quantity, was very promising. This encouraged us to make another attempt to clone the whole SpFtsEX overlapping operon into a pETDuet based vector in order to extract SpFtsEX as a complex from the membrane pellet, so that we can avoid the confusion about the start site for SpFtsX. To improve the protein expression, the pETDuet1 vector was modified by replacing the existing translation initiation site (TIS) by a new one that include an efficient RBS site (TTTGTTTAACTTTAAGAAGGAGA), was cloned from *pET-22b(+)* vector. This *pETDuet* based vector backbone with a highly efficient translation initiation site (HETIS), named as *pETDuetHETIS* (Table 2.4). A *S. pneumoniae* *ftsEX* overlapping operon with a 10-histidine (*his₁₀*) tag at the 3' end, was cloned from the previous *pET-52b(+)-strep-SpftsEX-his₁₀* and inserted into MCS1 of above modified plasmid that associate a 6-histidine (*his₆*) tag at the 5'-end of *SpftsEX-his₁₀*. This newly modified expression construct, presented as *pETDuetHETIS-his₆-SpftsEX-his₁₀* (Table 2.4), was created aiming to co-express SpFtsEX as complex, with a 6-histidine tag on the N-terminus of SpFtsE (His₆-SpFtsE) and a 10-histidine tag on the C-terminus of SpFtsX (His₆-SpFtsE).

4.2.3.1. SMALP successfully coextracted and co-purified *S. pneumoniae* FtsEX complex with high purity and good yield

The expression of newly made modified plasmid *pETDuetHETIS-his₆-SpftsEX-his₁₀* was tested heterologously in *E. coli* cells. This time we also changed our induction protocol slightly (2.4.3.1.2.) in order to increase the yield of overexpressed proteins. A single colony from freshly transformed *E. coli* *BL21(DE3)ΔacrB::kan^R* cells with above plasmid, was inoculated and induced using optimised expression and protein production protocol as mentioned in section

(2.4.3.1. and 2.4.3.1.2.). Isolation of *E. coli* membranes that expressed with SpFtsEX, followed by solubilization of the membrane protein fraction using detergent free SMALP extraction and subsequent purification by IMAC (His/Ni-NTA) and SEC/GF chromatography (**Figure 4.15.a**), allowed the isolation of the SpFtsEX complex in high yield and purity as shown by Native-PAGE (**Figure 4.15.b**), SDS-PAGE (**Figure 4.15.c**), and Western blots (**Figure 4.15.d**).

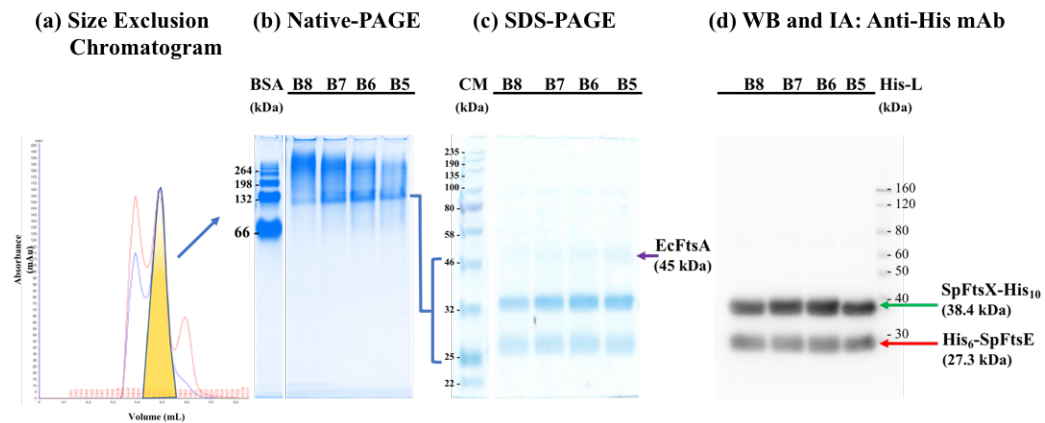


Figure 4.15. *SpFtsEX* successfully purified as complex in SMALP nanodisc.

Size exclusion chromatography following IMAC purification of SMALP extracted *SpFtsEX* with peak fractions indicated in yellow (**a**) and accompanying native PAGE that indicate a formation of *SpFtsEX* complex (**b**). The same fractions when reduced and separated on SDS-PAGE (**c**), showed two clear bands for *SpFtsE* and *SpFtsX*, which further identified using monoclonal anti his-tag antibody (*mAb* anti-His-HRP) immunoassay (IA) on Western blot (WB) analysis (**d**). A weakly staining band for *EcFtsA* observed in the SDS-PAGE analysis (**c**) which was subsequently confirmed by mass spectrometry analysis. Red and blue traces in SEC chromatogram indicates traces at 260 nm and 280 nm respectively.

The *SpFtsEX* complex in SMALP nanodisc migrated as broad band at approximately 200 kDa on Native-PAGE and mass spectrometry of a trypsin digest of these bands confirmed the presence of unique peptides from both *SpFtsE* and *SpFtsX* proteins (**Figure 4.16**). In addition, this analysis revealed the presence of peptide sequences for *E. coli* FtsA (*EcFtsA*) as shown in **Figure 4.16.b**. The same samples analyzed by reducing SDS-PAGE, showed clear bands for the *FtsE* and *FtsX* at 27 kDa and 36 kDa respectively, and the presence of a 46 kDa (**Figure 4.15.c**) that identified as *EcFtsA* when sequenced using mass spectrometry (**Figure**

4.17), highly suggestive therefore of a chimeric associative complex between SpFtsEX and EcFtsA. The association has been consistent through our previous trials (Figure 4.4; Figure 4.10; Figure 4.14) and has not been demonstrated or reported by any research group before this study.

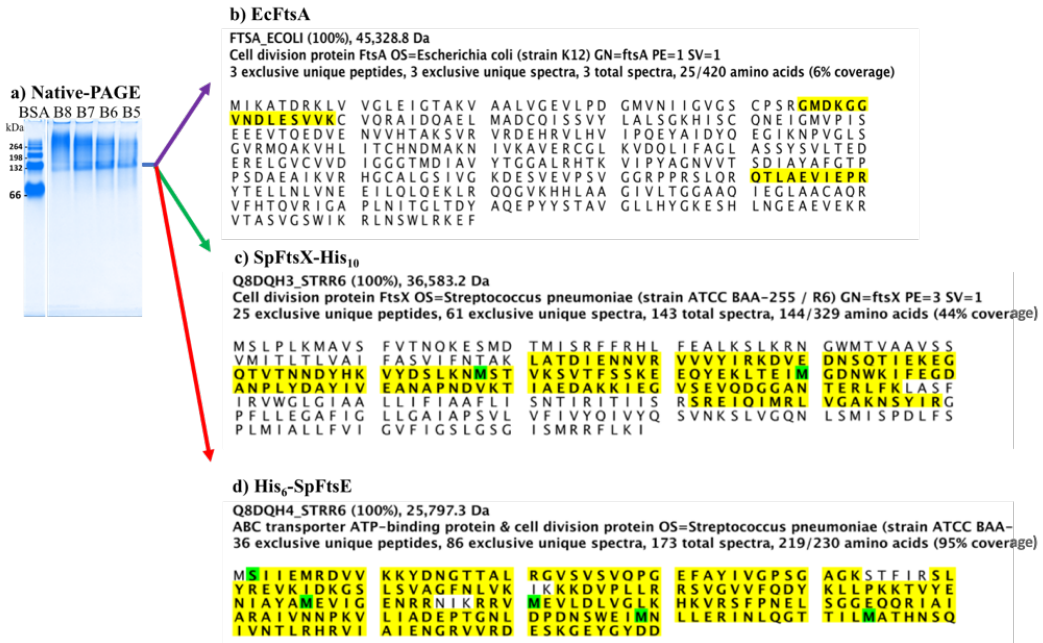


Figure 4.16. LC-MS/MS analysis of SpFtsEX-SMALP band on Native PAGE.

SMALP extraction and purification of SpFtsEX copurify traces of *E. coli* FtsA as observed when the Native-PAGE bands (a) for the complex were analysed and sequenced through LC-MS/MS mass spectrometry. Yellow lines indicate sequence coverage by exclusive unique peptides. Overall 6%, 44% and 95% coverages were achieved with EcFtsA (b), SpFtsX (c) and SpFtsE (d) exclusive unique peptides respectively.

4.2.3.2. Heterologous expression of *S. pneumoniae* *ftsEX* overlapping operon in *E. coli* produced elongated and concatenated cells

To analyse phenotypic consequences of expression of *S. pneumoniae* FtsEX, and later as complex with PcsB and FtsA (discussed in next chapter), we adopted a strategy of synchronous cell culture (Ferullo et al., 2009) using pre-treatment of inoculates using DL-serine hydroxamate to ensure all samples were harvested for analysis at the same point in growth following induction (**Figure 4.19.a**). Fluorescent microscopy of cells harvested at late exponential phase and labelled with FM4-64 (which allows visualization of the cell membrane) allowed comparison of empty vector control cells (**Figure 4.19.b**) with those expressing SpFtsEX (**Figure 4.19.c**) showed an aberrant cell division phenotype in the latter, where we observe long undivided concatenated cells. This is type of dominant negative effect on cell growth is a signature morphological defect in the bacterial cell division apparatus and is highly suggestive of a heterologous interaction between SpFtsEX and other components of the *E. coli* host divisome, as has been seen previous with other ‘Fts’ proteins (Du et al., 2016; Ng et al., 2004; Ng et al., 2003; Schmidt et al., 2004). Expression of empty vector when analysed *in-vitro* in similar way as FtsEX, no prominent overexpressed protein bands that purified with his-tag, are observed (**Figure 4.18**), and results no phenotypic abnormality during its heterologous expression (**Figure 4.19.b**).

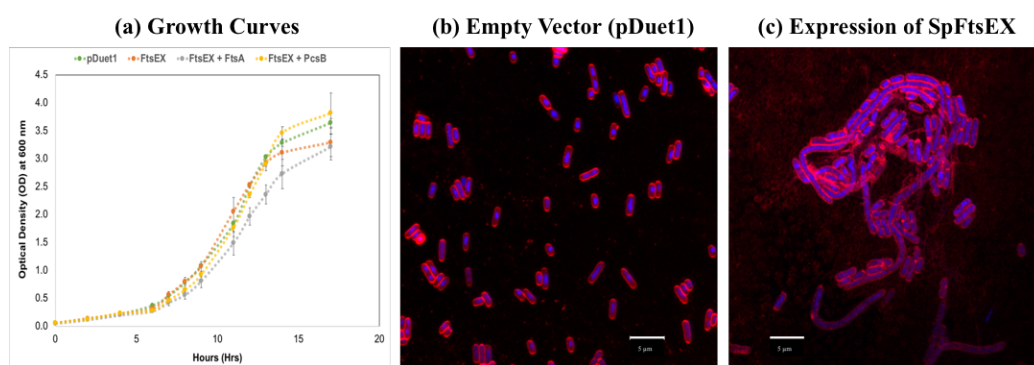


Figure 4.19. Heterologous expression of SpFtsEX in *E. coli* cells is showing a phenotypic effect.

Synchronous cell culture growth curve comparison for cells expressing FtsEX alone and when co-expressing with PcsB and FtsA (a). FM4-64 and DAPI stained *E. coli* cells under fluorescent microscope (at 100x magnification), harboring empty vector pETDuet empty vector(b) and pETDuetHETIS-SpFtsEX (c). Scale indicates 5 microns.

4.2.4. SpFtsEX complex in SMALP is functional in *in-vitro* assays

The phenotypic anomalies indicate the overproduced SpFtsEX must functionally active *in-vivo* even in the context of heterologous expression. In order to investigate this, we turned our focus into *in-vitro* functional assay with SMALP extracted and purified SpFtsEX protein complex. Amino acid sequence analysis of FtsE predicted the presence of the Walker A and B consensus motifs (John E. Walker, Saraste, and Gay, 1982) that involved in ATP binding, and commonly found in most proteins from ATP-binding cassette (ABC) transporter superfamily (Higgins, 1992). We tested this hypothesis on our successfully purified functional (*in-vitro*) *S. pneumoniae* complex of FtsEX that contain FtsE and its ATP binding site.

4.2.4.1. ATP binding assay with SpFtsEX complex in SMALP nanodisc

In order to assess the ATP binding ability of these SMALP purified SpFtsEX complex *in-vitro* we first examined purified sample in the presence and absence of fluorescent ATP analogue, BODIPY™ FL ATP- γ -S, Thioester (Adenosine 5'-O-(3-Thiotriphosphate)) (ThermoFisher Scientific, UK) as mentioned in methods and materials (2.4.6.5.). All purified protein samples assayed as above were analysed using non-reduced Native-PAGE by fluorescent imaging with excitation at 488 nm and imaged 510 nm for the BODIPY fluorophore and compared to a BSA standard that provides a convenient ATP binding control and native gel molecular weight estimation in this instance (Bauer, Baumann, and Trommer, 1992; Jameson, Smith, Annunziata, and Dzyuba, 2016). The purified SpFtsEX in SMALP, using both reconstitution and Co-EEP methods, are tested for its ATP binding ability. Samples that assayed in presence of BODIPY™ FL ATP- γ -S and Mg^{2+} are observed with prominent fluorescent band at their corresponding molecular weight on Native-PAGE as found in Coomassie staining of the same gel following fluorescent imaging (**Figure 4.20**). Strangely, purified SpFtsEX complex assayed in presence of Mg^{2+} migrated to higher order molecular weight band that could be the higher oligomeric form of SpFtsEX. The same bands are not visible enough in controls, in absence of Mg^{2+} (**Figure 4.20**). One possible explanation could be that the Mg^{+2}

is chelating SMALP disks during the assay, which may be destabilising the protein complex and leading to aggregate into higher order oligomeric form.

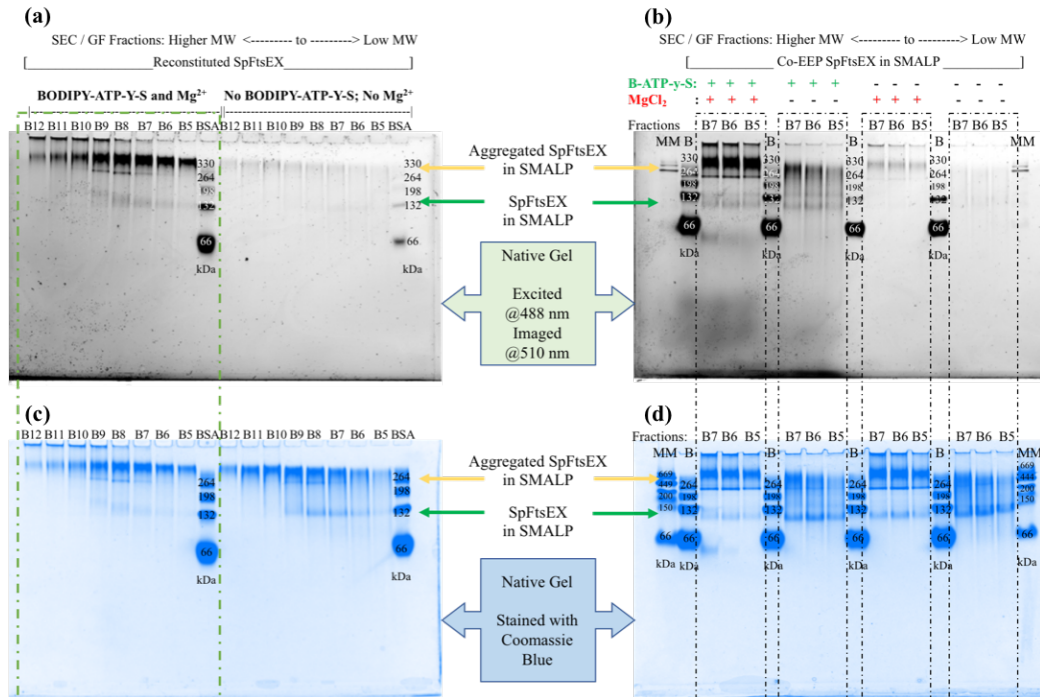


Figure 4.20. ATP-binding assays with purified SpFtsEX in SMALP.

ATP binding assays were performed by inducing BODIPY™ FL ATP-γ-S (a fluorescent analogue) with SEC fractions from reconstituted SpFtsEX in SMALP (a) and Co-EEP SpFtsEX in SMALP (b), followed by Native-PAGE run and imaging under laser scanning (excitation 488 nm and images with filter 510 nm) (a and b). Corresponding Coomassie stain of the same Native-gels (c and d) showing the possible dimmers (~150 kDa) of FtsSpEX is only excited at 488 nm when BODIPY™ FL ATP-γ-S is introduced to samples and in presence of Mg²⁺. This confirms the ATP binding ability of SpFtsE as predicted before (Bajaj et. al. 2016, Sham et. al. 2013). The co-factor Mg²⁺ probably chelated out SMALP from protein complex, as evident in Coomassie (d) as well as in fluorescent images (b). This consequently destabilised the protein complex, hence it is aggregated in presence of Mg²⁺. SEC: Size-exclusion chromatography; GF: Gel filtration; Co-EEP: Co-expressed, co-extracted and co-purified proteins; B: Bovine serum albumin (BSA); MM: Molecular markers; B12-B5: SEC fraction number from higher MW to lower MW.

4.2.4.2. ATP hydrolysis assay with SpFtsEX in SMALP nanodisc

When we verified successful binding of ATP molecules to SMALP purified complex of *S. pneumoniae* FtsEX, the same does not confirm ATP-hydrolysing ability of the purified protein complex. Previous studies had indicated a low level of ATP hydrolytic activity for FtsE in isolation (Bajaj et al., 2016). In order to address this question, we followed a classical, ADP release enzyme coupled assay that can detect ATP hydrolysis *in-vitro* as described in methods and materials (2.4.6.6.). The result shows a low level of activity for FtsEX (**Figure 4.21**).

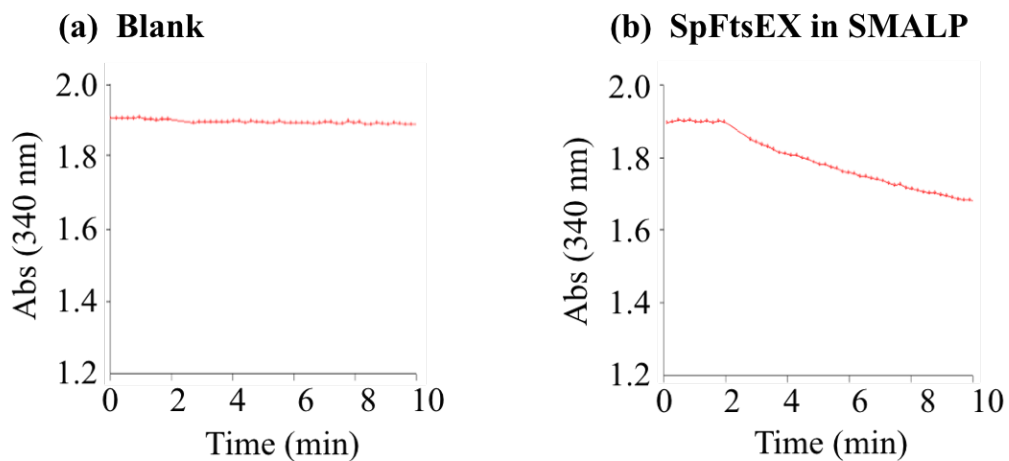


Figure 4.21. ATP-hydrolysing assay with purified SpFtsEX in SMALP. Absorbance based kinetic traces for ATP hydrolysis assays with blank (a) and SpFtsEX (b). The purified SpFtsEX complex in SMALP shows a low-level of activity compared to blank, which suggests the complex is functional *in-vitro*. Abs (340 nm): Absorbance at 340 nm.

4.2.5. A comparison of particle distributions of SpFtsEX that purified by reconstitution and Co-EEP methods, using negative stain electron microscopy

Negative stain electron microscopy studies (**Figure 4.22**) were performed with reconstituted SpFtsEX protein complex using SMALP, DDM, SMALP-TritonX-100 (**Figure 4.22. a, b and c** respectively), also with Co-EEP SpFtsEX complex using SMALP-TritonX-100 combination (**Figure 4.22.d**). Although all treatments show good number of particles, particles reconstituted using SMALP and DDM alone, shows a fraction of particles are aggregated (**Figure 4.22. a and b**), as observed in SEC chromatogram, Native PAGE and SDS-PAGE analysis with same samples (section **4.2.2.6.** above; **Figure 4.14**). Consistent with the same comparative study, the SMALP-TritonX-100 combination method reduced the aggregation in samples (SpFtsEX protein complex) prepared by both reconstitution and Co-EEP methods. The trend also noticed before in SEC, Native-PAGE and SDS-PAGE analysis with same samples (**Figure 4.14. d, e and f**). In both cases, negative stain EM micrograph shows a good distribution of the particles that ranges between 12 nm and 20 nm. The measurements on negative stained individual particles supports the dynamic light scattering analysis (Appendix **Figure A 2.c**) that measured particle sizes about 13 nm (+/- 3 nm) in diameter compared to its complex with PcsB (discussed in Chapter 5; also see **Appendix A1**) that showed about 16 nm (+/-4 nm) (Appendix **Figure A 5.c**) and to SMALP nanodisc alone approximately 9 nm. This is indicative of single particles representative of the FtsEX dimer encapsulated in a SMALP nanodisc.

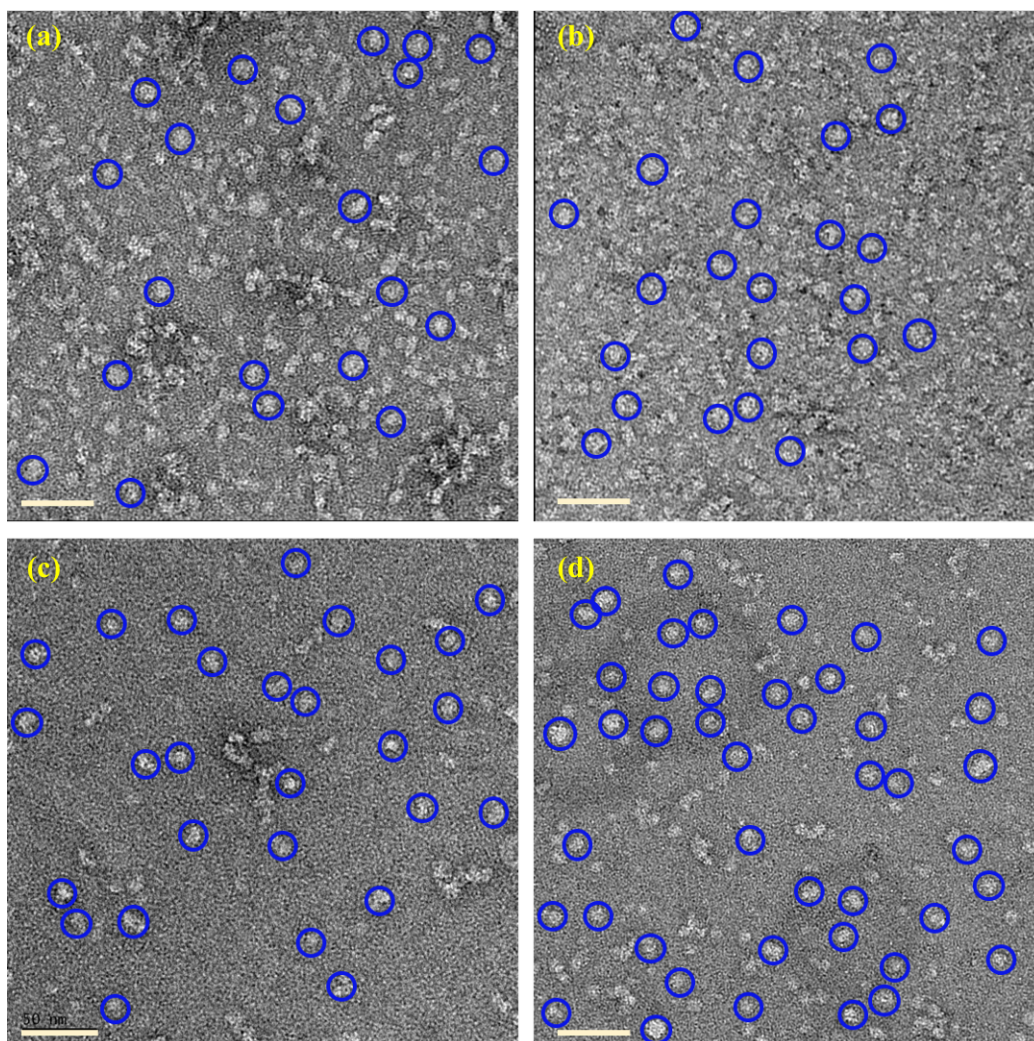


Figure 4.22. Negative stain EM micrographs of purified SpFtsEX using SMALP, DDM and SMALP-Tx100.

EM micrographs show the particle distribution of negative stained reconstituted SpFtsEX (**a**, **b** and **c**) that purified using SMALP extraction (**a**), DDM extraction (**b**) and using SMALP extraction and low CMC short Triton-X-100 incubation following reconstitution (**c**). Another EM micrograph shows the particle distribution of negative stained SpFtsEX in SMALP (co-expressed and co-purified using Co-EEP method) (**d**). The concentration of SpFtsEX on the EM micrographs are as follows (**a**) 200 µg/mL, (**b**) 200 µg/mL, (**c**) 100 µg/mL and (**d**) 120 µg/mL. The SMALP-Tx100 treated SpFtsEX showed better distribution and single particles (**c** and **d**) compared to individual SMALP (**a**) or DDM (**b**) extracted SpFtsEX. SMALP-Tx100 combination in both reconstitution and Co-EEP methods reduced aggregation of particles and showed good number of monodispersed particles (Blue circles). Scale bar represent 50 nm.

4.3. DISCUSSION: *S. pneumoniae* FtsEX is co-ordinately expressed as a functional protein complex and has a phenotypic effect on *E. coli* when heterologously expressed

Previous published studies examined the complementation of an *E. coli ftsEX* chromosomal knockout strain by complementation with recombinant *ftsEX* in defined media conditions, where chromosomal FtsEX function can be bypassed in high salt, complex media conditions (S. J. R. Arends, R. J. Kustus, and D. S. Weiss, 2009). It was found that site directed mutants of the *E. coli* FtsE, where ATP binding or ATP hydrolysis is abolished, could not complement the *ftsEX* knockout strains, highly suggestive that ATP hydrolysis is required for proper FtsEX function. By contrast to *E. coli*, FtsEX function in *S. pneumoniae* is essential in serotype strains (Ng et al., 2004; Ng et al., 2003; Sham et al., 2013) and causes diminished growth and severe cell division defects when inactivated in other strains (Giefing et al., 2008; Giefing-Kroll et al., 2011). In our study, we did not have access to comparable strains as described above for the *E. coli* system (Arends et al., 2009), which would not be compatible for heterologous expression of the *S. pneumoniae* proteins in any case using T7 promotor-based plasmids. We chose therefore to clone the entire genomic region encompassing *S. pneumoniae* FtsEX genes into the *E. coli* expression vector producing an expression construct with either a Strep- or 6-Histidine tag on the N-terminus of SpFtsE and a 10-Histidine-tag C-terminus of SpFtsX (Table 2.4). This approach has never been reported or tested before and this study is first of its kind.

In our very initial attempt, an expression construct *pET-52b(+)-strep-SpftsEX-his10* that carrying the overlapping operon *SpftsEX* along with a Strep-tag and a 10-His-tag (His₁₀) at the N-terminal and C-terminal respectively, was tested for its expression in two different *E. coli* cells lines, namely *Lemo21(DE3)::cam^R* and *BL21(DE3)ΔacrB::kan^R*. The expression condition was initially optimised in a small-scale study in *Lemo21(DE3)::cam^R* strain in order to access its *pLemo* system to control the overexpression of proteins and toxicity to the cells. While this

titration for SpFtsE and SpFtsX protein overexpression through L-rhamnose *P_{rhaBAD}* promoter could be very useful to reduce the toxicity of these overexpressed proteins at 37 °C and 42 °C, the same may not be necessary at low temperature. Results from our small-scale studies concluded that higher concentration L-rhamnose (thus inhibition of T7RNAP) has no beneficial effect in overexpression of SpFtsEX qualitatively and quantitatively, at moderate (25 °C) or low temperature (15°C). Instead, induction of cells (transformed with above plasmid) at moderate/low temperature and without L-rhamnose showed no aggregation or degradation and better yields for both proteins (SpFtsE and SpFtsX) in longer overnight inductions. In addition, small-scale expression studies with same above construct in both *E. coli Lemo21(DE3)::cam^R* and *BL21(DE3)ΔacrB::kan^R* strains revealed both SpFtsE and SpFtsX proteins are expressed in membrane fraction (MF), a very low-level of SpFtsE can be traced in the high-speed supernatant (HSS) but no trace of SpFtsX has been observed in HSS. These findings are consistent with SpFtsX forming an integral membrane protein, and the presence of low-level of SpFtsE in HSS suggests a small fraction of SpFtsE population can be unattached/unbound to membrane. This result together with successful SMALP extraction of SpFtsE (3.2.2.1.) for the very first time indicates SpFtsE may have membrane insertion/attachment/association site(s) at the cytoplasmic side of the inner membrane.

In large-scale study induction trials, we have shown successful purification of SpFtsEX as protein complex for the first time within its host lipid environment. We have shown this could be achieved either co-expressing the proteins from a natural overlapping operon followed by co-extraction and co-purification (Co-EEP) of SpFtsEX as complex using SMALP; or reconstituting these two proteins that are SMALP extracted and purified from separate expressions, in SMALP nanodisc context. In order to achieve the same, we initially utilized a tandem affinity purification strategy to purify the SpFtsEX complex using their associated His-tag (with SpFtsX) and Strep-tag (with SpFtsE) respectively. However, initial large-scale inductions of both *E. coli Lemo21(DE3)::cam^R* and *BL21(DE3)ΔacrB::kan^R* cells that transformed with *pET-52b(+)-strep-SpftsEX-his₁₀*, showed disparities in

the quantities of protein of SpFtsE and SpFtsX after SMALP extraction and purification. The SpFtsX (His-tagged C-terminally) has been purified in good quantity but the yield of SpFtsE that is strep-tagged N-terminally, has been relatively unsatisfactory possibly due to the high salt concentrations in buffers used in the purifications. In the past, *E. coli* FtsE was suspected as potential conditional salt-dependent essential protein (de Leeuw et al., 1999) and to have a possible role in translocating potassium-proton pump proteins (Ukai, Matsuzawa, Ito, Yamada, and Nishimura, 1998). Yet, it is still not clear how high salt osmolarity is affecting FtsE expression and potentially its ability to form a complex with FtsX and its functional essentiality during cell division. Considering above speculation, we tested varying salt concentrations in extraction and purification buffers to improve FtsE expression. The low salt concentration used in buffers for FtsE extraction and purification, appeared to improve the expression for this protein which was enhanced further by increased translation of the same using a modified *pETDuetHETIS* vector that was discussed.

Our initial assumption about losing FtsE yield compared to FtsX in high salt buffers, is that the high salt concentration (500 mM) possibly effecting the binding of FtsE to the inner membrane and its membrane partner FtsX. These two proteins possibly have some weak ionic interaction between them, which could have been lost during more stringent SMALP extraction using buffers with high salt concentration. Our strategy was therefore to use, low to moderate (100 to 300 mM) salt concentrations in extraction and IMAC purification buffers and low-salt concentration in SEC buffer for final purification and storage. Alternatively, the use of Magnesium (Mg^{2+}) salts in low concentration in all buffers could have improved the expression of both SpFtsE and SpFtsX, as indicated in previous study (Gill and Salmond, 1987; C. Jones and Holland, 1985). Where absence of Mg^{2+} in the buffer removed loosely associated membrane proteins during successive washing procedures. Unfortunately, a limitation of SMALP techniques is that the polymers disassemble in the presence of divalent cations (Mg^{2+} , Ca^{2+} etc.) that chelates and precipitate SMALP at concentration above 5 mM (Lee et al., 2016),

thus restricts the use of any divalent salts in buffers to stabilise the membrane association of the proteins.

In successive large-scale trials, where the construct *pET-52b(+)-strep-SpftsEX-his₁₀* was expressed in *E. coli Lemo21(DE3)*, the quantity of purified SpFtsE marginally improved with the use of low concentration salts in SMALP extraction and purification buffer. However, the overall ratio between SpFtsE and SpFtsX in SEC fractions was not judged to be acceptable for further study. In addition, AcrB has been co-purified with SpFtsEX when the complex was extracted from overexpressed membrane using SMALP. AcrB has been reported as common contaminants to SMALP extraction of membrane protein (Veesler et al., 2008). While introducing an *acrB* knocked-out *E. coli BL21(DE3)ΔacrB::kan^R* strain solved the contamination issue, it could not improve the yield of Strep-tagged SpFtsE at level proportionate to SpFtsX. Although our primary aim was to extract and purify this complex in detergent free environment using SMALP technique, at this point, we also tested detergent DDM extraction and purification in order to achieve a proportionate yield of both protein in complex. However, the attempt was frustrating with poor yield of Strep-tagged or untagged SpFtsE. Also, the purity of the DDM extracted and purified samples was not good enough compared to SMALP extracted and purified samples. When all these failed attempts resulted in disproportionate protein yields, successful purifications of SMALP extracted individual SpFtsE and SpFtsX proteins (both His-tagged and expressed from *pET-22b* and *pETDuet* based vectors) in good quantity (3.2.2.1. and 3.2.2.2.), was very encouraging. This led us to explore an alternate strategy that is to reconstitute these two SMALP extracted proteins immediately after IMAC and purify further through SEC. This resulted a successful reconstitution of SpFtsEX as heterodimeric complex in SMALP. This possibility has been shown for the first time, in this study. Also, a slight modification in general SMALP extraction and purification protocol, that is to use detergent before concentrating the purified protein in order to reduce any possible aggregation of SMALP nanodisc, is suggested in this study.

Among all failed attempts, a co-expression from duet plasmid system (*pET-Duet1-SpFtsEX-His₆-SpFtsX-His₁₀*) was one that showed completely opposite result. This construct produced more SpFtsE than SpFtsX protein, which expressed from their respective genes that cloned into two different multiple cloning sites (MCS1 and MCS2, respectively) of the same construct. This indicated a possible weaker RBS site before MCS2 compared to RBS located upstream of MCS1. Consequently, a modification in the pETDuet1 backbone was performed by substituting the original translation initiation site with a highly efficient translation initiation site (HETIS) that was tested previously while expressing SpFtsE (His-tagged) individually from plasmid construct *pET22b(+)-SpftsE-his₁₀* and showed very positive and strong overexpression of SpFtsE-His₆. This modification of *pETDuet* based vectors, has not only improved the expression of SpFtsE and SpFtsX in isolation from separate vectors (3.2.2.1. and 3.2.2.2. respectively), it also improved the co-expression of SpFtsEX (His-tagged on N-terminal of SpFtsE and C-terminal of SpFtsX) from the overlapping *SpftsEX* operon (as reported and discussed in this Chapter 4). Using the plasmid construct *pETDuetHETIS-his₆-SpftsEX-his₁₀*, a successful co-expression, co-extraction and co-purification of SpFtsEX as complex in SMALP nanodisc, is one of the major successes of this study. Creating this construct to co-express SpFtsEX proteins reduced the cost and labour involved with a large-scale reconstitution process where two large number of cultures (4 to 6 L in total for each protein) were induced parallelly. Additionally, it also provides another free MCS to accommodate an extra gene(s) for a protein of interest, in order to study their protein-protein interaction.

While the strong overexpression of *SpftEX* overlapping operon ensured a successful and well proportionate co-purification of SpFtsEX in SMALP nanodisc, it is utmost important to study its function *in-vivo* as well as *in-vitro* conditions. Subsequently, when SpFtsEX heterologously expressed in *E. coli* cells, we observed elongated and concatenated cells with cell division defects as also evident and reported in other occasions (de Leeuw et al., 1999; Du et al., 2016). One possible explanation of this phenotypic anomalies could be due to a high trafficking at membrane, overactivity or dominant negative activity of overproduced SpFtsEX complex at

the divisome. This may disrupt the ABC signal transducing system that involves SpFtsEX as well as PG hydrolase PcsB. However, co-purification of *E. coli* FtsA (EcFtsA) along with *S. pneumoniae* FtsEX in SMALP nanodisc, indicates a cross-species protein interaction between SpFtsEX and EcFtsA. Therefore, we cannot ignore the possibility of “cross communication” between *S. pneumoniae* FtsEX with *E. coli* divisome components, which indeed may disrupt the harmonization of the cell division process. On positive note, the *S. pneumoniae* FtsEX that has been found interacting with *E. coli* FtsA and other divisome components and showing phenotypic anomalies, confirms SpFtsEX protein complex is functional in heterologous *E. coli* system. Likewise, the purified SpFtsEX protein complex in SMALP, has been observed functional in *in-vitro* experiments with capabilities of binding ATP analogues as well as of hydrolysing ATP.

Since first identification of FtsE and FtsX proteins over 30 years ago (Gill et al., 1986; Hirota et al., 1968; Ricard and Hirota, 1973), researchers so far have been unsuccessful in purify this FtsEX as a complex in anyway (that is either in detergent micelle or in any kind of nanodisc). As a consequence, the bacterial cell divisome research is lacking a crucial and urgent structural study with this FtsEX complex and its structural-functional relationship with other proteins in divisome. In this study, we have optimised and demonstrated two pioneering and successful strategies (reconstitution and Co-EEP) to purify these two proteins as functional FtsEX protein complex, moreover in its most native form within host lipid environment in a SMALP nanodisc. These strategies and all *in-vitro* characterisation would be major prerequisites for detailed biophysical analysis and high-resolution single molecule structural studies with this complex.

CHAPTER 5. An investigation into the association of *S. pneumoniae* FtsEX with other divisome proteins FtsA, FtsZ and PcsB

5.1. INTRODUCTION

Bacterial cell division starts with the formation “Z-ring” around midcell, reinforced by GTP-dependent polymerisation of the tubulin homologue protein, FtsZ (Bi and Lutkenhaus, 1991; Erickson, Anderson, and Osawa, 2010; Pichoff and Lutkenhaus, 2002). The Z-ring provides the platform to number of divisome proteins to assemble into much bigger macromolecular complex and function coordinately to form septum and complete the cell division. The assembly of divisome in many organisms starts with recruiting an actin homologue FtsA that is thought to tether the FtsZ protofilament to the membrane and assist in the assembly other divisome protein complexes during different stages of cell division (Pichoff and Lutkenhaus, 2005; Sánchez et al., 1994; van den Ent and Lowe, 2000). FtsA has been identified as essential in *E. coli* as well as in *S. pneumoniae*, because inactivation of this protein caused static growth and filamentous cell phenotype in *E. coli* (Donachie et al., 1979; Lutkenhaus and Donachie, 1979) whereas depletion of the *ftsA* gene was not tolerated in *S. pneumoniae* cells (Lara et al., 2005; Mura et al., 2017). FtsEX is recruited to Z-ring at the early-to-mid cell division stage, however how both these proteins are precisely recruited to Z-ring is still not clear. FtsE has been shown to interact with FtsZ (Corbin et al., 2007), while recent studies indicate FtsE and FtsX are co-dependent on each other for their localisation at the Z-ring as complex, where FtsE is the main determinant for this recruitment (Du et al., 2019).

In *E. coli* Z-ring, FtsX has been shown to interact FtsA and FtsQ using a two-hybrid approach (Karimova et al., 2005) and later Du et al. (Du et al., 2019; Du et al., 2016) coupled the same findings with genetic studies, which also revealed the interaction between FtsA and FtsX is an important factor to recruit downstream protein

interactions required to activate the divisome. Point mutation in the *ftsA* (*ftsA^{R63H}* and *ftsA^{G366D}*) has been reported to nullify the effect of their divisome association in *E. coli* cells (Du et al., 2016). Additionally, the same group very recently have shown the N-terminal (4-69) cytoplasmic domain of FtsX has been critical for its association with FtsA, thus to assemble late stage divisome proteins; but the same association is not necessary for FtsEX to localise at the Z-ring (Du et al., 2019). However, this interaction along with the requirement of ZipA (an early cell division protein in *E. coli* but not universally conserved) (Hale and de Boer, 1997) has been shown could be bypassed either impairing the polymerisation of FtsA or promoting the interaction between FtsA and FtsN (Pichoff, Du, and Lutkenhaus, 2015). Therefore, it has been hypothesised that the FtsEX possibly stops self-interaction of FtsA and thus channels the FtsA pathways to assemble and activate the divisome (Du et al., 2016) (**Figure 5.1**). While all these findings are related to *E. coli* divisome and septal PG (sPG) synthesis, the same interaction studies are missing and consequences only just being explored in *S. pneumoniae* or other Gram-positive bacteria (Mura et al., 2017).

By contrast, another postulated conserved function of the FtsEX complex is its role in hydrolysis of PG to enable cell separation during the division process. In *E. coli*, PG hydrolysis is mediated by three autoinhibitory amidases AmiA, AmiB and AmiC (Heidrich, Ursinus, Berger, Schwarz, and Holtje, 2002). Inhibition of their hydrolytic function is required only at the septum during PG hydrolysis to prevent otherwise, deleterious breakdown of new PG layers formed at the division site. A periplasmic protein EnvC, is thought to activate and release inhibition of AmiA and AmiB, whereas NlpD has been found to activate AmiC in order to complement the PG hydrolysis process in *E. coli* (Peters et al., 2011). A failure in these interactions caused *E. coli* cells to elongate and concatenate in case of the above three amidases mutants, so as for mutants with loss of function of their regulator EnvC and NlpD (Heidrich et al., 2002; Peters et al., 2011). The periplasmic protein EnvC has been found to bind to FtsEX; and ATPase mutants of FtsE still bind EnvC but do not support cell separation (Yang et al., 2011). Also mutant *E. coli* strains defective in

FtsEX or EnvC become dependent on NlpD for their cell separation (Pichoff, Du, and Lutkenhaus, 2019).

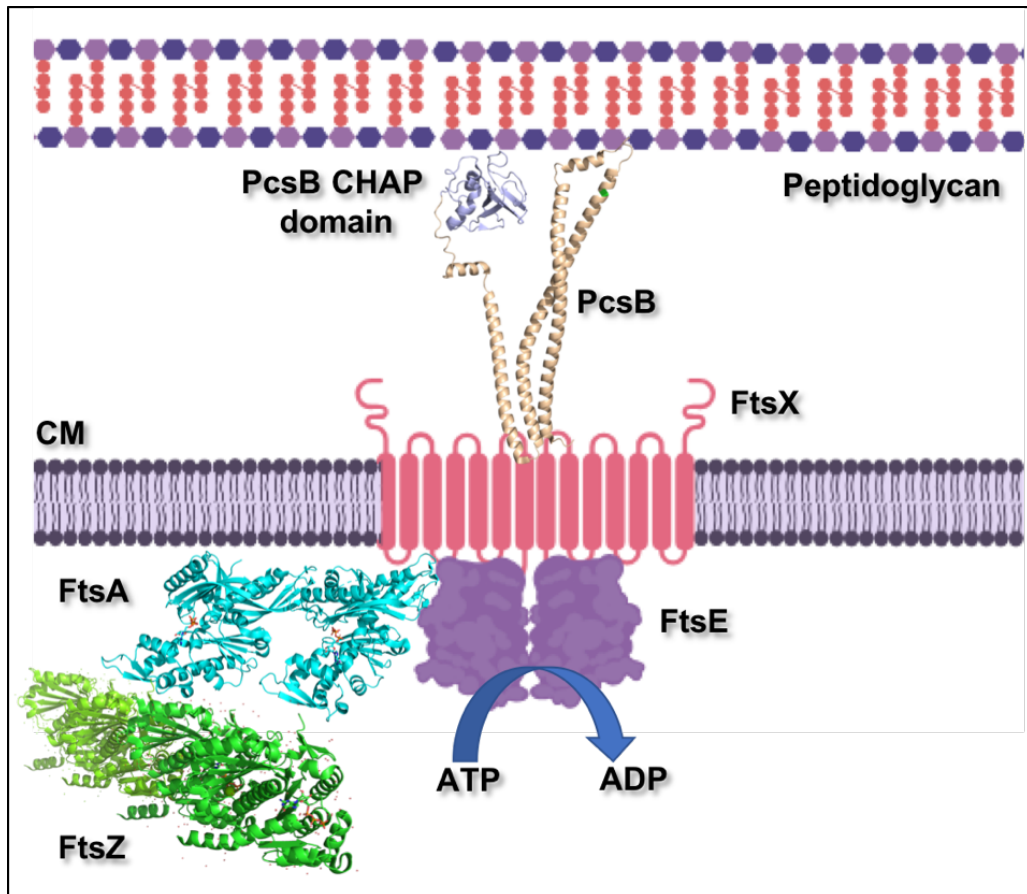


Figure 5.1. Schematic diagram of FtsEX, PcsB FtsA and FtsZ in context. The FtsEX complex is shown as a schematic dimer structure and resembles an ABC transporter protein structure with PcsB (PDB:4CKG) (Bartual et al., 2014) docking in the extracellular environment. The polymer structure of ATP bound FtsA (PDB: 3wqu) (Fujita et al., 2011) provides an anchoring point for FtsZ (PDB:1w5a) (Olivia et al., 2004). The peptidoglycan layer is shown above the cytoplasmic membrane (CM) as indicated.

In comparison, *S. pneumoniae* apparently employ a simpler overall set of protein-protein interactions to enable PG hydrolysis. The mechanism has been hypothesized to mediate through a direct interaction between FtsX and the PG hydrolase PcsB (Bajaj et al., 2016; Bartual et al., 2014; Massidda et al., 2013; Rued et al., 2019; Shak et al., 2013; Sham et al., 2011) (**Figure 5.1**). Recently, a series of genetic studies indicated a long coiled-coiled (CC) domain of the PcsB interact with the extracellular loops (ECL1 and ECL2) of FtsX at the periplasmic side of

the membrane (**Figure 5.2**) (Rued et al., 2019; Sham et al., 2011; Sham et al., 2013). A crystal structure of full-length PcsB provides the structural organization of its domain that includes a CC domain, alanine-rich linker region and a catalytic cysteine, histidine-dependent amidohydrolase/peptidase (CHAP) domain (Bartual et al., 2014).

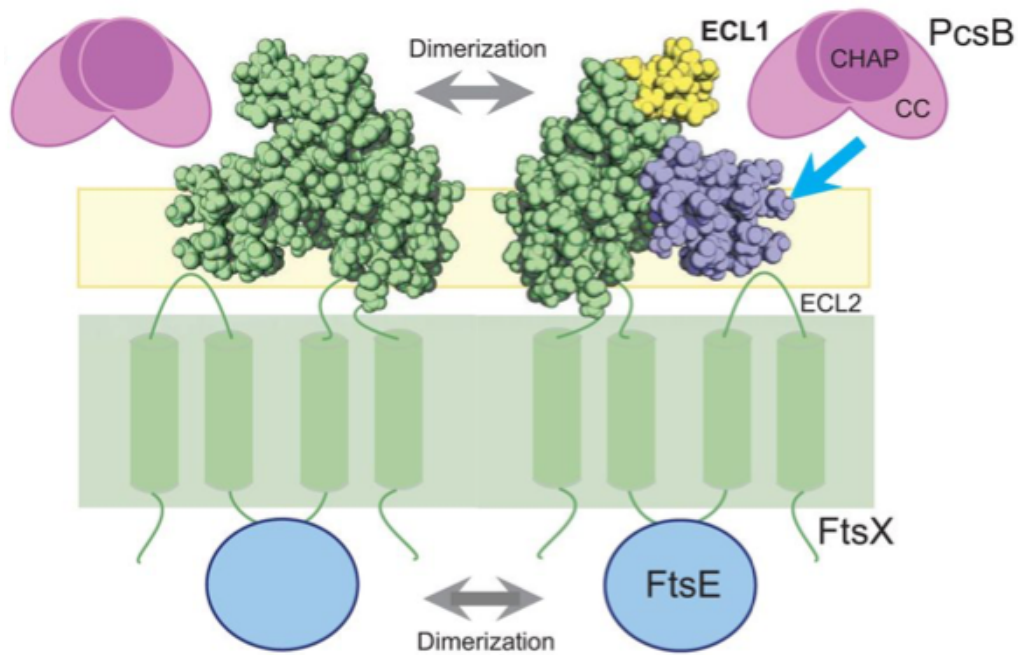


Figure 5.2. PcsB interacts with FtsEX extracellular loops for its activation.

At plasma membrane the FtsEX complex dimerises to form a functionally active complex with a PG hydrolase, PcsB that docks on FtsX extracellular loops (ECL1 and ECL2) at the extracellular side of the plasma membrane. Following an ATP hydrolysis event at FtsE, the activation of PcsB has been suspected to be mediated by an interaction between the coiled-coiled domain of the PcsB and the ECL1 of FtsX. The ECL1 of FtsX is coloured in green, whereas the yellow and blue lobes represent β -hairpin and α -helical lobes, respectively. This figure is adopted and modified from Rued et al. (2019).

All three proteins in this complex i.e. FtsE, FtsX and PcsB are found to be essential for *S. pneumoniae* to grow (Giefing et al., 2008; Giefing-Kroll et al., 2011; Ng et al., 2004; Ng et al., 2003; Sham et al., 2013) contrasting with the conditional essentiality of FtsEX in *E. coli* (Schmidt et al., 2004). The hydrolysis of ATP by FtsE at the cytoplasmic membrane interface is thought to transduce a signal through its integral membrane partner, FtsX, into to the CHAP domain of PcsB. This in

turn may cause a conformational change of the CHAP domain relative to majority CC portion of the PcsB protein, releasing suspected autoinhibitory/self-inhibitory conformation of the CHAP domain and promote PG hydrolysis (Bajaj et al., 2016; Bartual et al., 2014; Rued et al., 2019; Sham et al., 2013). However, the precise mechanism, including the events promoting ATP hydrolysis by FtsE leading to the proposed conformational changes is still unknown and inferred through a variety of data.

The hypothesis that FtsEX plays a pivotal role in between sPG synthesis and PG hydrolysis appears to be well supported, therefore. These two processes are highly dynamic and crucial to complete the cell division without any fatal damage to the daughter cells. While an interaction between FtsEX and FtsA has been found to have an indirect role in sPG synthesis by assembling the downstream protein to divisome appropriately and finally activating the divisome, the interaction between FtsEX and its periplasmic hydrolase partner (EnvC in *E. coli* or PcsB in *S. pneumoniae*) play a direct role in PG hydrolysis that couples through an ATP-hydrolysis event at the FtsE. Therefore, a structural and functional analysis of both these complexes are required to shed light on their mechanism of action. However, so far researchers have not been successful in the purification of these proteins in the form of complexes to enable such studies.

Aiming to study these complexes, in this Chapter we first explored the effect of heterologous co-expression of *S. pneumoniae* FtsEX (SpFtsEX) with its reported interactor proteins such as SpFtsA, PcsB and SpFtsZ (**Figure 5.1**). In the next step, we attempted to purify two distinct tripartite complex SpFtsEX-FtsA and SpFtsEX-PcsB in SMALP nanodisc. Finally, we also tested whether or not is it feasible to purify the bigger macromolecular complex composed of SpFtsE, SpFtsX, SpFtsA, SpFtsZ and PcsB?

5.2. RESULTS

5.2.1. An investigation into the association between FtsA and FtsEX complex

As described in chapter 4, our experiments on expression of the SpFtsEX complex, produced a clear cell division phenotype and allowed the purification of that complex *in-vitro*. In this analysis, we investigate the observation that EcFtsA was apparently copurifying with the complex (Chapter 4, **Figure 4.15**). Therefore, to explore this further we decided to co-express and purify the *S. pneumoniae* FtsA (SpFstA) protein along with SpFtsEX protein complex in order to examine their cognate interaction and its consequence on the host cell phenotype. In order to co-express SpFtsA, which has been reported to have toxic effect on the *E. coli* cells (Krupka et al., 2014), we took the advantage of *pACYCDuet1* plasmid backbone that contains a low-copy-number origin of replication *p15A*. In addition, this strategy would also allow propagation of the same plasmid into *E. coli* cells that containing a plasmid with medium-copy-number origin of replication *ColE*, such as the case for *pETDuet1* or *pETDuetHETIS* plasmids.

5.2.1.1. Heterologous co-expression of SpFtsEX and SpFtsA elongates *E. coli* cells and shows aberrant phenotypes

To test the co-expression of these proteins, the *E. coli* BL21(DE3) Δ *acrB::kan^R* cell line (**Table 2.3**) that containing *pETDuetHETIS-His₆-SpFtsEX-His₁₀* plasmid (**Table 2.4**), selectable with ampicillin and used to successfully express SpFtsEX previously, was also transformed with the chloramphenicol selectable plasmid *pACYCDuet1-SpftsA* (**Table 2.4**). In the latter plasmid the *SpftsA* gene has no tag for copurification. The transformed cells are induced and grown overnight in AIM as mentioned in section (2.2.3. and 4.2.3.2.). Compared to empty vector cells (**Figure 5.3.a**), transformed *E. coli* cell line that co-expressing SpFtsEX and SpFtsA produced a striking loss of normal rod shaped growth phenotype (**Figure 5.3.b**) indicating that the interaction of FtsA may enhance the phenotype of FtsEX

expression alone and in general agreement with expression of FtsA as previously reported for the *E. coli* proteins (Du et al., 2016). Similar to individual expression of SpFtsE, SpFtsX and SpFtsA (**Figure 3.1**) in *E. coli*, the co-expression of these proteins also showed elongated cells and patchy membrane staining by FM4.64. This uneven, patchy membrane staining is very characteristic to heterologous overexpression of FtsA (Krupka et al., 2014). Although co-overexpressed (SpFtsEX and SpFtsA) cells showed phenotypic defects and rate of division was lower than the empty vector induced cells during log phase (**Figure 4.19**), no significant difference between them was noticed at the stationary phase.

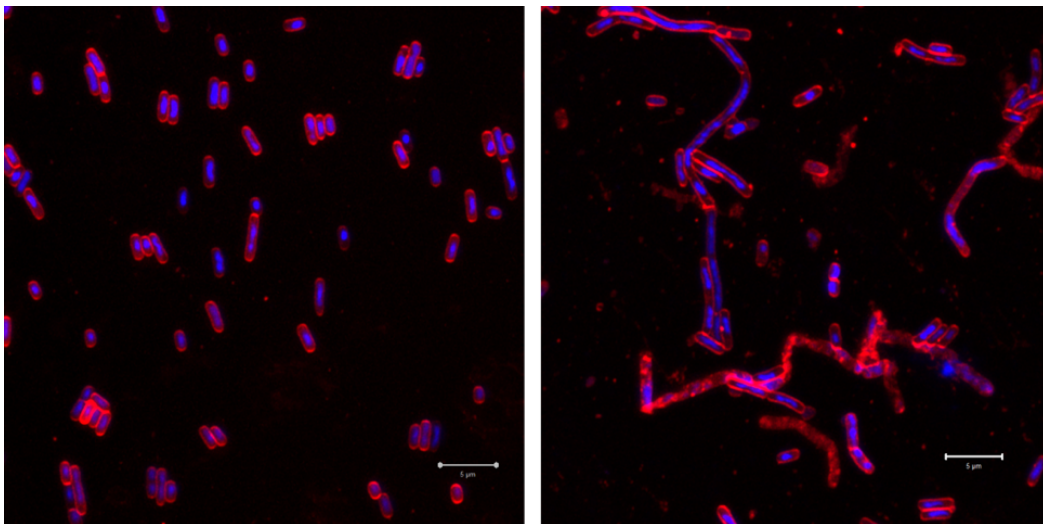


Figure 5.3. Heterologous co-expression of SpFtsEX and SpFtsA in *E. coli* cells.

*FM4-64 and DAPI stained *E. coli* cells at 100x magnification co-transformed with empty vectors pETDuet1 and pACYCDuet1 plasmids (a) compared to the same cell line harbouring expression constructs for SpFtsEX and SpFtsA respectively (b). Scale indicates 5 microns (μm).*

5.2.1.2. SpFtsA forms a tripartite complex with SpFtsEX, which extracted and purified successfully using SMALP nanodisc

In the next step, we examined the possibility of a direct *in-vivo* interaction between SpFtsEX and SpFtsA in *E. coli* host cells as well as the feasibility of purifying the same complex in its native form in SMALP nanodisc. The same *E. coli* cell line that expressing His-tagged SpFtsEX (His₆-SpFtsE and SpFtsX-His₁₀), was freshly transformed with *pACYCDuet1-SpftsA* as well. Transformed cells were grown and

induced overnight in AIM and membrane pellet was solubilised using SMALP as described in methods and material (2.4.3.1.2.). Finally, the high molecular weight tripartite complex in SMALP nanodisc was achieved by purifying the complex against the histidine-tags associated with SpFtsEX through Ni-NTA IMAC and further through SEC column (Superdex 200 Increase 10/300 GL) and thus any SpFtsA found associated with FtsEX must be occur as a consequence of its direct interaction. The formation of a high molecular weight complex was confirmed by native PAGE analysis followed by SDS-PAGE analysis with same SEC fractions (Figure 5.4. a and b). The analysis clearly shows the high molecular weight band on native PAGE, is composed of three major bands that identified as SpFtsE (~ 27 kDa), SpFtsX (~ 38 kDa) and SpFtsA (~ 49 kDa) as observed on SDS-PAGE and by LC-MS/MS mass spectrometry and peptide sequence analysis.

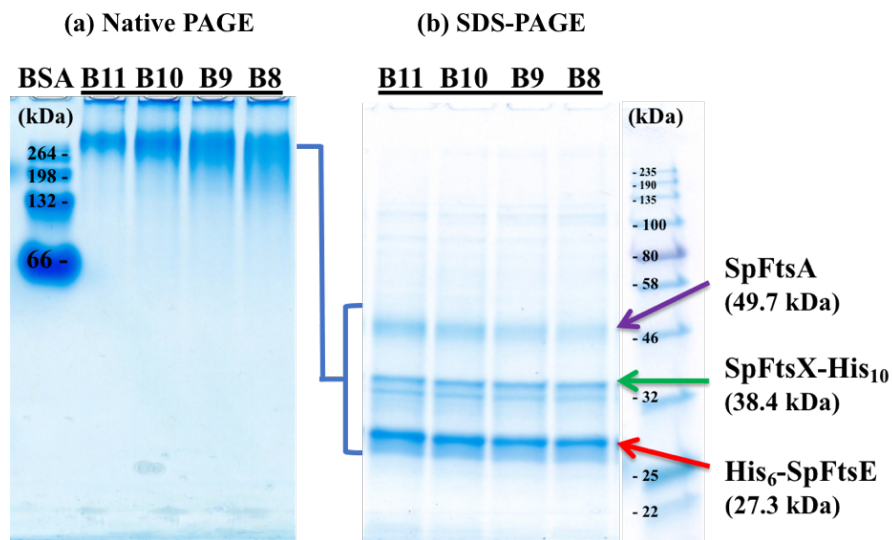


Figure 5.4. Purification of tripartite complex of SpFtsEX-SpFtsA in SMALP.

Expression and purification of a SpFtsEX-SpFtsA complex examined by native-PAGE (a) and SDS-PAGE (b).

5.2.1.3. FtsA interacts with FtsX but not with FtsE

Heterologous co-expression study with *S. pneumoniae* FtsEX and FtsA, and subsequent purification of these proteins as complex in SMALP nanodisc confirms a direct interaction between SpFtsEX and SpFtsA. However, it is not clear from this experiment whether is it SpFtsE or SpFtsX or both that interacts with SpFtsA?

In order to investigate this further, we expressed SpFtsE and SpFtsX separately in the presence of recombinant SpFtsA. We constructed *pETDuet* based expression vectors for SpFtsE-His₆ and SpFtsX-His₁₀ (**Table 2.4**) in isolation in which each protein was provided with a histidine tags on their carboxyl termini for subsequent purification and western blot detection. Expression of SpFtsE-His₆ or SpFtsX-His₁₀ protein individually (**Figure 3.2**, **Figure 3.4** and Appendix **Figure A 13**), produced comparable phenotypic observations (**Figure 3.1**) as seen for expression of the FtsEX complex described in Chapter 4 (**Figure 4.19**), indicative of interaction with the *E. coli* divisome. This interaction also observed *in-vitro* when *S. pneumoniae* proteins FtsX-His₁₀ and His₆-FtsA co-purified a low amount of *E. coli* FtsA and FtsX respectively (**Figure 3.4** and **Figure 3.5**, respectively). However, when the SMALP extracted untagged SpFtsA attempted purify through Ni-NTA IMAC resins, neither SpFtsA or SpFtsX protein bands are observed on the Coomassie stained SDS-PAGE gel (Appendix **Figure A 13**). We next co-transformed the individual FtsE-His₆ and FtsX-His₁₀ expression strains with an pACYC based plasmid expressing an untagged form of *S. pneumoniae* FtsA and SMALP purified any potential complexes using sequential IMAC and SEC to test if the FtsA association was specific to either FtsE or FtsX. Strikingly, SpFtsA was only recovered in the presence of FtsX indicating a direct interaction with FtsX alone (**Figure 5.5**). The sequence identities of purified SpFtsE-His₆ and co-purified proteins (SpFtsX-His₁₀ and SpFtsA) are confirmed by mass spectrometry as shown in **Figure 5.6** and **Figure 5.7** respectively. Whilst previous genetic experiments indicate an interaction between FtsX and FtsA in *E. coli* (Du et al., 2016), this is the first direct biochemical demonstration of this interaction and its potential in controlling early steps in cell division between cytoplasmic and membrane division components.

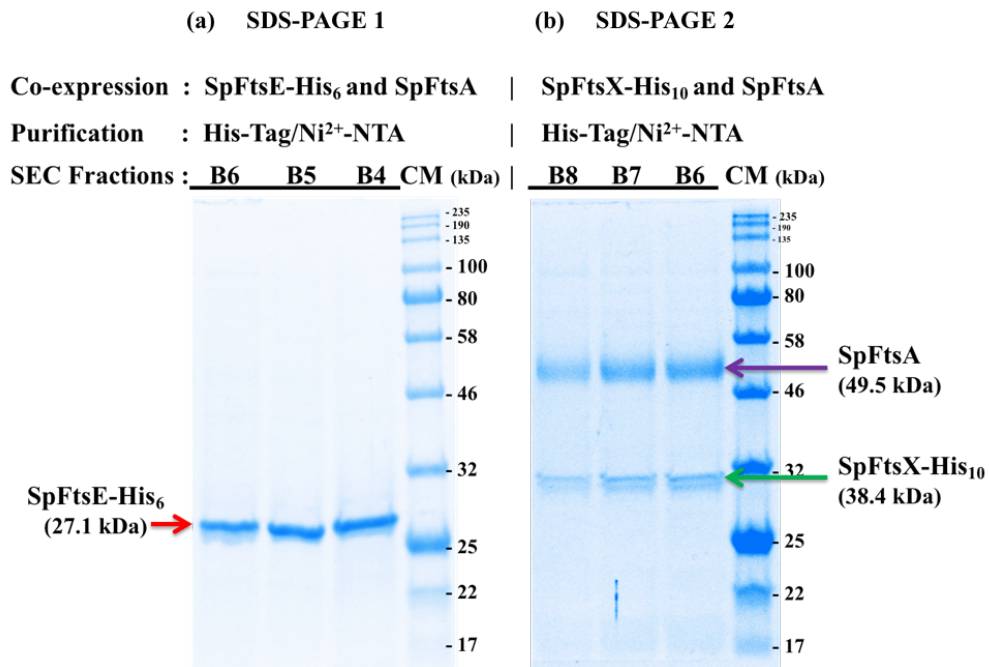
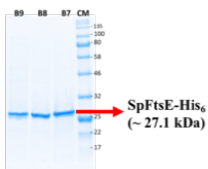


Figure 5.5. SpFtsX interacts with SpFtsA, but not SpFtsE.
SMALP mediated IMAC and SEC purification of his-tagged SpFtsE (a) and SpFtsX (b) in isolation, demonstrate copurification of untagged FtsA with FtsX alone.

Co-expression : FtsE-His₆ and FtsA
Purification : His-Tag/Ni²⁺-NTA

SDS-PAGE



Sequence identification by Mass Spectrometry

Q8DQH4_STRR6 (100%), 25,797.3 Da
ABC transporter ATP-binding protein & cell division protein OS=Streptococcus pneumoniae (strain ATCC BAA-36 exclusive unique peptides, 86 exclusive unique spectra, 173 total spectra, 219/230 amino acids (95% coverage))

| | | | | |
|---------------------|---------------------|---------------------|---------------------|---------------------|
| M S I I E M R D V V | K K Y D N G T T A L | R G V S V S V O P G | E F A Y I V G P S G | A G K S T F I R S L |
| Y R E V K I D K G S | L S V A G F N L V K | I K K K D V P L L R | R S V G V V F O D Y | K L L P K K T V Y E |
| N I A Y A M E V I G | E N R R N I K R R V | M E V L D L V G L K | H K V R S F P N E L | S G G E Q O R I A I |
| A R A I V N N P K V | L I A D E P T G N L | D P D N S W E I M N | L L E R I N L Q G T | T I L M A T H N S Q |
| I V N T L R H R V I | A I E N G R V V R D | E S K G E Y G Y D D | | |

Figure 5.6. Identification of SpFtsE through LC-MS/MS.
Sequence identification of purified SpFtsE band (~27 kDa) on SDS-PAGE, using mass-spectrometry (LC-MS/MS) analysis.

Co-expression : FtsX-His₁₀ and FtsA

Purification : His-Tag/Ni²⁺-NTA

SDS-PAGE

Sequence identification by Mass Spectrometry

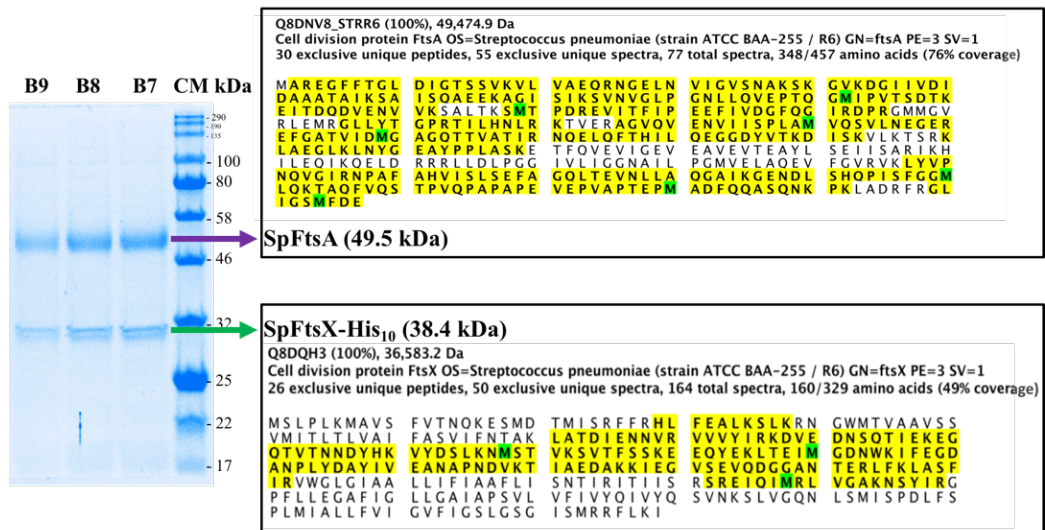


Figure 5.7. Identification of SpFtsX and SpFtsA through LC-MS/MS. Sequence identification of purified SpFtsA (untagged, ~ 49 kDa band) and SpFtsX (his-tagged, ~ 32 kDa band) on SDS-PAGE, using mass-spectrometry (LC-MS/MS) analysis.

5.2.2. The complex between FtsEX and PcsB play a significant role PG remodelling and separation

Previous genetic (Sham et al., 2013) and biochemical (Bajaj et al., 2016) studies provide some evidence for a interaction between FtsX and PcsB on the surface of the *S. pneumoniae* bacterial cell membrane. However, it has been shown that full length PcsB alone has no peptidoglycan hydrolytic activity in contrast to its isolated hydrolytic CHAP domain, highly suggestive that the full-length protein may require a conformational change upon docking to its cell membrane partner in order to be activated (Bartual et al., 2014). Given our ability to produce the FtsEX proteins in sufficient quantities for biochemical and structural investigations, coupled with our observations of phenotypic consequence of such expression, we next turned our attention to a potential complex between the FtsEX complex and PcsB to test the above hypothesis. In this regard, we created a modified *pCDFDuet1* vector based PcsB construct (Table 2.4), the design of which is quite similar to plasmid construct *pETDuetHETIS-his₆-SpftsEX-his₁₀*, but has a distinct origin of replication (*CloDF13*) and a *pelB* sequence (for a leader peptide) was fused at the 5'-end to full length *pcsB* gene. This leader peptide is very specific to *E. coli* system, is fused N-terminally to PcsB in order to guide PcsB to the *E. coli* bacterial periplasm and thus able to interact with FtsX on the extracytoplasmic environment (Sham et al., 2013).

5.2.2.1. Co-expression of SpFtsEX and PcsB rescue *E. coli* cells from cell division defect

Co-transformation of *E. coli* with separate plasmids constructs for the expression of FtsEX and PcsB in *pETDuetHETIS* and *pCDFDuetHETIS* (Table 2.4) respectively allowed a direct comparison of phenotype to cells transformed with the FtsEX expression construct alone (Figure 4.19) with the phenotype of cells carrying empty vector (Figure 5.8.a) to those co-expressing SpFtsEX and PcsB (Figure 5.8.b). Strikingly, when expression of SpFtsEX alone shows elongated cell phenotype (Chapter 4, Figure 4.19.c), co-expression of SpFtsEX and PcsB revealed that the previous cell division apparent phenotype had been rescued to a

normal rod shaped, consistent with a functional complex between FtsEX and PcsB which is able to hydrolyse *E. coli* peptidoglycan and thus re-establish normal cellular division.

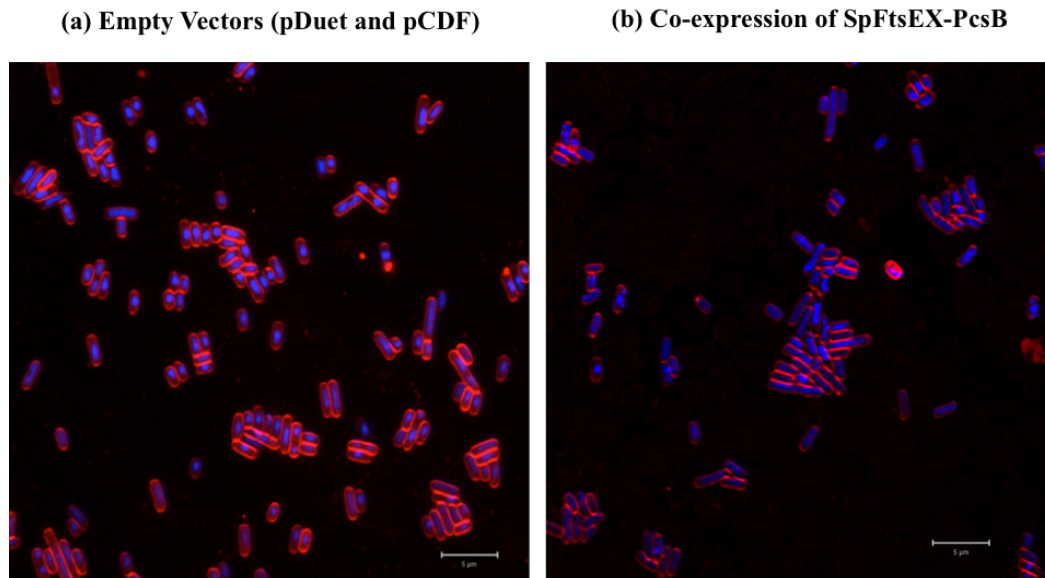


Figure 5.8. Heterologous co-expression of SpFtsEX and PcsB in *E. coli* cells.

FM4-64 and *DAPI* stained *E. coli* cells at 100x magnification co-transformed with empty vectors *pETDuet* and *pCDFDuet* plasmids (a) compared to the same cell line harbouring expression constructs for *SpFtsEX* and *PcsB* respectively (b). Scale indicates 5 microns (μm).

5.2.2.2. SpFtsEX and PcsB complex successfully extracted and purified using SMALP nanodisc

The heterologous co-expression study, shows a potential complex of PcsB with SpFtsEX prevented the severe cells division defects caused by expression of SpFtsEX alone, reverting to normal cell phenotype. While the cell phenotype is very obvious and comparable to normal *E. coli* cells or to same cells induced with empty vectors (that used to express above proteins), the question obviously arises whether or not these proteins are actually expressed, functional and interacting? To confirm the same, we decided to investigate further and purify the potential SpFtsEX-PcsB complex. Similar to co-expression study, the same *E. coli* *BL21(DE3)* $\Delta\text{acrB}::\text{kan}^R$ cell line was co-transformed with plasmid constructs

pETDuetHETIS-his₆-SpftsEX-his₁₀ and *pCDFDuetHETIS-pelB-PcsB-his₆* (Table 2.4). Proteins are expressed and produced inducing this co-transformed cell following optimised protocol as mentioned in Chapter 2 (section 2.4.3.1.2.). Expressed proteins are extracted from the membrane pellet using SMALP and purified sequentially by His-tag/Ni-NTA IMAC followed by SEC where a clear peak appeared through the SEC column at high molecular weight volume indicate a formation of complex (Figure 5.9.a). Further *in-vitro* biochemical characterization of SMALP purified PcsB and its complex with SpFtsEX (SpFtsEX-PcsB) showed a complex of the three proteins can be isolated together as a high molecular weight complex as judged by the native gel (Figure 5.9.b), SDS-PAGE gel (Figure 5.9.c) and Western blot (Figure 5.9.d) of the same SEC fractions. Although the Western blot signal from PcsB using an anti-his-tag antibody was relatively weak compared to FtsEX, its presence was confirmed through mass spectrometry sequence (Figure 5.10). Further, a preliminary biophysical characterisation was performed, and single molecule Cryo-EM feasibility was tested with this purified complex of SpFtsEX-PcsB in SMALP nanodisc as described in Appendix A1.

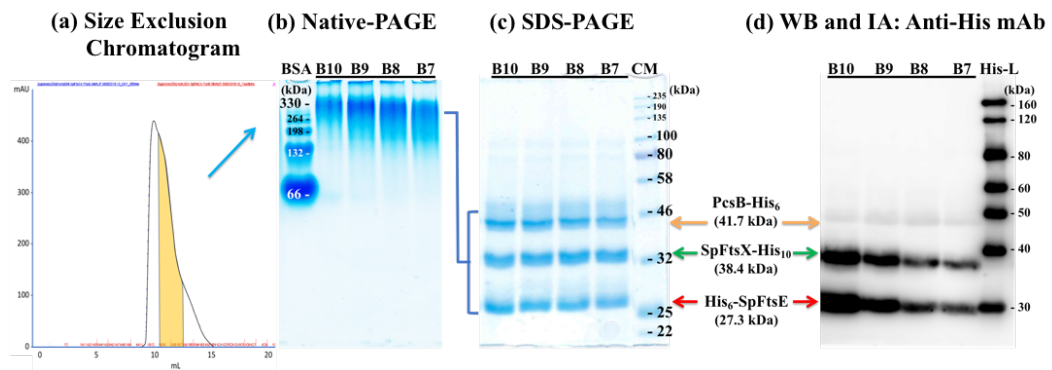


Figure 5.9. Purification of SpFtsEX-PcsB complex using SMALP. SMALP mediated IMAC and SEC purification of his-tagged SpFtsEX-PcsB peak fractions indicated in yellow (a), were analysed by native (b), SDS-PAGE (c) and Western blot and immunoassay analysis using anti-his tag monoclonal antibody (d).

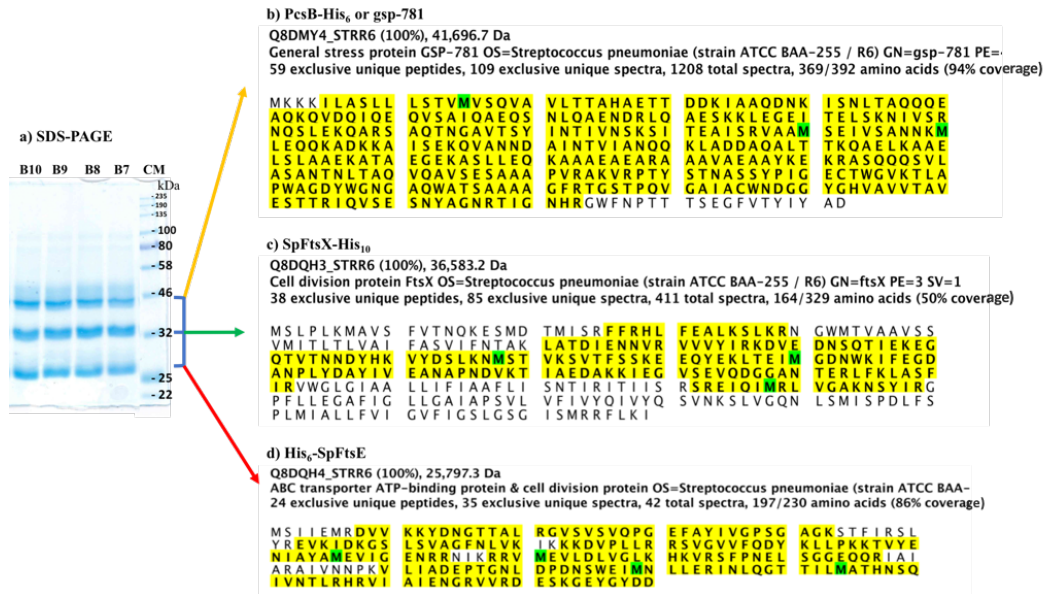


Figure 5.10. Identification of SpFtsE, SpFtsX and PcsB in a complex. SMALP extraction and purification of SpFtsEX-PcsB complex when separated upon SDS-PAGE (a) three bands (~ 42 kDa, 36 kDa and 27 kDa) were detected through Coomassie staining. These bands are analysed and sequenced through LC-MS/MS mass spectrometry, which them as PcsB (b), SpFtsX (c) and SpFtsE (d) with overall 94%, 50% and 86% sequence coverage respectively with their corresponding exclusive unique peptides. Yellow lines indicate sequence coverage by exclusive unique peptides.

In all of these experiments the SMA polymer is used to preserve the membrane lipid environment into which the FtsEX complex in particular is being expressed and we decided therefore to investigate if these membrane lipids in the context of the SMALP were important to observe the copurified proteins. This was examined comparing the quality of SMALP and DDM extracted and purified protein complexes. To achieve this, we directly compared cells expressing the proteins as described above to extracting from the membrane using the detergent DDM and purified in the same manner as described for SMALP using as above IMAC and SEC. The SEC chromatogram shows multiple peaks along with a major peak at high molecular weight volume (Figure 5.11.a). Interestingly, the SDS-PAGE analysis clearly shows the three proteins are absent with appropriate ratio in the same SEC fractions, when they are extracted by DDM (Figure 5.11.c). Similarly, the native-PAGE analysis also shows presence of multiple bands in the same lane (Figure 5.11.b). This result reveals that when purified in a detergent context, the complex is apparently destabilised in a detergent micelle. The inference is that the

membrane lipid context of these proteins is a key feature of the complex formation and that previous attempts to purify using detergents was flawed. In contrast to the SMALP extracted and purified situation these three proteins are clear forming a complex together and are quite stable with surrounding lipid environment. This may indicate the membrane lipids are important to purify these three proteins together as a complex in its stable form and for this complex to be functional appropriately in *in-vitro* condition.

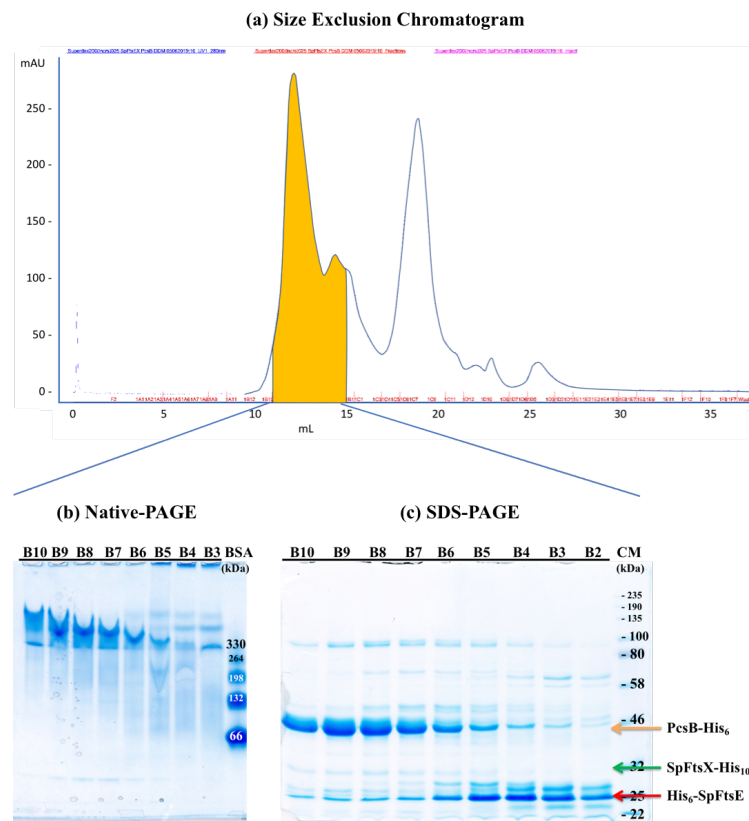
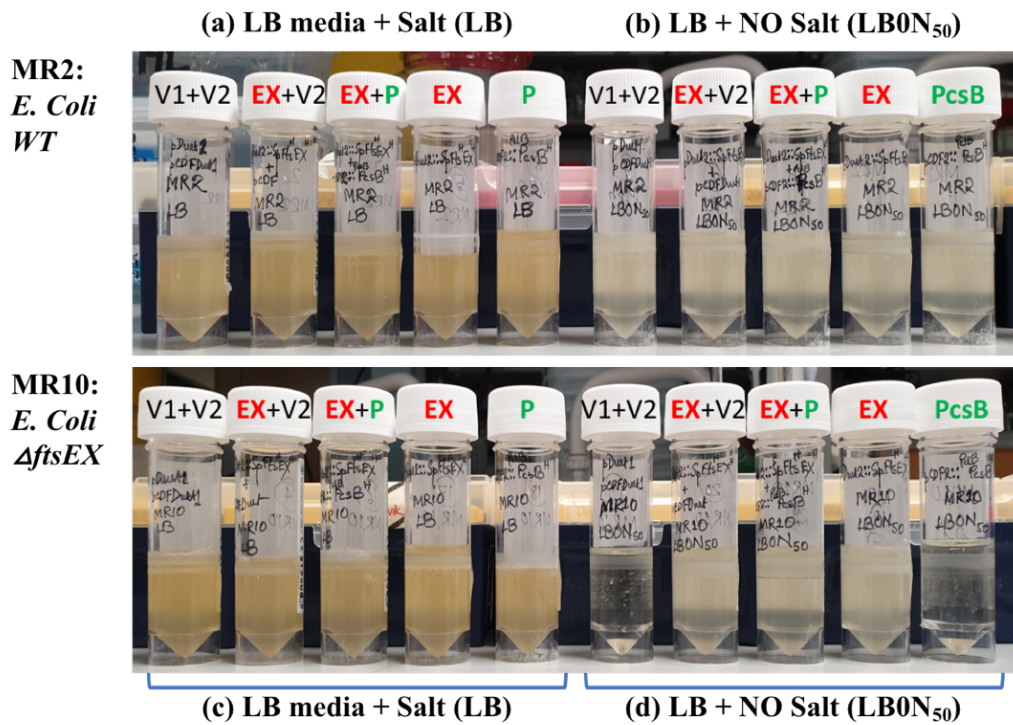


Figure 5.11. Purification of SpFtsEX and PcsB as complex using DDM. DDM mediated IMAC and SEC purification of his-tagged SpFtsEX-PcsB peak fractions indicated in yellow (a), were analysed by native (b), SDS-PAGE (c).

5.2.2.3. Expression of SpFtsEX or its co-expression with PcsB helps *E. coli ftsEX* knock-out mutant (MR10) strain growing in low-salt media

Since we observed heterologous expression of *S. pneumoniae* FtsEX in *E. coli* causing elongation of cell size as a result of dominant negative effect. We planned to test if the complexes of SpFtsEX or SpFtsEX-PcsB could actually compensate the loss of function of *E. coli* $\Delta ftsEX$ (MR10) mutant strain thus viability in no-salt media such as LB0N₅₀ (2.1.1.). This mutant strain *E. coli* MR10 lacks its chromosomal *ftsEX* gene and consequently this strain cannot survive in no-salt media LB0N₅₀ (Reddy, 2007). However, the same strain found survived in LB media with normal 1% (w/v) NaCl (LB) and the parent strain, MR2 can survive in both conditions. This is highly suggestive that *E. coli* FtsEX function is conditional but essential in no-salt or low-salt condition (Reddy, 2007). In our experiment we planned to use this conditional essentiality of MR10 mutant strain to test our SpFtsEX complexes in trans. We transformed both *E. coli* wild type MR2 and *E. coli* $\Delta ftsEX$ mutant strain MR10 with combination of plasmid constructs that express SpFtsEX, SpFtsEX-PcsB and PcsB as separate transformants. These transformants when induced in both normal LB (**Figure 5.12. a and c**) and LB0N₅₀ (**Figure 5.12. b and d**) media; both MR2 and MR10 transformants were found to grow normally in LB media (**Figure 5.12. a and c**, respectively). All MR2 transformants were also observed to grow in LB0N (**Figure 5.12.b**). However, among MR10 transformants only those which expressed SpFtsEX were survived in LB0N₅₀ media (**Figure 5.12.d**). Transformants with plasmids containing only PcsB or empty vectors did not survive under same no salt condition (**Figure 5.12.d**). The conclusion from this experiment therefore is that SpFtsEX is necessary and sufficient to complement the lack of EcFtsEX in the MR10 strain and this effect does not require the SpPcsB cognate hydrolase.



**V1: pDuet (Empty Vector); V2: pCDF-Duet (Empty Vector);
EX: SpFtsEX (pDuet) ; P : PcsB (pCDFDuet)**

Figure 5.12. SpFtsEX compensate the loss of function of *E. coli* Δ ftsEX mutant (MR10) in no salt LB media.

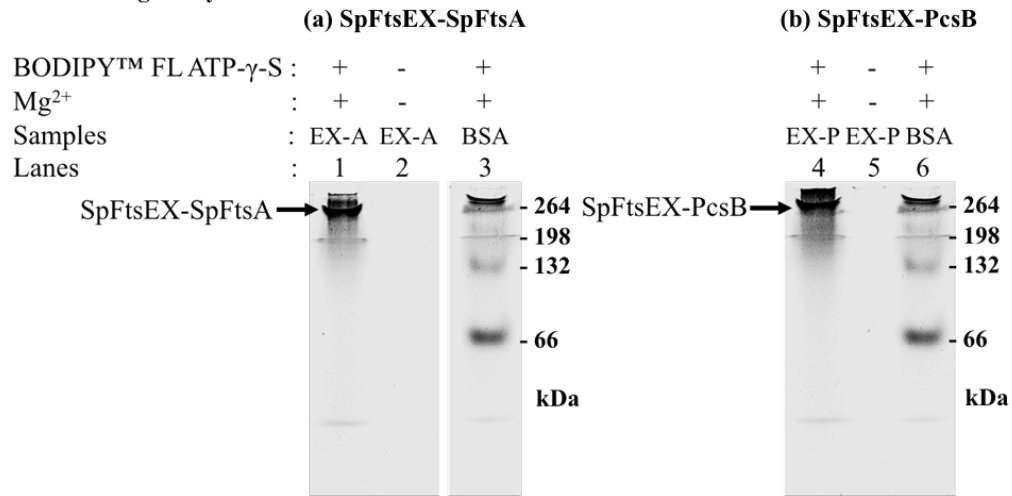
E. coli wild type (MR2) transformants co-expressing empty vectors (V1+V2), SpFtsEX and V2, SpFtsEX and PcsB, SpFtsEX and PcsB, were induced in LB media with 1% (w/v) NaCl salt (a) and in LB0N₅₀ media that is LB without any salt (b). Simultaneously, *E. coli* Δ ftsEX (MR10) mutant strain also transformed with above plasmid constructs in same order induced in LB (c) and LB0N₅₀ media (d).

5.2.3. Purified SMALP complexes of FtsEX-FtsA and FtsEX-PcsB can bind and hydrolyse ATP.

As described above, heterologous expression of *S. pneumoniae* FtsEX complex and its co-expression with FtsA or PcsB full length proteins in *E. coli* has demonstrated striking morphological changes on *E. coli* cell shape and provides strong evidence for these complexes having functional activity *in-vivo*. In order to understand their specific mechanism behind those phenotypical anomalies, we tested their *in-vitro* functional ability using ATP binding and hydrolysis assays as described in Chapter 4 (section 4.2.4.),

As described in the same section, all these purified SpFtsEX complexes either with SpFtsA or PcsB theoretically should contain the ATP-binding motifs Walker A and B with SpFtsE (John E. Walker et al., 1982). ATP-binding assays were performed in the presence and absence of a fluorescence ATP analogue BODIPY™ FL ATP- γ -S and Mg^{2+} as described in section 2.4.6.5. Samples of both SpFtsEX-SpFtsA and SpFtsEX-PcsB complex showed a positive fluorescent band (excitation at 488 nm and imaged 510 nm) at their corresponding molecular weight on the non-reduced native-PAGE gel only when these are assayed in presence of BODIPY™ FL ATP- γ -S and Mg^{2+} . The results indicate our purified SMALP complexes of FtsEX-FtsA (**Figure 5.13.a**) and FtsEX-PcsB (**Figure 5.13.b**) bind ATP molecules. In those samples containing FtsA as well, direct binding of the ATP analogue to FtsA is also possible since its polymerization is ATP dependent process (Krupka et al., 2014). However, when FtsA is absent (**Figure 5.13.b**) we also see ATP binding which can be directly attributed to the ATP binding site on FtsE. In these experiments we used BSA as a marker and positive control for ATP binding since it is known to bind ATP (Bauer et al., 1992).

ATP Binding Assay:



ATP Hydrolysis Assay:

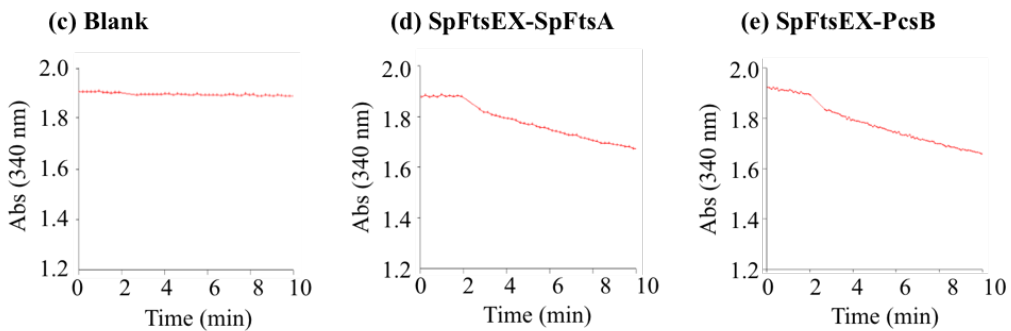


Figure 5.13. In-vitro functional assays with purified SpFtsEX-SpFtsA and SpFtsEX-PcsB complexes in SMALP.

ATP-binding assays (top): Native gel analysis of BODIPY-ATP-γ-S binding for (a) SpFtsEX-FtsA and (b) SpFtsEX-PcsB compared to BSA. Combinations of proteins labelled ATP and Mg²⁺ are indicated.

ATP-hydrolysis assays (bottom): Absorbance based kinetic traces for ATP hydrolysis assays with Blank (c), SpFtsEX-SpFtsA (d) and SpFtsEX-PcsB (e) shows very low-level of activity, however the concentration of the proteins was very low as well. In each assay about 2-4 μg of total protein was used per assays (200 μl).

In each of these figures, BSA: Bovine serum albumin, EX-A: SpFtsEX-SpFtsA complex in SMALP, EX-P: SpFtsEX-PcsB complex in SMALP; Abs (340 nm): Absorbance at 340 nm.

We next turned our attention to the role of ATP binding and hydrolysis with respect to PcsB activation linking events inside the cytoplasm of the cell to hydrolytic events outside the cell membrane. Following confirmation of ATP-binding ability of purified SpFtsEX-SpFtsA and SpFtsEX-PcsB complexes in SMALP, the obvious question arises about their ATP-hydrolysing ability, could these complexes

hydrolyse ATP under *in-vitro* conditions? To examine this, *in-vitro* ATP-hydrolysis assays were performed with above complexes in the same experiment as performed for SpFtsEX as described section 2.4.6.6. using the same blank (**Figure 5.13.c**) for all these purified complexes. The assay shows similar low-level activity for both complexes (**Figure 5.13. d and e**) as also observed for SpFtsEX (Chapter 4 **Figure 4.21**). However, these initial observations with the complexes of FtsEX is not yet conclusive due to lack of sufficient concentration of the samples and needs more careful further exploration in the future. Altogether results from two different *in-vitro* functional assays, one for ATP-binding and other for ATP-hydrolysis suggests, our SMALP extracted and copurified *S. pneumoniae* complexes of FtsEX-FtsA and FtsEX-PcsB binds ATP, shows low level of ATPase activity that requires further investigation.

5.3. Building up a larger macromolecular divisome complex with FtsZ, FtsA, FtsEX, and PcsB

In the next move, we planned to test the feasibility to build-up the complete macromolecular complex that involved in ATP-hydrolysis dependent PG hydrolysis and subsequent cell division, in a SMALP nanodisc context. So far, we have explored previous hypothesis about the interaction between SpFtsEX and PcsB, we have provided for the first time, direct evidence of the interaction between SpFtsX and SpFtsA. In addition, we have documented very distinct phenotypes in *E. coli* cells associated with SpFtsEX alone or co-expressed with either SpFtsA or PcsB. Moreover, we have been successful to purify these two-tripartite complex (SpFtsEX-SpFtsA and SpFtsEX-PcsB) using the SMALP nanodisc. We have seen PcsB successfully rescue *E. coli* cells from aberrant cell division defect caused by expression of SpFtsEX alone. Now the question is, can PcsB revert the effect of co-expression of SpFtsEX and SpFtsA? We also learned from previous findings that FtsZ interacts with FtsE and helps recruiting the latter into divisome (Corbin et al., 2007). Expressing SpFtsZ along with all four proteins (SpFtsE, SpFtsX, SpFtsA and PcsB) can we build-up the complete macromolecular complex? and purify the whole complex within host membrane lipids in SMALP nanodisc?

5.3.1. PcsB fails to rescue *E. coli* cells from severe cell division defect when SpFtsA co-expressed with SpFtsEX

In sections 5.2.1.1. and 5.2.2.1. we observed an *E. coli* cell line that expressing SpFtsEX, are able to avert aberrant cell division phenotypes when co-expressed with PcsB (**Figure 5.8**) but not when co-expressed with SpFtsA (**Figure 5.3**). The latter caused slower cell division (**Figure 4.19.a**) among all other co-expression and showed phenotypic defects. Therefore, at first, we attempted to co-express PcsB along with SpFtsEX and SpFtsA in *E. coli* cells (*BL21(DE3)* Δ *acrB::kan^R*) in order to salvage cells from similar phenotype. However, to our surprise, the cells were found severely elongated (**Figure 5.14.b**) compared to all other expression tested before in this study, and to cells harbouring and expressing their respective empty

vector plasmids *pCDFDuet*, *pETDuet* and *pACYCDuet* respectively, in our initial attempts (**Figure 5.14.a**). This excessive filamentous phenotype associated to co-expression of SpFtsEX, SpFtsA and PcsB, clearly suggest PcsB could not revert the combined effect of SpFtsEX and SpFtsA. This may indicate that overproduction of SpFtsA and its interaction with SpFtsEX either dislocate the complex from the divisome site because *S. pneumoniae* FtsA are reported to have roles in peripheral as well as septal PG synthesis (Mura et al., 2017), or it may be competing with PcsB for interaction with SpFtsEX at septum.

5.3.2. A combined effect of FtsZ and PcsB counterbalance the phenotypic abnormalities of SpFtsEX-SpFtsA complex

In the next phase, we tested whether expressing *S. pneumoniae* FtsZ along with other four proteins as mentioned above, could also affect the division of *E. coli* cells in this context? In order to examine this, we cloned the whole *S. pneumoniae* *ftsAZ* operon that containing adjacent *S. pneumoniae* genes for FtsA (*SpftsA*) and FtsZ (*SpftsZ*) (Appendix **Figure A 14**), into a modified plasmid vector *pACYCDuetHETIS* (**Table 2.4**). This modified plasmid construct (*pACYCDuetHETIS-his₆-SpftsAZ*) provides a 6-histidines tag at the N-terminal of SpFtsA and leave SpFtsZ untagged. To test this construct, when the same *E. coli* cell line (*BL21(DE3)ΔacrB::kan^R*) was co-transformed using respective expression constructs for SpFtsEX and SpFtsAZ (**Table 2.4**), expression of all four proteins associated to these constructs showed a very similar excessive filamentous phenotype (**Figure 5.14.c**) as seen in co-expression of SpFtsA, SpFtsEX, PcsB without SpFtsZ (**Figure 5.14.b**).

By contrast, when the same cell line was co-transformed with expression constructs for SpFtsEX, SpFtsAZ and PcsB (**Table 2.4**), the cells did not show the excessive filamentous phenotype (**Figure 5.14.d**) as observed before in co-expression studies without PcsB (**Figure 5.3** and **Figure 5.14**). In this situation with the *E. coli* cells expressing all above five proteins (**Figure 5.14.d**), their growth was associated with a much more usual phenotype observed with cells harbouring and co-expressing

their respective empty vectors (**Figure 5.14.a**). This result can be interpreted as direct effect of the expression of the *S. pneumoniae* proteins upon the division of the *E. coli* cells and that SpFtsZ possibly plays an important role to localise SpFtsA and SpFtsEX at the septum, so that these divisome proteins assemble further interactor protein(s) and function appropriately (El-Hajj and Newman, 2015). In this case, SpFtsZ possibly guides the SpFtsEX complex and SpFtsA towards the septum, where an interaction between SpFtsEX and PcsB occurs at a later stage, allowing hydrolysis of the PG layer and thus separation of the daughter cells, enabling a normal rod-shaped phenotype of the host *E. coli* cell.

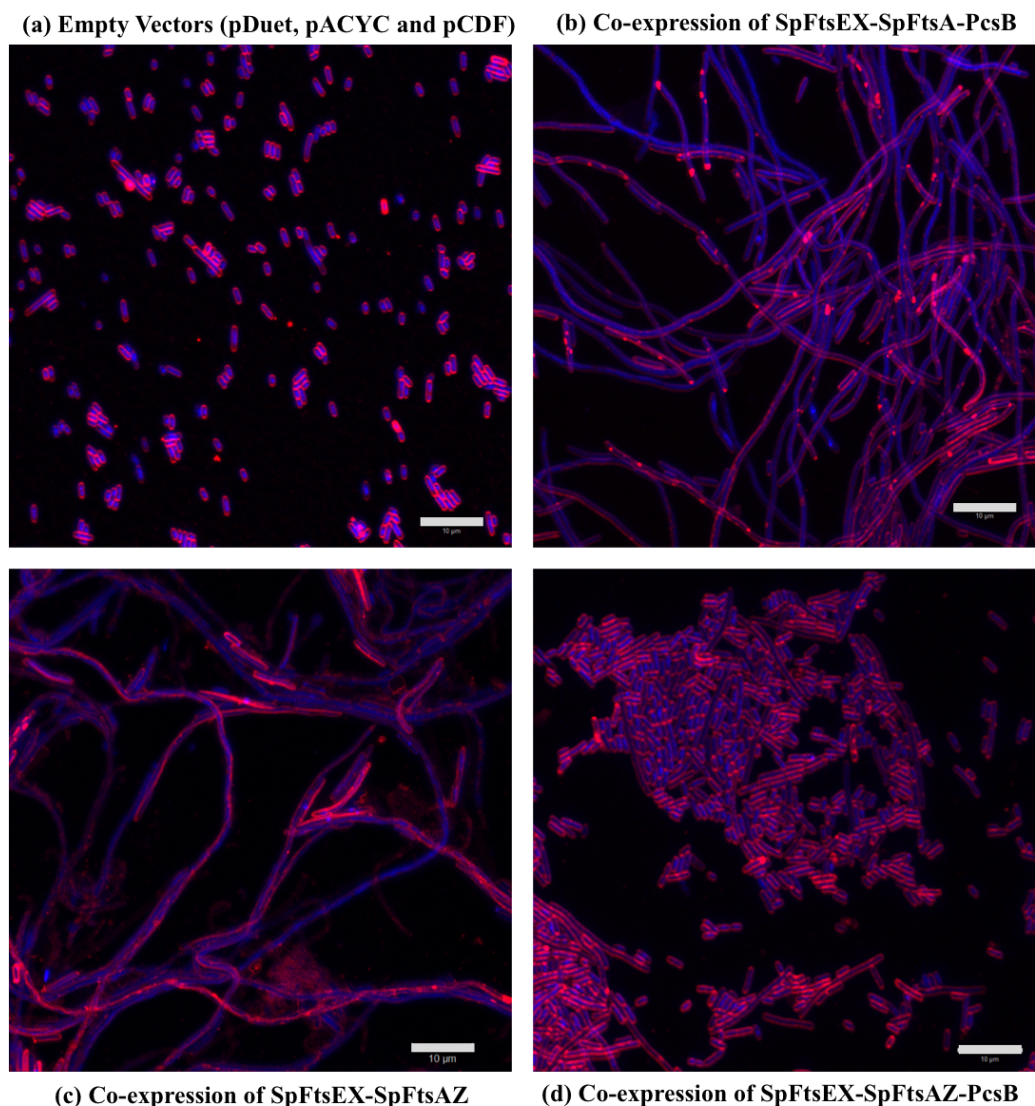


Figure 5.14. Effects of co-expression of macromolecular complexes in combination.

FM4-64 and DAPI stained E. coli cells at 40x magnification co-transformed with empty vectors pETDuet, pACYCDuet and pCDFDuet plasmids (a)

compared to the same cell line harbouring expression constructs for *SpFtsEX*, *SpFtsA* and *PcsB* respectively **(b)**, for *SpFtsEX* and *SpFtsAZ* respectively **(c)**, for *SpFtsEX*, *SpFtsAZ* and *PcsB* respectively **(d)**. Scale indicates 10 microns (μm).

5.3.3. A macromolecular cell divisome complex can be successfully purified in SMALP nanodisc by co-expressing *SpFtsEX*, *SpFtsAZ* and *PcsB*

Initially, we tried to purify the possible *SpFtsA*-*SpFtsEX*-*PcsB* complex by co-expressing these four proteins without co-expressing *SpFtsZ*, using SMALP. However, we failed to co-purify these four proteins together as complex. This failure to form a functional complex possibly links the reason why *PcsB* failed to rescue the aberrant cell division phenotype due to co-expression *SpFtsEX* and *SpFtsA*. This possibly supports the speculation (as mentioned in **5.3.1.**) about the role of *SpFtsZ* in localising and assembling the same complex at divisome correctly, so that it can function appropriately as a complex and hydrolyse PG through *PcsB*. In this initial attempt, failure to form such functional complex possibly resulted as incomplete septum PG hydrolysis and cell separation.

By contrast, successful co-expression of the five cell division proteins: *SpFtsE*, *SpFtsX*, *SpFtsA*, *SpFtsZ* and *PcsB*, in *E. coli* cells appears to occur without a significant effect on cell phenotype (**Figure 5.14.d**) in compare to several of these proteins expressed in isolation (**Figure 3.1**) or co-expressed in combination (**Figure 5.14.b,c**). This prompted us to investigate the nature of the interaction of these proteins further and to purify the complete macromolecular complex. Given that the phenotypic observation is suggestive of a functional cell division complex it is possible that such a complex is also representing one capable of ATP-hydrolysis dependent PG hydrolysis.

Using the same *E. coli* BL21(DE3) $\Delta\text{acrB}::\text{kan}^R$ cell line as previously described we co-transformed it with plasmids *pETDuetHETIS-his6-SpftsEX-his10*, *pACYCDuetHETIS-his6-SpftsAZ* and *pCDFDuetHETIS-pelB-pcsB-his6*.

Transformed cells were induced overnight at 20 °C and overexpressed proteins in its complex form were extracted using SMALP as per the optimised protocol as described in section 2.4.3.1.2. The SMALP extracted membrane protein complex was purified using His-tag/Ni-NTA IMAC and further purified through SEC using a Superdex 200 Increase 10/300 GL column. The purified SEC peak fractions (**Figure 5.15.a**) when analysed on native-PAGE, a wide band migrated over 300 kDa was observed (**Figure 5.15.b**). The same peak fractions when analysed under reduced condition on SDS-PAGE, four clear bands for SpFtsE (~ 27 kDa), SpFtsX (~ 38 kDa), PcsB (~ 42 kDa) and SpFtsA (~ 50 kDa) were observed (**Figure 5.15.c**). The same separated bands on Western blot also showed positive staining for Histidine-tag that associated to each of these four proteins, when the blot immunoassayed using monoclonal primary anti-His-HRP antibody (**Figure 5.15.d**). While this result for the very first time indicates a possible macromolecular complex that consist of SpFtsA, SpFtsE, SpFtsX and PcsB; we could not identify a band for SpFtsZ on SDS-PAGE along with other proteins. If purified, the untagged SpFtsZ (predicted MW 44.4 kDa) band would be difficult to distinguish since it would be very close to the PcsB band (~ 42 kDa) on SDS-PAGE. Alternatively, if we consider SpFtsZ did not co-purify with the above complex despite its reported interaction with SpFtsE (Corbin et al., 2007), then this might possibly be explained by either a weak interaction between SpFtsZ and SpFtsE, or the interaction only exists within a stable in cytoplasmic environment. The latter would infer that there is no direct association of SpFtsZ to the cell membrane, thus limiting the interaction in the soluble fraction. Therefore, extraction of above complex from the membrane fraction apparently restricts any co-purification of SpFtsZ along with other four membrane associated proteins. We must also bear in mind that this complex protein-protein interaction is demonstrated in a heterologous overexpression scenario and thus subject to a number of possible interpretations. In all cases, whether or not the SpFtsZ co-purified with other four proteins, it requires further repetition of the same experiment using different tags, peptide sequence analysis and detailed investigation about their interactions.

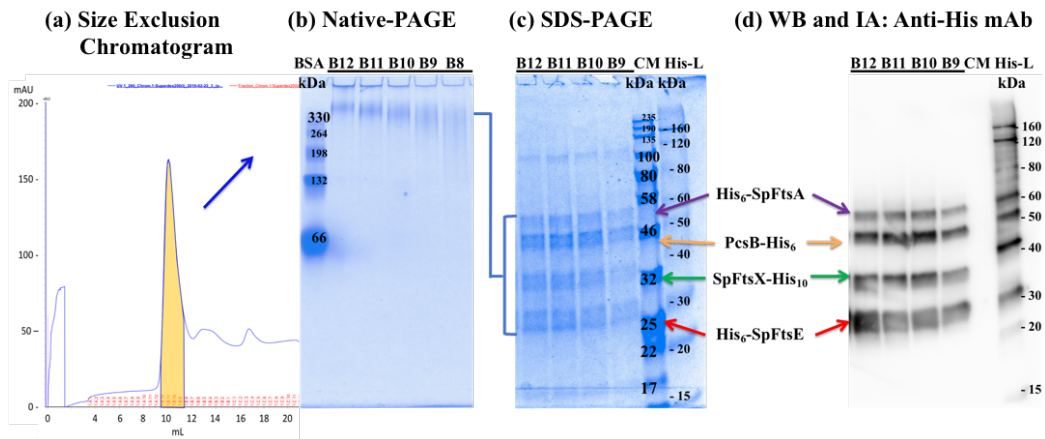


Figure 5.15. Successful purification of macromolecular complex, consists of SpFtsEX, SpFtsA and PcsB, in SMALP nanodisc. SMALP mediated IMAC and SEC purification of his-tagged SpFtsEX-SpFtsA-PcsB peak fractions in yellow (a) analysed by native-PAGE (b), SDS-PAGE (c) and Western blot and immunoassay analysis using anti-his tag monoclonal antibody (d). The band on native-PAGE gradually migrate wider in lower fractions, may possibly indicate a dissociation of proteins from the complex

5.4. DISCUSSION: PcsB forms functional complex with FtsEX and rescue cells from concatenation and aberrant cell division that observed with co-expression of SpFtsEX-SpFtsA complex

The bacterial protein complex of FtsEX sits at the hub of a complex choreography of cellular activities linking cell division events across the bacterial cell membrane. FtsEX is required in the early steps of cell division, coordinating events in the cytoplasm and also appears to be a “docking platform” and regulator of hydrolytic enzymes in the extra-cytoplasmic space in both Gram-positive and Gram-negative bacteria. In our heterologous expression study, we observed aberrant cell division defects in *Escherichia coli* cell when subject to expression of the *Streptococcus pneumoniae* FtsEX mimicking the phenotype of existing natural product antibacterial agents as well as antibiotic drugs. Moreover, previous reports have investigated the host cytokine CLCX10 as an inhibitor of FtsEX function as well as other targets (Bruce et al., 2018; Crawford et al., 2011; Margulieux et al., 2016). This suggest that FtsEX may provide a suitable focus for future antimicrobial strategies since its function is essential in Gram-positive bacteria and conditionally essential (low salt) in *E. coli* (it is not known if the same is true for other Gram-negative bacteria). We now show that the aberrant cell division phenotype, as a consequence of SpFtsEX expression, can be rescued by expression of SpPcsB in trans. This remarkable observation of the consequence of FtsEX expression in isolation or in complex with SpFtsA, is consistent with interruption of cell division process as yet by an ill-defined mechanism. Our working hypothesis is that an imbalance in the levels of certain cell division proteins, sequesters additional proteins in unproductive complexes; and that the SpFtsEX-PcsB complex is probably functionally active and in addition it can hydrolyse *Escherichia coli* PG required for PG remodelling during cell separation. This hypothesis requires the *S. pneumoniae* cell division proteins to be able to interact with the corresponding interaction partners from the host *E. coli* proteome and we demonstrate a direct copurification of *E. coli* FtsA with the SpFtsEX complex and specifically with SpFtsX.

Consistent with this overall hypothesis, a previous biochemical demonstration that shows the PcsB hydrolytic CHAP domain in isolation has the ability to digest isolated peptidoglycan from a different bacterial specie (Bartual et al., 2014). In addition, the same study shows that the vast majority of the extracellular full-length protein in isolation, is not active as a PG hydrolase in the same assays. The authors attribute this lack of activity in the full-length protein to a shielding of the CHAP domain by the rest of the protein and consequent conformational change required for activity. Such events are consistent with the hypothesis that docking of PcsB with SpFtsEX at the membrane and/or ATP hydrolysis by FtsE inside the cytoplasm is required for PcsB peptidoglycan hydrolytic activity. Whilst FtsEX has sequence similarity to archetypical: ABC transporters, there is no evidence of such a transport mechanism of cargo (Bajaj et al., 2016). However, the recent structure of MacB which is an ABC transporter that collaborates with the MacA adaptor protein and TolC exit duct to drive efflux of antibiotics out of the bacterial cell suggests the hydrolysis of ATP inside the cytoplasm drives conformational changes in the protein outside the cell membrane (Crow, Greene, Kaplan, and Koronakis, 2017). This may provide a mechanism for ATP dependent hydrolysis of the FtsEX in concert with activation and possible regulation of PcsB peptidoglycan hydrolytic activity.

Additionally, we have shown that these membrane protein complexes can be isolated *in-vitro* using styrene-maleic-acid-lipid-particles (SMALP) nanodisc, preserving a representative membrane lipid environment (without detergents) (Lee et al., 2016). In this study, we have overexpressed FtsEX along with FtsA and PcsB from *Streptococcus pneumoniae* in *E. coli*, and purified them as a complex in SMALPs, for enzymatic, biochemical and high-resolution single-molecule structural studies. The protein-protein interaction studies described indicate SpFtsX (but not SpFtsE), interacts with the essential divisome protein SpFtsA, and PcsB successfully docks with SpFtsEX to form an active peptidoglycan hydrolytic complex. Moreover, these complexes are competent for ATP binding as shown by *BODIPY-ATP- γ -S*. Recent studies on the *E. coli* FtsEX system using genetic and

phenotypic screens (Du et al., 2016) shows the EcFtsEX acts on EcFtsA to regulate both divisome assembly and activity. An interaction between EcFtsX and EcFtsA was indicated in a genetic screen and that this interaction was required for divisome assembly and inhibition of divisome function by ATPase mutants of EcFtsEX. Our results provide phenotypic and for the first-time biochemical data in support of this hypothesis.

Furthermore, in a series of ambitious efforts, we have shown the heterologous effects of macromolecular co-expression of SpFtsEX with three other proteins that has been reported to interact and involve in both processes of PG synthesis and PG hydrolysis. The FtsEX complex play a crucial role to counterbalance these two processes precisely. Since, in *S. pneumoniae* all these proteins are essential and the model system lacks a suitable expression strain to perform any such macromolecular co-expression study, we took the advantage of heterologous *E. coli* system, where we co-expressed these proteins in various combination and observed their phenotypes. We noticed a filamentous phenotype whenever SpFtsA co-expressed with FtsEX, even co-expression of either PcsB or SpFtsZ could not rescue cells from the same fate, the condition rather appeared poor and cells showed strikingly filamentous phenotype. However, the same *E. coli* cells that co-expressing SpFtsEX-SpFtsA, are observed to establish a normal cell division phenotype when co-expressed with SpFtsZ and PcsB together. These results indicate that these five proteins are interconnected and dependent on each other for their proper localization and function at the divisome site. Incorrect ratio of these proteins at the septum could cause a fatal damage to divisome site and so its function, as also observed in previous studies (Dai and Lutkenhaus, 1992; Dewar et al., 1992). Consequences of such damaged divisome and/or loss of functions possibly noticed in our heterologous co-expression studies with inappropriate complex and combination of co-expression of these proteins.

In *E. coli*, it has been showed that the FtsEX complex is dependent of FtsZ for its correct localization at the Z-ring (Du et al., 2019) and precisely through an interaction between FtsZ and FtsE (Corbin et al., 2007; Du et al., 2019). However,

mild overexpression of this EcFtsEX caused a divisional cellular defect due to delocalization of FtsA from divisome (Du et al., 2019; Du et al., 2018). Such an observation would also be consistent with our hypothesis that the ratios of the individual proteins with respect to each other is also an important factor in cell division, which when imbalanced, can lead to the sequestration of key proteins into non-productive protein-protein interactions.

Localization of *E. coli* FtsA at the divisional site also depends on the preceding location of FtsZ but not the way around (Addinall, Bi, and Lutkenhaus, 1996; Addinall and Lutkenhaus, 1996; Mura et al., 2017). Similarly, in *S. pneumoniae* FtsA has been found essential and dependent on FtsZ for its localization at divisome (Lara et al., 2005). However, the same protein has very distinct role in two different bacteria. Unlike *E. coli* FtsA, *S. pneumoniae* FtsA is involved in both peripheral and septal PG synthesis and a complete depletion of the same cause an isotropic cell expansion and cell death (Mura et al., 2017). Together with all these previous findings and recent observations from our heterologous co-expression studies with above five proteins, we can conclude the overexpression of SpFtsEX and its interaction with SpFtsA possibly displacing the complex from divisome site to peripheral site. As a result, we noticed elongated cells and the phenotype observed could not be prevented with co-expression of PcsB, possibly because the displacement of SpFtsEX-SpFtsA complex more towards the peripheral site may not be allowing the majority of PcsB to access the SpFtsEX to dock correctly at the divisome site. This situation also supports the idea that the SpFtsEX interacts with SpFtsA before PcsB, or that the interaction and function of SpFtsEX-PcsB is dependent on correct localization and interaction of SpFtsEX with SpFtsA; and may be influenced by SpFtsZ as observed in our co-expression study with all above five proteins.

In the case where the SpFtsA was absent, the heterologous expression of SpFtsEX in *E. coli* possibly restricts the same complex at divisome site through a chimeric interaction between SpFtsEX and *E. coli* FtsA, as EcFtsA is only reported to be involved in sPG synthesis (Du et al., 2019; Du et al., 2016). As a result, although

we noticed a dominant negative effect on overexpression of SpFtsEX in *E. coli* possibly due to an antagonistic nature of its very minimal interaction with EcFtsA (Du et al., 2016), but when these cells co-expressed these proteins in presence of PcsB, the hydrolase activity of PcsB evidently has a role in enabling PG hydrolysis. These experiments require additional *in-vitro* verification that the tripartite complex of SpFtsEX-PcsB can hydrolyse PG. But the fact that we can isolate the tripartite complex in SMALP and that the presence of PcsB rescues the phenotype of SpFtsEX expression in isolation, is an important step in support of the above hypothesis.

Similarly, the cells that co-expressing all five proteins (SpFtsEX, SpFtsAZ and PcsB), were able to escape from severe phenotypic defects as observed in cells co-expressing four proteins without either SpFtsZ or PcsB. However, a lack of biochemical evidence about the presence of SpFtsZ in the macromolecular complex that is composed of SpFtsA, SpFtsEX and PcsB in SMALP nanodisc, suggests the SpFtsZ possibly have no stable interaction with above complex. Whilst the latter experiments with all above five proteins are preliminary and more controls are required, together these *in-vivo* and *in-vitro* observations could indicate that SpFtsZ has important role to localize SpFtsA and SpFtsEX at the divisome site, but it may not form a stable macromolecular complex that involved in PG hydrolysis. While this result is for the very first time has been shown that these five proteins can be co-expressed together in a heterologous system like *E. coli* and a possible macromolecular complex that composed of SpFtsA, SpFtsEX and PcsB, could be purified using SMALP nanodisc. Clearly this provides the basis for future investigation of their precise interaction and role in regulating divisome activity and PG hydrolysis.

CHAPTER 6. General discussion and future perspectives

6.1. The global concern with β -lactam and other antibiotic resistance

Since the discovery of penicillin as an antibiotic almost 90 years ago, the discovery of as many as 20 new classes followed in next three to four decades (Coates, Halls, and Hu, 2011; Powers, 2004). However, overuse and misuse of these classes of antibiotics and their analogues have made many of these drugs ineffective due to counter-resistance mechanism in bacteria. This is a result of the effective selection pressure applied to bacteria which has prompted fast adaptation giving rise to multidrug-resistance bacteria world-wide (Levy and Marshall, 2004); (O'Neill's report 2016). This threat, in addition to the fact that it has taken just over 50 years for some bacterial strains to evolve resistance against most of these 20 existing classes of antibiotics, combined with a drop in industrial efforts to find new class of antibiotics (only three classes has been discovered) (Cheesman, Ilanko, Blonk, and Cock, 2017; Coates et al., 2011) is a serious global concern. Furthermore, what is concerning is that the resistance mechanism for a certain class of antibiotics varies between Gram-positive bacteria and Gram-negative bacteria, and even species to species within same category. Taking the example of β -lactam antibiotics (including penicillin, carbapenem, cephalosporin and monobactam subfamilies) which are clinically important and still relevant to date, we find completely different primary resistance mechanisms employed by Gram-negative and Gram-positive bacteria (Fisher and Mobashery, 2016). The β -lactam antibiotics target PBP proteins and inactivates their activity and thus inhibits transpeptidation of PG, which consequently disrupt the cell wall and ultimate cell lysis (Macheboeuf, Contreras-Martel, Job, Dideberg, and Dessen, 2006). While this class of antibiotics had a legacy to combat severe bacterial infections for decades, the battle between the two put a selection pressure on many bacteria to develop various resistance mechanisms. Gram-negative bacteria such as *E. coli* and

Pseudomonas aeruginosa (*P. aeruginosa*) have developed the ability to produce β -lactamase enzyme into their periplasmic spaces to hydrolyse the β -lactam before it can interact with a PBP and thus shield themselves from β -lactam action. In addition, many Gram-negatives, in particular certain strains of *Pseudomonas Sp.* as well as *Klebsiella Sp.* are able to remove antibiotics from the periplasmic space by the use of efflux pumps eg MexA, B-OprM pumps (Macheboeuf et al., 2006; Nehme and Poole, 2005).

By contrast, Gram-positive bacteria such as *S. pneumoniae* and *Staphylococcus aureus* (*S. aureus*) and certain *Enterococci*, they do not generally secrete β -lactamase, instead they modify or mutate their PBPs to avoid β -lactam inactivation (Macheboeuf et al., 2006; Pinho, de Lencastre, and Tomasz, 2001; S. W. Wu, de Lencastre, and Tomasz, 2001). This is best exemplified by the acquisition of a class B PBP with reduced susceptibility to β -lactams as seen in methicillin-resistant *Staphylococcus aureus* (MRSA), and mutational resistance by genetic recombination and mosaic gene formation providing resistance to β -lactams seen in naturally transformable strains including *S. pneumoniae*. Finally, some strains including *Enterococci Sp* and *Mycobacterium tuberculosis* switch their mode for cell wall crosslinking from PBP DD-transpeptidase dependent 3-4 crosslinks to LD-transpeptidase dependent 3-3 crosslinking upon β -lactam challenge, in which the chemistry of the latter enzymes' active sites makes them susceptible to only a very limited set of β -lactam compounds (e.g. imipenem). Production of these highly mutated PBPs that are insensitive to most β -lactam antibiotics but capable of synthesizing PG, help these bacteria emerge as multidrug-resistant bacteria and continue the endless battle between the antibiotics and bacteria.

6.2. *S. pneumoniae* PBPs and β -lactam resistance

S. pneumoniae is one most frequently resistance bacteria of human healthcare relevance, which has developed highly altered mosaic PBPs, that contain as many as 100 mutations (Albarracin Orio, Pinas, Cortes, Cian, and Echenique, 2011; Macheboeuf et al., 2006; Spratt, 1994). As previously discussed *S. pneumoniae* produce six functional PBPs among which three: PBP1a, PBP1b and PBP2 are class A bifunctional and shows both GTase and TPase activities, whereas two: PBP2b and PBP2x are class B monofunctional and shows only TPase activity. The remaining enzyme, PBP3 is class C enzyme shows carboxypeptidase activity and is required for peptidoglycan modification and shape determination.

Interestingly, in the same bacterial species the monofunctional PBP2b and PBP2x which are involved directly in PG synthesis as a component of elongasome and divisome complexes respectively, are also found essential (Berg et al., 2013; Philippe et al., 2014) and crucial to compensate and tolerate the individual or paired functional redundancy of three monofunctional PBPs (Fisher and Mobashery, 2016). This clearly indicates there might be other component(s) from divisome or elongasome or from completely different pathway, are involved. Indeed, recently a divisome component FtsW has been shown to have GTase activity that is inter-reliant on coupling to TPase activity of class B PBP2x to accomplish the PG synthesis (Taguchi et al., 2019), suggests divisome components may play a vital role in developing β -lactam related resistance by continuing PG synthesis using alternate mechanisms and maintaining cell viability. This give rise one of the fundamental questions about this β -lactam or other antibacterial resistance is that what other additional factor(s) or pathway(s) are involved with and contributing to this resistance? Genome wide analysis of single nucleotide polymorphism suggests *mraW* and *mraY* genes from cell wall synthesis pathways are associated to β -lactam resistance, so as genes from cell division pathway (*ftsL*, *gpsB* etc.), recombination pathway (*recU*) and genes that encodes chaperons such as *clpL* and *clpX* (Chewapreecha et al., 2014; Fisher and Mobashery, 2016). Interestingly the ClpX protein is involved in Z-ring disassembly process and many of these are directly or

indirectly involved with cell division mechanism. This indicates that, to understand β -lactam or other antibacterial resistance mechanisms, we do need to understand the mechanistic links between macromolecular complexes that involved in cell division mechanism and cell wall synthesis.

6.3. Targeting divisome complexes could restrict bacterial infections

Bacteria generally need to be able to multiply and be present in sufficient numbers in order to overcome the response often mounted by the immune system. Thus, if we are able to restrict or interfere with their reproduction, the immune system is able to mount a successful attack and clearance of any such infection. Therefore, novel ways to interfere with bacterial growth could be a very efficient strategy to deal any fast spreading infection. With the concern caused by existing antibiotic resistance, investigation of the fundamental bacterial cell division mechanisms could provide new targets and/or alternate synergistic approach to combat bacterial resistance and pathogens. As discussed above, this requires a more detailed understanding of the macromolecular complexes concerned to identify what targets are viable and study their structural and functional relationship. Finding a new potential macromolecular target is also a crucial step in AMR related research considering the fact that conducting a research involving a study about structural-functional relationship of a macromolecular complex, is not just time consuming but it also needs bigger collaboration and a substantial amount of money. The general speed of similar study or exploring a new drug/antibiotic is no match to the rate at which bacteria has been evolving and developing resistance against existing antibiotics. Therefore, we need a very careful consideration in choosing target molecule(s) or macromolecular complexes. To achieve this, the similarities and difference of bacterial cell division mechanisms in three different bacteria are discussed in the Chapter 1. In the same chapter we also discussed several essential divisome proteins or macromolecular complexes that could potentially be good target(s) for a new class of antibiotics. The macromolecular complex of FtsEX with their extra-cytoplasmic/periplasmic hydrolase partner, is one those prime targets.

As mentioned in the Chapter 1 and throughout this thesis, this molecular machine is absolutely crucial in cell wall separation process in *S. pneumoniae* and to some plays an important role also in *E. coli*. In other species it has been observed with varied roles such as regulating a the PG hydrolase CwlO during elongation in *B. subtilis* and regulating a protease (RipC) in pathogenic and non-pathogenic Corynebacterineae (*M. tuberculosis* and *C. glutamicum* respectively) (see Chapter 1, section 1.7.).

However, no previous study has been able to purify this complex in its native form to study the structural-functional relationships of these proteins and understand the molecular mechanics about how the FtsEX complex is operated in conjunction with an ATP-hydrolysis event. Moreover, the other proposed macromolecular interactions of FtsEX with FtsA and FtsZ as described in Chapter 1 (1.7.) and Chapter 5, raises interesting question about their roles in localizing and regulating this FtsEX-hydrolase molecular machine. Also, it would be interesting to know whether inhibiting/disrupting their functions using novel inhibitors or changing their stoichiometry at the divisome site by overproducing these molecules, resulting in an inability of bacteria to divide or does the same actions change their phenotype during homologous or heterologous expression?

6.4. Technical challenges and achievements associated with isolation of divisome protein complexes

In order to investigate about questions as mentioned above, (6.3.), we first and foremost need to build-up and purify this whole macromolecular complex in sufficient quantities to perform all the necessary *in-vitro* structural and functional analysis. This is technically very challenging since components of this macromolecular complex are mostly membrane proteins or membrane associated proteins, which are less abundant due to their location. In addition, the lack of suitable homologous expression systems in certain bacterial species, restricts the overproduction of these MP and MAPs in the same bacterial species. Such as the case for this study where we made efforts to purify the *S. pneumoniae* FtsEX-PcsB

and FtsEX-FtsA complexes as well as the possible macromolecular complex composed of all these four components, which never have been attempted before.

To deal these technical challenges we decided to use the robust and well-developed heterologous *E. coli* expression system to express and overproduce these *S. pneumoniae* proteins. In addition, we chose to explore purification of these proteins as complex, hence we used SMALP nanodiscs which extracts the membrane lipids portion that includes the recombinant overproduced tagged proteins of our interest. Before this study, there was a single report of a successful purification of FtsE and FtsX in isolation in a detergent micelle context (Bajaj et al., 2016) but not as a complex or with other interacting proteins. Looking further, identification of most known divisome proteins and knowledge of their interactions as complexes in various bacterial species, there are almost no known cases that report purification of large complexes that containing more than two divisome proteins together. Among these reports, the largest isolated complex being 1 MDa, was reported to contain seven *E. coli* divisome proteins as follows FtsZ, ZipA, FtsK, FtsQ, FtsL, FtsB, and FtsN (Trip and Scheffers, 2015). Another similar successful attempt was reported to isolate *S. pneumoniae* divisome complex containing five proteins as follows DivIB (FtsQ), FtsL, DivIC (FtsB), FtsW and PBP2x were co-expressed in heterologous *E. coli* system (Noirclerc-Savoie et al., 2013). While these reports of successful isolation of macromolecular divisome complexes are encouraging, both have been isolated using detergents which replaces lipid particles. Interestingly (Noirclerc-Savoie et al., 2013) did not report any phenotypic changes as a result of expression of these *S. pneumoniae* divisome complex proteins in *E. coli* which are clearly evident in our study. Also, there is no report about purifying the complexes or macromolecular complexes composed of FtsA, FtsE, FtsX and PcsB.

6.5. Key achievements and findings from this study

The unique success of this study is to isolate all possible complexes of *S. pneumoniae* FtsEX with FtsA, PcsB and all four proteins together surrounded by their lipid environment as shown in Chapter 5. In aiming to achieve purification of these macromolecular complexes, we initially also isolated them individually, which indicated lipid association/interaction of *S. pneumoniae* FtsE, FtsA and PcsB (Chapter 3). All these proteins have been predicted to have lipid/membrane association; however, these proteins have never been isolated in its membrane attached state or using any lipid nanodisc which has been shown in this study (Chapter 3). This membrane attachment observation is possibly crucial to retain the functional ability of MPs and MAPs, and so it is also an important consideration in the isolation of the above *S. pneumoniae* proteins under *in-vitro* condition. Perhaps this membrane associated state of the macromolecular complex may reflect the actual interlinks and mechanics between these molecules during the hydrolysis event. One of the reasons behind the unsuccessful isolation of FtsEX as complex in previous studies where isolations of these proteins and their reconstitution were attempted using detergent, was the lack of an appropriate membrane lipid context. In this study we report for the very first time, the isolation of FtsEX within this lipid membrane context. In our observation it has been clear that the formation of FtsEX complex requires membrane lipids for correct assembly as shown and discussed in Chapter 4.

Another unique observation of this study is the phenotypic changes in a host *E. coli* cell due to overexpression of heterologous *S. pneumoniae* proteins, some of which are characteristically different e.g. there is no direct homologue of PcsB in *E. coli*. Therefore, it is necessary to observe their effects on host system *in-vivo*. This has been performed simultaneously alongside *in-vitro* studies as mentioned above, where effects of individual and combined expression(s) of above *S. pneumoniae* proteins on phenotype of heterologous *E. coli* system were observed and discussed (Chapter 3, Chapter 4 and Chapter 5). In these phenotypic observations, we noticed the overexpression of SpFtsEX causes a filamentous phenotype in *E. coli* in trans. Overexpression of many other cell wall and divisome proteins also causes a

filamentous phenotype in *E. coli* but what is perhaps quite remarkable is that this phenotype is rescued by the overexpression of PcsB and that a tripartite FtsEX-PcsB complex to be purified on lipid bound nanodisc (SMALP). This raises the possibility that FtsEX causes the filamentous phenotype by sequestering *E. coli* divisome partnering proteins from *E. coli*; and the formation of FtsEX-PcsB may be functional in PG hydrolysis in *E. coli*. This isolation of FtsEX-PcsB (ABC-PG hydrolase) complex within membrane lipid context is one of the major successes of this study.

Similarly, successful isolation of another tripartite complex formed between FtsEX and FtsA, is another key achievement and the finding that the SpFtsX interacts with SpFtsA not SpFtsE, is one of the highlights this study. While EcFtsA has been shown to be linked to EcFtsX genetically there is no previous direct biochemical evidence of the same interaction reported for either *E. coli* or *S. pneumoniae* FtsX and FtsA. Also, this is for the very first time SpFtsA has been shown to form a complex with SpFtsEX. This similar link in *E. coli* has been proposed to be involved in assembling further downstream divisome proteins and in regulating the PG hydrolase activity by trapping FtsA in a monomer form (or preventing FtsA polymerization) during ATP-hydrolysis at FtsE (Du et al., 2016). In aiming to test such hypothesis, we made an attempt to isolate these four *S. pneumoniae* (FtsA, FtsE, FtsX and PcsB) in complex and observed their combined effect on phenotype of host *E. coli* cells. To our surprise, we did not observe the biochemical isolation of PcsB in complex with FtsA, FtsE, FtsX suggesting that the interaction of FtsA with FtsEX prevents co-association with PcsB. In the accompanying *in-vitro* phenotypic experiments, expression of PcsB also failed to rescue the long filamentous phenotype caused by co-expression of SpFtsEX and SpFtsA together. However, the rescue action by PcsB was restored when SpFtsZ was introduced in the co-expression trial. These findings indicate SpFtsZ possibly plays an important role in localizing and assembling these four divisome correctly at the division site; and that interaction of SpFtsEX with SpFtsA precedes the further macromolecular interaction with PcsB. Isolation of this macromolecular complex composed of SpFtsA, SpFtsE, SpFtsX and PcsB in our preliminary trials is very encouraging, but

missing SpFtsZ in the same macromolecular complex either suggests while it is crucial in assembling them correctly, it may not be directly involved to ABC-PG hydrolase machinery or contributing to the PG hydrolysis. However, this needs further investigation as discussed below.

6.6. Future investigations and experiments

In this study, a molecular and genetic ‘toolbox’ for the *S. pneumoniae* exemplar of divisome complexes FtsEX-PcsB and FtsEX-FtsA as well as macromolecular complex composed of all four proteins (FtsA-FtsEX-PcsB) have been assembled for the first time by use of a detergent free membrane protein isolation system. We have shown that these isolated complexes containing FtsE are capable of binding ATP and to some extent are capable of hydrolysing ATP as indicated in our preliminary experiments. However, we need to exploit these abilities using their specific mutants to understand their interlinked mechanism in PG hydrolysis in much more detail. We have already identified mutants of SpFtsE and are in the process of preparing relevant mutant constructs for SpFtsEX which contain mutants that are predicted to be defective in binding ATP such as SpFtsE(K43Q) or SpFtsE(D164A) and to be defective in hydrolysing ATP that is SpFtsE(E165A). When first two substitution at K43Q and at D164A in the Walker A and Walker B motif of SpFtsE respectively, proposed not be able to bind ATP, hence would not show any ATP hydrolysis (Arends et al., 2009). The last substitution at E165A in the Walker B motif of SpFtsE is proposed to be able to bind ATP but would fail to hydrolyse. These mutants of SpFtsEX would be very important tools to verify the ATP-binding and hydrolysing abilities of those *in-vitro* purified complexes as well as overexpression of these also may indicate whether or not the ATPase activity of FtsE has any role in aberrant phenotype due to overexpression of SpFtsEX in heterologous *E. coli* system.

In addition, the complex of above mutated SpFtsE with SpFtsX and PcsB may also probe the role of ATP hydrolysis in activation of the PcsB hydrolytic activity which is so far unresolved. In this regard, mutants of PcsB would be crucial to verify the

same. We have identified and are in progress to prepare a construct for mutated PcsB (C292A) in order to investigate further about PG hydrolysis ability of SpFtsEX-PcsB or SpFtsA-SpFtsEX-PcsB complexes as well as to access the role of ATP hydrolysis at FtsE (using ATP site mutants in FtsE as mentioned above) in those complexes in both *in-vivo* and *in-vitro* conditions. The prediction is that the C292A substitution at PcsB would not be able to rescue the SpFtsEX overexpression related aberrant cell division phenotype in *E. coli*. To compliment these experiments with an *in-vitro* biochemical assay verification with the same SpFtsEX complexes with PcsB, we wish to establish either a PG hydrolysis assay either using PG zymogram assay or investigate a spectroscopic assay to detect the clearance of PG crosslinking based on a change in turbidity. A similar spectrophotometric assay already exists for lysozyme activity and is based on the hydrolysis of lyophilised *Micrococcus lysodeikticus* in a solution and measured at 450nm. Such an assay could be developed using purified *E. coli* PG or PG of lyophilised cells from *S. pneumoniae*. Once the assay is established, we need to verify the same hypothesis using above mutated PcsB complex with SpFtsEX that should not ideally be able to hydrolyse PG despite receiving the signal of ATP hydrolysis at the SpFtsE end through possible conformational change in SpFtsX subunit. These experiments along with the isolation of the same complex without his-tag at the PcsB would certainly confirm their interaction between FtsEX and PcsB as well as verify the hypothesis about their molecular mechanism behind ATP-dependent PG hydrolysis.

Another set of interesting experiments could be designed by identifying and mutating the site of interaction(s) between SpFtsA and SpFtsX, and test whether or not their complex has any role in regulating PG hydrolysis by regulating PcsB? Also, a complex of SpFtsEX with SpFtsA that mutated at its self-polymerisation site or a complex of SpFtsEX with the FtsA*, which would show deficiency in FtsA polymerisation, this would be interesting to characterise phenotypically in *in-vivo* condition as well as in *in-vitro* assay such as ATP-related assays and PG-hydrolysis assay when in complexed with SpFtsEX-PcsB.

Apart from above crucial verification analysis, it would be good to repeat the same phenotypic studies (as performed in this project) using same *S. pneumoniae* proteins and their complexes but fusing them with some appropriate GFP or RFP or mCherry tags and expressing them in heterologous *E. coli* system. This would provide further evidence of their colocalization and possibly the order of interaction at different stages of cell division. This information would be crucial with regard to their spatio-temporal interaction in *in-vivo* condition. If possible, super resolution microscopy such as PALM or STED or STORM imaging of these same set of proteins and their complexes using appropriate tags, would certainly provide information about their strong correlation if within close proximity.

In regard to biophysical characterisation of the complexes, the very next step would be to perform SEC-MALS experiments with these complexes to estimate their molecular weight and stoichiometry in the same complex. Simultaneously, AUC experiments with SMALP isolated complexes in this study and their individual components would provide information about their monomeric or oligomeric or complex state in the buffer. DLS experiments could be designed alongside where the same samples as will be used for AUC, to check and compare particle distribution and temperature stability of these isolated individual proteins with their complex form. Testing their sample purity through biochemical and biophysical characterisation followed by negative staining EM, the purest fraction(s)/sample(s) could be taken for further SAXS/SANS experiments to get low-resolution envelop structural data to model the complex initially.

However, the most important above all is to perform the structural analysis of these isolated complexes using high-resolution cryo-EM study. In order to pursue this structural analysis first we need to screen the best conditions for high-resolution data collection. If achieved, high resolution single particle structure of the complex will be examined. Apart from structural analysis screening of inhibitors for SpFtsEX and PcsB functions would be another priority.

In addition, it would be interesting to investigate the mechanism surrounding the proposed antimicrobial activity of human cytokine CXCL10 that targets *B. anthracis* FtsEX (Margulieux et al., 2016). If similar interaction persists between SpFtsX and CXCL10, it could be interesting to explore their antagonistic effect in *in-vivo* condition in Gram-negative as well as Gram-positive system. This can be achieved by producing and purifying the protein from a human gene block for CXCL10, using an origami strain of *E. coli*, then observing the effect of cytokine on labelled FtsEX under *in-vivo* conditions.

6.7. Concluding remarks

This is for first time we are aware of that the *S. pneumoniae* divisome complexes containing more than two proteins, can be isolated within membrane lipid context. With this study, we presented a detergent free nanodisc extraction strategy that facilitated the purification of membrane protein complexes that specifically associated with cell divisome complexes of *S. pneumoniae*. This approach should not only help isolating the complexes as mentioned in this study, but it could extend to purify and identify even bigger macromolecular complexes comprising their associated divisome or elongasome proteins. As we learned the importance of studying complexes to deal with infections, our study extends the molecular tools and necessary preliminary steps to analyse the cell division events *in-vivo* as well as *in-vitro*. Certainly, the successful purification of all possible complexes of FtsEX with FtsA and PcsB, which are involved in the critical final steps of cell separation process, will help to understand the mechanism behind ATP-dependent PG-hydrolysis process in *S. pneumoniae*. In addition, a non-pathogenic Gram-negative heterologous expression system and phenotypic observation used in this study could facilitate the screen for potential inhibitors or antibiotics against essential protein or protein complexes of cell division mechanism from pathogenic bacteria, which otherwise difficult to test in native host.

BIBLIOGRAPHY AND REFERENCES

- Aarsman, M. E., Piette, A., Fraipont, C., Vinkenvleugel, T. M., Nguyen-Disteche, M., & den Blaauwen, T. (2005). Maturation of the Escherichia coli divisome occurs in two steps. *Mol Microbiol*, *55*(6), 1631-1645. doi:10.1111/j.1365-2958.2005.04502.x
- Abhayawardhane, Y., & Stewart, G. C. (1995). Bacillus subtilis possesses a second determinant with extensive sequence similarity to the Escherichia coli mreB morphogene. *Journal of bacteriology*, *177*(3), 765-773. doi:10.1128/jb.177.3.765-773.1995
- Adams, D. W., Wu, L. J., & Errington, J. (2014). Cell cycle regulation by the bacterial nucleoid. *Curr Opin Microbiol*, *22*, 94-101. doi:10.1016/j.mib.2014.09.020
- Adams, D. W., Wu, L. J., & Errington, J. (2015). Nucleoid occlusion protein Noc recruits DNA to the bacterial cell membrane. *EMBO J*, *34*(4), 491-501. doi:10.15252/embj.201490177
- Addinall, S. G., Bi, E., & Lutkenhaus, J. (1996). FtsZ ring formation in fts mutants. *Journal of bacteriology*, *178*(13), 3877-3884. doi:10.1128/jb.178.13.3877-3884.1996
- Addinall, S. G., Cao, C., & Lutkenhaus, J. (1997). FtsN, a late recruit to the septum in Escherichia coli. *Mol Microbiol*, *25*(2), 303-309. doi:10.1046/j.1365-2958.1997.4641833.x
- Addinall, S. G., & Lutkenhaus, J. (1996). FtsA is localized to the septum in an FtsZ-dependent manner. *Journal of bacteriology*, *178*(24), 7167-7172. doi:10.1128/jb.178.24.7167-7172.1996
- Adler, H. I., Fisher, W. D., Cohen, A., & Hardigree, A. A. (1967). MINIATURE escherichia coli CELLS DEFICIENT IN DNA. *Proc Natl Acad Sci U S A*, *57*(2), 321-326. doi:10.1073/pnas.57.2.321
- Agarwal, S., Agarwal, S., Pancholi, P., & Pancholi, V. (2011). Role of serine/threonine phosphatase (SP-STP) in Streptococcus pyogenes physiology and virulence. *J Biol Chem*, *286*(48), 41368-41380. doi:10.1074/jbc.M111.286690
- Albarracin Orio, A. G., Pinas, G. E., Cortes, P. R., Cian, M. B., & Echenique, J. (2011). Compensatory evolution of pbp mutations restores the fitness cost imposed by beta-lactam resistance in Streptococcus pneumoniae. *PLoS Pathog*, *7*(2), e1002000. doi:10.1371/journal.ppat.1002000
- Alexeeva, S., Gadella Jr, T. W. J., Verheul, J., Verhoeven, G. S., & Den Blaauwen, T. (2010). Direct interactions of early and late assembling division proteins in Escherichia coli cells resolved by FRET. *Molecular Microbiology*, *77*(2), 384-398. doi:10.1111/j.1365-2958.2010.07211.x
- Alexopoulos, J. A., Guarne, A., & Ortega, J. (2012). ClpP: a structurally dynamic protease regulated by AAA+ proteins. *J Struct Biol*, *179*(2), 202-210. doi:10.1016/j.jsb.2012.05.003
- Alyahya, S. A., Alexander, R., Costa, T., Henriques, A. O., Emonet, T., & Jacobs-Wagner, C. (2009). RodZ, a component of the bacterial core morphogenic

- apparatus. *Proc Natl Acad Sci U S A*, 106(4), 1239-1244. doi:10.1073/pnas.0810794106
- Appelbaum, P. C., Bhamjee, A., Scragg, J. N., Hallett, A. F., Bowen, A. J., & Cooper, R. C. (1977). Streptococcus pneumoniae resistant to penicillin and chloramphenicol. *Lancet*, 2(8046), 995-997. doi:10.1016/s0140-6736(77)92892-6
- Arends, S. J., Kustus, R. J., & Weiss, D. S. (2009). ATP-binding site lesions in FtsE impair cell division. *J Bacteriol*, 191(12), 3772-3784. doi:10.1128/JB.00179-09
- Arends, S. J. R., Kustus, R. J., & Weiss, D. S. (2009). ATP-Binding Site Lesions in FtsE Impair Cell Division. *Journal of bacteriology*, 191(12), 3772-3784. doi:10.1128/jb.00179-09
- Arigoni, F., Pogliano, K., Webb, C. D., Stragier, P., & Losick, R. (1995). Localization of protein implicated in establishment of cell type to sites of asymmetric division. *Science*, 270(5236), 637-640. doi:10.1126/science.270.5236.637
- Ayala, J. A., Garrido, T., De Pedro, M. A., & Vicente, M. (1994). Chapter 5 Molecular biology of bacterial septation. In J. M. Ghuyssen & R. Hakenbeck (Eds.), *New Comprehensive Biochemistry* (Vol. 27, pp. 73-101): Elsevier.
- Baba, T., Ara, T., Hasegawa, M., Takai, Y., Okumura, Y., Baba, M., . . . Mori, H. (2006). Construction of Escherichia coli K-12 in-frame, single-gene knockout mutants: the Keio collection. *Mol Syst Biol*, 2, 2006.0008. doi:10.1038/msb4100050
- Bailey, M. W., Bisicchia, P., Warren, B. T., Sherratt, D. J., & Mannik, J. (2014). Evidence for divisome localization mechanisms independent of the Min system and SlmA in Escherichia coli. *PLoS Genet*, 10(8), e1004504. doi:10.1371/journal.pgen.1004504
- Bajaj, R., Bruce, K. E., Davidson, A. L., Rued, B. E., Stauffacher, C. V., & Winkler, M. E. (2016). Biochemical characterization of essential cell division proteins FtsX and FtsE that mediate peptidoglycan hydrolysis by PcsB in Streptococcus pneumoniae. *Microbiologyopen*, 5(5), 738-752. doi:10.1002/mbo3.366
- Banzhaf, M., van den Berg van Saparoea, B., Terrak, M., Fraipont, C., Egan, A., Philippe, J., . . . Vollmer, W. (2012). Cooperativity of peptidoglycan synthases active in bacterial cell elongation. *Mol Microbiol*, 85(1), 179-194. doi:10.1111/j.1365-2958.2012.08103.x
- Barendt, S. M., Land, A. D., Sham, L. T., Ng, W. L., Tsui, H. C., Arnold, R. J., & Winkler, M. E. (2009). Influences of capsule on cell shape and chain formation of wild-type and pcsB mutants of serotype 2 Streptococcus pneumoniae. *Journal of bacteriology*, 191(9), 3024-3040. doi:10.1128/JB.01505-08
- Barendt, S. M., Sham, L. T., & Winkler, M. E. (2011). Characterization of mutants deficient in the L,D-carboxypeptidase (DacB) and WalRK (VicRK) regulon, involved in peptidoglycan maturation of Streptococcus pneumoniae serotype 2 strain D39. *Journal of bacteriology*, 193(9), 2290-2300. doi:10.1128/JB.01555-10
- Bartual, S. G., Straume, D., Stamsas, G. A., Munoz, I. G., Alfonso, C., Martinez-Ripoll, M., . . . Hermoso, J. A. (2014). Structural basis of PcsB-mediated

- cell separation in *Streptococcus pneumoniae*. *Nat Commun*, 5, 3842. doi:10.1038/ncomms4842
- Bauer, M., Baumann, J., & Trommer, W. E. (1992). ATP binding to bovine serum albumin. *FEBS Lett*, 313(3), 288-290. doi:10.1016/0014-5793(92)81211-4
- Beall, B., Lowe, M., & Lutkenhaus, J. (1988). Cloning and characterization of *Bacillus subtilis* homologs of *Escherichia coli* cell division genes *ftsZ* and *ftsA*. *Journal of bacteriology*, 170(10), 4855-4864. doi:10.1128/jb.170.10.4855-4864.1988
- Beall, B., & Lutkenhaus, J. (1989). Nucleotide sequence and insertional inactivation of a *Bacillus subtilis* gene that affects cell division, sporulation, and temperature sensitivity. *Journal of bacteriology*, 171(12), 6821-6834. doi:10.1128/jb.171.12.6821-6834.1989
- Beall, B., & Lutkenhaus, J. (1991). *FtsZ* in *Bacillus subtilis* is required for vegetative septation and for asymmetric septation during sporulation. *Genes Dev*, 5(3), 447-455. doi:10.1101/gad.5.3.447
- Beall, B., & Lutkenhaus, J. (1992). Impaired cell division and sporulation of a *Bacillus subtilis* strain with the *ftsA* gene deleted. *Journal of bacteriology*, 174(7), 2398-2403. doi:10.1128/jb.174.7.2398-2403.1992
- Begg, K. J., Dewar, S. J., & Donachie, W. D. (1995). A new *Escherichia coli* cell division gene, *ftsK*. *Journal of bacteriology*, 177(21), 6211-6222. doi:10.1128/jb.177.21.6211-6222.1995
- Beilharz, K., Novakova, L., Fadda, D., Branny, P., Massidda, O., & Veening, J. W. (2012). Control of cell division in *Streptococcus pneumoniae* by the conserved Ser/Thr protein kinase StkP. *Proc Natl Acad Sci U S A*, 109(15), E905-913. doi:10.1073/pnas.1119172109
- Ben-Yehuda, S., Fujita, M., Liu, X. S., Gorbatyuk, B., Skoko, D., Yan, J., . . . Losick, R. (2005). Defining a centromere-like element in *Bacillus subtilis* by identifying the binding sites for the chromosome-anchoring protein RacA. *Mol Cell*, 17(6), 773-782. doi:10.1016/j.molcel.2005.02.023
- Ben-Yehuda, S., Rudner, D. Z., & Losick, R. (2003). RacA, a bacterial protein that anchors chromosomes to the cell poles. *Science*, 299(5606), 532-536. doi:10.1126/science.1079914
- Bendezu, F. O., & de Boer, P. A. (2008). Conditional lethality, division defects, membrane involution, and endocytosis in *mre* and *mrd* shape mutants of *Escherichia coli*. *Journal of bacteriology*, 190(5), 1792-1811. doi:10.1128/JB.01322-07
- Berg, K. H., Stamsas, G. A., Straume, D., & Havarstein, L. S. (2013). Effects of low PBP2b levels on cell morphology and peptidoglycan composition in *Streptococcus pneumoniae* R6. *Journal of bacteriology*, 195(19), 4342-4354. doi:10.1128/JB.00184-13
- Bernhardt, T. G., & de Boer, P. A. (2003). The *Escherichia coli* amidase AmiC is a periplasmic septal ring component exported via the twin-arginine transport pathway. *Mol Microbiol*, 48(5), 1171-1182. doi:10.1046/j.1365-2958.2003.03511.x
- Bernhardt, T. G., & de Boer, P. A. (2005). SlmA, a nucleoid-associated, *FtsZ* binding protein required for blocking septal ring assembly over Chromosomes in *E. coli*. *Mol Cell*, 18(5), 555-564. doi:10.1016/j.molcel.2005.04.012

- Bertsche, U., Kast, T., Wolf, B., Fraipont, C., Aarsman, M. E., Kannenberg, K., . . . Vollmer, W. (2006). Interaction between two murein (peptidoglycan) synthases, PBP3 and PBP1B, in *Escherichia coli*. *Mol Microbiol*, *61*(3), 675-690. doi:10.1111/j.1365-2958.2006.05280.x
- Bhandari, P., & Gowrishankar, J. (1997). An *Escherichia coli* host strain useful for efficient overproduction of cloned gene products with NaCl as the inducer. *Journal of bacteriology*, *179*(13), 4403-4406. doi:10.1128/jb.179.13.4403-4406.1997
- Bi, E. F., & Lutkenhaus, J. (1991). FtsZ ring structure associated with division in *Escherichia coli*. *Nature*, *354*(6349), 161-164. doi:10.1038/354161a0
- Bisicchia, P., Noone, D., Lioliou, E., Howell, A., Quigley, S., Jensen, T., . . . Devine, K. M. (2007). The essential YycFG two-component system controls cell wall metabolism in *Bacillus subtilis*. *Mol Microbiol*, *65*(1), 180-200. doi:10.1111/j.1365-2958.2007.05782.x
- Bisson-Filho, A. W., Hsu, Y. P., Squyres, G. R., Kuru, E., Wu, F., Jukes, C., . . . Garner, E. C. (2017). Treadmilling by FtsZ filaments drives peptidoglycan synthesis and bacterial cell division. *Science*, *355*(6326), 739-743. doi:10.1126/science.aak9973
- Bradshaw, N., & Losick, R. (2015). Asymmetric division triggers cell-specific gene expression through coupled capture and stabilization of a phosphatase. *Elife*, *4*. doi:10.7554/eLife.08145
- Bramkamp, M., Emmins, R., Weston, L., Donovan, C., Daniel, R. A., & Errington, J. (2008). A novel component of the division-site selection system of *Bacillus subtilis* and a new mode of action for the division inhibitor MinCD. *Mol Microbiol*, *70*(6), 1556-1569. doi:10.1111/j.1365-2958.2008.06501.x
- Bramkamp, M., Weston, L., Daniel, R. A., & Errington, J. (2006). Regulated intramembrane proteolysis of FtsL protein and the control of cell division in *Bacillus subtilis*. *Mol Microbiol*, *62*(2), 580-591. doi:10.1111/j.1365-2958.2006.05402.x
- Broder, D. H., & Pogliano, K. (2006). Forespore engulfment mediated by a ratchet-like mechanism. *Cell*, *126*(5), 917-928. doi:10.1016/j.cell.2006.06.053
- Bruce, K. E., Rued, B. E., Tsui, H. T., & Winkler, M. E. (2018). The Opp (AmiACDEF) Oligopeptide Transporter Mediates Resistance of Serotype 2 *Streptococcus pneumoniae* D39 to Killing by Chemokine CXCL10 and Other Antimicrobial Peptides. *Journal of bacteriology*, *200*(11). doi:10.1128/JB.00745-17
- Brunet, Y. R., Wang, X., & Rudner, D. Z. (2019). SweC and SweD are essential co-factors of the FtsEX-CwlO cell wall hydrolase complex in *Bacillus subtilis*. *PLoS Genet*, *15*(8), e1008296. doi:10.1371/journal.pgen.1008296
- Buddelmeijer, N., & Beckwith, J. (2004). A complex of the *Escherichia coli* cell division proteins FtsL, FtsB and FtsQ forms independently of its localization to the septal region. *Mol Microbiol*, *52*(5), 1315-1327. doi:10.1111/j.1365-2958.2004.04044.x
- Busiek, K. K., Eraso, J. M., Wang, Y., & Margolin, W. (2012). The early divisome protein FtsA interacts directly through its 1c subdomain with the cytoplasmic domain of the late divisome protein FtsN. *Journal of bacteriology*, *194*(8), 1989-2000. doi:10.1128/JB.06683-11

- Buss, J., Coltharp, C., Shtengel, G., Yang, X., Hess, H., & Xiao, J. (2015). A multi-layered protein network stabilizes the Escherichia coli FtsZ-ring and modulates constriction dynamics. *PLoS Genet*, *11*(4), e1005128. doi:10.1371/journal.pgen.1005128
- Buss, J. A., Peters, N. T., Xiao, J., & Bernhardt, T. G. (2017). ZapA and ZapB form an FtsZ-independent structure at midcell. *Mol Microbiol*, *104*(4), 652-663. doi:10.1111/mmi.13655
- Camberg, J. L., Hoskins, J. R., & Wickner, S. (2009). ClpXP protease degrades the cytoskeletal protein, FtsZ, and modulates FtsZ polymer dynamics. *Proc Natl Acad Sci U S A*, *106*(26), 10614-10619. doi:10.1073/pnas.0904886106
- Camberg, J. L., Hoskins, J. R., & Wickner, S. (2011). The interplay of ClpXP with the cell division machinery in Escherichia coli. *Journal of bacteriology*, *193*(8), 1911-1918. doi:10.1128/JB.01317-10
- Carballido-Lopez, R., Formstone, A., Li, Y., Ehrlich, S. D., Noirot, P., & Errington, J. (2006). Actin homolog MreBH governs cell morphogenesis by localization of the cell wall hydrolase LytE. *Dev Cell*, *11*(3), 399-409. doi:10.1016/j.devcel.2006.07.017
- Carniol, K., Ben-Yehuda, S., King, N., & Losick, R. (2005). Genetic dissection of the sporulation protein SpoIIE and its role in asymmetric division in Bacillus subtilis. *Journal of bacteriology*, *187*(10), 3511-3520. doi:10.1128/jb.187.10.3511-3520.2005
- Cha, J. H., & Stewart, G. C. (1997). The divIVA minicell locus of Bacillus subtilis. *Journal of bacteriology*, *179*(5), 1671-1683. doi:10.1128/jb.179.5.1671-1683.1997
- Cheesman, M. J., Ilanko, A., Blonk, B., & Cock, I. E. (2017). Developing New Antimicrobial Therapies: Are Synergistic Combinations of Plant Extracts/Compounds with Conventional Antibiotics the Solution? *Pharmacogn Rev*, *11*(22), 57-72. doi:10.4103/phrev.phrev_21_17
- Chewapreecha, C., Marttinen, P., Croucher, N. J., Salter, S. J., Harris, S. R., Mather, A. E., . . . Parkhill, J. (2014). Comprehensive identification of single nucleotide polymorphisms associated with beta-lactam resistance within pneumococcal mosaic genes. *PLoS Genet*, *10*(8), e1004547. doi:10.1371/journal.pgen.1004547
- Cho, H., & Bernhardt, T. G. (2013). Identification of the SlmA active site responsible for blocking bacterial cytokinetic ring assembly over the chromosome. *PLoS Genet*, *9*(2), e1003304. doi:10.1371/journal.pgen.1003304
- Cho, H., McManus, H. R., Dove, S. L., & Bernhardt, T. G. (2011). Nucleoid occlusion factor SlmA is a DNA-activated FtsZ polymerization antagonist. *Proc Natl Acad Sci U S A*, *108*(9), 3773-3778. doi:10.1073/pnas.1018674108
- Claessen, D., Emmins, R., Hamoen, L. W., Daniel, R. A., Errington, J., & Edwards, D. H. (2008). Control of the cell elongation-division cycle by shuttling of PBP1 protein in Bacillus subtilis. *Mol Microbiol*, *68*(4), 1029-1046. doi:10.1111/j.1365-2958.2008.06210.x
- Cleverley, R. M., Barrett, J. R., Basle, A., Bui, N. K., Hewitt, L., Solovyova, A., . . . Lewis, R. J. (2014). Structure and function of a spectrin-like regulator of bacterial cytokinesis. *Nat Commun*, *5*, 5421. doi:10.1038/ncomms6421

- Coates, A. R., Halls, G., & Hu, Y. (2011). Novel classes of antibiotics or more of the same? *Br J Pharmacol*, *163*(1), 184-194. doi:10.1111/j.1476-5381.2011.01250.x
- Conti, J., Viola, M. G., & Camberg, J. L. (2015). The bacterial cell division regulators MinD and MinC form polymers in the presence of nucleotide. *FEBS Lett*, *589*(2), 201-206. doi:10.1016/j.febslet.2014.11.047
- Cook, W. R., de Boer, P. A., & Rothfield, L. I. (1989). Differentiation of the bacterial cell division site. *Int Rev Cytol*, *118*, 1-31. doi:10.1016/s0074-7696(08)60871-2
- Corbin, B. D., Geissler, B., Sadasivam, M., & Margolin, W. (2004). Z-ring-independent interaction between a subdomain of FtsA and late septation proteins as revealed by a polar recruitment assay. *Journal of bacteriology*, *186*(22), 7736-7744. doi:10.1128/jb.186.22.7736-7744.2004
- Corbin, B. D., Wang, Y., Beuria, T. K., & Margolin, W. (2007). Interaction between cell division proteins FtsE and FtsZ. *Journal of bacteriology*, *189*(8), 3026-3035. doi:10.1128/JB.01581-06
- Crawford, M. A., Lowe, D. E., Fisher, D. J., Stibitz, S., Plaut, R. D., Beaber, J. W., . . . Hughes, M. A. (2011). Identification of the bacterial protein FtsX as a unique target of chemokine-mediated antimicrobial activity against *Bacillus anthracis*. *Proc Natl Acad Sci U S A*, *108*(41), 17159-17164. doi:10.1073/pnas.1108495108
- Crawford, M. A., Margulieux, K. R., Singh, A., Nakamoto, R. K., & Hughes, M. A. (2019). Mechanistic insights and therapeutic opportunities of antimicrobial chemokines. *Seminars in Cell & Developmental Biology*, *88*, 119-128. doi:<https://doi.org/10.1016/j.semcdb.2018.02.003>
- Crow, A., Greene, N. P., Kaplan, E., & Koronakis, V. (2017). Structure and mechanotransmission mechanism of the MacB ABC transporter superfamily. *Proc Natl Acad Sci U S A*, *114*(47), 12572-12577. doi:10.1073/pnas.1712153114
- Dai, K., & Lutkenhaus, J. (1992). The proper ratio of FtsZ to FtsA is required for cell division to occur in *Escherichia coli*. *Journal of bacteriology*, *174*(19), 6145-6151. doi:10.1128/jb.174.19.6145-6151.1992
- Dai, K., Xu, Y., & Lutkenhaus, J. (1996). Topological characterization of the essential *Escherichia coli* cell division protein FtsN. *Journal of bacteriology*, *178*(5), 1328-1334. doi:10.1128/jb.178.5.1328-1334.1996
- Dajkovic, A., Lan, G., Sun, S. X., Wirtz, D., & Lutkenhaus, J. (2008). MinC spatially controls bacterial cytokinesis by antagonizing the scaffolding function of FtsZ. *Curr Biol*, *18*(4), 235-244. doi:10.1016/j.cub.2008.01.042
- Dajkovic, A., Pichoff, S., Lutkenhaus, J., & Wirtz, D. (2010). Cross-linking FtsZ polymers into coherent Z rings. *Mol Microbiol*, *78*(3), 651-668. doi:10.1111/j.1365-2958.2010.07352.x
- Daniel, R. A., & Errington, J. (2000). Intrinsic instability of the essential cell division protein FtsL of *Bacillus subtilis* and a role for DivIB protein in FtsL turnover. *Mol Microbiol*, *36*(2), 278-289. doi:10.1046/j.1365-2958.2000.01857.x
- Daniel, R. A., Harry, E. J., Katis, V. L., Wake, R. G., & Errington, J. (1998). Characterization of the essential cell division gene *ftsL*(yIID) of *Bacillus*

- subtilis and its role in the assembly of the division apparatus. *Mol Microbiol*, 29(2), 593-604. doi:10.1046/j.1365-2958.1998.00954.x
- Daniel, R. A., Noirot-Gros, M. F., Noirot, P., & Errington, J. (2006). Multiple interactions between the transmembrane division proteins of *Bacillus subtilis* and the role of FtsL instability in divisome assembly. *Journal of bacteriology*, 188(21), 7396-7404. doi:10.1128/jb.01031-06
- Daniel, R. A., Williams, A. M., & Errington, J. (1996). A complex four-gene operon containing essential cell division gene *pbpB* in *Bacillus subtilis*. *Journal of bacteriology*, 178(8), 2343-2350. doi:10.1128/jb.178.8.2343-2350.1996
- Das, U., Hariprasad, G., Ethayathulla, A. S., Manral, P., Das, T. K., Pasha, S., . . . Srinivasan, A. (2007). Inhibition of Protein Aggregation: Supramolecular Assemblies of Arginine Hold the Key. *PLoS One*, 2(11), e1176. doi:10.1371/journal.pone.0001176
- de Boer, P., Crossley, R., & Rothfield, L. (1992). The essential bacterial cell-division protein FtsZ is a GTPase. *Nature*, 359(6392), 254-256. doi:10.1038/359254a0
- de Boer, P. A. (2010). Advances in understanding *E. coli* cell fission. *Curr Opin Microbiol*, 13(6), 730-737. doi:10.1016/j.mib.2010.09.015
- de Boer, P. A., Crossley, R. E., Hand, A. R., & Rothfield, L. I. (1991). The MinD protein is a membrane ATPase required for the correct placement of the *Escherichia coli* division site. *EMBO J*, 10(13), 4371-4380. Retrieved from <https://www.ncbi.nlm.nih.gov/pubmed/1836760>
- de Boer, P. A., Crossley, R. E., & Rothfield, L. I. (1989). A division inhibitor and a topological specificity factor coded for by the minicell locus determine proper placement of the division septum in *E. coli*. *Cell*, 56(4), 641-649. doi:10.1016/0092-8674(89)90586-2
- De Las Rivas, B., García, J. L., López, R., & García, P. (2002). Purification and polar localization of pneumococcal LytB, a putative endo-beta-N-acetylglucosaminidase: the chain-dispersing murein hydrolase. *Journal of bacteriology*, 184(18), 4988-5000. doi:10.1128/jb.184.18.4988-5000.2002
- de Leeuw, E., Graham, B., Phillips, G. J., ten Hagen-Jongman, C. M., Oudega, B., & Luirink, J. (1999). Molecular characterization of *Escherichia coli* FtsE and FtsX. *Mol Microbiol*, 31(3), 983-993. Retrieved from <https://www.ncbi.nlm.nih.gov/pubmed/10048040>
- Defeu Soufo, H. J., & Graumann, P. L. (2006). Dynamic localization and interaction with other *Bacillus subtilis* actin-like proteins are important for the function of MreB. *Mol Microbiol*, 62(5), 1340-1356. doi:10.1111/j.1365-2958.2006.05457.x
- Defeu Soufo, H. J., Reimold, C., Breddermann, H., Mannherz, H. G., & Graumann, P. L. (2015). Translation elongation factor EF-Tu modulates filament formation of actin-like MreB protein in vitro. *J Mol Biol*, 427(8), 1715-1727. doi:10.1016/j.jmb.2015.01.025
- den Blaauwen, T., Andreu, J. M., & Monasterio, O. (2014). Bacterial cell division proteins as antibiotic targets. *Bioorg Chem*, 55, 27-38. doi:10.1016/j.bioorg.2014.03.007
- den Blaauwen, T., de Pedro, M. A., Nguyen-Disteche, M., & Ayala, J. A. (2008). Morphogenesis of rod-shaped sacculi. *FEMS Microbiol Rev*, 32(2), 321-344. doi:10.1111/j.1574-6976.2007.00090.x

- den Blaauwen, T., Hamoen, L. W., & Levin, P. A. (2017). The divisome at 25: the road ahead. *Curr Opin Microbiol*, 36, 85-94. doi:10.1016/j.mib.2017.01.007
- den Blaauwen, T., & Luirink, J. (2019). Checks and Balances in Bacterial Cell Division. *MBio*, 10(1). doi:10.1128/mBio.00149-19
- Dewachter, L., Verstraeten, N., Fauvart, M., & Michiels, J. (2018). An integrative view of cell cycle control in Escherichia coli. *FEMS Microbiology Reviews*, 42(2), 116-136. doi:10.1093/femsre/fuy005
- Dewar, S. J., Begg, K. J., & Donachie, W. D. (1992). Inhibition of cell division initiation by an imbalance in the ratio of FtsA to FtsZ. *Journal of bacteriology*, 174(19), 6314-6316. doi:10.1128/jb.174.19.6314-6316.1992
- Di Lallo, G., Fagioli, M., Barionovi, D., Ghelardini, P., & Paolozzi, L. (2003). Use of a two-hybrid assay to study the assembly of a complex multicomponent protein machinery: bacterial septosome differentiation. *Microbiology*, 149(Pt 12), 3353-3359. doi:10.1099/mic.0.26580-0
- Doan, T., Coleman, J., Marquis, K. A., Meeske, A. J., Burton, B. M., Karatekin, E., & Rudner, D. Z. (2013). FisB mediates membrane fission during sporulation in Bacillus subtilis. *Genes Dev*, 27(3), 322-334. doi:10.1101/gad.209049.112
- Dominguez-Cuevas, P., Porcelli, I., Daniel, R. A., & Errington, J. (2013). Differentiated roles for MreB-actin isologues and autolytic enzymes in Bacillus subtilis morphogenesis. *Mol Microbiol*, 89(6), 1084-1098. doi:10.1111/mmi.12335
- Dominguez-Escobar, J., Chastanet, A., Crevenna, A. H., Fromion, V., Wedlich-Soldner, R., & Carballido-Lopez, R. (2011). Processive movement of MreB-associated cell wall biosynthetic complexes in bacteria. *Science*, 333(6039), 225-228. doi:10.1126/science.1203466
- Donachie, W. D., Begg, K. J., Lutkenhaus, J. F., Salmond, G. P., Martinez-Salas, E., & Vincente, M. (1979). Role of the ftsA gene product in control of Escherichia coli cell division. *Journal of bacteriology*, 140(2), 388-394. Retrieved from <https://www.ncbi.nlm.nih.gov/pubmed/387733>
- Dorr, J. M., Koorengevel, M. C., Schafer, M., Prokofyev, A. V., Scheidelaar, S., van der Cruijssen, E. A. W., . . . Killian, J. A. (2014). Detergent-free isolation, characterization, and functional reconstitution of a tetrameric K⁺ channel: The power of native nanodiscs. *Proceedings of the National Academy of Sciences of the United States of America*, 111(52), 18607-18612. Retrieved from <Go to ISI>://WOS:000347444400054
- Dorr, J. M., Scheidelaar, S., Koorengevel, M. C., Dominguez, J. J., Schafer, M., van Walree, C. A., & Killian, J. A. (2016). The styrene-maleic acid copolymer: a versatile tool in membrane research. *Eur Biophys J*, 45(1), 3-21. doi:10.1007/s00249-015-1093-y
- Dramsi, S., Magnet, S., Davison, S., & Arthur, M. (2008). Covalent attachment of proteins to peptidoglycan. *FEMS Microbiol Rev*, 32(2), 307-320. doi:10.1111/j.1574-6976.2008.00102.x
- Drew, D., Klepsch, M. M., Newstead, S., Flaig, R., De Gier, J. W., Iwata, S., & Beis, K. (2008). The structure of the efflux pump AcrB in complex with bile acid. *Mol Membr Biol*, 25(8), 677-682. doi:10.1080/09687680802552257

- Du, S., Henke, W., Pichoff, S., & Lutkenhaus, J. (2019). How FtsEX localizes to the Z ring and interacts with FtsA to regulate cell division. *Mol Microbiol*, *112*(3), 881-895. doi:10.1111/mmi.14324
- Du, S., & Lutkenhaus, J. (2014). SlmA antagonism of FtsZ assembly employs a two-pronged mechanism like MinCD. *PLoS Genet*, *10*(7), e1004460. doi:10.1371/journal.pgen.1004460
- Du, S., & Lutkenhaus, J. (2017). Assembly and activation of the Escherichia coli divisome. *Mol Microbiol*, *105*(2), 177-187. doi:10.1111/mmi.13696
- Du, S., Pichoff, S., Kruse, K., & Lutkenhaus, J. (2018). FtsZ filaments have the opposite kinetic polarity of microtubules. *Proc Natl Acad Sci U S A*, *115*(42), 10768-10773. doi:10.1073/pnas.1811919115
- Du, S., Pichoff, S., & Lutkenhaus, J. (2016). FtsEX acts on FtsA to regulate divisome assembly and activity. *Proc Natl Acad Sci U S A*, *113*(34), E5052-5061. doi:10.1073/pnas.1606656113
- Durand-Heredia, J., Rivkin, E., Fan, G., Morales, J., & Janakiraman, A. (2012). Identification of ZapD as a cell division factor that promotes the assembly of FtsZ in Escherichia coli. *Journal of bacteriology*, *194*(12), 3189-3198. doi:10.1128/JB.00176-12
- Durand-Heredia, J. M., Yu, H. H., De Carlo, S., Lesser, C. F., & Janakiraman, A. (2011). Identification and characterization of ZapC, a stabilizer of the FtsZ ring in Escherichia coli. *Journal of bacteriology*, *193*(6), 1405-1413. doi:10.1128/JB.01258-10
- Ebersbach, G., Galli, E., Moller-Jensen, J., Lowe, J., & Gerdes, K. (2008). Novel coiled-coil cell division factor ZapB stimulates Z ring assembly and cell division. *Mol Microbiol*, *68*(3), 720-735. doi:10.1111/j.1365-2958.2008.06190.x
- Edwards, D. H., & Errington, J. (1997). The Bacillus subtilis DivIVA protein targets to the division septum and controls the site specificity of cell division. *Molecular Microbiology*, *24*(5), 905-915. doi:10.1046/j.1365-2958.1997.3811764.x
- Egan, A. J., Cleverley, R. M., Peters, K., Lewis, R. J., & Vollmer, W. (2017). Regulation of bacterial cell wall growth. *FEBS J*, *284*(6), 851-867. doi:10.1111/febs.13959
- Egan, A. J., & Vollmer, W. (2013). The physiology of bacterial cell division. *Ann NY Acad Sci*, *1277*, 8-28. doi:10.1111/j.1749-6632.2012.06818.x
- El-Hajj, Z. W., & Newman, E. B. (2015). An Escherichia coli mutant that makes exceptionally long cells. *Journal of bacteriology*, *197*(8), 1507-1514. doi:10.1128/JB.00046-15
- Emami, K., Guyet, A., Kawai, Y., Devi, J., Wu, L. J., Allenby, N., . . . Errington, J. (2017). RodA as the missing glycosyltransferase in Bacillus subtilis and antibiotic discovery for the peptidoglycan polymerase pathway. *Nat Microbiol*, *2*, 16253. doi:10.1038/nmicrobiol.2016.253
- Erickson, H. P., Anderson, D. E., & Osawa, M. (2010). FtsZ in bacterial cytokinesis: cytoskeleton and force generator all in one. *Microbiol Mol Biol Rev*, *74*(4), 504-528. doi:10.1128/MMBR.00021-10
- Errington, J. (2003). Regulation of endospore formation in Bacillus subtilis. *Nat Rev Microbiol*, *1*(2), 117-126. doi:10.1038/nrmicro750

- Errington, J., Daniel, R. A., & Scheffers, D. J. (2003). Cytokinesis in bacteria. *Microbiol Mol Biol Rev*, 67(1), 52-65, table of contents. doi:10.1128/membr.67.1.52-65.2003
- Errington, J., & Wu, L. J. (2017). Cell Cycle Machinery in *Bacillus subtilis*. *Subcell Biochem*, 84, 67-101. doi:10.1007/978-3-319-53047-5_3
- Espeli, O., Borne, R., Dupaigne, P., Thiel, A., Gigant, E., Mercier, R., & Boccard, F. (2012). A MatP-divisome interaction coordinates chromosome segregation with cell division in *E. coli*. *EMBO J*, 31(14), 3198-3211. doi:10.1038/emboj.2012.128
- Esue, O., Cordero, M., Wirtz, D., & Tseng, Y. (2005). The assembly of MreB, a prokaryotic homolog of actin. *J Biol Chem*, 280(4), 2628-2635. doi:10.1074/jbc.M410298200
- Esue, O., Wirtz, D., & Tseng, Y. (2006). GTPase Activity, Structure, and Mechanical Properties of Filaments Assembled from Bacterial Cytoskeleton Protein MreB. *Journal of bacteriology*, 188(3), 968-976. doi:10.1128/jb.188.3.968-976.2006
- Eswaramoorthy, P., Erb, M. L., Gregory, J. A., Silverman, J., Pogliano, K., Pogliano, J., & Ramamurthi, K. S. (2011). Cellular architecture mediates DivIVA ultrastructure and regulates min activity in *Bacillus subtilis*. *MBio*, 2(6). doi:10.1128/mBio.00257-11
- Fadda, D., Pischedda, C., Caldara, F., Whalen, M. B., Anderluzzi, D., Domenici, E., & Massidda, O. (2003). Characterization of divIVA and other genes located in the chromosomal region downstream of the dcw cluster in *Streptococcus pneumoniae*. *Journal of bacteriology*, 185(20), 6209-6214. doi:10.1128/jb.185.20.6209-6214.2003
- Fadda, D., Santona, A., D'Ulisse, V., Ghelardini, P., Ennas, M. G., Whalen, M. B., & Massidda, O. (2007). *Streptococcus pneumoniae* DivIVA: Localization and Interactions in a MinCD-Free Context. *Journal of bacteriology*, 189(4), 1288-1298. doi:10.1128/jb.01168-06
- Fenton, A. K., & Gerdes, K. (2013). Direct interaction of FtsZ and MreB is required for septum synthesis and cell division in *Escherichia coli*. *EMBO J*, 32(13), 1953-1965. doi:10.1038/emboj.2013.129
- Ferullo, D. J., Cooper, D. L., Moore, H. R., & Lovett, S. T. (2009). Cell cycle synchronization of *Escherichia coli* using the stringent response, with fluorescence labeling assays for DNA content and replication. *Methods*, 48(1), 8-13. doi:10.1016/j.ymeth.2009.02.010
- Feucht, A., Lucet, I., Yudkin, M. D., & Errington, J. (2001). Cytological and biochemical characterization of the FtsA cell division protein of *Bacillus subtilis*. *Molecular Microbiology*, 40(1), 115-125. doi:10.1046/j.1365-2958.2001.02356.x
- Fimlaid, K. A., & Shen, A. (2015). Diverse mechanisms regulate sporulation sigma factor activity in the Firmicutes. *Curr Opin Microbiol*, 24, 88-95. doi:10.1016/j.mib.2015.01.006
- Fisher, J. F., & Mobashery, S. (2016). beta-Lactam Resistance Mechanisms: Gram-Positive Bacteria and *Mycobacterium tuberculosis*. *Cold Spring Harb Perspect Med*, 6(5). doi:10.1101/cshperspect.a025221
- Fleurie, A., Cluzel, C., Guiral, S., Freton, C., Galisson, F., Zanella-Cleon, I., . . . Grangeasse, C. (2012). Mutational dissection of the S/T-kinase StkP reveals

- crucial roles in cell division of *Streptococcus pneumoniae*. *Mol Microbiol*, *83*(4), 746-758. doi:10.1111/j.1365-2958.2011.07962.x
- Fleurie, A., Lesterlin, C., Manuse, S., Zhao, C., Cluzel, C., Lavergne, J. P., . . . Grangeasse, C. (2014). MapZ marks the division sites and positions FtsZ rings in *Streptococcus pneumoniae*. *Nature*, *516*(7530), 259-262. doi:10.1038/nature13966
- Formstone, A., Carballido-Lopez, R., Noirot, P., Errington, J., & Scheffers, D. J. (2008). Localization and interactions of teichoic acid synthetic enzymes in *Bacillus subtilis*. *Journal of bacteriology*, *190*(5), 1812-1821. doi:10.1128/JB.01394-07
- Foulquier, E., Pompeo, F., Bernadac, A., Espinosa, L., & Galinier, A. (2011). The YvcK protein is required for morphogenesis via localization of PBP1 under gluconeogenic growth conditions in *Bacillus subtilis*. *Mol Microbiol*, *80*(2), 309-318. doi:10.1111/j.1365-2958.2011.07587.x
- Fraipont, C., Alexeeva, S., Wolf, B., van der Ploeg, R., Schloesser, M., den Blaauwen, T., & Nguyen-Disteche, M. (2011). The integral membrane FtsW protein and peptidoglycan synthase PBP3 form a subcomplex in *Escherichia coli*. *Microbiology*, *157*(Pt 1), 251-259. doi:10.1099/mic.0.040071-0
- Fu, G., Huang, T., Buss, J., Coltharp, C., Hensel, Z., & Xiao, J. (2010). In vivo structure of the *E. coli* FtsZ-ring revealed by photoactivated localization microscopy (PALM). *PLoS One*, *5*(9), e12682. doi:10.1371/journal.pone.0012680
- Fujita, J., Maeda, Y., Nagao, C., Tsuchiya, Y., Miyazaki, Y., Hirose, M., . . . Matsumura, H. (2014). Crystal structure of FtsA from *Staphylococcus aureus*. *FEBS Lett*, *588*(10), 1879-1885. doi:10.1016/j.febslet.2014.04.008
- Gamba, P., Rietkotter, E., Daniel, R. A., & Hamoen, L. W. (2015). Tetracycline hypersensitivity of an *ezaA* mutant links GalE and TseB (YpmB) to cell division. *Front Microbiol*, *6*, 346. doi:10.3389/fmicb.2015.00346
- Gamba, P., Veening, J. W., Saunders, N. J., Hamoen, L. W., & Daniel, R. A. (2009). Two-step assembly dynamics of the *Bacillus subtilis* divisome. *Journal of bacteriology*, *191*(13), 4186-4194. doi:10.1128/JB.01758-08
- Garcia, P., Paz Gonzalez, M., Garcia, E., Garcia, J. L., & Lopez, R. (1999). The molecular characterization of the first autolytic lysozyme of *Streptococcus pneumoniae* reveals evolutionary mobile domains. *Mol Microbiol*, *33*(1), 128-138. doi:10.1046/j.1365-2958.1999.01455.x
- Garcia, P. S., Simorre, J. P., Brochier-Armanet, C., & Grangeasse, C. (2016). Cell division of *Streptococcus pneumoniae*: think positive! *Curr Opin Microbiol*, *34*, 18-23. doi:10.1016/j.mib.2016.07.014
- Garner, E. C., Bernard, R., Wang, W., Zhuang, X., Rudner, D. Z., & Mitchison, T. (2011). Coupled, circumferential motions of the cell wall synthesis machinery and MreB filaments in *B. subtilis*. *Science*, *333*(6039), 222-225. doi:10.1126/science.1203285
- Garti-Levi, S., Hazan, R., Kain, J., Fujita, M., & Ben-Yehuda, S. (2008). The FtsEX ABC transporter directs cellular differentiation in *Bacillus subtilis*. *Mol Microbiol*, *69*(4), 1018-1028. doi:10.1111/j.1365-2958.2008.06340.x
- Geissler, B., Elraheb, D., & Margolin, W. (2003). A gain-of-function mutation in *ftsA* bypasses the requirement for the essential cell division gene *zipA* in

- Escherichia coli. *Proc Natl Acad Sci U S A*, 100(7), 4197-4202. doi:10.1073/pnas.0635003100
- Gerdes, K. (2009). RodZ, a new player in bacterial cell morphogenesis. *EMBO J*, 28(3), 171-172. doi:10.1038/emboj.2008.287
- Gerding, M. A., Liu, B., Bendezu, F. O., Hale, C. A., Bernhardt, T. G., & de Boer, P. A. (2009). Self-enhanced accumulation of FtsN at Division Sites and Roles for Other Proteins with a SPOR domain (DamX, DedD, and RlpA) in Escherichia coli cell constriction. *Journal of bacteriology*, 191(24), 7383-7401. doi:10.1128/jb.00811-09
- Gerding, M. A., Ogata, Y., Pecora, N. D., Niki, H., & de Boer, P. A. (2007). The trans-envelope Tol-Pal complex is part of the cell division machinery and required for proper outer-membrane invagination during cell constriction in E. coli. *Mol Microbiol*, 63(4), 1008-1025. doi:10.1111/j.1365-2958.2006.05571.x
- Ghosal, D., Trambaiolo, D., Amos, L. A., & Lowe, J. (2014). MinCD cell division proteins form alternating copolymeric cytomotive filaments. *Nat Commun*, 5, 5341. doi:10.1038/ncomms6341
- Giefing, C., Jelencsics, K. E., Gelbmann, D., Senn, B. M., & Nagy, E. (2010). The pneumococcal eukaryotic-type serine/threonine protein kinase StkP colocalizes with the cell division apparatus and interacts with FtsZ in vitro. *Microbiology*, 156(Pt 6), 1697-1707. doi:10.1099/mic.0.036335-0
- Giefing, C., Meinke, A. L., Hanner, M., Henics, T., Bui, M. D., Gelbmann, D., . . . Nagy, E. (2008). Discovery of a novel class of highly conserved vaccine antigens using genomic scale antigenic fingerprinting of pneumococcus with human antibodies. *J Exp Med*, 205(1), 117-131. doi:10.1084/jem.20071168
- Giefing-Kroll, C., Jelencsics, K. E., Reipert, S., & Nagy, E. (2011). Absence of pneumococcal PcsB is associated with overexpression of LysM domain-containing proteins. *Microbiology*, 157(Pt 7), 1897-1909. doi:10.1099/mic.0.045211-0
- Gill, D. R., Hatfull, G. F., & Salmond, G. P. (1986). A new cell division operon in Escherichia coli. *Mol Gen Genet*, 205(1), 134-145. doi:10.1007/bf02428043
- Gill, D. R., & Salmond, G. P. (1987). The Escherichia coli cell division proteins FtsY, FtsE and FtsX are inner membrane-associated. *Mol Gen Genet*, 210(3), 504-508. doi:10.1007/bf00327204
- Gill, D. R., & Salmond, G. P. (1990). The identification of the Escherichia coli ftsY gene product: an unusual protein. *Mol Microbiol*, 4(4), 575-583. doi:10.1111/j.1365-2958.1990.tb00626.x
- Goehring, N. W., & Beckwith, J. (2005). Diverse paths to midcell: assembly of the bacterial cell division machinery. *Curr Biol*, 15(13), R514-526. doi:10.1016/j.cub.2005.06.038
- Goehring, N. W., Gueiros-Filho, F., & Beckwith, J. (2005). Premature targeting of a cell division protein to midcell allows dissection of divisome assembly in Escherichia coli. *Genes Dev*, 19(1), 127-137. doi:10.1101/gad.1253805
- Goffin, C., & Ghuysen, J. M. (1998). Multimodular penicillin-binding proteins: an enigmatic family of orthologs and paralogs. *Microbiol Mol Biol Rev*, 62(4),

1079-1093.

Retrieved

from

<https://www.ncbi.nlm.nih.gov/pubmed/9841666>

- Gram, H. C. J., & Friedlaender, C. (1884). *Ueber die isolirte Färbung der Schizomyceten : in Schnitt-und Trockenpräparaten*. Berlin: Theodor Fischer's medicinischer Buchhandlung.
- Greene, N. P., Kaplan, E., Crow, A., & Koronakis, V. (2018). Antibiotic Resistance Mediated by the MacB ABC Transporter Family: A Structural and Functional Perspective. *Front Microbiol*, *9*, 950. doi:10.3389/fmicb.2018.00950
- Gregory, J. A., Becker, E. C., & Pogliano, K. (2008). Bacillus subtilis MinC destabilizes FtsZ-rings at new cell poles and contributes to the timing of cell division. *Genes Dev*, *22*(24), 3475-3488. doi:10.1101/gad.1732408
- Guberman, J. M., Fay, A., Dworkin, J., Wingreen, N. S., & Gitai, Z. (2008). PSICIC: noise and asymmetry in bacterial division revealed by computational image analysis at sub-pixel resolution. *PLoS Comput Biol*, *4*(11), e1000233. doi:10.1371/journal.pcbi.1000233
- Gueiros-Filho, F. J., & Losick, R. (2002). A widely conserved bacterial cell division protein that promotes assembly of the tubulin-like protein FtsZ. *Genes Dev*, *16*(19), 2544-2556. doi:10.1101/gad.1014102
- Gulati, S., Jamshad, M., Knowles, T. J., Morrison, K. A., Downing, R., Cant, N., . . . Rothnie, A. J. (2014). Detergent-free purification of ABC (ATP-binding-cassette) transporters. *Biochem J*, *461*(2), 269-278. doi:10.1042/BJ20131477
- Gundogdu, M. E., Kawai, Y., Pavlendova, N., Ogasawara, N., Errington, J., Scheffers, D. J., & Hamoen, L. W. (2011). Large ring polymers align FtsZ polymers for normal septum formation. *EMBO J*, *30*(3), 617-626. doi:10.1038/emboj.2010.345
- Haeusser, D. P., Garza, A. C., Buscher, A. Z., & Levin, P. A. (2007). The division inhibitor EzrA contains a seven-residue patch required for maintaining the dynamic nature of the medial FtsZ ring. *Journal of bacteriology*, *189*(24), 9001-9010. doi:10.1128/JB.01172-07
- Haeusser, D. P., & Margolin, W. (2016). Splitsville: structural and functional insights into the dynamic bacterial Z ring. *Nat Rev Microbiol*, *14*(5), 305-319. doi:10.1038/nrmicro.2016.26
- Haeusser, D. P., Schwartz, R. L., Smith, A. M., Oates, M. E., & Levin, P. A. (2004). EzrA prevents aberrant cell division by modulating assembly of the cytoskeletal protein FtsZ. *Mol Microbiol*, *52*(3), 801-814. doi:10.1111/j.1365-2958.2004.04016.x
- Hajduk, I. V., Mann, R., Rodrigues, C. D. A., & Harry, E. J. (2019). The ParB homologs, SpoJ and Noc, together prevent premature midcell Z ring assembly when the early stages of replication are blocked in Bacillus subtilis. *Mol Microbiol*, *112*(3), 766-784. doi:10.1111/mmi.14319
- Hajduk, I. V., Rodrigues, C. D., & Harry, E. J. (2016). Connecting the dots of the bacterial cell cycle: Coordinating chromosome replication and segregation with cell division. *Semin Cell Dev Biol*, *53*, 2-9. doi:10.1016/j.semcdb.2015.11.012

- Hale, C. A., & de Boer, P. A. (1997). Direct binding of FtsZ to ZipA, an essential component of the septal ring structure that mediates cell division in *E. coli*. *Cell*, *88*(2), 175-185. doi:10.1016/s0092-8674(00)81838-3
- Hale, C. A., Meinhardt, H., & de Boer, P. A. (2001). Dynamic localization cycle of the cell division regulator MinE in *Escherichia coli*. *EMBO J*, *20*(7), 1563-1572. doi:10.1093/emboj/20.7.1563
- Hale, C. A., Shiomi, D., Liu, B., Bernhardt, T. G., Margolin, W., Niki, H., & de Boer, P. A. (2011). Identification of *Escherichia coli* ZapC (YcbW) as a component of the division apparatus that binds and bundles FtsZ polymers. *Journal of bacteriology*, *193*(6), 1393-1404. doi:10.1128/JB.01245-10
- Hamoen, L. W., & Errington, J. (2003). Polar targeting of DivIVA in *Bacillus subtilis* is not directly dependent on FtsZ or PBP 2B. *Journal of bacteriology*, *185*(2), 693-697. doi:10.1128/jb.185.2.693-697.2003
- Hamoen, L. W., Meile, J. C., de Jong, W., Noirot, P., & Errington, J. (2006). SepF, a novel FtsZ-interacting protein required for a late step in cell division. *Mol Microbiol*, *59*(3), 989-999. doi:10.1111/j.1365-2958.2005.04987.x
- Hamon, M. A., & Lazazzera, B. A. (2001). The sporulation transcription factor Spo0A is required for biofilm development in *Bacillus subtilis*. *Mol Microbiol*, *42*(5), 1199-1209. doi:10.1046/j.1365-2958.2001.02709.x
- Hanahan, D. (1983). Studies on transformation of *Escherichia coli* with plasmids. *J Mol Biol*, *166*(4), 557-580. doi:10.1016/s0022-2836(83)80284-8
- Handler, A. A., Lim, J. E., & Losick, R. (2008). Peptide inhibitor of cytokinesis during sporulation in *Bacillus subtilis*. *Mol Microbiol*, *68*(3), 588-599. doi:10.1111/j.1365-2958.2008.06173.x
- Hansman, D., & Bullen, M. M. (1967). A RESISTANT PNEUMOCOCCUS. *The Lancet*, *290*(7509), 264-265. doi:[https://doi.org/10.1016/S0140-6736\(67\)92346-X](https://doi.org/10.1016/S0140-6736(67)92346-X)
- Haydon, D. J., Stokes, N. R., Ure, R., Galbraith, G., Bennett, J. M., Brown, D. R., . . . Czaplewski, L. G. (2008). An inhibitor of FtsZ with potent and selective anti-staphylococcal activity. *Science*, *321*(5896), 1673-1675. doi:10.1126/science.1159961
- Heidrich, C., Templin, M. F., Ursinus, A., Merdanovic, M., Berger, J., Schwarz, H., . . . Holtje, J. V. (2001). Involvement of N-acetylmuramyl-L-alanine amidases in cell separation and antibiotic-induced autolysis of *Escherichia coli*. *Mol Microbiol*, *41*(1), 167-178. doi:10.1046/j.1365-2958.2001.02499.x
- Heidrich, C., Ursinus, A., Berger, J., Schwarz, H., & Holtje, J. V. (2002). Effects of multiple deletions of murein hydrolases on viability, septum cleavage, and sensitivity to large toxic molecules in *Escherichia coli*. *Journal of bacteriology*, *184*(22), 6093-6099. doi:10.1128/jb.184.22.6093-6099.2002
- Henriques, A. O., & Moran, C. P., Jr. (2007). Structure, assembly, and function of the spore surface layers. *Annu Rev Microbiol*, *61*, 555-588. doi:10.1146/annurev.micro.61.080706.093224
- Hernandez-Rocamora, V. M., Reija, B., Garcia, C., Natale, P., Alfonso, C., Minton, A. P., . . . Vicente, M. (2012). Dynamic interaction of the *Escherichia coli* cell division ZipA and FtsZ proteins evidenced in nanodiscs. *J Biol Chem*, *287*(36), 30097-30104. doi:10.1074/jbc.M112.388959

- Higgins, C. F. (1992). ABC transporters: from microorganisms to man. *Annu Rev Cell Biol*, 8, 67-113. doi:10.1146/annurev.cb.08.110192.000435
- Higgins, M. L., & Shockman, G. D. (1970). Model for Cell Wall Growth of *Streptococcus faecalis*. *Journal of bacteriology*, 101(2), 643-648. Retrieved from <https://jb.asm.org/content/jb/101/2/643.full.pdf>
- Higgins, M. L., & Shockman, G. D. (1976). Study of cycle of cell wall assembly in *Streptococcus faecalis* by three-dimensional reconstructions of thin sections of cells. *Journal of bacteriology*, 127(3), 1346-1358. Retrieved from <https://www.ncbi.nlm.nih.gov/pubmed/821928>
- Hirota, Y., Ryter, A., & Jacob, F. (1968). Thermosensitive mutants of *E. coli* affected in the processes of DNA synthesis and cellular division. *Cold Spring Harb Symp Quant Biol*, 33, 677-693. doi:10.1101/sqb.1968.033.01.077
- Holeckova, N., Doubravova, L., Massidda, O., Molle, V., Buriankova, K., Benada, O., . . . Branny, P. (2014). LocZ is a new cell division protein involved in proper septum placement in *Streptococcus pneumoniae*. *MBio*, 6(1), e01700-01714. doi:10.1128/mBio.01700-14
- Holtje, J. V. (1998). Growth of the stress-bearing and shape-maintaining murein sacculus of *Escherichia coli*. *Microbiol Mol Biol Rev*, 62(1), 181-203. Retrieved from <https://www.ncbi.nlm.nih.gov/pubmed/9529891>
- Hu, Z., & Lutkenhaus, J. (1999). Topological regulation of cell division in *Escherichia coli* involves rapid pole to pole oscillation of the division inhibitor MinC under the control of MinD and MinE. *Mol Microbiol*, 34(1), 82-90. doi:10.1046/j.1365-2958.1999.01575.x
- Hu, Z., & Lutkenhaus, J. (2003). A conserved sequence at the C-terminus of MinD is required for binding to the membrane and targeting MinC to the septum. *Molecular Microbiology*, 47(2), 345-355. doi:10.1046/j.1365-2958.2003.03321.x
- Huang, K. H., Durand-Heredia, J., & Janakiraman, A. (2013). FtsZ ring stability: of bundles, tubules, crosslinks, and curves. *Journal of bacteriology*, 195(9), 1859-1868. doi:10.1128/JB.02157-12
- Hugonnet, J. E., Mengin-Lecreux, D., Monton, A., den Blaauwen, T., Carbonnelle, E., Veckerle, C., . . . Arthur, M. (2016). Factors essential for L,D-transpeptidase-mediated peptidoglycan cross-linking and beta-lactam resistance in *Escherichia coli*. *Elife*, 5. doi:10.7554/eLife.19469
- Ishikawa, S., Kawai, Y., Hiramatsu, K., Kuwano, M., & Ogasawara, N. (2006). A new FtsZ-interacting protein, YlmF, complements the activity of FtsA during progression of cell division in *Bacillus subtilis*. *Mol Microbiol*, 60(6), 1364-1380. doi:10.1111/j.1365-2958.2006.05184.x
- Ito, K., & Akiyama, Y. (2005). Cellular functions, mechanism of action, and regulation of FtsH protease. *Annu Rev Microbiol*, 59, 211-231. doi:10.1146/annurev.micro.59.030804.121316
- Jacobs, M. R., Koornhof, H. J., Robins-Browne, R. M., Stevenson, C. M., Vermaak, Z. A., Freiman, I., . . . Austrian, R. (1978). Emergence of multiply resistant pneumococci. *N Engl J Med*, 299(14), 735-740. doi:10.1056/NEJM197810052991402
- Jameson, L. P., Smith, N. W., Annunziata, O., & Dzyuba, S. V. (2016). Interaction of BODIPY dyes with bovine serum albumin: a case study on the

- aggregation of a click-BODIPY dye. *Phys Chem Chem Phys*, 18(21), 14182-14185. doi:10.1039/c6cp00420b
- Jamshad, M., Charlton, J., Lin, Y. P., Routledge, S. J., Bawa, Z., Knowles, T. J., . . . Wheatley, M. (2015). G-protein coupled receptor solubilization and purification for biophysical analysis and functional studies, in the total absence of detergent. *Biosci Rep*, 35(2). doi:10.1042/bsr20140171
- Jensen, S. O., Thompson, L. S., & Harry, E. J. (2005). Cell division in *Bacillus subtilis*: FtsZ and FtsA association is Z-ring independent, and FtsA is required for efficient midcell Z-Ring assembly. *Journal of bacteriology*, 187(18), 6536-6544. doi:10.1128/JB.187.18.6536-6544.2005
- Jones, C., & Holland, I. B. (1985). Role of the SulB (FtsZ) protein in division inhibition during the SOS response in *Escherichia coli*: FtsZ stabilizes the inhibitor SulA in maxicells. *Proc Natl Acad Sci U S A*, 82(18), 6045-6049. doi:10.1073/pnas.82.18.6045
- Jones, L. J., Carballido-Lopez, R., & Errington, J. (2001). Control of cell shape in bacteria: helical, actin-like filaments in *Bacillus subtilis*. *Cell*, 104(6), 913-922. doi:10.1016/s0092-8674(01)00287-2
- Kaimer, C., Gonzalez-Pastor, J. E., & Graumann, P. L. (2009). SpoIIIE and a novel type of DNA translocase, SftA, couple chromosome segregation with cell division in *Bacillus subtilis*. *Mol Microbiol*, 74(4), 810-825. doi:10.1111/j.1365-2958.2009.06894.x
- Kaimer, C., Schenk, K., & Graumann, P. L. (2011). Two DNA translocases synergistically affect chromosome dimer resolution in *Bacillus subtilis*. *Journal of bacteriology*, 193(6), 1334-1340. doi:10.1128/JB.00918-10
- Karimova, G., Dautin, N., & Ladant, D. (2005). Interaction network among *Escherichia coli* membrane proteins involved in cell division as revealed by bacterial two-hybrid analysis. *Journal of bacteriology*, 187(7), 2233-2243. doi:10.1128/JB.187.7.2233-2243.2005
- Katis, V. L., Harry, E. J., & Wake, R. G. (1997). The *Bacillus subtilis* division protein DivIC is a highly abundant membrane-bound protein that localizes to the division site. *Mol Microbiol*, 26(5), 1047-1055. doi:10.1046/j.1365-2958.1997.6422012.x
- Katis, V. L., & Wake, R. G. (1999). Membrane-bound division proteins DivIB and DivIC of *Bacillus subtilis* function solely through their external domains in both vegetative and sporulation division. *Journal of bacteriology*, 181(9), 2710-2718. Retrieved from <https://www.ncbi.nlm.nih.gov/pubmed/10217758>
- Katis, V. L., Wake, R. G., & Harry, E. J. (2000). Septal Localization of the Membrane-Bound Division Proteins of *Bacillus subtilis* DivIB and DivIC Is Codependent Only at High Temperatures and Requires FtsZ. *Journal of bacteriology*, 182(12), 3607-3611. doi:10.1128/jb.182.12.3607-3611.2000
- Katz, C., & Ron, E. Z. (2008). Dual role of FtsH in regulating lipopolysaccharide biosynthesis in *Escherichia coli*. *Journal of bacteriology*, 190(21), 7117-7122. doi:10.1128/jb.00871-08
- Kawai, Y., Asai, K., & Errington, J. (2009). Partial functional redundancy of MreB isoforms, MreB, Mbl and MreBH, in cell morphogenesis of *Bacillus*

- subtilis. *Mol Microbiol*, 73(4), 719-731. doi:10.1111/j.1365-2958.2009.06805.x
- Kawai, Y., Daniel, R. A., & Errington, J. (2009). Regulation of cell wall morphogenesis in *Bacillus subtilis* by recruitment of PBP1 to the MreB helix. *Mol Microbiol*, 71(5), 1131-1144. doi:10.1111/j.1365-2958.2009.06601.x
- Kawai, Y., Marles-Wright, J., Cleverley, R. M., Emmins, R., Ishikawa, S., Kuwano, M., . . . Errington, J. (2011). A widespread family of bacterial cell wall assembly proteins. *EMBO J*, 30(24), 4931-4941. doi:10.1038/emboj.2011.358
- Kawai, Y., & Ogasawara, N. (2006). *Bacillus subtilis* EzrA and FtsL synergistically regulate FtsZ ring dynamics during cell division. *Microbiology*, 152(4), 1129-1141. doi:<https://doi.org/10.1099/mic.0.28497-0>
- Kell, C. M., Sharma, U. K., Dowson, C. G., Town, C., Balganes, T. S., & Spratt, B. G. (1993). Deletion analysis of the essentiality of penicillin-binding proteins 1A, 2B and 2X of *Streptococcus pneumoniae*. *FEMS Microbiol Lett*, 106(2), 171-175. doi:10.1111/j.1574-6968.1993.tb05954.x
- Kennedy, M. J., Reader, S. L., & Swierczynski, L. M. (1994). Preservation records of micro-organisms: evidence of the tenacity of life. *Microbiology*, 140 (Pt 10), 2513-2529. doi:10.1099/00221287-140-10-2513
- Klugman, K. P. (2011). Contribution of vaccines to our understanding of pneumococcal disease. *Philos Trans R Soc Lond B Biol Sci*, 366(1579), 2790-2798. doi:10.1098/rstb.2011.0032
- Krupka, M., Cabre, E. J., Jimenez, M., Rivas, G., Rico, A. I., & Vicente, M. (2014). Role of the FtsA C terminus as a switch for polymerization and membrane association. *MBio*, 5(6), e02221. doi:10.1128/mBio.02221-14
- Krupka, M., Sobrinos-Sanguino, M., Jimenez, M., Rivas, G., & Margolin, W. (2018). *Escherichia coli* ZipA Organizes FtsZ Polymers into Dynamic Ring-Like Protofilament Structures. *MBio*, 9(3). doi:10.1128/mBio.01008-18
- Kruse, T., Bork-Jensen, J., & Gerdes, K. (2005). The morphogenetic MreBCD proteins of *Escherichia coli* form an essential membrane-bound complex. *Mol Microbiol*, 55(1), 78-89. doi:10.1111/j.1365-2958.2004.04367.x
- Kuhn, A., Koch, H. G., & Dalbey, R. E. (2017). Targeting and Insertion of Membrane Proteins. *EcoSal Plus*, 7(2). doi:10.1128/ecosalplus.ESP-0012-2016
- Laemmli, U. K. (1970). Cleavage of structural proteins during the assembly of the head of bacteriophage T4. *Nature*, 227(5259), 680-685. doi:10.1038/227680a0
- Land, A. D., Luo, Q., & Levin, P. A. (2014). Functional domain analysis of the cell division inhibitor EzrA. *PLoS One*, 9(7), e102616. doi:10.1371/journal.pone.0102616
- Land, A. D., Tsui, H. C., Kocaoglu, O., Vella, S. A., Shaw, S. L., Keen, S. K., . . . Winkler, M. E. (2013). Requirement of essential Pbp2x and GpsB for septal ring closure in *Streptococcus pneumoniae* D39. *Mol Microbiol*, 90(5), 939-955. doi:10.1111/mmi.12408
- Land, A. D., & Winkler, M. E. (2011). The requirement for pneumococcal MreC and MreD is relieved by inactivation of the gene encoding PBP1a. *Journal of bacteriology*, 193(16), 4166-4179. doi:10.1128/JB.05245-11

- Lara, B., Rico, A. I., Petruzzelli, S., Santona, A., Dumas, J., Biton, J., . . . Massidda, O. (2005). Cell division in cocci: localization and properties of the *Streptococcus pneumoniae* FtsA protein. *Mol Microbiol*, *55*(3), 699-711. doi:10.1111/j.1365-2958.2004.04432.x
- LB (Luria-Bertani) liquid medium. (2006). *Cold Spring Harbor Protocols*, *2006*(1), pdb.rec8141. doi:10.1101/pdb.rec8141
- Le Gouellec, A., Roux, L., Fadda, D., Massidda, O., Vernet, T., & Zapun, A. (2008). Roles of pneumococcal DivIB in cell division. *Journal of bacteriology*, *190*(13), 4501-4511. doi:10.1128/JB.00376-08
- Leaver, M., & Errington, J. (2005). Roles for MreC and MreD proteins in helical growth of the cylindrical cell wall in *Bacillus subtilis*. *Mol Microbiol*, *57*(5), 1196-1209. doi:10.1111/j.1365-2958.2005.04736.x
- LeDeaux, J. R., Yu, N., & Grossman, A. D. (1995). Different roles for KinA, KinB, and KinC in the initiation of sporulation in *Bacillus subtilis*. *Journal of bacteriology*, *177*(3), 861-863. doi:10.1128/jb.177.3.861-863.1995
- Lee, M. E., Baker, T. A., & Sauer, R. T. (2010). Control of substrate gating and translocation into ClpP by channel residues and ClpX binding. *J Mol Biol*, *399*(5), 707-718. doi:10.1016/j.jmb.2010.04.027
- Lee, S. C., Knowles, T. J., Postis, V. L. G., Jamshad, M., Parslow, R. A., Lin, Y. P., . . . Dafforn, T. R. (2016). A method for detergent-free isolation of membrane proteins in their local lipid environment. *Nature Protocols*, *11*(7), 1149-1162. Retrieved from <Go to ISI>://WOS:000377489200001
- Lee, S. C., & Pollock, N. L. (2016). Membrane proteins: is the future disc shaped? *Biochem Soc Trans*, *44*(4), 1011-1018. doi:10.1042/BST20160015
- Lenarcic, R., Halbedel, S., Visser, L., Shaw, M., Wu, L. J., Errington, J., . . . Hamoen, L. W. (2009). Localisation of DivIVA by targeting to negatively curved membranes. *EMBO J*, *28*(15), 2272-2282. doi:10.1038/emboj.2009.129
- Lennox, E. S. (1955). Transduction of linked genetic characters of the host by bacteriophage P1. *Virology*, *1*(2), 190-206. doi:10.1016/0042-6822(55)90016-7
- Levin, P. A., Kurtser, I. G., & Grossman, A. D. (1999). Identification and characterization of a negative regulator of FtsZ ring formation in *Bacillus subtilis*. *Proc Natl Acad Sci U S A*, *96*(17), 9642-9647. doi:10.1073/pnas.96.17.9642
- Levin, P. A., & Losick, R. (1996). Transcription factor Spo0A switches the localization of the cell division protein FtsZ from a medial to a bipolar pattern in *Bacillus subtilis*. *Genes Dev*, *10*(4), 478-488. doi:10.1101/gad.10.4.478
- Levin, P. A., Margolis, P. S., Setlow, P., Losick, R., & Sun, D. (1992). Identification of *Bacillus subtilis* genes for septum placement and shape determination. *Journal of bacteriology*, *174*(21), 6717-6728. doi:10.1128/jb.174.21.6717-6728.1992
- Levy, S. B., & Marshall, B. (2004). Antibacterial resistance worldwide: causes, challenges and responses. *Nat Med*, *10*(12 Suppl), S122-129. doi:10.1038/nm1145
- Li, Q., Li, Z., Li, X., Xia, L., Zhou, X., Xu, Z., . . . Zhang, R. (2018). FtsEX-CwlO regulates biofilm formation by a plant-beneficial rhizobacterium *Bacillus*

- velezensis SQR9. *Research in Microbiology*, 169(3), 166-176. doi:<https://doi.org/10.1016/j.resmic.2018.01.004>
- Lim, H. C., Sher, J. W., Rodriguez-Rivera, F. P., Fumeaux, C., Bertozzi, C. R., & Bernhardt, T. G. (2019). Identification of new components of the RipC-FtsEX cell separation pathway of Corynebacterineae. *PLoS Genet*, 15(8), e1008284. doi:10.1371/journal.pgen.1008284
- Liu, B., Persons, L., Lee, L., & de Boer, P. A. (2015). Roles for both FtsA and the FtsBLQ subcomplex in FtsN-stimulated cell constriction in *Escherichia coli*. *Mol Microbiol*, 95(6), 945-970. doi:10.1111/mmi.12906
- Liu, G., Draper, G. C., & Donachie, W. D. (1998). FtsK is a bifunctional protein involved in cell division and chromosome localization in *Escherichia coli*. *Mol Microbiol*, 29(3), 893-903. doi:10.1046/j.1365-2958.1998.00986.x
- Lleo, M. M., Canepari, P., & Satta, G. (1990). Bacterial cell shape regulation: testing of additional predictions unique to the two-competing-sites model for peptidoglycan assembly and isolation of conditional rod-shaped mutants from some wild-type cocci. *Journal of bacteriology*, 172(7), 3758-3771. doi:10.1128/jb.172.7.3758-3771.1990
- Lowe, J., & Amos, L. A. (1998). Crystal structure of the bacterial cell-division protein FtsZ. *Nature*, 391(6663), 203-206. doi:10.1038/34472
- Lu, Z., Takeuchi, M., & Sato, T. (2007). The LysR-type transcriptional regulator YofA controls cell division through the regulation of expression of ftsW in *Bacillus subtilis*. *Journal of bacteriology*, 189(15), 5642-5651. doi:10.1128/JB.00467-07
- Lucet, I., Feucht, A., Yudkin, M. D., & Errington, J. (2000). Direct interaction between the cell division protein FtsZ and the cell differentiation protein SpoIIE. *EMBO J*, 19(7), 1467-1475. doi:10.1093/emboj/19.7.1467
- Lutkenhaus, J. (1997). Bacterial cytokinesis: let the light shine in. *Curr Biol*, 7(9), R573-575. doi:10.1016/s0960-9822(06)00285-5
- Lutkenhaus, J., Pichoff, S., & Du, S. (2012). Bacterial cytokinesis: From Z ring to divisome. *Cytoskeleton (Hoboken)*, 69(10), 778-790. doi:10.1002/cm.21054
- Lutkenhaus, J. F., & Donachie, W. D. (1979). Identification of the ftsA gene product. *Journal of bacteriology*, 137(3), 1088-1094. Retrieved from <https://www.ncbi.nlm.nih.gov/pubmed/374336>
- Macheboeuf, P., Contreras-Martel, C., Job, V., Dideberg, O., & Dessen, A. (2006). Penicillin binding proteins: key players in bacterial cell cycle and drug resistance processes. *FEMS Microbiol Rev*, 30(5), 673-691. doi:10.1111/j.1574-6976.2006.00024.x
- Maggi, S., Massidda, O., Luzi, G., Fadda, D., Paolozzi, L., & Ghelardini, P. (2008). Division protein interaction web: identification of a phylogenetically conserved common interactome between *Streptococcus pneumoniae* and *Escherichia coli*. *Microbiology*, 154(Pt 10), 3042-3052. doi:10.1099/mic.0.2008/018697-0
- Manuse, S., Jean, N. L., Guinot, M., Lavergne, J. P., Laguri, C., Bougault, C. M., . . . Simorre, J. P. (2016). Structure-function analysis of the extracellular domain of the pneumococcal cell division site positioning protein MapZ. *Nat Commun*, 7, 12071. doi:10.1038/ncomms12071

- Margolin, W. (2009). Sculpting the bacterial cell. *Curr Biol*, 19(17), R812-822. doi:10.1016/j.cub.2009.06.033
- Margulieux, K. R., Fox, J. W., Nakamoto, R. K., & Hughes, M. A. (2016). CXCL10 Acts as a Bifunctional Antimicrobial Molecule against Bacillus anthracis. *MBio*, 7(3). doi:10.1128/mBio.00334-16
- Marston, A. L., & Errington, J. (1999). Selection of the midcell division site in Bacillus subtilis through MinD-dependent polar localization and activation of MinC. *Mol Microbiol*, 33(1), 84-96. doi:10.1046/j.1365-2958.1999.01450.x
- Marston, A. L., Thomaidis, H. B., Edwards, D. H., Sharpe, M. E., & Errington, J. (1998). Polar localization of the MinD protein of Bacillus subtilis and its role in selection of the mid-cell division site. *Genes Dev*, 12(21), 3419-3430. doi:10.1101/gad.12.21.3419
- Marteyn, B. S., Karimova, G., Fenton, A. K., Gazi, A. D., West, N., Touqui, L., . . . Tang, C. M. (2014). ZapE is a novel cell division protein interacting with FtsZ and modulating the Z-ring dynamics. *MBio*, 5(2), e00022-00014. doi:10.1128/mBio.00022-14
- Massey, T. H., Mercogliano, C. P., Yates, J., Sherratt, D. J., & Lowe, J. (2006). Double-stranded DNA translocation: structure and mechanism of hexameric FtsK. *Mol Cell*, 23(4), 457-469. doi:10.1016/j.molcel.2006.06.019
- Massidda, O., Anderluzzi, D., Friedli, L., & Feger, G. (1998). Unconventional organization of the division and cell wall gene cluster of Streptococcus pneumoniae. *Microbiology*, 144 (Pt 11), 3069-3078. doi:10.1099/00221287-144-11-3069
- Massidda, O., Novakova, L., & Vollmer, W. (2013). From models to pathogens: how much have we learned about Streptococcus pneumoniae cell division? *Environ Microbiol*, 15(12), 3133-3157. doi:10.1111/1462-2920.12189
- Masson, S., Kern, T., Le Gouellec, A., Giustini, C., Simorre, J. P., Callow, P., . . . Zapun, A. (2009). Central domain of DivIB caps the C-terminal regions of the FtsL/DivIC coiled-coil rod. *J Biol Chem*, 284(40), 27687-27700. doi:10.1074/jbc.M109.019471
- Mavrici, D., Marakalala, M. J., Holton, J. M., Prigozhin, D. M., Gee, C. L., Zhang, Y. J., . . . Alber, T. (2014). Mycobacterium tuberculosis FtsX extracellular domain activates the peptidoglycan hydrolase, RipC. *Proceedings of the National Academy of Sciences of the United States of America*, 111(22), 8037-8042. doi:10.1073/pnas.1321812111
- Maxwell, A. (1993). The interaction between coumarin drugs and DNA gyrase. *Mol Microbiol*, 9(4), 681-686. doi:10.1111/j.1365-2958.1993.tb01728.x
- McKenney, P. T., Driks, A., & Eichenberger, P. (2013). The Bacillus subtilis endospore: assembly and functions of the multilayered coat. *Nat Rev Microbiol*, 11(1), 33-44. doi:10.1038/nrmicro2921
- McKenney, P. T., & Eichenberger, P. (2012). Dynamics of spore coat morphogenesis in Bacillus subtilis. *Mol Microbiol*, 83(2), 245-260. doi:10.1111/j.1365-2958.2011.07936.x
- McPherson, D. C., & Popham, D. L. (2003). Peptidoglycan synthesis in the absence of class A penicillin-binding proteins in Bacillus subtilis. *Journal of bacteriology*, 185(4), 1423-1431. doi:10.1128/jb.185.4.1423-1431.2003

- Meeske, A. J., Riley, E. P., Robins, W. P., Uehara, T., Mekalanos, J. J., Kahne, D., . . . Rudner, D. Z. (2016). SEDS proteins are a widespread family of bacterial cell wall polymerases. *Nature*, *537*(7622), 634-638. doi:10.1038/nature19331
- Meisner, J., Montero Llopis, P., Sham, L. T., Garner, E., Bernhardt, T. G., & Rudner, D. Z. (2013). FtsEX is required for CwlO peptidoglycan hydrolase activity during cell wall elongation in *Bacillus subtilis*. *Mol Microbiol*, *89*(6), 1069-1083. doi:10.1111/mmi.12330
- Mercier, R., Petit, M. A., Schbath, S., Robin, S., El Karoui, M., Boccard, F., & Espeli, O. (2008). The MatP/matS site-specific system organizes the terminus region of the *E. coli* chromosome into a macrodomain. *Cell*, *135*(3), 475-485. doi:10.1016/j.cell.2008.08.031
- Meyer, P., Gutierrez, J., Pogliano, K., & Dworkin, J. (2010). Cell wall synthesis is necessary for membrane dynamics during sporulation of *Bacillus subtilis*. *Mol Microbiol*, *76*(4), 956-970. doi:10.1111/j.1365-2958.2010.07155.x
- Miller, A. K., Brown, E. E., Mercado, B. T., & Herman, J. K. (2016). A DNA-binding protein defines the precise region of chromosome capture during *Bacillus* sporulation. *Mol Microbiol*, *99*(1), 111-122. doi:10.1111/mmi.13217
- Mir, M. A., Arumugam, M., Mondal, S., Rajeswari, H. S., Ramakumar, S., & Ajitkumar, P. (2015). Mycobacterium tuberculosis cell division protein, FtsE, is an ATPase in dimeric form. *Protein J*, *34*(1), 35-47. doi:10.1007/s10930-014-9593-7
- Mir, M. A., Rajeswari, H. S., Veeraghavan, U., & Ajitkumar, P. (2006). Molecular characterisation of ABC transporter type FtsE and FtsX proteins of *Mycobacterium tuberculosis*. *Arch Microbiol*, *185*(2), 147-158. doi:10.1007/s00203-005-0079-z
- Mohammadi, T., van Dam, V., Sijbrandi, R., Vernet, T., Zapun, A., Bouhss, A., . . . Breukink, E. (2011). Identification of FtsW as a transporter of lipid-linked cell wall precursors across the membrane. *EMBO J*, *30*(8), 1425-1432. doi:10.1038/emboj.2011.61
- Morlot, C., Noirclerc-Savoye, M., Zapun, A., Dideberg, O., & Vernet, T. (2004). The D,D-carboxypeptidase PBP3 organizes the division process of *Streptococcus pneumoniae*. *Mol Microbiol*, *51*(6), 1641-1648. doi:10.1046/j.1365-2958.2003.03953.x
- Morlot, C., Zapun, A., Dideberg, O., & Vernet, T. (2003). Growth and division of *Streptococcus pneumoniae*: localization of the high molecular weight penicillin-binding proteins during the cell cycle. *Mol Microbiol*, *50*(3), 845-855. doi:10.1046/j.1365-2958.2003.03767.x
- Mosyak, L., Zhang, Y., Glasfeld, E., Haney, S., Stahl, M., Seehra, J., & Somers, W. S. (2000). The bacterial cell-division protein ZipA and its interaction with an FtsZ fragment revealed by X-ray crystallography. *EMBO J*, *19*(13), 3179-3191. doi:10.1093/emboj/19.13.3179
- Muchova, K., Chromikova, Z., & Barak, I. (2013). Control of *Bacillus subtilis* cell shape by RodZ. *Environ Microbiol*, *15*(12), 3259-3271. doi:10.1111/1462-2920.12200

- Muchova, K., Chromikova, Z., Valencikova, R., & Barak, I. (2017). Interaction of the Morphogenic Protein RodZ with the Bacillus subtilis Min System. *Front Microbiol*, 8, 2650. doi:10.3389/fmicb.2017.02650
- Mulder, E., & Woldringh, C. L. (1989). Actively replicating nucleoids influence positioning of division sites in Escherichia coli filaments forming cells lacking DNA. *Journal of bacteriology*, 171(8), 4303-4314. doi:10.1128/jb.171.8.4303-4314.1989
- Muller, P., Ewers, C., Bertsche, U., Anstett, M., Kallis, T., Breukink, E., . . . Vollmer, W. (2007). The essential cell division protein FtsN interacts with the murein (peptidoglycan) synthase PBP1B in Escherichia coli. *J Biol Chem*, 282(50), 36394-36402. doi:10.1074/jbc.M706390200
- Mura, A., Fadda, D., Perez, A. J., Danforth, M. L., Musu, D., Rico, A. I., . . . Massidda, O. (2017). Roles of the Essential Protein FtsA in Cell Growth and Division in Streptococcus pneumoniae. *Journal of bacteriology*, 199(3). doi:10.1128/JB.00608-16
- Nanninga, N. (1998). Morphogenesis of Escherichia coli. *Microbiology and molecular biology reviews : MMBR*, 62(1), 110-129. Retrieved from <https://www.ncbi.nlm.nih.gov/pubmed/9529889>
<https://www.ncbi.nlm.nih.gov/pmc/articles/PMC98908/>
- Nehme, D., & Poole, K. (2005). Interaction of the MexA and MexB components of the MexAB-OprM multidrug efflux system of Pseudomonas aeruginosa: identification of MexA extragenic suppressors of a T578I mutation in MexB. *Antimicrob Agents Chemother*, 49(10), 4375-4378. doi:10.1128/AAC.49.10.4375-4378.2005
- Neuhaus, F. C., & Baddiley, J. (2003). A continuum of anionic charge: structures and functions of D-alanyl-teichoic acids in gram-positive bacteria. *Microbiol Mol Biol Rev*, 67(4), 686-723. doi:10.1128/mubr.67.4.686-723.2003
- Ng, W. L., Kazmierczak, K. M., & Winkler, M. E. (2004). Defective cell wall synthesis in Streptococcus pneumoniae R6 depleted for the essential PcsB putative murein hydrolase or the VicR (YycF) response regulator. *Mol Microbiol*, 53(4), 1161-1175. doi:10.1111/j.1365-2958.2004.04196.x
- Ng, W. L., Robertson, G. T., Kazmierczak, K. M., Zhao, J., Gilmour, R., & Winkler, M. E. (2003). Constitutive expression of PcsB suppresses the requirement for the essential VicR (YycF) response regulator in Streptococcus pneumoniae R6. *Mol Microbiol*, 50(5), 1647-1663. doi:10.1046/j.1365-2958.2003.03806.x
- Ng, W. L., Tsui, H. C., & Winkler, M. E. (2005). Regulation of the pspA virulence factor and essential pcsB murein biosynthetic genes by the phosphorylated VicR (YycF) response regulator in Streptococcus pneumoniae. *Journal of bacteriology*, 187(21), 7444-7459. doi:10.1128/JB.187.21.7444-7459.2005
- Nicholson, W. L., Munakata, N., Horneck, G., Melosh, H. J., & Setlow, P. (2000). Resistance of Bacillus endospores to extreme terrestrial and extraterrestrial environments. *Microbiol Mol Biol Rev*, 64(3), 548-572. doi:10.1128/mubr.64.3.548-572.2000
- Nikolaichik, Y. A., & Donachie, W. D. (2000). Conservation of gene order amongst cell wall and cell division genes in Eubacteria, and ribosomal genes in

- Eubacteria and Eukaryotic organelles. *Genetica*, 108(1), 1-7. doi:10.1023/a:1004077806910
- Nogales, E., Downing, K. H., Amos, L. A., & Lowe, J. (1998). Tubulin and FtsZ form a distinct family of GTPases. *Nat Struct Biol*, 5(6), 451-458. doi:10.1038/nsb0698-451
- Noirclerc-Savoye, M., Lantez, V., Signor, L., Philippe, J., Vernet, T., & Zapun, A. (2013). Reconstitution of membrane protein complexes involved in pneumococcal septal cell wall assembly. *PLoS One*, 8(9), e75522. doi:10.1371/journal.pone.0075522
- Noirclerc-Savoye, M., Le Gouellec, A., Morlot, C., Dideberg, O., Vernet, T., & Zapun, A. (2005). In vitro reconstitution of a trimeric complex of DivIB, DivIC and FtsL, and their transient co-localization at the division site in *Streptococcus pneumoniae*. *Mol Microbiol*, 55(2), 413-424. doi:10.1111/j.1365-2958.2004.04408.x
- Novakova, L., Bezouskova, S., Pompach, P., Spidlova, P., Saskova, L., Weiser, J., & Branny, P. (2010). Identification of multiple substrates of the StkP Ser/Thr protein kinase in *Streptococcus pneumoniae*. *Journal of bacteriology*, 192(14), 3629-3638. doi:10.1128/JB.01564-09
- O'Brien, K. L., Wolfson, L. J., Watt, J. P., Henkle, E., Deloria-Knoll, M., McCall, N., . . . Pneumococcal Global Burden of Disease Study, T. (2009). Burden of disease caused by *Streptococcus pneumoniae* in children younger than 5 years: global estimates. *Lancet*, 374(9693), 893-902. doi:10.1016/S0140-6736(09)61204-6
- Oliva, M. A., Cordell, S. C., & Lowe, J. (2004). Structural insights into FtsZ protofilament formation. *Nat Struct Mol Biol*, 11(12), 1243-1250. doi:10.1038/nsmb855
- Olshausen, P. V., Defeu Soufo, H. J., Wicker, K., Heintzmann, R., Graumann, P. L., & Rohrbach, A. (2013). Superresolution imaging of dynamic MreB filaments in *B. subtilis*--a multiple-motor-driven transport? *Biophys J*, 105(5), 1171-1181. doi:10.1016/j.bpj.2013.07.038
- Orelle, C., Ayvaz, T., Everly, R. M., Klug, C. S., & Davidson, A. L. (2008). Both maltose-binding protein and ATP are required for nucleotide-binding domain closure in the intact maltose ABC transporter. *Proceedings of the National Academy of Sciences*, 105(35), 12837-12842. doi:10.1073/pnas.0803799105
- Osaki, M., Arcondeguy, T., Bastide, A., Touriol, C., Prats, H., & Trombe, M. C. (2009). The StkP/PhpP signaling couple in *Streptococcus pneumoniae*: cellular organization and physiological characterization. *Journal of bacteriology*, 191(15), 4943-4950. doi:10.1128/jb.00196-09
- Pacheco-Gomez, R., Cheng, X., Hicks, M. R., Smith, C. J., Roper, D. I., Addinall, S., . . . Dafforn, T. R. (2013). Tetramerization of ZapA is required for FtsZ bundling. *Biochem J*, 449(3), 795-802. doi:10.1042/BJ20120140
- Pagliari, E., Dideberg, O., Vernet, T., & Di Guilmi, A. M. (2005). The PECACE domain: a new family of enzymes with potential peptidoglycan cleavage activity in Gram-positive bacteria. *BMC Genomics*, 6, 19. doi:10.1186/1471-2164-6-19
- Paradis-Bleau, C., Markovski, M., Uehara, T., Lupoli, T. J., Walker, S., Kahne, D. E., & Bernhardt, T. G. (2010). Lipoprotein cofactors located in the outer

- membrane activate bacterial cell wall polymerases. *Cell*, 143(7), 1110-1120. doi:10.1016/j.cell.2010.11.037
- Patrick, J. E., & Kearns, D. B. (2008). MinJ (YvjD) is a topological determinant of cell division in *Bacillus subtilis*. *Mol Microbiol*, 70(5), 1166-1179. doi:10.1111/j.1365-2958.2008.06469.x
- Pazos, M., Natale, P., & Vicente, M. (2013). A specific role for the ZipA protein in cell division: stabilization of the FtsZ protein. *J Biol Chem*, 288(5), 3219-3226. doi:10.1074/jbc.M112.434944
- Pedrido, M. E., de Ona, P., Ramirez, W., Lenini, C., Goni, A., & Grau, R. (2013). Spo0A links de novo fatty acid synthesis to sporulation and biofilm development in *Bacillus subtilis*. *Mol Microbiol*, 87(2), 348-367. doi:10.1111/mmi.12102
- Pelczar, P. L., Igarashi, T., Setlow, B., & Setlow, P. (2007). Role of GerD in Germination of *Bacillus subtilis* Spores. *Journal of bacteriology*, 189(3), 1090-1098. doi:10.1128/jb.01606-06
- Perez, A. J., Cesbron, Y., Shaw, S. L., Bazan Villicana, J., Tsui, H. T., Boersma, M. J., . . . Winkler, M. E. (2019). Movement dynamics of divisome proteins and PBP2x:FtsW in cells of *Streptococcus pneumoniae*. *Proc Natl Acad Sci USA*, 116(8), 3211-3220. doi:10.1073/pnas.1816018116
- Peters, N. T., Dinh, T., & Bernhardt, T. G. (2011). A fail-safe mechanism in the septal ring assembly pathway generated by the sequential recruitment of cell separation amidases and their activators. *Journal of bacteriology*, 193(18), 4973-4983. doi:10.1128/jb.00316-11
- Philippe, J., Vernet, T., & Zapun, A. (2014). The elongation of ovococci. *Microb Drug Resist*, 20(3), 215-221. doi:10.1089/mdr.2014.0032
- Pichoff, S., Du, S., & Lutkenhaus, J. (2015). The bypass of ZipA by overexpression of FtsN requires a previously unknown conserved FtsN motif essential for FtsA-FtsN interaction supporting a model in which FtsA monomers recruit late cell division proteins to the Z ring. *Mol Microbiol*, 95(6), 971-987. doi:10.1111/mmi.12907
- Pichoff, S., Du, S., & Lutkenhaus, J. (2018). Disruption of divisome assembly rescued by FtsN-FtsA interaction in *Escherichia coli*. *Proc Natl Acad Sci USA*, 115(29), E6855-E6862. doi:10.1073/pnas.1806450115
- Pichoff, S., Du, S., & Lutkenhaus, J. (2019). Roles of FtsEX in cell division. *Res Microbiol*. doi:10.1016/j.resmic.2019.07.003
- Pichoff, S., & Lutkenhaus, J. (2002). Unique and overlapping roles for ZipA and FtsA in septal ring assembly in *Escherichia coli*. *EMBO J*, 21(4), 685-693. doi:10.1093/emboj/21.4.685
- Pichoff, S., & Lutkenhaus, J. (2005). Tethering the Z ring to the membrane through a conserved membrane targeting sequence in FtsA. *Molecular Microbiology*, 55(6), 1722-1734. Retrieved from <Go to ISI>://WOS:000227381000009
- Pichoff, S., Shen, B., Sullivan, B., & Lutkenhaus, J. (2012). FtsA mutants impaired for self-interaction bypass ZipA suggesting a model in which FtsA's self-interaction competes with its ability to recruit downstream division proteins. *Mol Microbiol*, 83(1), 151-167. doi:10.1111/j.1365-2958.2011.07923.x
- Piette, A., Fraipont, C., Den Blaauwen, T., Aarsman, M. E., Pastoret, S., & Nguyen-Disteche, M. (2004). Structural determinants required to target penicillin-

- binding protein 3 to the septum of *Escherichia coli*. *Journal of bacteriology*, *186*(18), 6110-6117. doi:10.1128/JB.186.18.6110-6117.2004
- Pinho, M. G., de Lencastre, H., & Tomasz, A. (2001). An acquired and a native penicillin-binding protein cooperate in building the cell wall of drug-resistant staphylococci. *Proc Natl Acad Sci U S A*, *98*(19), 10886-10891. doi:10.1073/pnas.191260798
- Pinho, M. G., Kjos, M., & Veening, J. W. (2013). How to get (a)round: mechanisms controlling growth and division of coccoid bacteria. *Nat Rev Microbiol*, *11*(9), 601-614. doi:10.1038/nrmicro3088
- Porath, J., Carlsson, J., Olsson, I., & Belfrage, G. (1975). Metal chelate affinity chromatography, a new approach to protein fractionation. *Nature*, *258*(5536), 598-599. doi:10.1038/258598a0
- Porath, J., & Olin, B. (1983). Immobilized metal ion affinity adsorption and immobilized metal ion affinity chromatography of biomaterials. Serum protein affinities for gel-immobilized iron and nickel ions. *Biochemistry*, *22*(7), 1621-1630. doi:10.1021/bi00276a015
- Powers, J. H. (2004). Antimicrobial drug development--the past, the present, and the future. *Clin Microbiol Infect*, *10 Suppl 4*, 23-31. doi:10.1111/j.1465-0691.2004.1007.x
- Pucci, M. J., Thanassi, J. A., Discotto, L. F., Kessler, R. E., & Dougherty, T. J. (1997). Identification and characterization of cell wall-cell division gene clusters in pathogenic gram-positive cocci. *Journal of bacteriology*, *179*(17), 5632-5635. doi:10.1128/jb.179.17.5632-5635.1997
- Ramamurthi, K. S., & Losick, R. (2009). Negative membrane curvature as a cue for subcellular localization of a bacterial protein. *Proc Natl Acad Sci U S A*, *106*(32), 13541-13545. doi:10.1073/pnas.0906851106
- Randich, A. M., & Brun, Y. V. (2015). Molecular mechanisms for the evolution of bacterial morphologies and growth modes. *Front Microbiol*, *6*, 580. doi:10.3389/fmicb.2015.00580
- Raskin, D. M., & de Boer, P. A. (1997). The MinE ring: an FtsZ-independent cell structure required for selection of the correct division site in *E. coli*. *Cell*, *91*(5), 685-694. doi:10.1016/s0092-8674(00)80455-9
- Raskin, D. M., & de Boer, P. A. (1999). Rapid pole-to-pole oscillation of a protein required for directing division to the middle of *Escherichia coli*. *Proc Natl Acad Sci U S A*, *96*(9), 4971-4976. doi:10.1073/pnas.96.9.4971
- Reddy, M. (2007). Role of FtsEX in cell division of *Escherichia coli*: viability of ftsEX mutants is dependent on functional SufI or high osmotic strength. *Journal of bacteriology*, *189*(1), 98-108. doi:10.1128/JB.01347-06
- Reeve, J. N., Mendelson, N. H., Coyne, S. I., Hallock, L. L., & Cole, R. M. (1973). Minicells of *Bacillus subtilis*. *Journal of bacteriology*, *114*(2), 860-873. Retrieved from <https://www.ncbi.nlm.nih.gov/pubmed/4196259>
- Reimold, C., Defeu Soufo, H. J., Dempwolff, F., & Graumann, P. L. (2013). Motion of variable-length MreB filaments at the bacterial cell membrane influences cell morphology. *Mol Biol Cell*, *24*(15), 2340-2349. doi:10.1091/mbc.E12-10-0728
- Reshes, G., Vanounou, S., Fishov, I., & Feingold, M. (2008). Cell shape dynamics in *Escherichia coli*. *Biophys J*, *94*(1), 251-264. doi:10.1529/biophysj.107.104398

- Ricard, M., & Hirota, Y. (1973). Process of cellular division in *Escherichia coli*: physiological study on thermosensitive mutants defective in cell division. *Journal of bacteriology*, *116*(1), 314-322.
- Robson, S. A., Michie, K. A., Mackay, J. P., Harry, E., & King, G. F. (2002). The *Bacillus subtilis* cell division proteins FtsL and DivIC are intrinsically unstable and do not interact with one another in the absence of other septosomal components. *Mol Microbiol*, *44*(3), 663-674. doi:10.1046/j.1365-2958.2002.02920.x
- Rosano, G. L., & Ceccarelli, E. A. (2014). Recombinant protein expression in *Escherichia coli*: advances and challenges. *Front Microbiol*, *5*, 172. doi:10.3389/fmicb.2014.00172
- Rowlett, V. W., & Margolin, W. (2015). The Min system and other nucleoid-independent regulators of Z ring positioning. *Front Microbiol*, *6*, 478. doi:10.3389/fmicb.2015.00478
- Rued, B. E., Alcorlo, M., Edmonds, K. A., Martinez-Caballero, S., Straume, D., Fu, Y., . . . Giedroc, D. P. (2019). Structure of the Large Extracellular Loop of FtsX and Its Interaction with the Essential Peptidoglycan Hydrolase PcsB in *Streptococcus pneumoniae*. *MBio*, *10*(1). doi:10.1128/mBio.02622-18
- Rueff, A. S., Chastanet, A., Dominguez-Escobar, J., Yao, Z., Yates, J., Prejean, M. V., . . . Carballido-Lopez, R. (2014). An early cytoplasmic step of peptidoglycan synthesis is associated to MreB in *Bacillus subtilis*. *Mol Microbiol*, *91*(2), 348-362. doi:10.1111/mmi.12467
- Sackett, M. J., Kelly, A. J., & Brun, Y. V. (1998). Ordered expression of ftsQA and ftsZ during the *Caulobacter crescentus* cell cycle. *Mol Microbiol*, *28*(3), 421-434. doi:10.1046/j.1365-2958.1998.00753.x
- Salje, J., van den Ent, F., de Boer, P., & Lowe, J. (2011). Direct membrane binding by bacterial actin MreB. *Mol Cell*, *43*(3), 478-487. doi:10.1016/j.molcel.2011.07.008
- Sánchez, M., Valencia, A., Ferrándiz, M. J., Sander, C., & Vicente, M. (1994). Correlation between the structure and biochemical activities of FtsA, an essential cell division protein of the actin family. *The EMBO Journal*, *13*(20), 4919-4925. doi:10.1002/j.1460-2075.1994.tb06819.x
- Sass, P., & Brotz-Oesterhelt, H. (2013). Bacterial cell division as a target for new antibiotics. *Curr Opin Microbiol*, *16*(5), 522-530. doi:10.1016/j.mib.2013.07.006
- Sass, P., Josten, M., Famulla, K., Schiffer, G., Sahl, H. G., Hamoen, L., & Brotz-Oesterhelt, H. (2011). Antibiotic acyldepsipeptides activate ClpP peptidase to degrade the cell division protein FtsZ. *Proc Natl Acad Sci U S A*, *108*(42), 17474-17479. doi:10.1073/pnas.1110385108
- Schmidt, K. L., Peterson, N. D., Kustusch, R. J., Wissel, M. C., Graham, B., Phillips, G. J., & Weiss, D. S. (2004). A predicted ABC transporter, FtsEX, is needed for cell division in *Escherichia coli*. *Journal of bacteriology*, *186*(3), 785-793. Retrieved from <https://www.ncbi.nlm.nih.gov/pubmed/14729705>
- Schumacher, M. A., & Zeng, W. (2016). Structures of the nucleoid occlusion protein SlmA bound to DNA and the C-terminal domain of the cytoskeletal protein FtsZ. *Proc Natl Acad Sci U S A*, *113*(18), 4988-4993. doi:10.1073/pnas.1602327113

- Scott, J. R., & Barnett, T. C. (2006). Surface proteins of gram-positive bacteria and how they get there. *Annu Rev Microbiol*, 60, 397-423. doi:10.1146/annurev.micro.60.080805.142256
- Setlow, P., & Johnson, E. A. (2007). Spores and Their Significance. In *Food Microbiology: Fundamentals and Frontiers, Third Edition*: American Society of Microbiology.
- Shak, J. R., Vidal, J. E., & Klugman, K. P. (2013). Influence of bacterial interactions on pneumococcal colonization of the nasopharynx. *Trends Microbiol*, 21(3), 129-135. doi:10.1016/j.tim.2012.11.005
- Sham, L. T., Barendt, S. M., Kopecky, K. E., & Winkler, M. E. (2011). Essential PcsB putative peptidoglycan hydrolase interacts with the essential FtsXSpn cell division protein in *Streptococcus pneumoniae* D39. *Proc Natl Acad Sci U S A*, 108(45), E1061-1069. doi:10.1073/pnas.1108323108
- Sham, L. T., Butler, E. K., Lebar, M. D., Kahne, D., Bernhardt, T. G., & Ruiz, N. (2014). Bacterial cell wall. MurJ is the flippase of lipid-linked precursors for peptidoglycan biogenesis. *Science*, 345(6193), 220-222. doi:10.1126/science.1254522
- Sham, L. T., Jensen, K. R., Bruce, K. E., & Winkler, M. E. (2013). Involvement of FtsE ATPase and FtsX extracellular loops 1 and 2 in FtsEX-PcsB complex function in cell division of *Streptococcus pneumoniae* D39. *MBio*, 4(4). doi:10.1128/mBio.00431-13
- Sham, L. T., Tsui, H. C., Land, A. D., Barendt, S. M., & Winkler, M. E. (2012). Recent advances in pneumococcal peptidoglycan biosynthesis suggest new vaccine and antimicrobial targets. *Curr Opin Microbiol*, 15(2), 194-203. doi:10.1016/j.mib.2011.12.013
- Shih, Y. L., & Zheng, M. (2013). Spatial control of the cell division site by the Min system in *Escherichia coli*. *Environ Microbiol*, 15(12), 3229-3239. doi:10.1111/1462-2920.12119
- Shiomi, D., Sakai, M., & Niki, H. (2008). Determination of bacterial rod shape by a novel cytoskeletal membrane protein. *EMBO J*, 27(23), 3081-3091. doi:10.1038/emboj.2008.234
- Shiomi, D., Toyoda, A., Aizu, T., Ejima, F., Fujiyama, A., Shini, T., . . . Niki, H. (2013). Mutations in cell elongation genes mreB, mrdA and mrdB suppress the shape defect of RodZ-deficient cells. *Mol Microbiol*, 87(5), 1029-1044. doi:10.1111/mmi.12148
- Sievers, J., & Errington, J. (2000a). Analysis of the essential cell division gene ftsL of *Bacillus subtilis* by mutagenesis and heterologous complementation. *Journal of bacteriology*, 182(19), 5572-5579. doi:10.1128/jb.182.19.5572-5579.2000
- Sievers, J., & Errington, J. (2000b). The *Bacillus subtilis* cell division protein FtsL localizes to sites of septation and interacts with DivIC. *Mol Microbiol*, 36(4), 846-855. doi:10.1046/j.1365-2958.2000.01895.x
- Silhavy, T. J., Kahne, D., & Walker, S. (2010). The bacterial cell envelope. *Cold Spring Harb Perspect Biol*, 2(5), a000414. doi:10.1101/cshperspect.a000414
- Small, E., Marrington, R., Rodger, A., Scott, D. J., Sloan, K., Roper, D., . . . Addinall, S. G. (2007). FtsZ polymer-bundling by the *Escherichia coli* ZapA

- orthologue, YgfE, involves a conformational change in bound GTP. *J Mol Biol*, 369(1), 210-221. doi:10.1016/j.jmb.2007.03.025
- Song, J. H., Ko, K. S., Lee, J. Y., Baek, J. Y., Oh, W. S., Yoon, H. S., . . . Chun, J. (2005). Identification of essential genes in *Streptococcus pneumoniae* by allelic replacement mutagenesis. *Mol Cells*, 19(3), 365-374. Retrieved from <https://www.ncbi.nlm.nih.gov/pubmed/15995353>
- Spratt, B. G. (1994). Resistance to antibiotics mediated by target alterations. *Science*, 264(5157), 388-393. doi:10.1126/science.8153626
- Stouf, M., Meile, J. C., & Cornet, F. (2013). FtsK actively segregates sister chromosomes in *Escherichia coli*. *Proc Natl Acad Sci U S A*, 110(27), 11157-11162. doi:10.1073/pnas.1304080110
- Studier, F. W., & Moffatt, B. A. (1986). Use of bacteriophage T7 RNA polymerase to direct selective high-level expression of cloned genes. *J Mol Biol*, 189(1), 113-130. doi:10.1016/0022-2836(86)90385-2
- Surdova, K., Gamba, P., Claessen, D., Siersma, T., Jonker, M. J., Errington, J., & Hamoen, L. W. (2013). The conserved DNA-binding protein WhiA is involved in cell division in *Bacillus subtilis*. *Journal of bacteriology*, 195(24), 5450-5460. doi:10.1128/jb.00507-13
- Szeto, T. H., Rowland, S. L., Rothfield, L. I., & King, G. F. (2002). Membrane localization of MinD is mediated by a C-terminal motif that is conserved across eubacteria, archaea, and chloroplasts. *Proc Natl Acad Sci U S A*, 99(24), 15693-15698. doi:10.1073/pnas.232590599
- Szwedziak, P., Wang, Q., Freund, S. M., & Lowe, J. (2012). FtsA forms actin-like protofilaments. *EMBO J*, 31(10), 2249-2260. doi:10.1038/emboj.2012.76
- Taguchi, A., Welsh, M. A., Marmont, L. S., Lee, W., Sjodt, M., Kruse, A. C., . . . Walker, S. (2019). FtsW is a peptidoglycan polymerase that is functional only in complex with its cognate penicillin-binding protein. *Nat Microbiol*, 4(4), 587-594. doi:10.1038/s41564-018-0345-x
- Tamames, J., Gonzalez-Moreno, M., Mingorance, J., Valencia, A., & Vicente, M. (2001). Bringing gene order into bacterial shape. *Trends Genet*, 17(3), 124-126. doi:10.1016/s0168-9525(00)02212-5
- Tan, I. S., & Ramamurthi, K. S. (2014). Spore formation in *Bacillus subtilis*. *Environ Microbiol Rep*, 6(3), 212-225. doi:10.1111/1758-2229.12130
- Taschner, P. E., Huls, P. G., Pas, E., & Woldringh, C. L. (1988). Division behavior and shape changes in isogenic ftsZ, ftsQ, ftsA, pbpB, and ftsE cell division mutants of *Escherichia coli* during temperature shift experiments. *Journal of bacteriology*, 170(4), 1533-1540. doi:10.1128/jb.170.4.1533-1540.1988
- Tavares, J. R., de Souza, R. F., Meira, G. L., & Gueiros-Filho, F. J. (2008). Cytological characterization of YpsB, a novel component of the *Bacillus subtilis* divisome. *Journal of bacteriology*, 190(21), 7096-7107. doi:10.1128/JB.00064-08
- Teo, A. C. K., Lee, S. C., Pollock, N. L., Stroud, Z., Hall, S., Thakker, A., . . . Roper, D. I. (2019). Analysis of SMALP co-extracted phospholipids shows distinct membrane environments for three classes of bacterial membrane protein. *Sci Rep*, 9(1), 1813. doi:10.1038/s41598-018-37962-0
- Teo, A. C. K., Lee, S. C., Pollock, N. L., Stroud, Z., Hall, S., Thakker, A., . . . Roper, D. I. (2019). Analysis of SMALP co-extracted phospholipids shows

- distinct membrane environments for three classes of bacterial membrane protein. *Scientific Reports*, 9(1), 1813. doi:10.1038/s41598-018-37962-0
- Thanassi, J. A., Hartman-Neumann, S. L., Dougherty, T. J., Dougherty, B. A., & Pucci, M. J. (2002). Identification of 113 conserved essential genes using a high-throughput gene disruption system in *Streptococcus pneumoniae*. *Nucleic Acids Research*, 30(14), 3152-3162. doi:10.1093/nar/gkf418
- Thanbichler, M., & Shapiro, L. (2008). Getting organized--how bacterial cells move proteins and DNA. *Nat Rev Microbiol*, 6(1), 28-40. doi:10.1038/nrmicro1795
- Tocheva, E. I., Lopez-Garrido, J., Hughes, H. V., Fredlund, J., Kuru, E., Vannieuwenhze, M. S., . . . Jensen, G. J. (2013). Peptidoglycan transformations during *Bacillus subtilis* sporulation. *Mol Microbiol*, 88(4), 673-686. doi:10.1111/mmi.12201
- Tonthat, N. K., Arold, S. T., Pickering, B. F., Van Dyke, M. W., Liang, S., Lu, Y., . . . Schumacher, M. A. (2011). Molecular mechanism by which the nucleoid occlusion factor, SlmA, keeps cytokinesis in check. *EMBO J*, 30(1), 154-164. doi:10.1038/emboj.2010.288
- Trip, E. N., & Scheffers, D.-J. (2015). A 1 MDa protein complex containing critical components of the *Escherichia coli* divisome. *Scientific Reports*, 5, 18190. doi:10.1038/srep18190
<https://www.nature.com/articles/srep18190#supplementary-information>
- Tsang, M. J., & Bernhardt, T. G. (2015a). Guiding divisome assembly and controlling its activity. *Curr Opin Microbiol*, 24, 60-65. doi:10.1016/j.mib.2015.01.002
- Tsang, M. J., & Bernhardt, T. G. (2015b). A role for the FtsQLB complex in cytokinetic ring activation revealed by an ftsL allele that accelerates division. *Mol Microbiol*, 95(6), 925-944. doi:10.1111/mmi.12905
- Typas, A., Banzhaf, M., Gross, C. A., & Vollmer, W. (2011). From the regulation of peptidoglycan synthesis to bacterial growth and morphology. *Nat Rev Microbiol*, 10(2), 123-136. doi:10.1038/nrmicro2677
- Typas, A., & Sourjik, V. (2015). Bacterial protein networks: properties and functions. *Nat Rev Microbiol*, 13(9), 559-572. doi:10.1038/nrmicro3508
- Uehara, T., Parzych, K. R., Dinh, T., & Bernhardt, T. G. (2010). Daughter cell separation is controlled by cytokinetic ring-activated cell wall hydrolysis. *EMBO J*, 29(8), 1412-1422. doi:10.1038/emboj.2010.36
- Ukai, H., Matsuzawa, H., Ito, K., Yamada, M., & Nishimura, A. (1998). ftsE(Ts) affects translocation of K⁺-pump proteins into the cytoplasmic membrane of *Escherichia coli*. *Journal of bacteriology*, 180(14), 3663-3670. Retrieved from <https://www.ncbi.nlm.nih.gov/pubmed/9658012>
<https://www.ncbi.nlm.nih.gov/pmc/articles/PMC107337/>
- Ursinus, A., van den Ent, F., Brechtel, S., de Pedro, M., Höltje, J.-V., Löwe, J., & Vollmer, W. (2004). Murein (Peptidoglycan) Binding Property of the Essential Cell Division Protein FtsN from *Escherichia coli*. *Journal of bacteriology*, 186(20), 6728-6737. doi:10.1128/jb.186.20.6728-6737.2004
- van Baarle, S., & Bramkamp, M. (2010). The MinCDJ system in *Bacillus subtilis* prevents minicell formation by promoting divisome disassembly. *PLoS One*, 5(3), e9850. doi:10.1371/journal.pone.0009850

- van den Berg van Saparoea, H. B., Glas, M., Vernooij, I. G., Bitter, W., den Blaauwen, T., & Luirink, J. (2013). Fine-mapping the contact sites of the Escherichia coli cell division proteins FtsB and FtsL on the FtsQ protein. *J Biol Chem*, 288(34), 24340-24350. doi:10.1074/jbc.M113.485888
- van den Ent, F., Amos, L. A., & Lowe, J. (2001). Prokaryotic origin of the actin cytoskeleton. *Nature*, 413(6851), 39-44. doi:10.1038/35092500
- van den Ent, F., Izore, T., Bharat, T. A., Johnson, C. M., & Lowe, J. (2014). Bacterial actin MreB forms antiparallel double filaments. *Elife*, 3, e02634. doi:10.7554/eLife.02634
- van den Ent, F., Johnson, C. M., Persons, L., de Boer, P., & Lowe, J. (2010). Bacterial actin MreB assembles in complex with cell shape protein RodZ. *EMBO J*, 29(6), 1081-1090. doi:10.1038/emboj.2010.9
- van den Ent, F., Leaver, M., Bendezu, F., Errington, J., de Boer, P., & Lowe, J. (2006). Dimeric structure of the cell shape protein MreC and its functional implications. *Mol Microbiol*, 62(6), 1631-1642. doi:10.1111/j.1365-2958.2006.05485.x
- van den Ent, F., & Lowe, J. (2000). Crystal structure of the cell division protein FtsA from Thermotoga maritima. *EMBO J*, 19(20), 5300-5307. doi:10.1093/emboj/19.20.5300
- van der Ploeg, R., Verheul, J., Vischer, N. O., Alexeeva, S., Hoogendoorn, E., Postma, M., . . . den Blaauwen, T. (2013). Colocalization and interaction between elongasome and divisome during a preparative cell division phase in Escherichia coli. *Mol Microbiol*, 87(5), 1074-1087. doi:10.1111/mmi.12150
- Varley, A. W., & Stewart, G. C. (1992). The divIVB region of the Bacillus subtilis chromosome encodes homologs of Escherichia coli septum placement (minCD) and cell shape (mreBCD) determinants. *Journal of bacteriology*, 174(21), 6729-6742. doi:10.1128/jb.174.21.6729-6742.1992
- Vats, P., & Rothfield, L. (2007). Duplication and segregation of the actin (MreB) cytoskeleton during the prokaryotic cell cycle. *Proc Natl Acad Sci U S A*, 104(45), 17795-17800. doi:10.1073/pnas.0708739104
- Vats, P., Shih, Y. L., & Rothfield, L. (2009). Assembly of the MreB-associated cytoskeletal ring of Escherichia coli. *Mol Microbiol*, 72(1), 170-182. doi:10.1111/j.1365-2958.2009.06632.x
- Veesler, D., Blangy, S., Cambillau, C., & Sciara, G. (2008). There is a baby in the bath water: AcrB contamination is a major problem in membrane-protein crystallization. *Acta Crystallogr Sect F Struct Biol Cryst Commun*, 64(Pt 10), 880-885. doi:10.1107/s1744309108028248
- Vega, D. E., & Margolin, W. (2019). Direct Interaction between the Two Z Ring Membrane Anchors FtsA and ZipA. *Journal of bacteriology*, 201(4). doi:10.1128/JB.00579-18
- Vicente, M., & García-Ovalle, M. (2007). Making a Point: the Role of DivIVA in Streptococcal Polar Anatomy^v. *Journal of bacteriology*, 189(4), 1185-1188. doi:10.1128/jb.01710-06
- Vicente, M., Rico, A. I., Martinez-Arteaga, R., & Mingorance, J. (2006). Septum enlightenment: assembly of bacterial division proteins. *Journal of bacteriology*, 188(1), 19-27. doi:10.1128/JB.188.1.19-27.2006

- Vinella, D., Joseleau-Petit, D., Thevenet, D., Bouloc, P., & D'Ari, R. (1993). Penicillin-binding protein 2 inactivation in *Escherichia coli* results in cell division inhibition, which is relieved by FtsZ overexpression. *Journal of bacteriology*, *175*(20), 6704-6710. doi:10.1128/jb.175.20.6704-6710.1993
- Vollmer, W., Blanot, D., & de Pedro, M. A. (2008). Peptidoglycan structure and architecture. *FEMS Microbiol Rev*, *32*(2), 149-167. doi:10.1111/j.1574-6976.2007.00094.x
- Wachi, M., Doi, M., Tamaki, S., Park, W., Nakajima-Iijima, S., & Matsushashi, M. (1987). Mutant isolation and molecular cloning of mre genes, which determine cell shape, sensitivity to mecillinam, and amount of penicillin-binding proteins in *Escherichia coli*. *Journal of bacteriology*, *169*(11), 4935-4940. doi:10.1128/jb.169.11.4935-4940.1987
- Wagner, S., Klepsch, M. M., Schlegel, S., Appel, A., Draheim, R., Tarry, M., . . . de Gier, J.-W. (2008). Tuning *Escherichia coli* for membrane protein overexpression. *Proceedings of the National Academy of Sciences*, *105*(38), 14371-14376. doi:10.1073/pnas.0804090105
- Wagner-Herman, J. K., Bernard, R., Dunne, R., Bisson-Filho, A. W., Kumar, K., Nguyen, T., . . . Rudner, D. Z. (2012). RefZ facilitates the switch from medial to polar division during spore formation in *Bacillus subtilis*. *Journal of bacteriology*, *194*(17), 4608-4618. doi:10.1128/jb.00378-12
- Wagstaff, J. M., Tsim, M., Oliva, M. A., Garcia-Sanchez, A., Kureisaite-Ciziene, D., Andreu, J. M., & Lowe, J. (2017). A Polymerization-Associated Structural Switch in FtsZ That Enables Treadmilling of Model Filaments. *MBio*, *8*(3). doi:10.1128/mBio.00254-17
- Walker, J. E., Saraste, M., & Gay, N. J. (1982). *E. coli* F1-ATPase interacts with a membrane protein component of a proton channel. *Nature*, *298*(5877), 867-869. doi:10.1038/298867a0
- Walker, J. E., Saraste, M., Runswick, M. J., & Gay, N. J. (1982). Distantly related sequences in the alpha- and beta-subunits of ATP synthase, myosin, kinases and other ATP-requiring enzymes and a common nucleotide binding fold. *EMBO J*, *1*(8), 945-951. Retrieved from <https://www.ncbi.nlm.nih.gov/pubmed/6329717>
- Walsh, C. (2003). Where will new antibiotics come from? *Nature Reviews Microbiology*, *1*(1), 65-70. doi:10.1038/nrmicro727
- Wang, G., Yi, X., Li, Y. Q., & Setlow, P. (2011). Germination of individual *Bacillus subtilis* spores with alterations in the GerD and SpoVA proteins, which are important in spore germination. *Journal of bacteriology*, *193*(9), 2301-2311. doi:10.1128/JB.00122-11
- Wang, L., Khattar, M. K., Donachie, W. D., & Lutkenhaus, J. (1998). FtsI and FtsW are localized to the septum in *Escherichia coli*. *Journal of bacteriology*, *180*(11), 2810-2816. Retrieved from <https://www.ncbi.nlm.nih.gov/pubmed/9603865>
- Wang, X., & Lutkenhaus, J. (1993). The FtsZ protein of *Bacillus subtilis* is localized at the division site and has GTPase activity that is dependent upon FtsZ concentration. *Mol Microbiol*, *9*(3), 435-442. doi:10.1111/j.1365-2958.1993.tb01705.x
- Weiss, D. S. (2004). Bacterial cell division and the septal ring. *Mol Microbiol*, *54*(3), 588-597. doi:10.1111/j.1365-2958.2004.04283.x

- Weiss, D. S. (2015). Last but not least: new insights into how FtsN triggers constriction during *Escherichia coli* cell division. *Mol Microbiol*, *95*(6), 903-909. doi:10.1111/mmi.12925
- Weiss, D. S., Chen, J. C., Ghigo, J. M., Boyd, D., & Beckwith, J. (1999). Localization of FtsI (PBP3) to the septal ring requires its membrane anchor, the Z ring, FtsA, FtsQ, and FtsL. *Journal of bacteriology*, *181*(2), 508-520. Retrieved from <https://www.ncbi.nlm.nih.gov/pubmed/9882665>
- White, S. H. (2015). The messy process of guiding proteins into membranes. *Elife*, *4*, e12100. doi:10.7554/eLife.12100
- Wissel, M. C., & Weiss, D. S. (2004). Genetic analysis of the cell division protein FtsI (PBP3): amino acid substitutions that impair septal localization of FtsI and recruitment of FtsN. *Journal of bacteriology*, *186*(2), 490-502. doi:10.1128/jb.186.2.490-502.2004
- Woldringh, C. L., Mulder, E., Valkenburg, J. A., Wientjes, F. B., Zaritsky, A., & Nanninga, N. (1990). Role of the nucleoid in the toporegulation of division. *Res Microbiol*, *141*(1), 39-49. doi:10.1016/0923-2508(90)90096-9
- Woldringh, C. L., & Nanninga, N. (2006). Structural and physical aspects of bacterial chromosome segregation. *J Struct Biol*, *156*(2), 273-283. doi:10.1016/j.jsb.2006.04.013
- Wu, L. J., & Errington, J. (2004). Coordination of cell division and chromosome segregation by a nucleoid occlusion protein in *Bacillus subtilis*. *Cell*, *117*(7), 915-925. doi:10.1016/j.cell.2004.06.002
- Wu, L. J., & Errington, J. (2011). Nucleoid occlusion and bacterial cell division. *Nat Rev Microbiol*, *10*(1), 8-12. doi:10.1038/nrmicro2671
- Wu, L. J., Feucht, A., & Errington, J. (1998). Prespore-specific gene expression in *Bacillus subtilis* is driven by sequestration of SpoIIE phosphatase to the prespore side of the asymmetric septum. *Genes Dev*, *12*(9), 1371-1380. doi:10.1101/gad.12.9.1371
- Wu, L. J., Ishikawa, S., Kawai, Y., Oshima, T., Ogasawara, N., & Errington, J. (2009). Noc protein binds to specific DNA sequences to coordinate cell division with chromosome segregation. *EMBO J*, *28*(13), 1940-1952. doi:10.1038/emboj.2009.144
- Wu, S. W., de Lencastre, H., & Tomasz, A. (2001). Recruitment of the *mecA* gene homologue of *Staphylococcus sciuri* into a resistance determinant and expression of the resistant phenotype in *Staphylococcus aureus*. *Journal of bacteriology*, *183*(8), 2417-2424. doi:10.1128/jb.183.8.2417-2424.2001
- Yang, D. C., Peters, N. T., Parzych, K. R., Uehara, T., Markovski, M., & Bernhardt, T. G. (2011). An ATP-binding cassette transporter-like complex governs cell-wall hydrolysis at the bacterial cytokinetic ring. *Proc Natl Acad Sci U S A*, *108*(45), E1052-1060. doi:10.1073/pnas.1107780108
- Yang, X., Lyu, Z., Miguel, A., McQuillen, R., Huang, K. C., & Xiao, J. (2017). GTPase activity-coupled treadmilling of the bacterial tubulin FtsZ organizes septal cell wall synthesis. *Science*, *355*(6326), 744-747. doi:10.1126/science.aak9995
- Yanouri, A., Daniel, R. A., Errington, J., & Buchanan, C. E. (1993). Cloning and sequencing of the cell division gene *pbpB*, which encodes penicillin-binding protein 2B in *Bacillus subtilis*. *Journal of bacteriology*, *175*(23), 7604-7616. doi:10.1128/jb.175.23.7604-7616.1993

- Yin, J., Sun, Y., Mao, Y., Jin, M., & Gao, H. (2015). PBP1a/LpoA but not PBP1b/LpoB are involved in regulation of the major beta-lactamase gene blaA in *Shewanella oneidensis*. *Antimicrob Agents Chemother*, *59*(6), 3357-3364. doi:10.1128/AAC.04669-14
- Yoshii, Y., Niki, H., & Shiomi, D. (2019). Division-site localization of RodZ is required for efficient Z ring formation in *Escherichia coli*. *Mol Microbiol*, *111*(5), 1229-1244. doi:10.1111/mmi.14217
- Zapun, A., Philippe, J., Abrahams, K. A., Signor, L., Roper, D. I., Breukink, E., & Vernet, T. (2013). In vitro reconstitution of peptidoglycan assembly from the Gram-positive pathogen *Streptococcus pneumoniae*. *ACS Chem Biol*, *8*(12), 2688-2696. doi:10.1021/cb400575t
- Zapun, A., Vernet, T., & Pinho, M. G. (2008). The different shapes of cocci. *FEMS Microbiol Rev*, *32*(2), 345-360. doi:10.1111/j.1574-6976.2007.00098.x
- Zucchini, L., Mercy, C., Garcia, P. S., Cluzel, C., Gueguen-Chaignon, V., Galisson, F., . . . Grangeasse, C. (2018). PASTA repeats of the protein kinase StkP interconnect cell constriction and separation of *Streptococcus pneumoniae*. *Nat Microbiol*, *3*(2), 197-209. doi:10.1038/s41564-017-0069-3

Citation for reports

- O'Neil, J (2016) *Tackling drug-resistant infections globally: final report and recommendation: A review on antimicrobial resistance*. AMR Review.
- Sheehan, E (2016) *The molecular cloning and overexpression of divisome proteins, FtsE and FtsX*. An MIBTP reserch project report. University of Warwick.

Citation for thesis and dissertation

- de Sousa Borges, A. (2017). *Come out and play: Exploring bacterial cell wall synthesis and cell division*. [Groningen]: University of Groningen.
- Naskar, S (2016) *Towards the bacterial divisome: Molecular cloning and purification of the FtsEX protein complex, essential for bacterial cell division*. An MSc mini-project dissertation. University of Warwick.

APPENDIX

Appendix A1

Initial biophysical and structural analysis of FtsEX, FtsEX-FtsA and FtsEX-PcsB complexes

A detailed structural description for FtsEX and its interaction with cognate cell division proteins is still lacking in the literature with only the extracellular region of mycobacterium tuberculosis FtsX (Mavrici et al., 2014) described so far. Since our *in-vitro* purification strategy provided very highly purified samples of FtsEX alone and in complex with other proteins, we choose to investigate preliminary biophysical and structural studies. The AUC analysis with SMALP-SpFtsEX and SMALP-SpFtsEX-PcsB complexes clearly showed a difference in their sedimentation co-efficient (**Figure A 1**). In the same experiment SMALP-FtsEX showed single peak around 11.5 whereas the SMALP-FtsEX-PcsB complex showed two prominent peaks at around 11 and 14.5 (**Figure A 1**). This possibly indicates the peak around 11 or 11.5 is for SMALP-SpFtsEX whereas the peak around 14.5 possibly represent the SMALP-SpFtsEX-PcsB complex (**Figure A 1**). Negative stain electron microscopy studies with SMALP-FtsEX (**Figure A 2.a**) and SMALP-FtsEX-PcsB (**Figure A 3.b**) showed a good distribution of the particles that ranges between 12 nm and 16 nm for SMALP-FtsEX and between 16 and 22 for SMALP-FtsEX-PcsB. This allowed particle picking and sorting as demonstrated in **Figure A 2.b** for SMALP-SpFtsEX complex. The measurements on negative stained individual particles supports the dynamic light scattering analysis (**Figure A 2.c** and **Figure A 5.c**) that measured particle sizes about 13 nm (+/- 3 nm) and 16 nm (+/- 4) for SMALP-FtsEX and SMALP-FtsEX-PcsB complexes respectively. Average Sizes of both these complexes are larger compared to SMALP disc alone that sizes approximately 9 to 10 nm. This is indicative of single particles representative of the FtsEX dimer or its complex with PcsB encapsulated in a SMALP nanodisc. Examination of individual particles at higher magnification (**Figure A 2.d**) shows the SMALP-SpFtsEX particle in a number of orientations on the EM grid and allowed the generation of a low-

resolution model for FtsEX as demonstrated in **Figure A 2.e**. In addition, we also detected monodispersed SpFtsEX-SpFtsA complex and SPFtsEX-PcsB complex in SMALP disk in negative stain EM micrographs (**Figure A 3.a** and **Figure A 3.b**, respectively). Whilst these results are preliminary and further higher resolution studies are required, all these analyses show promise for future detailed structural studies on the FtsEX core complex and the proteins that bind to it. An initial Cryo-EM screening, micrographs that shows very good distribution of monodispersed particles with all three complexes are shown in **Figure A 4**. Among these the SMALP-SpFtsEX-PcsB complex showed good monodispersed particles distribution on Graphene oxide coated grids for Cryo-EM (**Figure A 4.c**; and **Figure A 5.a**), which when further analyzed by extracting single particles (**Figure A 5.b**) for initial 2D and 3D classification, and an initial model was generated along with its projections using EMAN2 program as shown in **Figure A 5. d, e, f**. This initial analysis is indicative of existence of possible SpFtsEX-PcsB complex in our purified samples, however this work needs further screening for best cryo-EM condition and grid preparation for high resolution structural studies with these complexes.

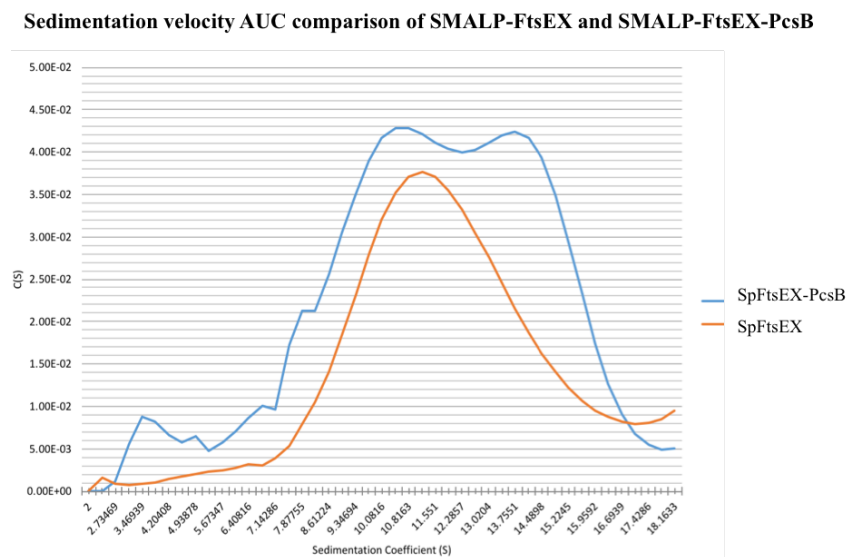


Figure A 1. AUC plots for SpFtsEX and SpFtsEX-PcsB complexes in SMALP

(The AUC experiments were set and run by Dr. Pooja Sridhar and AUC data were analysed by Dr. Sara Lee in my presence. I was under their supervision for AUC related experiments).

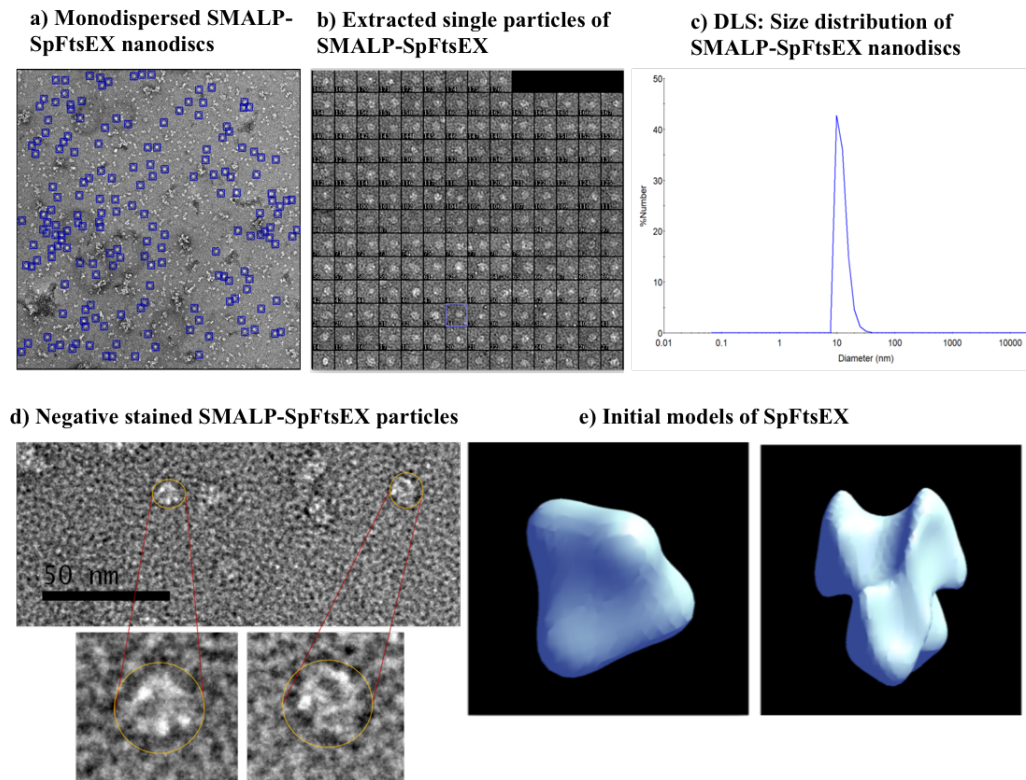


Figure A 2. Negative Stain EM and DLS with SMALP-SpFtsEX.

Negative staining of purified SMALP-SpFtsEX sample (at 0.2 mg/ml) using Uranyl Acetate (UA, 2%) showed particles are monodispersed **(a)** and when single particles are screened extracted using appropriate box size in EMAN2 program, particles are found disc-like structure and evenly distributed in their size **(b)**. The DLS of the same sample also measured the size about 15.46 nm \pm 3 nm **(c)**. An amplified image with scale bar 50 nm shows the size of those discs is between 12 nm and 20 nm **(d)** Yellow circles are directing few of those disc-like structures. 2D-class averaging of those single particles (performed with \sim 2500 particles) lead to generate initial models **(e, left)** and its further refinement **(e, right)**, which indicate a possible heterodimeric arrangement between SpFtsE and SpFtsX.

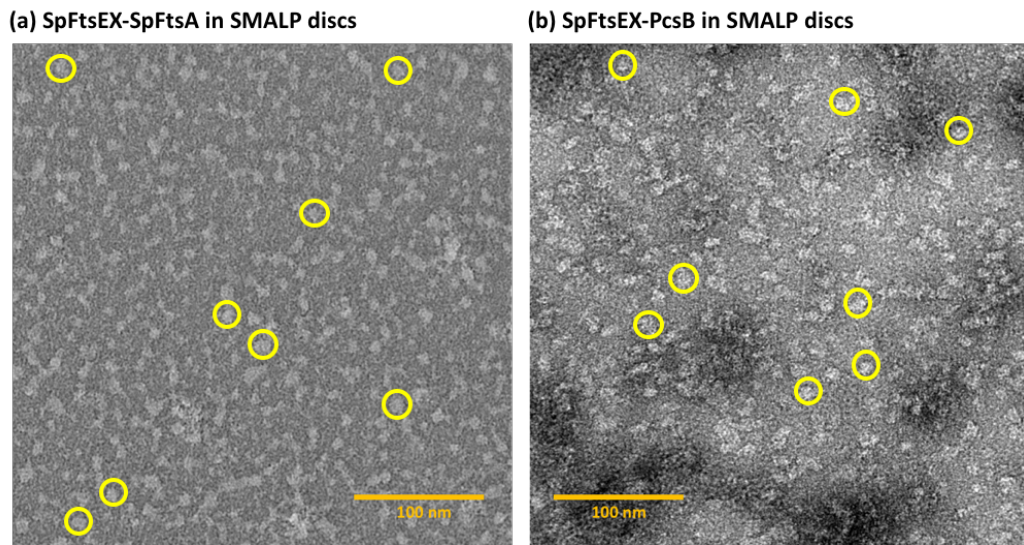


Figure A 3. Negative Stain EM with *SpFtsEX-SpFtsA* and *SpFtsEX-PcsB*
 Negative stain (UA 2%) electron micrograph of *SpFtsEX-SpFtsA* complex (a), and *SpFtsEX-PcsB* complex (b) in SMALP discs, sizes between 12 nm – 20 nm, shows monodispersed. Yellow circles are directing few of those disc like structure. Scale bar 100 nm.

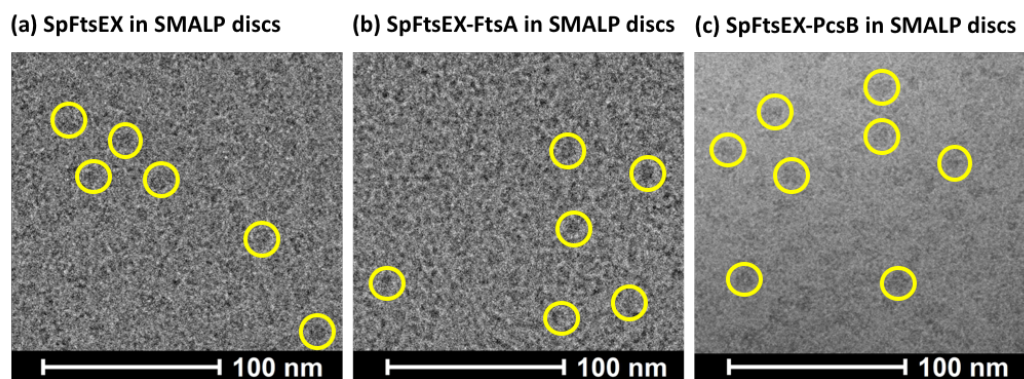


Figure A 4. Cryo-EM with *SpFtsEX*, *SpFtsEX-SpFtsA* and *SpFtsEX-PcsB* In SMALP.
 Cryo-electron micrograph of *SpFtsEX* complex (a), *SpFtsEX-SpFtsA* complex (b), and *SpFtsEX-PcsB* complex (b) in SMALP discs, shows good contrast of monodispersed particles. Yellow circles are directing few of those disc like structure. Scale bar 100 nm.

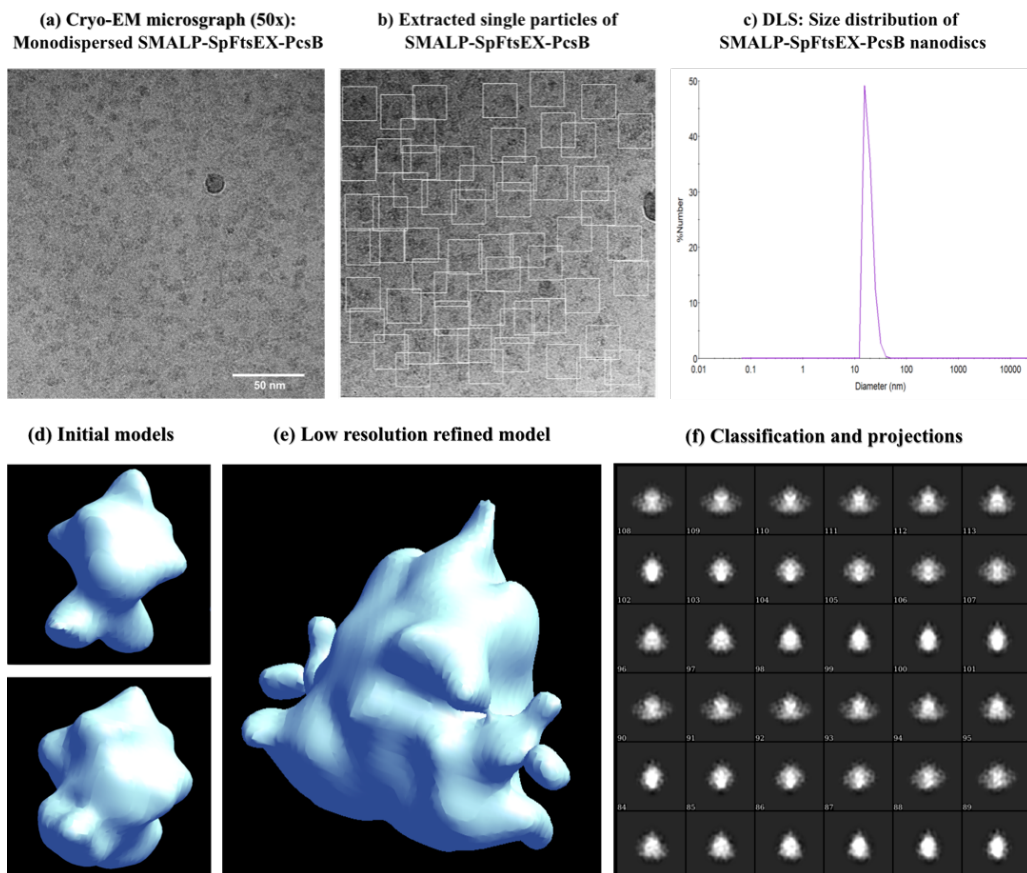


Figure A 5. DLS and preliminary Cryo-EM screening with SMALP-SpFtsEX-PcsB complex.

Initial screening and Cryo-electron micrograph of SpFtsEX-PcsB complex **(a)**; Single particles of the same complex picked and extracted using particle picker program (EMAN2) **(b)**; The initial images showed good particle distributions on the Cryo-EM grids that coated with graphene oxide **(a-b)**. Initial measurement on the Cryo-EM images as well as DLS experiment with same complex indicated the size of the SMALP-SpFtsEX-PcsB disc is about 16-18 nm **(c)**, which is slightly larger than the size of SMALP-FtsEX complex (12-14 nm). An initial analysis with extracted small number of particles (about 1200) generated an initial model **(d, top)** and a further refinement is shown in **(d, bottom)**. A low resolution ($>18 \text{ \AA}$) initial 3D model also projected from selection of few good classes **(e)**; related classification showing the projections of the same model **(f)**. Scale bar 50 nm.

Appendix A2.

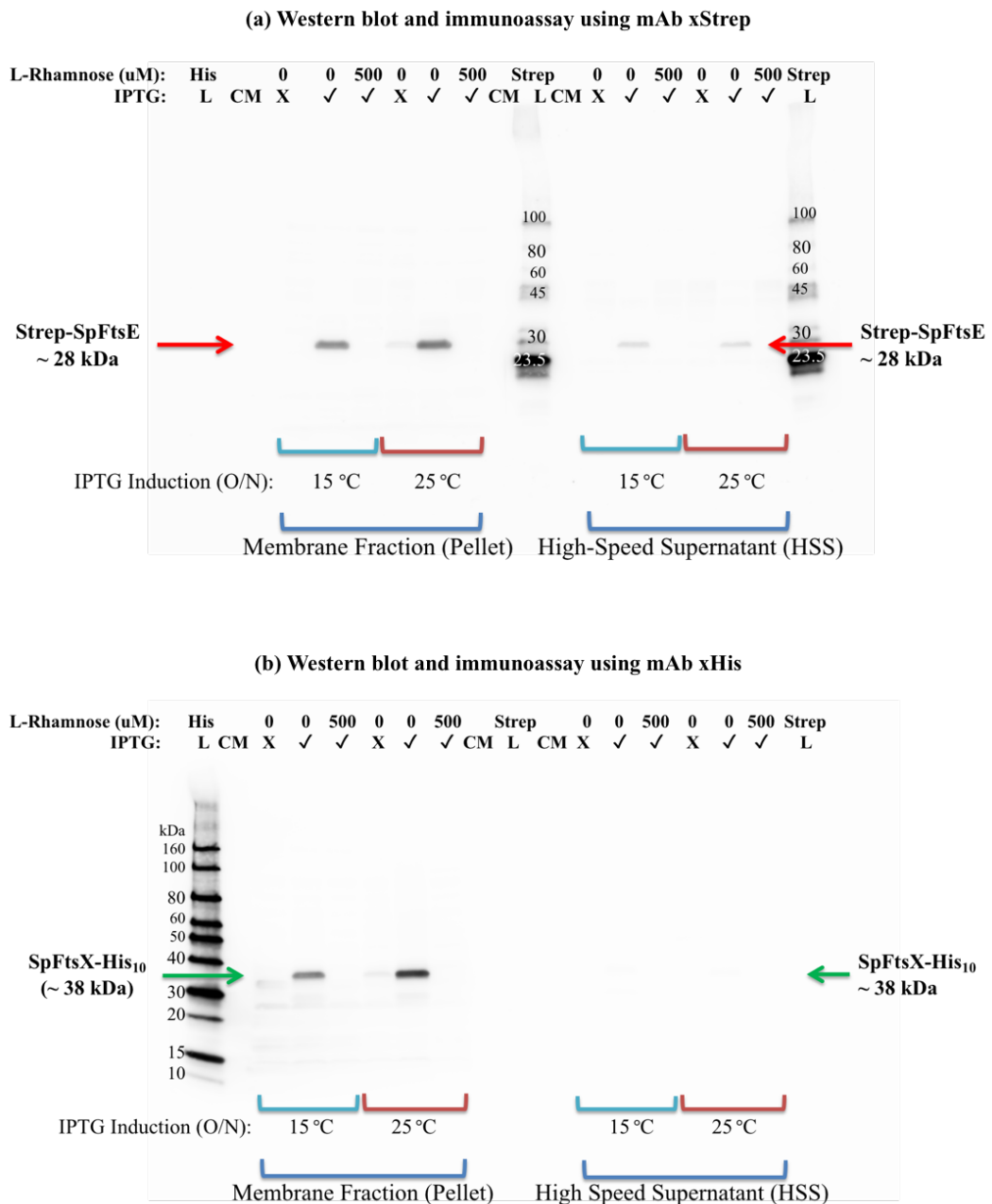
The following study was performed during one of my MSc mini-project and results are included in the dissertation submitted for the fulfilment of the MSc study. I have re-written the following section summarising the same small-scale study which was important to optimise the right condition for further large-scale expression and protein production as described in the main thesis.

Small-scale heterologous overexpression studies with *S. pneumoniae ftsEX* in *E. coli Lemo21(DE3)::cam^R* cells

In a small-scale study, *Lemo21(DE3)::cam^R* competent cells were transformed with *pET-52b(+)-strep-SpftsEX-his₁₀* construct. Cells were grown in LB media with or without varied concentration of L-rhamnose, and induced by IPTG at different temperatures and lengths as detailed in methods (2.4.1.). All these variables were selected initially based on a previous similar optimisation study with *E. coli ftsEX* (*EcftsEX*), which was performed on the same strain inducing for 4 hours and overnight at different temperatures (37 °C, 25 °C and 15 °C) using varied concentrations of L-rhamnose. In this experiment, low L-rhamnose concentrations in the LB media, and low temperatures (15 °C and 25 °C) evidently showed better expression of both EcFtsE and EcFtsX proteins at these lower temperatures (MSc thesis: Sheehan, 2016; Naskar, 2016). Likewise, in the same study, for *S. pneumoniae ftsEX*, cells were induced overnight, in presence and absence of L-rhamnose (500 µM) in the LB media, including one batch without induction as control, at 15 °C as well as 25 °C. All overnight induced cells were harvested the next morning and membranes were prepared from these cells following standard membrane preparation protocol (2.4.1.). The proteins from membrane fractions (MF) and high-speed supernatants (HSS) were measured in order to load same amount of total proteins and separate them on SDS-PAGE. Reduced and separated proteins were further immunoassayed on separate western blots for two proteins,

using HRP conjugated antibodies against the Strep and Histidine tags associated with SpFtsE and SpFtsX respectively. Clearly, Strep-SpFtsE and SpFtsX-His₁₀ were detected in the membrane fractions with band size approximately ~27 kDa and ~38 kDa respectively (**Figure A 6. a and b**). Both bands appeared very clear, compact and without any noticeable proteolytic degradation/truncation. The quality and quantity of both proteins are very satisfying in the MF (**Figure A 6**). This confirms their high abundance in bacterial cell membrane. However, a very low abundance of Strep-SpFtsE also evident in HSS. This suggest a fraction of SpFtsE population may also stay in cytoplasm, in a state that probably unbound to membrane. Whereas, expression of SpFtsX-His₁₀ was observed very specific to membrane fraction and not in HSS, suggesting this protein is very much stable as integral membrane protein as has been reported in several previous studies (Bajaj et al., 2016; Gill et al., 1986; Schmidt et al., 2004; Sham et al., 2011). In cases of variables, while induction at low temperatures overnight showed satisfying expression for both proteins in MFs, the sugar L-rhamnose (500) in the culture media (LB media) did not improve the protein yield or expression quality at all.

In the case of control cultures without IPTG induction, no visible protein bands for Strep-SpFtsE, and very faint bands for SpFtsX-His₁₀, were observed in the same western blot and immunoassay. This could be consequence of contamination during sample preparation or an indication of extremely low level of SpFtsX leaky expression. Overall, this small-scale study with varying conditions, hinted a low temperature induction without L-rhamnose is preferable to express and produce both Strep-SpFtsE and SpFtsX-His₁₀ recombinant proteins in high quality and quantity.



Appendix 3:

This section includes all additional information and figures to support main thesis.

Escherichia coli **ftsYEX**:

```
ATGGCGAAAGAAAAAACCTGGCTTTTTTTCCTGGCTGGGCTTTGGTCAAAAAGAGCAGACCCCGGAAA
AAGAGACAGAAGTTCAGAATGAACAACCGGTTGTAGAAGAAATCGTTTCAGGCGCAAGAGCCTGTGAAGGC
CTCTGAACAAGCCGTTGAAGAGCAGCCGCAAGCGCATACTGAAGCCGAGGCGGAAAACCTTTGTGTCGCGAC
GTTGTGGAAAGTCACTGAACAGGTTGCTGAAAAGTAAAAAGCGCAGCCTGAAGCGGAAGTCGTTGCACAGC
CGGAACCGGTCGTAGAAGAAACGCCGAGCCAGTGGCTATCGAACGTGAAGAGCTGCCGTTGCCGGAAGA
CGTCAACGCCGAAAGCGGTTTCGCCAGAAGAGTGGCAGGCTGAAGCGGAAACCGTAGAGATTGTGCGAAGCG
GCGGAAGAAGAAGCGGCTAAAGAAGAAATTACCAGCAAGAGCTGGAACCGGCGCTGGCTGCCGAAGCG
GCAGAAGAGCGGTTGATGTTGGTTCTCCGGCAGAAGAAGAGCAGCCGGTGAAGAATAATCGCTCAGGAGC
AGGAAAAACCGACCAAGAAGGTTTTTTCGCGCGCCTGAAACGCAGCCTGTAAAAAACCAAGAAAAATCT
CGGTTCCGGATTTATCAGCCTGTTCCGCGGTAAAAAATCGACGATGATCTGTTTGAGGAGCTGGAAGAGCA
GCTTTTATCGCCGATGTGGGTGTGGAACCACACGTAAAAATTATACCAATCTGACGGAAGGCGCATCCCG
CAAGCAGCTTCGTGACGCCGAGGCGCTCTATGGCCTGTGAAAGAAGAGATGGGCGAGATTCTGGCGAAA
GTCGATGAGCCGCTGAATGTTGAAGGCAAGCGCCGTTTGTGATCCTGATGTTGGGCGTCAACGGTGTGGG
TAAAACCCAGCAGATTGTAAGCTGGCGCGTCAGTTTGAAGCAGCGGTAATCGGTGATGCTGGCGGCGG
GTGATACTTTCCGTGCAGCTGCGGTTGAACAGCTTCAGGTCTGGGGTCAAGCGCAACAATATTCCGGTATTG
CCCAGCATACCGGGGCGGATTCCGCCTCTGTATCTTCGACGCCATTACAGCAGCTAAAGCGCGTAATATCG
ACGCTCTGATTGCCGATACAGCCGGACGCCTGCAGAACAATCGCACCTGATGGAAGAGTTGAAGAAAAATC
CTCCCGTGATGAAGAAACTCGACGTTGAAGCGCCGCATGAAGTTATGCTGACTATTGATGCCAGCACCGG
GCAGAACCGGTAAGCCAGGCCAAACTGTTCCATGAAGCCGTTGGCTTAACCGGCATCACGTAACGAAAC
TGGACGGCACGGGAAAGGCGGGGTAATTTCTCGGTGGCTGACAGTTTGGTATCCCTATCCGCTACATTG
GTGTCGGGAAACGTATTGAGGATTTGCGTCCGTTAAAGCGGACGACTTTATAGAGCACTTTTTCGCCGAG
AGGATTAACAATGATTTCGCTTTGAACATGTCAGCAAGGCTTATCTCGGTGGGAGACAGGCGCTGACGGCGG
TTACGTTCCATATGCAGCCGGGTGAGATGGCGTTTCTGACCGGTCATTCCGGCGCAGGGAAAAAGTACCCTCC
TGAAGCTGATCTGTGGGATTGAGCGGCCAGCGCCGGGAAAAATCTGGTTTAGCGGCCATGACATCACGCGT
CTGAAAAACCGTGAAGTTCCGTTTCTGCGCCGCCAGATTGGCATGATTTCCAGGATCACCATCTACTGATG
GACCGTACTGTCTACGATAACGTGGCGATCCCGCTGATTATCGCCGGTGCCAGCGGTGACGATATTCTGCGCC
GGGTGTGCGGCGGCGCTGGATAAAGTCCGGCTACTGGACAAAGCGAAGAACTCCCTATTACGCTTTCCGGG
GGTGAACAACAGCGTGTGGCATTGCCCGCGGTTGGTGAACAAGCCCGGTAAGTCTGCTGGCGGACGAAC
CGACTGGTAACTGGACGACGCGCTGTGCGAAGGCATTTACGCTCTGTTGAAGAGTTTAAACCGGTTGGG
GTAACCGTATTGATGGCAACGCACGACATCAACCTGATCTCGCGGCGTTCCCTATCGCATGCTCACCTGAGC
GTTGTCACTTGCATGGAGGCGTGGGCCATGAATAAGCGCGATGCAATCAATCATATTCCGCGAGTTTGGCGG
GCGTCTTGATCGCTTCCGTAAATCGGTCCGGCGCTCAGGCGACGGCGGTCGTAACGCACCAAAAACGCGCGA
AATCCTCGCCAAAACCGGTAATCGCAAAACCAACGTTTTCAACGAACAGGTGCGCTATGCCTTCCACGGC
GCATTGCAGGATCTGAAAAGCAAACCGTTCCGCCAGTTTTTAAACGGTGTGTTATCGCCATTCTCTGACG
CTGCCAGCGTCTGTTATATGGTGTACAAAAACGTTAACAGGCGGCGACGCAAGTATTATCCGTCACCGCAA
ATCAGCTGTTTATCTGCAAAAAACGTTGGACGATGACGCTGCTGCGGGCGTGGTGGCACAGTTGCAGGCCGA
GCAAGGCGTGGAGAAAGTGAATATCTTCTCGTGAAGACGCACTGGGTGAGTTCCGTAACCTGGTCTGGTT
TTGGTGGTGGCTGGATATGCTGGAAGAAAACCGCTTCCGGCAGTGGCGGTTGGTATCCCGAAACTCGAT
TTCCAGGGGACGGAATCACTGAATACGCTGCGTATCGTATCACGCAGATTAACGGCATTGACGAAGTGGCG
ATGGATGACAGCTGGTTTCCCGTCTGGCGGCGTTGACCGGGCTGGTGGGCGCGTTTCCGGCATGATCGG
CGTGTGATGGTGGCGCCGTTTCCCTCGTATCGGTAACAGTGTGCGTCTGAGTATCTTGTCTGCCGTGA
CTCCATTAACGTACAGAACTGATTTGGTGGCACAGATGGATTATCCTGCGCCCGTTCTGTATGGTGGCGC
ACTGTGGGATTTCTGGCGCATTGTTGTCATTAATTTGTGCAAAAATCTGGTGGTGGTGGTGGTGGTGGTGG
GTTGCGGAAGTGGCACAGGTTTTCGGAACGAAGTTGATATCAATGGCTTATCATTGATGAATGCCTGCTAT
TGCTGCTGGTATGCTCGATGATTGGCTGGGTGGCAGCGTGGCTTGGCACGGTACAACATTTACGCCACTTTA
CGCCTGAATAA
```

Adjacent *ftsY-ftsE* genes in the same *ftsYEX* operon:

```
AGGATTAACAATG
```

Overlap *ftsE-ftsX* genes in the same *ftsYEX* operon::

ORF 1: GTCACTTGCATGGAGGCGTGGGCCATGAATAA

ORF2: ATGAATAA

START Codon; STOP Codon; RBS

Figure A 7. Genetic organisation of *E. coli* *ftsYEX* operon.

***Streptococcus pneumoniae* ftsEX:**

ATGGGCAGCAGCCATCACCATCACCACAGCCAGGATATGTCAATTATTGAAATGAGAGATGTCGTTAAA
 AAATACGACAACGGAAACGACTGCTCTACGCGGTGTTTCGGTTAGCGTTCAACCGGGGAATTTGCTTACAT
 CGTAGGACCTTCAGGAGCAGGGAAGTCAACTTTTATTCGTTCTCTGTATCGTGAAGTAAAAATCGATAAAG
 GAAGTCTATCAGTTGCTGGTTTTAATCTGGTTAAGATCAAAAAGAAAGATGTCGCCGCTTCTACGTCGTAGTG
 TTGGGGTTGCTTCCAAGATTATAAATTGTTACCAAAGAAAACGTCTATGAAAATATTGCTTACGCTATGGA
 AGTAATCGGGGAAAAATCGCCGTAATATCAAAAGACGAGTGATGGAAGTTTTGGACTTGGTTGGATTGAAGC
 ATAAGGTTTCGTTCTTCCCAAATGAACTCTCAGGTGGGGAGCAACAGCGGATTGCGATTGCGCGTGAATTT
 GTAAATAATCCCAAAGTATTGATAGCTGATGAGCCAACAGGAAATCTGGATCCGGATAATTCATGGGAAAT
 ATGAATCTTTGGAACGGATTAACCTACAAGGAACAATATTTTGGTGGCGACTCATAATAGCCAGATTGTA
 AATACCTTGCGCCACC TCATTGCCATTGAAAATGGCCGTGTCGTTTCGTGACGAATCAAAGGAGAGTA
 TGGATACGATGATGTAGATTTTTTCGCCATTTATTGAAGCCTTAAAAAGTTTGAACGAAATGGTTGGAT
 GACAGTAGCTGCTGTCAGTTTCAGTCATGATTACTTTGACCTTGGTGGCAATATTGTCATCTGTTATTTTCAAT
 ACAGCGAAACTAGCTACAGATATTGAAAATAATGTCGGTGTAGTAGTTTATATCCGAAAAGGATGTTGGAAGAT
 AATAGTACAGCAATGAAAAAGAAGGTCAAACCTGTTACAATAATGACTACCACAAGGTATATGATTCTTTG
 AAGAATCATGCTACGGTTAAAAGTGTACCTTTTCAAGTAAAGAAGAACAATATGAAAAATTAACCGAGAT
 AATGGGAGATAACTGGAAAATCTTTGAAGGAGATGCCAATCTCTCTATGATGCCTATATTGTAGAGGCAAA
 CGTCCAAAATGATGAAAAACTATAGCCGAAGATGCTAAAAAATGAAGGTGCTCTGAGGTTCAAGATG
 GCGGTGCCAATACAGAAAAGACTCTTCAAGTTAGCTTCAATTTACCGTGTGGGGACTAGGGATTGCTGCTT
 TGTTAATTTTATCGCAGCTTCTTGATTCAAATACCATTCTGATTACCAATTTCCCGCAGTCGCGAAAT
 CAAATCATGCGCTTGGTCGGAGCTAAAAACAGTTATATCCGTGGACCGTCTTGTGTAAGGAGCCTTTATC
 GGTTTATTTGGGAGCTATCGCACCATCTGTTTGGTCTTATTGTTTATCAAATGTTTACCAATCTGTCAACA
 AATCGTTGGTAGGGCAAAATCTATCCATGATTAGTCCAGATTATTTAGTCCGTTGATGATTGCCTACTATT
 GTGATTGGGTTTTTCATTGGTTCATTGGGATCAGGAATATCCATGCGCCGATTCTTGAAGATTGAGCTCGCT
 CTGGTCCACGCGGTAGTTCGGTCTATCACCACCATCATCACCATCACCACCAC TAA

Overlap operon 1:

TCATTGCCATTGAAAATGGCCGTGTCGTTTCGTGACGAATCAAAGGAGAGTATGGATACGATGATTA

Or

Overlap operon 2:

ATGGCCGTGTCGTTTCGTGACGAATCAAAGGAGAGTATGGATACGATGATTA

START Codon; STOP Codon

Figure A 8. Genetic organisation of *S. pneumoniae* ftsEX operon.

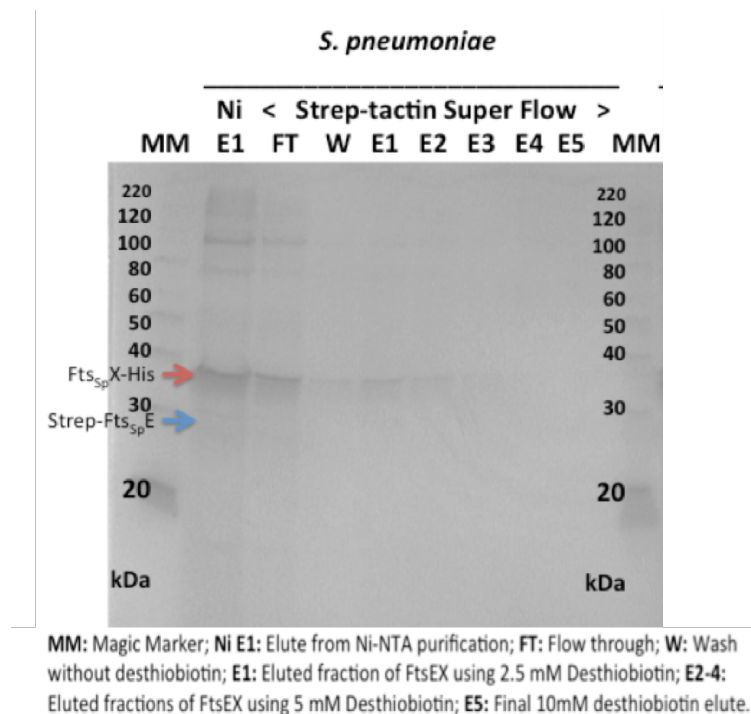


Figure A 9. Second purification of *Strep-SpFtsEX-His₁₀* using *Streptactin* resin.

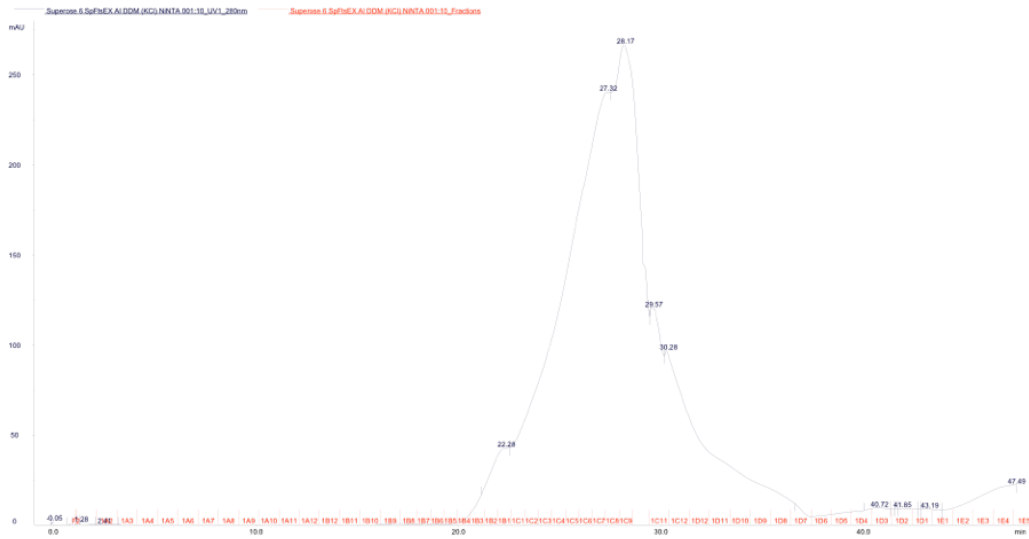


Figure A 10. SEC chromatogram of *Strep-SpFtsEX-His₁₀* complex that extracted and purified using DDM.

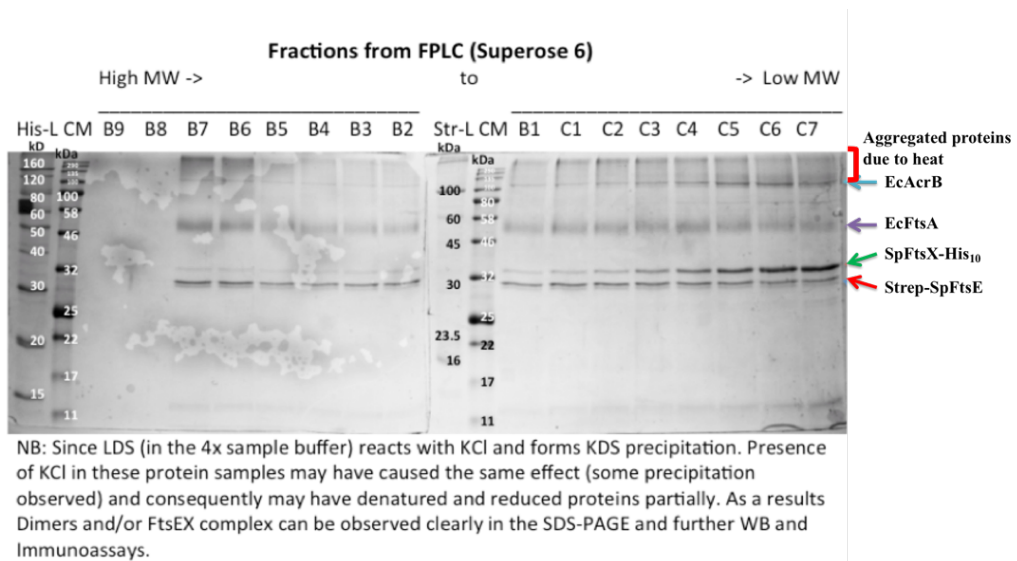


Figure A 11. SDS-PAGE analysis of purified (IMAC and SEC) *Strep-SpFtsE* and *SpFtsX-His₁₀* complex that heated at 95 °C.

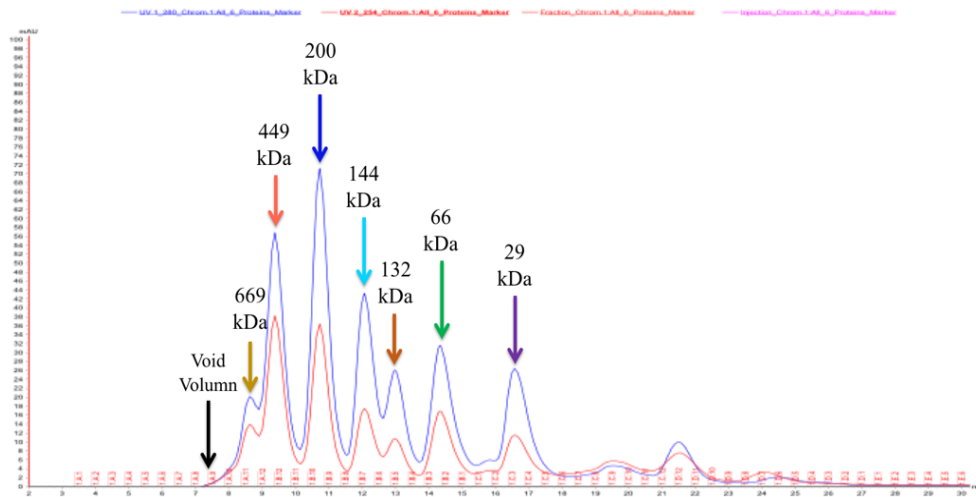


Figure A 12. Protein markers run on SEC column.

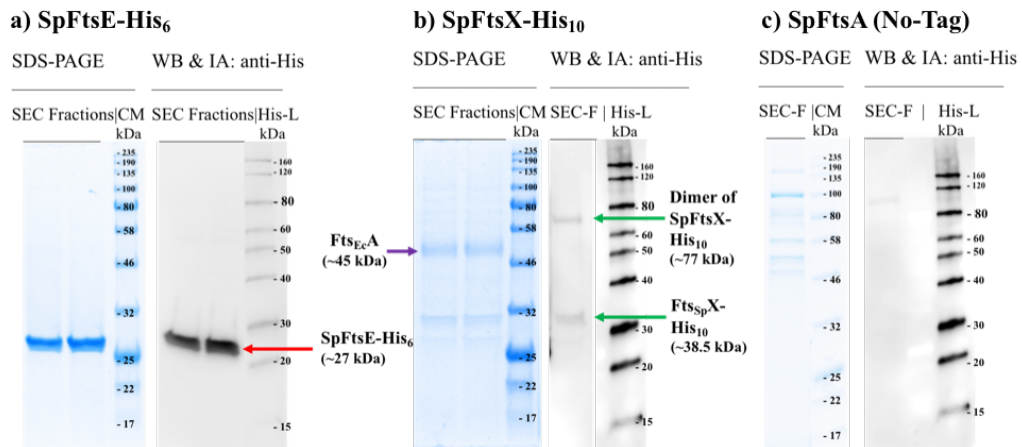


Figure A 13. Individual expressions and purifications of SpFtsE-His₆, SpFtsX-His₁₀ and untagged-SpFtsA.

SpFtsE-His, SpFtsX-His and untagged SpFtsA when purified individually following standard SMALP extraction, IMAC and SEC purification, we observed SpFtsE-His purified as single protein and migrated as single band (~27 kDa) upon SDS-PAGE and western blot (WB) and immunoassay (IA) against its his-tag (**a**); SpFtsX-His (~ 32 kDa) co-purified with another band around 46 kDa as observed in SDS-PAGE gel (**b**), however the same band is not detected in WB and IA with anti-his antibody. The 46 kDa band contain traces of *E. coli* FtsA peptides as found through mass spectrometry. In case of SpFtsA (untagged) expression and purification, no detectable and strong band is observed for SpFtsA in SDS-PAGE as well as in WB and IA (**c**).

S. pneumoniae ftsAZ

ATCGGCAGCAGCCATCACCATCATCACACAGCCAGGATATGGCTAGAGAAGGCTTTTTTACAGGTCTAGATATT
GGAACAAGCTCTGTCAAGGTGCTTGTGGCCGAGCAGAGAAATGGTGAATTAATGTAATTGGCGTGAGTAATGC
CAAAAGTAAAGGTGTAAAGGATGGAATTATTGTTGATATTGATGCAGCAGCAACTGCTATCAAGTCAGCCATTC
CCAAGCGGAAGAAAAGGCAGGCATTTGATTAATCAGTGAATGTCGGCTTGCCTGGTAATCTTTTGCAGGTAG
AACCAACTCAGGGGATGATTCCAGTAACATCTGATACTAAGGAAATTACGGATCAAGATGTTGAAAATGTTGTCA
AATCAGCTTTGACAAAGAGTATGACACCTGACCGTGAAGTCATTACCTTTATCCTGAAGAATTTATTGTGGATG
GTTTCCAAGGATTCGTGACCCACGTGGCATGATGGGGTTCGCCTTGAATGCGTGGTTTGTCTTATACAGGAC
CTCGTACTATCTTGACAATTTGCGTAAGACGGTTGAGCGTGCAGGTGTTACAGTTGAAAATGTTATCATTTCAC
CCTAGCAATGGTTCAAGTCTGTTTTGAACGAAGGGGAACGTGAATTTGGTGCTACAGTGATTGATATGGGGGCA
GGTCAAACGACTGTCGCTACAATCCGTAATCAAGAATCCAGTTCACACATATTCTCCAAGAAGGTGGAGATTAT
GTAATAAGATATCTCCAAGTTTTGAAAACCTCTCGCAAATTAGCGGAAGGCTTAAAACGTAATACGGGGGA
AGCCTATCCGCTCTTGAAGCAAAGAAACCTTCAAAGTAGAGGTATTGGAGAAGTAGAAGCAGTCGAAGTAG
ACGGAAGCCTTGTGAGAAATTTTCTGCACGAATCAAGCACATCCTTGAACAAATCAAGATAAGAAATTAGA
TAGAAGGCGTCTATTGACCTCCCTGGTGGTATTGTCTTAATCGGTGGGAATGCCATTTTACCAGGTATGGTTGAG
CTTGCTCAGGAAGTCTTTGGCGTCCGTGTCAAGCTTTATGTTCCAAATCAAGTTGGTATCCGTAATCCAGCCTT
GCGCATGTGATTAGTTTATCAGAATTTGCGGGTCAATTAACAGAAGTAAATCTTTTGGCTCAGGAGCGATAAAA
GGTGAGAATGCTTAAGTCATCAGCCAATTAGTTTTGGTGGGATGCTGCAAAAAACAGCTCAGTTTGTACAATC
AACGCTGTCAACCAGTCTCTGCTCCAGAAGTAGAGCCGGTGGCGCTACAGAACCAATGGCGGATTTCCAA
CAAGCTTCAAAAATAAACCGAAATTAGCAGATCGTTTCCGTGGCTTGCAGGAAGCATGTTTGCAGAAATAAG
AGGAAAATAAATTTACATTTTCATTTGATACAGCTGCTGCTCAAGGGGCAGTGATTAAGTAATTGGTGTCTC
GTGGAGGTGGTGGCAATGCCATCAACCGTATGGTCGACGAAGGTGTTACAGGCGTAGAATTTATCGCAGCAAAC
ACAGATGTACAAGCATTGAGTAGTACAAAAGCTGAGACTGTTATTTCAGTTGGGACCTAAATGACTCGTGGTTT
GGGTGCAGGAGGTCAACCTGAGGTTGGTCGTAAAGCCGCTGAAGAAAGCGAAGAAACACTGACGGAAGCTAT
TAGTGGTCCGATATGGTCTTCATCACTGCTGGTATGGGAGGAGGCTCTGGAAGTGGAGCTGCTCCTGTTATTGC
TCGTATCGCCAAAGATTTAGGTGCGCTTACAGTTGGTGTGTAACACGTCCTTTGGTTTTGAAGGAAGTAAGCG
TGGACAATTTGCTGTAGAAGGAATCAATCAACTTCGTGAGCATGTAGACACTCTATTGATTATCTCAAACAACA
TTTGCTTGAATTTGTGATAAGAAAACACCGCTTTTGGAGGCTCTTAGCGAAGCGGATAACGTTCTTCGTCAAG
GTGTTCAAGGGATTACCGATTTGATTACCAATCCAGGATTGATTAACCTTGACTTTGCCGATGTGAAAACGGTAA
TGGCAAAACAAAGGGAATGCTCTTATGGGTATTGGTATCGGTAGTGGAGAAGAACGTGTGGTAGAAGCGGCACGT
AAGGCAATCTATCCACTTCTTGAACAACACTATTGACGGTGTGAGGATGTTATCGTCAACGTTACTGGTGGT
CTTGACTTAACCTTGATTGAGGCAGAAGAGGCTTCAAAAATTGTGAACCAGGCAGCAGGTCAAGGAGTGAACA
TCTGGCTCGTACTTCAATTGATGAAAGTATGCGTGATGAAATTCGTGTAACAGTTGTCGCAACGGGTGTTCTGTC
AAGACCGCGTAGAAAAGGTTGTGGCTCCACAAGCTAGATCTGCTACTAACTACCGTGAGACAGTGAAACAGC
TCATTACATGGCTTTGATCGTCATTTTGTATGGCAGAAACAGTTGAATTGCCAAAAACAAATCCACGTCGTTT
GGAACCAACTCAGGCATCTGCTTTTGGTATTGGGATCTTCGCCGTGAATCGATTGTTCTGTACAACAGATTCA
CGTTTCTCCAGTCGAGCGCTTTGAAGCCCCAATTTACAAGATGAAGATGAATTGGATACACCTCCATTTTCAA
AAATCGTTAA

START Codon; STOP Codon; RBS

Figure A 14. Genetic organization of *S. pneumoniae* ftsAZ operon.

Appendix A3

This section contains a draft manuscript that is prepared based on findings from this PhD project and from contents written in the main thesis and appendix sections under supervision and guidance of Professor David Roper. All experimental works were performed by Souvik Naskar, unless mentioned in the acknowledgement.

Heterologous expression and *in-vitro* analysis of *Streptococcus pneumoniae* FtsEX divisome complex with peptidoglycan (PG) hydrolase PcsB and actin homologue FtsA, required for PG remodelling and cell separation.

Souvik Naskar¹, Corinne Smith², Tim Dafforn³, Allister Crow², Malcom Winkler⁴
and David I Roper²

¹Warwick Medical School, University of Warwick, UK; ²School of Life Sciences, University of Warwick, UK; ³School of Biosciences, University of Birmingham, UK; ⁴Department of Biology, Indiana University Bloomington, Indiana 47405, US

Abstract:

Bacterial cell division is orchestrated by the divisome complex of proteins necessary for coordinated peptidoglycan (PG) synthesis and PG remodeling, with homologous proteins in all Gram-positive and Gram-negative species. The complex between FtsE and FtsX is recruited to the divisome at an early stage in division and is required in assembling further downstream divisome proteins as well as performing a specific role in cell wall separation. The molecular events controlling this overall process are largely unknown and may also provide insight into future chemotherapeutic strategies to inhibit bacterial growth. We now show that heterologous expression of *Streptococcus pneumoniae* FtsEX forms an ATP dependent protein complex not only with FtsA as previous thought but also with its cognate peptidoglycan hydrolase; PcsB. We demonstrate functional complementation of *E. coli* cell division phenotypic defects in the presence of a complex of *Streptococcus pneumoniae* FtsEX-PcsB *in-vivo* and ATP binding activity *in-vitro*. In these studies, we utilized styrene malic acid nanodisc technology to extract these complexes *in-vitro* with bacterial membrane lipids for biochemical studies providing new insight into the molecular function of the individual proteins and the complexes together. In addition, we demonstrate a complex between the bacterial actin homologue, FtsA with FtsX specifically linking cell division to peptidoglycan metabolism events across the cytoplasmic membrane.

1. Introduction:

Cell division represents one of the most fundamental and complex changes in morphology a bacterial cell can undertake. Because of its intimate association with cell wall biosynthesis required to support the formation of daughter cells, interruption of this process is the basis for the mechanism of action of many natural and semi-synthetic antibiotics. Bacterial cell division starts with the formation “Z-ring” inside the cell, underpinned by the polymerisation of the tubulin homologue protein; FtsZ. The Z-ring provides the foundation for the assembly of a number of discrete protein complexes to form a much larger structure, the bacterial divisome (Haeusser & Margolin, 2016). The coordinated interaction of these individual proteins and those downstream in the process is required for successful cell division (den Blaauwen et al., 2017). Whilst the proteins of the divisome induce constriction of the cytoplasmic membrane inside the cell required for division, they also coordinate a number of other cellular events outside the cell. These include degradation of the old cell wall peptidoglycan sacculus located outside the cell membrane and the creation of new peptidoglycan structures (Haeusser & Margolin, 2016). Ultimately understanding of how the cell division process is coordinated through the assembly of the divisome and other linked macromolecular structures outside the cell is of fundamental biological interest and may also provide further insight into future antimicrobial action. At present there is a crucial lack of understanding in this area, particularly regarding the coordination of cell division with new cell wall biosynthesis.

Previous microbiological studies of bacterial cell morphology, combined with detailed genetic, biochemical and light microscopy imaging studies have already provided a wealth of information on the identity of the key proteins and macromolecules in the divisome. FtsZ is first recruited to the division site inside the cell and undergoes polymerisation in a GTP dependent process. Common to all species, FtsZ is tethered to the inside of the membrane by the actin homologue FtsA which is ATP dependent (Szwedziak et al., 2012). This proto-ring complex of

proteins forms the foundation upon which successive individual proteins and protein complexes are recruited the first of which is the complex between integral membrane protein, FtsE and its associated ATP hydrolase FtsX. FtsEX is thought to form a heterodimer (Bajaj et al., 2016; Dominguez-Cuevas et al., 2013) (**Fig. 1**) and spans the bacterial membrane from cytoplasm to its outer membrane surface with the four predicted membrane spanning helices of FtsX which provide a two extracellular loops which are responsible for binding peptidoglycan (PG) hydrolytic enzymes required for hydrolysis of this extracellular macromolecule allowing the cell to divide. It is known that the large extracellular loop domain of pneumococcal FtsX (ECL1) interacts with the coiled-coil domain of PcsB(Sham et al., 2013), and in combination with the smaller ECL2 loop, are responsible in signal transduction thought to be required for PcsB PG hydrolase activity (Sham et al., 2013). A recent study has also implicated the direct interaction of PcsB with membrane lipids raising the possibility that the binding interface for PcsB is a combination of lipid and FtsX protein features(Bajaj et al., 2016). Although FtsE has sequence homology to ABC transporters, there is little evidence that it acts as a small molecule transporter in common with other proteins in that class.

PG (also known as murein) is a three-dimension mesh found outside the cell membrane and is unique to bacteria. Disruption of its biosynthesis by inhibition of the enzymes which are responsible for its formation and modulation is lethal to bacteria and has been the basis for life saving beta-lactam chemotherapy for decades. Recent X-ray crystallographic studies of PcsB have shown that the carboxy-terminal cysteine, histidine-dependent amidohydrolase/peptidase (CHAP) domain is linked to the rest of the protein by a series of extended alpha coiled-coil (CC) domain structures(Bartual et al., 2014). Moreover, the protein is arranged in a dimeric structure in which the CC domain of each monomer acts as a pair of molecular tweezers locking the catalytic domain CHAP of each dimeric partner in an inactive form. The inference therefore is that docking of PcsB to FtsEX activates the muralytic hydrolase activity, which may be linked to the ATP hydrolysis activity of FtsE. Biochemical studies of FtsE have identified mutants of the *E. coli* enzyme(S. J. Arends, R. J. Kustus, & D. S. Weiss, 2009) which are also

conserved elements of the classical Walker ATP binding motifs (J. E. Walker, Saraste, Runswick, & Gay, 1982). At the cytoplasmic membrane face, FtsA is known to interact with FtsEX and studies on the *E. coli* system indicate that FtsA interacts directly with FtsX regulating both divisome assembly and activity (Du et al., 2016) (**Figure 1**). This study with the *E. coli* system also suggests that FtsEX antagonizes, ATP dependent polymerization of FtsA to promote divisome assembly, since FtsE ATPase mutants block divisome activity by locking FtsA in the inactive form or preventing FtsA coordinating downstream protein-protein interactions required for divisome assembly (Du et al., 2016).

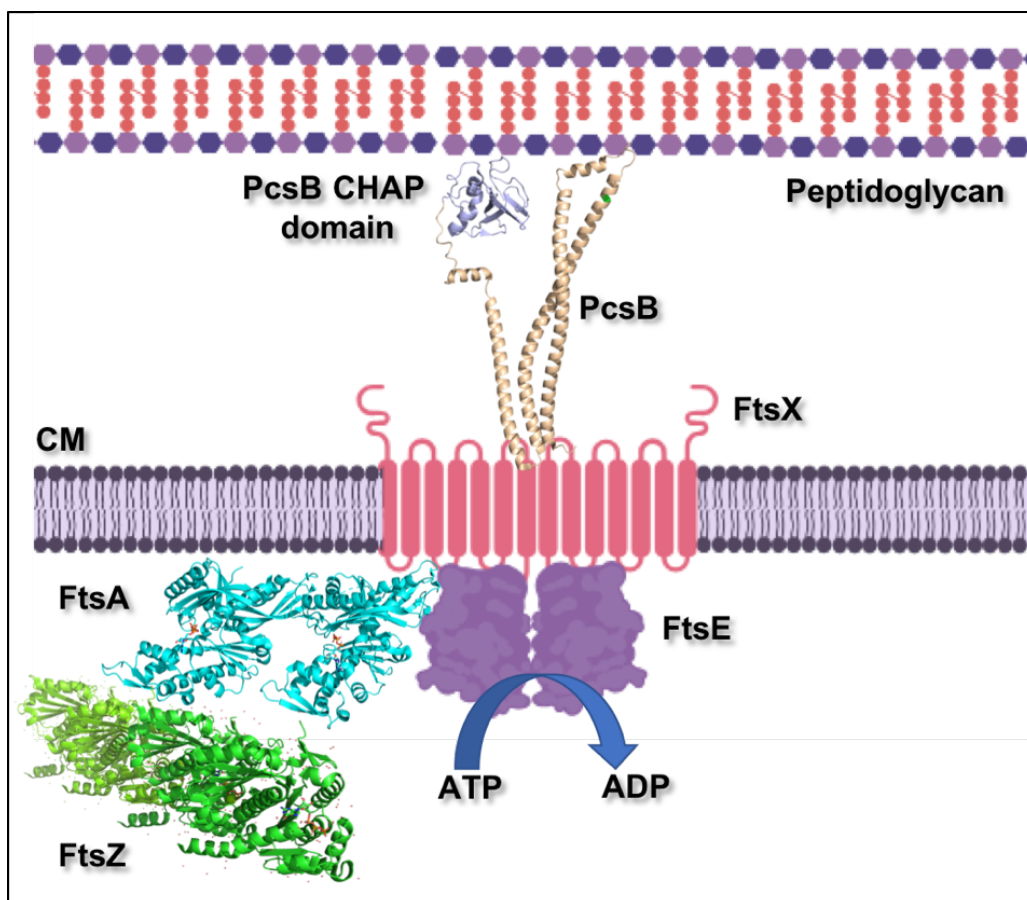


Fig. 1. Schematic diagram of FtsEX, PcsB, FtsA and FtsZ in context. The FtsEX complex is shown as a schematic dimer structure and resembles an ABC transporter protein structure with PcsB (PDB:4CKG (Bartual et al., 2014)) docking in the extracellular environment. The polymer structure of ATP bound FtsA (PDB: 3wqu (Fujita et al., 2014)) provides an anchoring point for FtsZ (PDB:1w5a (Oliva, Cordell, & Lowe, 2004)). The peptidoglycan layer is shown above the cytoplasmic membrane (CM) as indicated.

In this context we have focussed and extended previous observations on the Gram-positive human pathogen *Streptococcus pneumoniae* hydrolase enzyme PcsB and its complex with FtsEX. In addition, we also shown a direct interaction of *S. pneumoniae* FtsA with FtsX. Future structural and biochemical information on these protein-protein interactions would greatly aid in the interpretation of the molecular events surrounding the early steps in bacterial cell division (Bajaj et al., 2016). In order to achieve this we have utilised heterologous overexpression of the required *S. pneumoniae* enzymes in *E. coli* to facilitate biochemical study but utilising styrene malic acid lipidic particle (SMALP) nanodisc technology (Lee et al., 2016; Lee & Pollock, 2016) which in contrast to conventional detergent membrane protein extraction techniques, allows isolation of the membrane protein in question with such lipids (Teo et al., 2019). In addition, we have studied the morphology of these expressed proteins in different combination allowing insight into the molecular events and interactions of these *S. pneumoniae* enzymes within an *E. coli* context. Since these proteins represent core elements of the conserved divisome machinery and the nomenclature of these proteins resides with their effect on bacterial cell division and growth producing filamentous phenotype when perturbed or inhibited, this approach provides powerful insight into coordinating events inside and outside the membrane during cell division.

2. Results:

2.A. *S. pneumoniae* FtsEX is coordinately expressed as a protein complex and has a phenotypic effect on *E. coli* when heterologously expressed.

Previous studies examined the complementation of an *E. coli ftsEX* genetic knockout strains by complementation of recombinant *ftsEX* in defined media conditions where normal FtsEX function can be bypassed in high salt, complex media conditions (S. J. Arends et al., 2009). Site directed mutants of the *E. coli* recombinant *ftsE* gene, producing proteins where ATP binding or ATP hydrolysis is abolished, could not complement the *ftsEX* knockout strains, highly suggestive that ATP hydrolysis is required for proper FtsEX function. By contrast to *E. coli*, FtsEX function in *S. pneumoniae* (Sp) is essential in serotype strains (Ng et al., 2004; Ng et al., 2003; Sham et al., 2013) and causes diminished growth and severe cell division defects when inactivated in other strains (Giefing et al., 2008; Giefing-Kroll et al., 2011). In our study, we did not have access to comparable strains as described above for the *E. coli* system, which would not be compatible for heterologous expression of the *S. pneumoniae* proteins in any case. We chose therefore to clone the entire genomic region encompassing *S. pneumoniae* FtsEX genes into the *E. coli pETduet* vector producing an expression construct with a histidine tag on the N-terminus of SpFtsE (6) and a C-terminus of SpFtsX (10) (**Table 1**). This work therefore extends previous observation of SpFtsE and SpFtsX isolation and characterization (Bajaj et al., 2016).

To analyze phenotypic consequences of expression of *S. pneumoniae* FtsEX, PcsB and FtsA in this study, we adopted a strategy of synchronous cell culture (Ferullo et al., 2009) using pretreatment of inoculates using DL-serine hydroxamate to ensure all samples were harvested for analysis at the same point in growth following induction (**Fig. 2a**). Fluorescent microscopy of cells harvested at late exponential phase and labelled with FM4-64 allowed comparison of empty vector control cells (**Fig. 2b**) with those expressing FtsEX (**Fig. 2c**) showed an aberrant cell division phenotype in the latter, where we observe long undivided cells. This is type of dominant negative effect on cell growth is a signature morphological defect in the

bacterial cell division apparatus and is highly suggestive of a heterologous interaction between SpFtsEX and other components of the *E. coli* host divisome, as has been seen previous with other ‘Fts’ proteins (Du et al., 2016; Ng et al., 2004; Ng et al., 2003; Schmidt et al., 2004). We extended this observation by examination of the cellular location of heterologously expressed SpFtsEX *in-vitro* and found the FtsEX proteins located in the membrane fraction of the *E. coli* host cells, consistent with a complex between the two proteins. Expression of empty vector when analyzed *in-vitro* in similar way as FtsEX, no prominent overexpressed protein bands that purified with his-tag, are observed (Fig. S2), and results no phenotypic abnormality during its heterologous expression (Fig. S1).

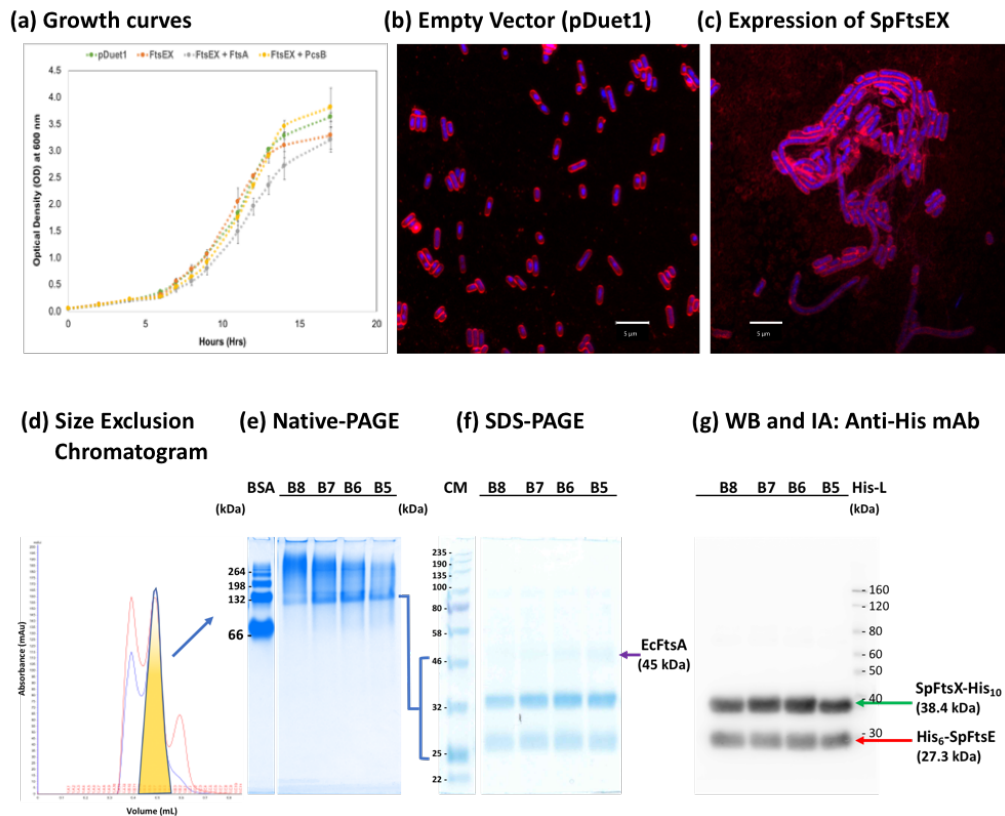


Fig. 2: Synchronous cell culture growth curve comparison for cells expressing *FtsEX* alone and when co-expressing with *PcsB* and *FtsA* (a). FM4-64 and DAPI stained *E. coli* cells under fluorescent microscope (at 100x magnification), harboring empty vector pETduet (b) and pETduet-SpFtsEX (c). Scale indicates 5 microns. Size exclusion chromatography (d) following IMAC purification of SMALP extracted SpFtsEX with peak fractions indicated in yellow (d) and accompanying native PAGE (e), SDS-PAGE (f) and anti his-tag antibody immunoassay (IA) on Western blot (WB) analysis

(g) of peak fractions. The bands for SpFtsE and SpFtsX are indicated by arrows, as is a weakly staining band for EcFtsA in the SDS-PAGE analysis which was subsequently confirmed by mass spectrometry analysis.

Isolation of *E. coli* membranes that expressed with SpFtsEX, followed by solubilization of the membrane protein fraction using detergent free, SMALP extraction and subsequent purification by IMAC and GF chromatography (Fig. 2d), allowed the isolation of the FtsEX complex in high yield and purity as shown by Native-PAGE (Fig. 2e), SDS-PAGE (Fig. 2f), Western blots (Fig. 2g). Moreover, the FtsEX complex in SMALP nanodisc migrated as broad band at approximately 200 kDa. Native-PAGE and mass spectrometry of a trypsin digest of these bands confirmed the presence of unique peptides from both SpFtsE and SpFtsX proteins (Fig. S5). In addition, this analysis revealed the presence of peptide sequences for *E. coli* FtsA (EcFtsA) as shown in Figure S5. The same samples analyzed by reducing SDS-PAGE, showed clear bands for the FtsE and FtsX at 27 kDa and 36 kDa respectively, and the presence of a 46 kDa (Fig. 2f) that identified as EcFtsA when sequenced using mass spectrometry (Fig. S6), highly suggestive therefore of a chimeric associative complex between SpFtsEX and EcFtsA which has not been previously observed.

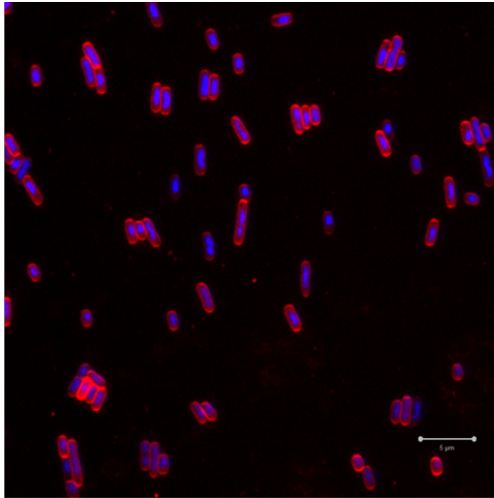
2.B. *S. pneumoniae* FtsA forms a complex with FtsX and not FtsE.

As described above, our experiments on expression of SpFtsEX in complex, produced a clear cell division phenotype and allowed the purification of that complex *in-vitro*. In this analysis, we also noted that EcFtsA was apparently copurifying with the complex (Fig. 1f). Compared to empty vector cells (Fig. 3a), transformation of an *E. coli* cell line expressing SpFtsEX with a plasmid expressing *S. pneumoniae* FtsA (SpFtsA) produced an even more striking loss of cell division phenotype (Fig. 3b) indicating that FtsA may interact with FtsEX as previously reported for the *E. coli* proteins (Du et al., 2016). In order to investigate this further, we expressed SpFtsE and SpFtsX separately in the presence of recombinant SpFtsA. We constructed pETDuet based expression vectors for SpFtsE-His₆ and SpFtsX-His₁₀ (Table 1) in isolation in which each protein was provided with a

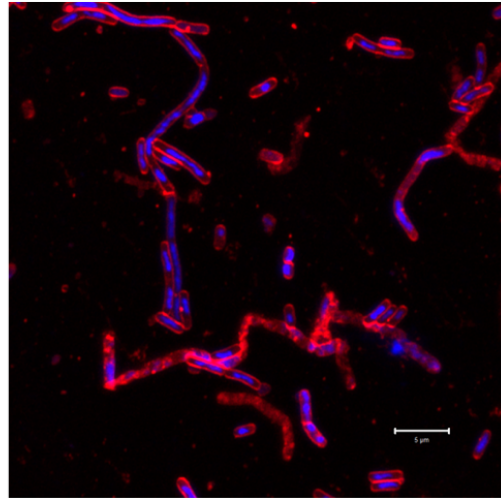
histidine tags on their carboxyl termini for subsequent purification and western blot detection. Expression of SpFtsE or SpFtsX protein individually (**Fig. S3**), produced comparable phenotypic observations (**Fig. S1**) as seen for expression of the FtsEX complex described above (**Fig. 2c**), indicative of interaction with the *E. coli* divisome. This interaction also observed *in-vitro* when *S. pneumoniae* proteins FtsX and FtsA co-purified a low amount of *E. coli* FtsA and FtsX respectively (**Fig. S3** and **Fig. S4**).

We next co-transformed the individual FtsE-His₆ and FtsX-His₁₀ expression strains with an pACYC based plasmid expressing an untagged form of *S. pneumoniae* FtsA and SMALP purified any potential complexes using sequential IMAC and SEC to test if the FtsA association was specific to either FtsE or FtsX. Strikingly, SpFtsA was only recovered in the presence of FtsX indicating a direct interaction with FtsX alone (**Fig. 3c-d**). The sequence identities of purified SpFtsE-His₆ and co-purified proteins (SpFtsX-His₁₀ and SpFtsA) are confirmed by mass spectrometry as shown in **Fig. S7** and **Fig. S8** respectively. Whilst previous genetic experiments indicate an interaction between FtsX and FtsA in *E. coli* (Du et al., 2016), this is the first direct biochemical demonstration of this interaction and its potential in controlling early steps in cell division between cytoplasmic and membrane division components. Co-expression of SpFtsA (no tag) with the SpFtsEX complex (His₆-FtsE and FtsX-His₁₀) (**Fig. 3e**) followed by SMALP mediated IMAC and SEC purification of the high molecular tripartite complex was also achieved (**Fig. 3e-f**). In a similar experiment, N-terminally tagged SpFtsA co-expressed with the SpFtsEX complex and co-purified following SMALP extraction, IMAC and SEC purification, which resulted similar tripartite complex and the His₆-SpFtsA band was identified along with His₆-SpFtsE and SpFtsX- His₁₀ on Western blot using anti-his antibody (**Fig. S9**).

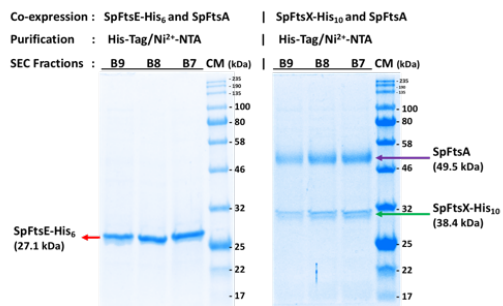
(a) Empty Vectors (pDuet and pACYC)



(b) Co-expression of SpFtsEX-SpFtsA



(c) SDS-PAGE 1 (d) SDS-PAGE 2



(e) Native-PAGE (f) SDS-PAGE

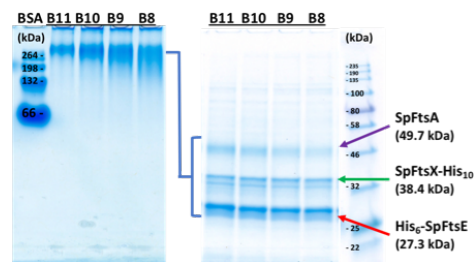


Fig. 3: (a-b) FM4-64 and DAPI stained *E. coli* cells at 100x magnification transformed with empty vector pETDuet and pACYC plasmids (a) compared to the same cell line harboring expression constructs for SpFtsEX and SpFtsA, respectively (b). Scale indicates 5 microns. SMALP mediated IMAC and SEC purification of his-tagged SpFtsE (c) and SpFtsX (d) in isolation, demonstrate copurification of untagged FtsA with FtsX alone. Expression and purification of a SpFtsEX-FtsA complex examined by native (e) and SDS-PAGE (f).

2.C. PcsB forms a functional complex with FtsEX rescuing the phenotype of FtsEX expression alone.

Previous genetic(Sham et al., 2013) and biochemical(Bajaj et al., 2016) studies provide some evidence for a direct interaction between FtsX and PcsB on the surface of the *S. pneumoniae* bacterial cell membrane. However, it has been shown that full length PcsB alone has no peptidoglycan hydrolytic activity in contrast to its isolated hydrolytic CHAP domain, highly suggestive that the full length protein may require a conformational change upon docking to its cell membrane partner in order to be activated(Bartual et al., 2014). Given our ability to produce the FtsEX proteins in sufficient quantities for biochemical and structural investigations, coupled with our observations of phenotypic consequence of such expression, we next turned our attention to a potential complex between the FtsEX complex and PcsB to test the above hypothesis.

Co-transformation of *E. coli* with separate plasmids constructs for the expression of FtsEX and PcsB in pHETIS-Duet2 and pHETIS-CDF2 (**Table 1**) respectively allowed a direct comparison of phenotype to cells transformed with the FtsEX expression construct alone. Comparison of the phenotype of cells carrying empty vector (**Fig. 4a**) to those co-expressing SpFtsEX and SpPcsB (**Fig. 4b**). When expression of SpFtsEX alone shows elongated cell phenotype (**Fig. 2c**), co-expression of SpFtsEX and PcsB revealed that the previous cell division aberrant phenotype had been rescued to a normal rod shaped, consistent with a functional complex between FtsEX and PcsB which is able to hydrolyse *E. coli* peptidoglycan and thus re-establish normal cellular division. Further *In-vitro* biochemical characterization of SMALP purified PcsB and its complex with SpFtsEX (SpFtsEX-PcsB) showed a complex of the three proteins can be isolated together as a high molecular weight complex as judged by the native gel (**Fig. 4c**) SDS-PAGE gel (**Fig. 4d**) and Western blot (**Fig. 4e**) of the same SEC fractions. Although the Western blot signal from PcsB using an anti-his-tag antibody was relatively weak compared to FtsEX, its presence was confirmed through mass spectrometry sequence (**Fig. S10**).

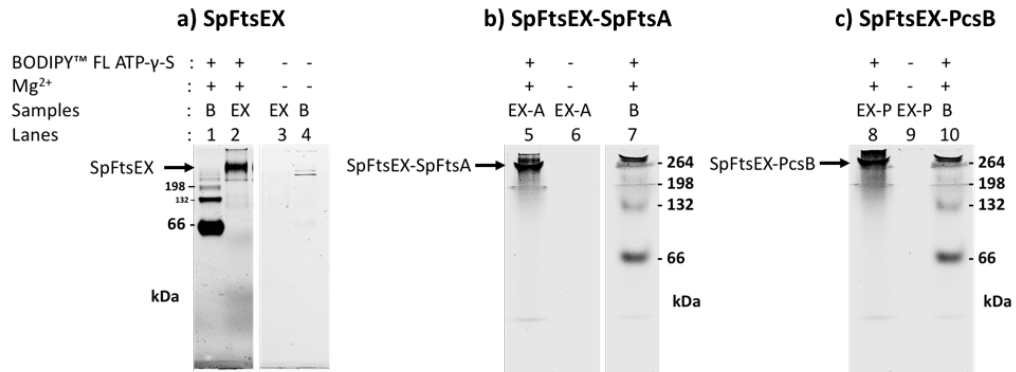
2.D. Purified SMALP complexes of FtsEX, FtsEX-FtsA and FtsEX-PcsB are functional in *in-vitro* condition and exhibits ATPase activity.

As described above heterologous expression of *S. pneumoniae* FtsEX complex and its co-expression with FtsA or PcsB full length proteins in *E. coli* has demonstrated striking morphological changes on *E. coli* cell shape and provides strong evidence for these complexes having functionally activity *in-vivo*. In order to understand their specific mechanism behind those phenotypical anomalies, we turned our focus into *in-vitro* functional assays with these complexes. Amino acid sequence analysis of FtsE predicted the presence of the Walker A and B consensus motifs (J. E. Walker et al., 1982) that involved in ATP binding, and commonly found in most proteins from ATP-binding cassette (ABC) transporter superfamily (Higgins, 1992). We tested this hypothesis on our successfully purified functional (*in-vitro*) *S. pneumoniae* complexes of FtsEX, FtsEX-FtsA and FtsEX-PcsB, which contain FtsE and its ATP binding site. In order to assess the ATP binding ability of these SMALP purified complexes *in-vitro* we first examined all three samples in the presence and absence of fluorescent ATP analogue, BODIPY™ FL ATP- γ -S, Thioester (Adenosine 5'-O-(3-Thiotriphosphate)) (ThermoFisher Scientific, UK) as mentioned in methods and materials (4.C). All purified protein samples were analyzed using non-reduced Native-PAGE by fluorescent imaging with excitation at 488 nm and imaged 510 nm for the BODIPY fluorophore and compared to a BSA standard that provides a convenient ATP binding control and native gel molecular weight estimation in this instance (Bauer et al., 1992; Jameson et al., 2016). Samples that assayed in presence of BODIPY™ FL ATP- γ -S and Mg²⁺ are observed with prominent fluorescent band at their corresponding molecular weight Native-PAGE as found in Coomassie staining of the same gel following fluorescent imaging (**Fig. S12**). The results indicate our purified SMALP complexes of FtsEX, (**Fig. 5a**) FtsEX-FtsA (**Fig. 5b**) and FtsEX-PcsB (**Fig. 5c**), all entraps ATP molecule, through FtsE. In those samples containing FtsA, direct binding of the ATP analogue to FtsA is also possible since its polymerization is ATP dependent (Krupka et al., 2014)

We next turned our attention to the role of ATP binding and hydrolysis with respect to PcsB activation linking events inside the cytoplasm of the cell to hydrolytic

events outside the cell membrane. When we verified successful binding of ATP molecules to SMALP purified complexes of *S. pneumoniae* FtsEX, FtsEx-FtsA and FtsEX-PcsB, the obvious question arises about their ATP-hydrolysing ability; Could these complexes hydrolyze ATP under *in-vitro* conditions? Previous studies had indicated a low level of ATP hydrolytic activity for FtsE in isolation (Bajaj et al., 2016). In order to address this question, we followed a classic ATPase, ADP release enzyme coupled assay that can detect ATP hydrolysis *in-vitro* as described in methods and materials (4.C). The result shows a low level of activity for FtsEX, and its complex with SpFtsA and PcsB. However, these initial observations with the complexes of FtsEX is not yet conclusive due to lack of sufficient concentration of the samples and needs more careful further exploration in the future. Altogether results from two different *in-vitro* functional assays: one for ATP-binding and other for ATP-hydrolysis suggests, our SMALP extracted and copurified *S. pneumoniae* complexes of FtsEX-FtsA and FtsEX-PcsB binds ATP, shows low level of ATPase activity that requires further investigation.

ATP Binding Assay:



ATP Hydrolysis Assay:

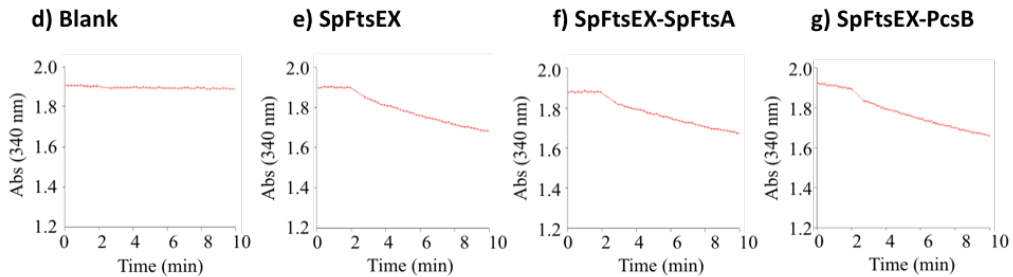


Fig. 5: Native gel analysis of BODIPY-ATP- γ -S binding for SpFtsEX (a), SpFtsEX-FtsA (b) and SpFtsEX-PcsB (c) compared to BSA. In each of these

figures, B: BSA, EX: SpFtsEX, EX-A: SpFtsEX-SpFtsA complex, EX-P: SpFtsEX-PcsB complex. Combinations of proteins labelled ATP and Mg²⁺ are indicated. Absorbance based kinetic traces for ATP hydrolysis assays with Blank (d), SpFtsEX (e), SpFtsEX-SpFtsA (f) and SpFtsEX-PcsB (g) shows very low-level of activity compared to the blank, however the concentration of the proteins was very low as well. In each assay about 2-4 µg of total protein was used per assays (200 µl). In each of these figures, BSA: Bovine serum albumin, EX-A: SpFtsEX-SpFtsA complex in SMALP, EX-P: SpFtsEX-PcsB complex in SMALP; Abs (340 nm): Absorbance at 340 nm.

2.E. Initial biophysical and structural analysis of FtsEX, FtsEX-FtsA and FtsEX-PcsB complexes.

A detailed structural description for FtsEX and its interaction with cognate cell division proteins is still lacking in the literature with only the extracellular region of mycobacterium tuberculosis FtsX (Mavrici et al., 2014) described so far. Since our *in-vitro* purification strategy provided very highly purified samples of FtsEX alone and in complex with other proteins, we choose to investigate preliminary biophysical and structural studies. The AUC analysis with SMALP-SpFtsEX and SMALP-SpFtsEX-PcsB complexes clearly showed a difference in their sedimentation co-efficient (**Fig. 6**). In the same experiment SMALP-FtsEX showed single peak around 11.5 whereas the SMALP-FtsEX-PcsB complex showed two prominent peaks at around 11 and 14.5 (**Fig. 6**). This possibly indicates the peak around 11 or 11.5 is for SMALP-SpFtsEX whereas the peak around 14.5 possibly represent the SMALP-SpFtsEX-PcsB complex (**Fig. 6**). Negative stain electron microscopy studies with SMALP-FtsEX (**Fig. 7a**) and SMALP-FtsEX-PcsB (**Fig. S13.b**) showed a good distribution of the particles that ranges between 12 nm and 16 nm for SMALP-FtsEX and between 16 and 22 for SMALP-FtsEX-PcsB. This allowed particle picking and sorting as demonstrated in **Fig. 7.b** for SMALP-SpFtsEX complex. The measurements on negative stained individual particles supports the dynamic light scattering analysis (**Fig. 7.c** and **Fig. 8.c**) that measured particle sizes about 13 nm (+/- 3 nm) and 16 nm (+/- 4) for SMALP-FtsEX and SMALP-FtsEX-PcsB complexes respectively. Average Sizes of both these complexes are larger compared to SMALP disc alone that sizes approximately 9 to

10 nm. This is indicative of single particles representative of the FtsEX dimer or its complex with PcsB encapsulated in a SMALP nanodisc. Examination of individual particles at higher magnification (**Fig. 7.d**) shows the SMALP-SpFtsEX particle in a number of orientations on the EM grid and allowed the generation of a low-resolution model for FtsEX as demonstrated in **Fig. 7.e**. In addition, we also detected monodispersed SpFtsEX-SpFtsA complex and SPFtsEX-PcsB complex in SMALP disk in negative stain EM micrographs (**Fig. S13a** and **S13b**, respectively). Whilst these results are preliminary and further higher resolution studies are required, all these analyses show promise for future detailed structural studies on the FtsEX core complex and the proteins that bind to it. An initial Cryo-EM screening, micrographs that shows good distribution of monodispersed particles with all three complexes are shown in **Fig. S14**. Among these the SMALP-SpFtsEX-PcsB complex showed very good monodispersed particles distribution on Graphene oxide coated grids for Cryo-EM (**Fig. S14.c**; and **Fig. 8.a**), which when further analyzed by extracting single particles (**Fig. 8.b**) for initial 2D and 3D classification, and an initial model was generated along with its projections using EMAN2 program as shown in **Fig. 8. d, e, f**. This initial analysis is indicative of existence of possible SpFtsEX-PcsB complex in our purified samples, however this work needs further screening for best cryo-EM condition and grid preparation for high resolution structural studies with these complexes.

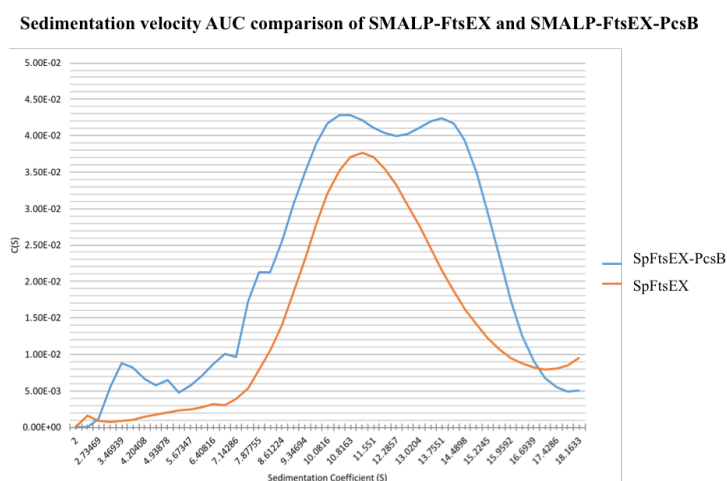


Fig. 6: AUC plots for SpFtsEX and SpFtsEX-PcsB complexes in SMALP. (The AUC experiments were set and run by Dr Pooja Sridhar and AUC data were analysed by Dr Sara Lee in my presence. I was under their supervision for AUC related experiments).

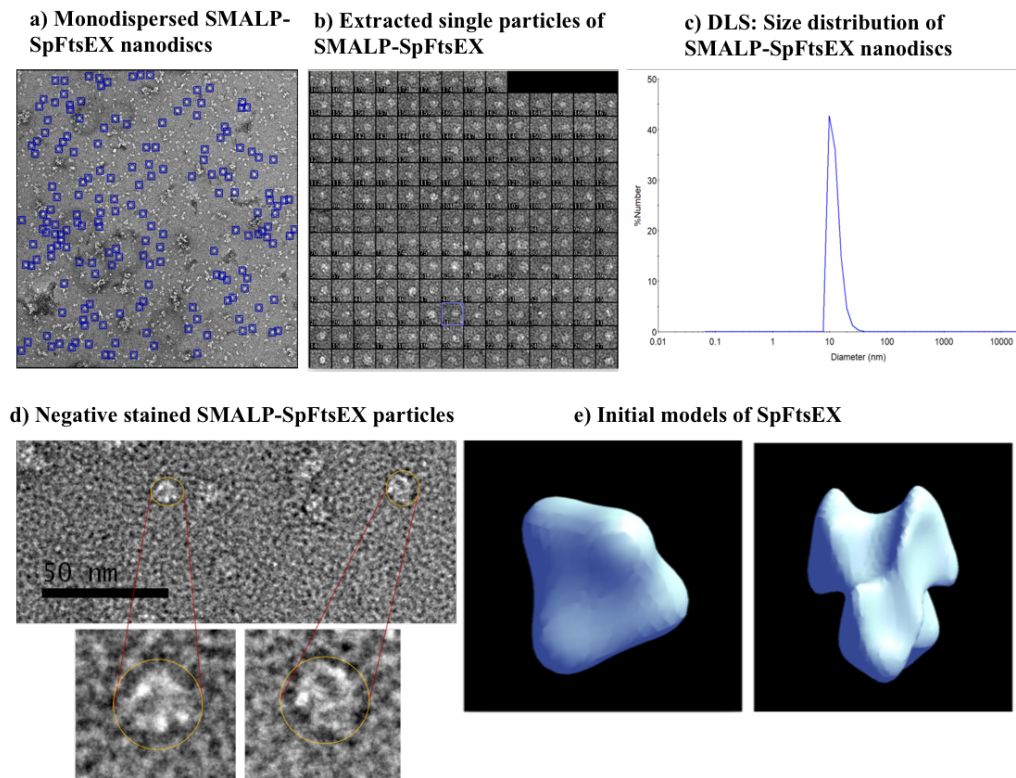


Fig. 7: Negative staining of purified SMALP-SpFtsEX sample (at 0.2 mg/ml) using Uranyl Acetate (UA, 2%) showed particles are monodispersed (a) and when single particles are screened extracted using appropriate box size in EMAN2 program, particles are found disc-like structure and evenly distributed in their size (b). The DLS of the same sample also measured the size about 15.46 nm \pm 3 nm (c). An amplified image with scale bar 50 nm shows the size of those discs is between 12 nm and 20 nm (d) Yellow circles are directing few of those disc-like structures. 2D-class averaging of those single particles (performed with \sim 2500 particles) lead to generate initial models (e, left) and its further low-resolution (>22 Å) refinement (e, right), which indicate a possible heterodimeric arrangement between SpFtsE and SpFtsX.

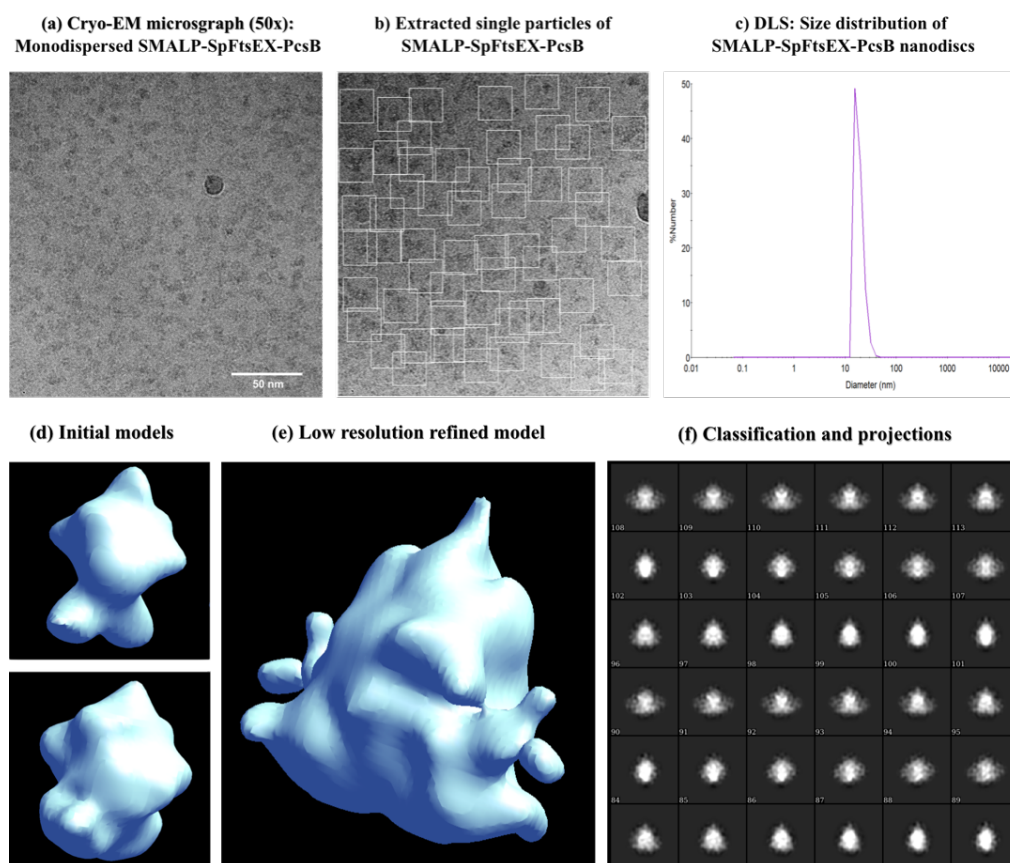


Fig. 8: Initial screening and Cryo-electron micrograph of SpFtsEX-PcsB complex **(a)**; Single particles of the same complex picked and extracted using particle picker program (EMAN2) **(b)**; The initial images showed good particle distributions on the Cryo-EM grids that coated with graphene oxide **(a-b)**. Initial measurement on the Cryo-EM images as well as DLS experiment with same complex indicated the size of the SMALP-SpFtsEX-PcsB disc is about 16-18 nm **(c)**, which is slightly larger than the size of SMALP-FtsEX complex (12-14 nm). An initial analysis with extracted small number of particles (about 1200) generated an initial model **(d, top)** and a further refinement is shown in **(d, bottom)**. A low resolution ($>18 \text{ \AA}$) initial 3D model also projected from selection of few good classes **(e)**; related classification is showing the projections of the same model **(f)**. Scale bar 50 nm..

3. Discussion:

The bacterial protein complex of FtsEX sits at the hub of a complex choreography of cellular activities linking cell division events across the bacterial cell membrane. FtsEX is required in the early steps of cell division, coordinating events in the cytoplasm and also appears to be a “docking platform” and regulator of hydrolytic enzymes in the extra-cytoplasmic space in both Gram-positive and Gram-negative bacteria. In our heterologous expression study, we observed aberrant cell division defects in *Escherichia coli* cell when subject to expression of the *Streptococcus pneumoniae* FtsEX mimicking the phenotype of existing natural product antibacterial agents as well as antibiotic drugs. Moreover, previous reports have investigated the host cytokine CLCX10 as an inhibitor of FtsEX function as well as other targets (Bruce et al., 2018; Crawford et al., 2011; Margulieux et al., 2016). This suggest that FtsEX may provide a suitable focus for future antimicrobial strategies since its function is essential in Gram-positive bacteria and conditionally essential (low salt) in *E. coli* (it is not known if the same is true for other Gram-negative bacteria). We now show that the aberrant cell division phenotype, as a consequence of SpFtsEX expression, can be rescued by expression of SpPcsB in trans. This remarkable observations of the consequence of FtsEX expression in isolation or in complex with SpFtsA, is consistent with interruption of cell division process as yet by an ill-defined mechanism. Our working hypothesis is that an imbalance in the levels of certain cell division proteins, sequesters additional proteins in unproductive complexes; and that the SpFtsEX-PcsB complex is probably functionally active and in addition it can hydrolyse *Escherichia coli* PG required for PG remodelling during cell separation. This hypothesis requires the *S. pneumoniae* cell division proteins to be able to interact with the corresponding interaction partners from the host *E. coli* proteome and we demonstrate a direct copurification of *E. coli* FtsA with the SpFtsEX complex and specifically with SpFtsX.

Consistent with this overall hypothesis, a previous biochemical demonstration that shows the PcsB hydrolytic CHAP domain in isolation has the ability to digest isolated peptidoglycan from a different bacterial specie (Bartual et al., 2014). In

addition, the same study shows that the vast majority of the extracellular full-length protein in isolation, is not active as a PG hydrolase in the same assays. The authors attribute this lack of activity in the full-length protein to a shielding of the CHAP domain by the rest of the protein and consequent conformational change required for activity. Such events are consistent with the hypothesis that docking of PcsB with SpFtsEX at the membrane and/or ATP hydrolysis by FtsE inside the cytoplasm is required for PcsB peptidoglycan hydrolytic activity. Whilst FtsEX has sequence similarity to archetypical: ABC transporters, there is no evidence of such a transport mechanism of cargo (Bajaj et al., 2016). However, the recent structure of MacB which is an ABC transporter that collaborates with the MacA adaptor protein and TolC exit duct to drive efflux of antibiotics out of the bacterial cell suggests the hydrolysis of ATP inside the cytoplasm drives conformational changes in the protein outside the cell membrane (Crow et al., 2017). This may provide a mechanism for ATP dependent hydrolysis of the FtsEX in concert with activation and possible regulation of PcsB peptidoglycan hydrolytic activity.

Additionally, we have shown that these membrane protein complexes can be isolated *in-vitro* using styrene-maleic-acid-lipid-particles (SMALP) nanodisc, preserving a representative membrane lipid environment (without detergents) (Lee et al., 2016). In this study, we have overexpressed FtsEX along with FtsA and PcsB from *Streptococcus pneumoniae* in *E. coli*, and purified them as a complex in SMALPs, for enzymatic, biochemical and high-resolution single-molecule structural studies. The protein-protein interaction studies described indicate SpFtsX (but not SpFtsE), interacts with the essential divisome protein SpFtsA, and PcsB successfully docks with SpFtsEX to form an active peptidoglycan hydrolytic complex. Moreover, these complexes are competent for ATP binding as shown by *BODIPY-ATP- γ -S*. Recent studies on the *E. coli* FtsEX system using genetic and phenotypic screens (Du et al., 2016) shows the EcFtsEX acts on EcFtsA to regulate both divisome assembly and activity. An interaction between EcFtsX and EcFtsA was indicated in a genetic screen and that this interaction was required for divisome assembly and inhibition of divisome function by ATPase mutants of EcFtsEX. Our results provide phenotypic and for the first-time biochemical data in support of this

hypothesis. Negative stain electron microscopy images and initial high resolution cryo-EM images of the complex provides a valuable prerequisite for investigating mechanistic insight about their structural-functional relationship and for further inhibitor screens for SpFtsA-FtsEX-PcsB complex as well as their high-resolution structure and function studies.

4. Methods and Materials:

4.A. Strains and plasmids:

Escherichia coli (*E. coli*) *BL21DE3ΔacrB::Km^R* strain³² that lacked *acrB* gene, was used for purifying SMALP extracted proteins or protein complexes. Because, AcrB has been found as common contaminant in SMALP extracted purified protein samples. Depending on the antibiotic selection of plasmid, ampicillin (100 μg/mL), chloramphenicol (18 μg/mL) and Streptomycin (25 μg/mL) were used in combination kanamycin (25 μg/mL), to select for transformants in *E. coli* *BL21DE3ΔacrB::Km^R*. Details of plasmids used in this study are listed in **Table 1**. Bacterial growth was estimated by measuring optical density (OD) of the culture at 600 nm.

Table 1: Plasmid details

| Recombinant construct | Expressed <i>S. pneumoniae</i> gene | Tag(s) and description | Plasmid used for cloning and expression study | Source of plasmid backbone | Origin of replication | Antibiotic resistance marker | Source of recombinant construct |
|--|--|--|---|--|-------------------------------|------------------------------|---------------------------------|
| <i>pET-52b(+)-strept-SpftsEX-his₁₀</i> | <i>ftsEX</i> | The <i>ftsE</i> is strep tagged N-terminally and <i>ftsX</i> is histidine (6) tagged C-terminally | <i>pET-52b(+)</i> | Novagen, UK (71554) | pBR322 | Ampicillin | In this study |
| <i>pETDuet1-His₆-SpftsE(MCS1)-SpftsX-his₁₀(MCS2)</i> | <i>ftsE</i> and <i>ftsX</i> from MCS1 and MCS2 respectively. | The <i>ftsE</i> is strep tagged N-terminally and <i>ftsX</i> is histidine (6) tagged C-terminally | <i>pETDuet1</i> | Novagen, UK (71146) | pBR322 | Ampicillin | In this study |
| <i>pET-22b(+)-SpftsE-His₆</i> | <i>ftsE</i> | The <i>ftsE</i> is histidine (6) tagged C-terminally | <i>pET-22b(+)</i> | Novagen, UK (69744) | pBR322 | Ampicillin | In this study |
| <i>pETDuet1-SpftsE-his₆</i> | <i>ftsE</i> | The <i>ftsE</i> is histidine (6) tagged C-terminally | <i>pETDuet1</i> | Novagen, UK (71146) | pBR322 | Ampicillin | In this study |
| <i>pETDuet1-SpftsXvol-his10</i> | <i>ftsX</i> with start codon valine (Vol); translation start as YSLP | The <i>ftsX</i> is histidine (10) tagged C-terminally (amplified from pET-52b(+)-strep-SpftsEX-his10) | <i>pETDuet1</i> | Novagen, UK (71146) | pBR322 | Ampicillin | In this study |
| <i>pETDuet1-SpftsX-His₁₀</i> | <i>ftsX</i> (translation starts as MAVS) | The <i>ftsX</i> is histidine (10) tagged C-terminally (amplified from pET-52b(+)-strep-SpftsEX-his10) | <i>pETDuet1</i> | Novagen, UK (71146) | pBR322 | Ampicillin | In this study |
| <i>pETDuet1-His₆-SpFtsA</i> | <i>ftsA</i> | The <i>ftsA</i> is histidine (6) tagged N-terminally | <i>pETDuet1</i> | Novagen, UK (71146) | pBR322 | Ampicillin | In this study |
| <i>pACYCDuet1-SpFtsA</i> | <i>ftsA</i> | The <i>ftsA</i> is untagged | <i>pACYC-Duet1</i> | Novagen, UK (71147) | P15A | Chloramphenicol | In this study |
| <i>pACYCDuet1-his6-SpftsAZ</i> | <i>ftsAZ</i> complete operon | The <i>ftsA</i> is histidine (6) tagged N-terminally and <i>ftsZ</i> is untagged. | <i>pACYC-Duet1</i> | Novagen, UK (71147) | P15A | Chloramphenicol | In this study |
| <i>pETDuetHETIS</i> | Empty Vector | The <i>pETDuet1</i> plasmid is modified at upstream of multiple cloning site-1 by introducing a highly efficient translation initiation site (HETIS) that contain a strong ribosome binding site. | <i>pETDuet1</i> | Novagen, UK (71146) | pBR322 | Ampicillin | In this study |
| <i>pCDFDuetHETIS</i> | Empty Vector | The <i>pCDFDuet1</i> plasmid is modified at upstream of first multiple cloning site-1 by introducing a HETIS sequence. | <i>pCDFDuet1</i> | Novagen, UK (71340) | ClonDF13-derived CDF replicon | streptomycin /spectinomycin | In this study |
| <i>pACYCDuetHETIS</i> | Empty Vector | The <i>pACYCDuet1</i> plasmid is modified at upstream of first multiple cloning site-1 by introducing a HETIS sequence. | <i>pACYC-Duet1</i> | Novagen, UK (71147) | P15A | Chloramphenicol | In this study |
| <i>pACYCDuetHETIS-His₆-SpFtsA</i> | <i>ftsA</i> | The <i>ftsA</i> is histidine (6) tagged N-terminally; a highly efficient translation initiation site (HETIS) is included at upstream of MCS-1 | <i>pACYC-DuetHETIS</i> | Original plasmid backbone was modified in this study | P15A | Chloramphenicol | In this study |
| <i>pETDuetHETIS-his₆-SpftsEX-his₁₀</i> | <i>ftsEX</i> complete operon | The overlapping operon of <i>ftsEX</i> is cloned into <i>pETDuetHETIS</i> . The <i>ftsE</i> is histidine (6) tagged N-terminally and <i>ftsX</i> is histidine (10) tagged C-terminally; a highly efficient translation initiation site (HETIS) is included at upstream of MCS-1. | <i>pETDuetHETIS</i> | Original plasmid backbone was modified in this study | pBR322 | Ampicillin | In this study |
| <i>pCDFDuetHETIS-pdB-ptsB-his₆</i> | <i>ptsB</i> or <i>gsp-781</i> (in R6 strain) | The <i>ptsB</i> is histidine (6) tagged C-terminally; a highly efficient translation initiation site (HETIS) is included at upstream of MCS-1. | <i>pHETIS-CDFDuet2</i> | Original plasmid backbone was modified in this study | ClonDF13-derived CDF replicon | streptomycin /spectinomycin | In this study |
| <i>pACYCDuetHETIS-his₆-SpftsAZ</i> | <i>ftsAZ</i> complete operon | The <i>ftsAZ</i> complete operon is cloned into <i>pACYCDuetHETIS</i> vector. The <i>ftsA</i> is histidine (6) tagged N-terminally and <i>ftsZ</i> is untagged. The plasmid containing a highly efficient translation initiation site (HETIS) at the upstream of MCS-1. | <i>pACYC-DuetHETIS</i> | Original plasmid backbone was modified in this study | P15A | Chloramphenicol | In this study |

4.B. Growth media, phenotypic studies and protein expression:

All transformed cell lines were grown aerobically in 100 mL Luria broth (LB) overnight (at 37 °C) before diluting the overnight cultures (OD_{600nm} is about 2) 10-folds into 900 mL 2YT autoinduction media (AIM, Formedium, UK) at 37 °C with appropriate antibiotics. This estimate starting OD_{600nm} of the overnight cultures in AIM were about 0.2. The cultures were incubated at 37 °C for at 180 rpm about 1 hr, till the optical density (OD) at 600 nm reaches 0.6. At this point, cells in AIM were immediately transferred to 20 °C or 15 °C incubator and grown overnight with continuous shaking at 180 rpm. For synchronous growth conditions of phenotypic studies, a starter culture in Luria broth was grown to $OD_{600}=1$ where DL-serine hydroxamate was added to a final concentration of 1mg/ml to induce the stringent response (Ferullo et al., 2009). Following further incubation for 90 mins these cultures were used to inoculate fresh media with antibiotic at 100 fold dilution, releasing the cells from stringent response and allowing further synchronous growth. Cells for purification were grown in up to 6L volumes as required and harvested by centrifugation at 10,000 rcf after for 10 mins at 4 °C. Harvested cells were washed and resuspended (at 5 ml per gram of cells) in lysis buffer (20 mM Tris-HCl/HEPES, pH – 8; 137 mM KCl; Glycerol 5% v/v) with protease inhibitor cocktail (EDTA free, Pierce, Thermo-scientific, UK). Resuspended cells were lysed using cell disrupter in two passes at 30 kpsi and 25 kpsi (Constant Systems, UK), centrifuged at 12,000xg for 10 minutes at 4°C. Supernatant from the spin was collected and further ultra-centrifuged (UC) at 150,000 rcf for 1 hour 15 minutes at 4° C. High-speed supernatants (HSS) were collected and stored at -20 °C for further analysis, while membrane pellets were dried and resuspended in SMALP extraction buffer (50 mM Tris-HCl/HEPES, 500 mM KCl, 5% v/v glycerol, pH 8) at 160 mg/mL concentration. Membrane pellets were solubilized using 2.5% (w/v) styrene-maleic acid (SMA) co-polymer in same extraction buffer as recommended by Lee et al., 2016 (Lee et al., 2016). The homogenized sample incubated for 3 hours at room temperature with gentle shaking on a roller, once the opaque sample become clear as a result of SMALP encapsulation of protein-lipid fragments, the sample was ultra-centrifuged at 150,000 rcf for 1 hour 30 minutes at 4 °C, and high-

speed soluble membrane fraction (in the supernatant) was collected and incubated with 1 or 2 ml Nickel-charged affinity resin (Ni-Nitrilotriacetic acid; Ni-NTA) overnight at 4 °C cold room on a rocker. SMALP-proteins bound to Ni²⁺-charged resins through recombinant histidine tags were purified through immobilized metal affinity chromatography (IMAC) where his-tagged SMALP proteins eluted with 500mM imidazole Ni-NTA buffer (50 mM Tris-HCl/HEPES, 500 mM KCl, 5% v/v glycerol, pH 8) by flowing through the over-night incubation and washed the beads with same above buffer except using 10mM (50mL), 20mM (50 ml) and 50mM (25 ml) imidazole in sequence. The eluted proteins were concentrated down to 500 µl using Viva-spin 20 (Sartorius, UK) filter tubes with appropriate molecular weight cut-off (MWCO). Finally the concentrated samples (~ 500 µL) centrifuged at 13500 ref for 15 min to pellet any precipitate before further separation and purification of the SMALP-Protein using size exclusion chromatography (SEC; Superose 6 10/300 GL or Superdex 200 Increase 10/300 GL). Fractions were monitored using UV-spectra associated with the ACTA pure device. SMALP-proteins were characterized using Native-PAGE, SDS-PAGE, standard western blot (WB) and immunoassay (IA) with HRP conjugated primary antibodies-Anti-His₆-Peroxidase (1:500; Roche, UK). Circular Dichroism of the SMALP-proteins were tested using J-815 CD Spectrometer (Jasco, UK).

4.C. ATP binding and ATP hydrolysis assay:

ATP binding assay was performed using an ATP fluorescent analogue BODIPYTM FL ATP-γ-S, (Adenosine 5'-O-(3-Thiotriphosphate), BODIPYTM FL Thioester, Sodium Salt) (A22184; ThermoFisher Scientific, UK). Purified protein samples (SpFtsEX, SpFtsEX-SpFtsA and SpFtsEX-PcsB) were incubated with BODIPY-ATP-γ-S (5 µM) and MgCl₂ (5 mM) for an hour, while their respective control assays did not incubated with any BODIPY-ATP-γ-S and MgCl₂. Following incubation all protein samples were separated upon non-reducing Native-PAGE and gels were imaged by exciting protein bands at 473 nm and filtered emission around 510 nm. Further the same gels were visualised under white light using Coomassie stain.

ATP hydrolysis ability of the purified protein complexes was determined by a standard pyruvate kinase and lactate dehydrogenase coupled enzyme assay as described in previous studies^{5,31}. Each assay was performed with 1 to 4 μg of purified protein complexes in total volume of 200 μL HEPES (50 mM, pH 8.0) buffer that containing 1.5 mM ATP, 5 mM MgCl_2 , 1 mM DTT, 50 mM KCl, 2 mM phosphoenolpyruvate (PEP), 0.3 mM NADH, pyruvate kinase 60 $\mu\text{g}/\text{mL}$, lactate dehydrogenase 32 $\mu\text{g}/\text{mL}$. The reduced absorbance for NADH at 340 nm, was an indicator of ATP-hydrolysis, recorded using spectrophotometer at 25°C for 30 min. Samples were normalised or corrected against blank which do not contain any ATP.

4.D. *E. coli* Membrane staining and confocal airyscan light microscopy:

Synchronised cells (as mentioned above) were grown until OD at 600 nm reaches approximately 3, when 100 μL of culture was spun on a bench-top centrifuge for 1 min at 8000 rpm. Cell pellet was washed by resuspending the pellet in 100 mL PBS and re-centrifuging the pellet again at 8000 rpm. The washed pellet resuspended in 100 μl PBS with FM4-64 (1:100; ThermoFisher, UK) and DAPI (4',6-diamidino-2-phenylindole; 1:100), and incubated for 5 minutes at 37 °C. Following incubation, 5-10 μl of sample pipetted onto agarose pad in order to immobilize live bacteria cells and covered carefully using cover slips. Bacterial membrane was stained and visualised with lipophilic dye FM4-64 (excitation/emission maxima \sim 488/640 nm), while bacterial nucleus was stained using DAPI (excitation/emission \sim 405/450 nm). Images were captured as a Z-stack (2-3 μm) of 20-25 optical slices (0.14 μm) processed under airy scan programme and projected based on maximum intensity calculation. Images with red fluorescent represent FM4-64 stain and blue represents DAPI stain.

4.E. Negative Staining and Electron Microscopy (EM):

Negative staining of the purified SMALP-protein (3 μL at a concentration of 0.1 mg/mL) was performed using uranyl-acetate stain (2%) on a glow-discharged EM grade continuous carbon grid, and imaged using Jeol 2100 (200kV). Negative stained EM images were processed using EMAN2 programme.

Grids (Quantifoil R1.2/1.3, UK) for cryo-electron microscopy (Cryo-EM) were glow-discharged (for 1 min) and coated with graphene oxide (GO) following standard protocol (1 min incubation with GO following 3 washes with double distilled water). Samples (3 μ L at a concentration of 0.1 mg/mL) were incubated for 30 seconds on GO coated grids before blotted for 7-8 seconds and plunged-frozen into liquid-ethane using Leica EM GP - Automatic Plunge Freezer (Leica Microsystem, UK). Frozen grids with protein were transferred to an FEG transmission electron microscope Jeol 2200FS (200kV). Images were captured using an estimated dose of 16 electrons/ \AA^2 for 0.5 s exposures.

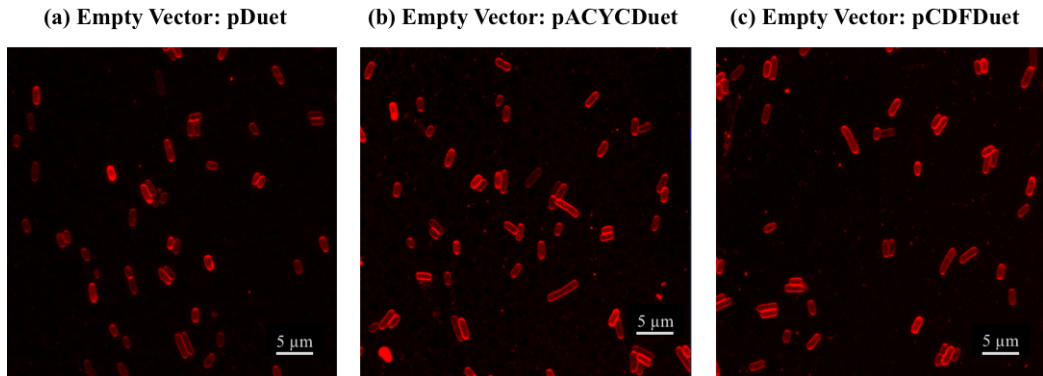
Acknowledgements:

We would like to thank Dr. Saskia Bakker (University of Warwick, UK) and Dr. Cristos Savva (University of Leicester, UK) for training and helping in Electron Microscopy; Mr. Ian Hands-Portman (University of Warwick, UK) for all guidance and training in Light Microscopy. We would like to thank Dr. Pooja Sridhar (University of Birmingham, UK) for setting up and running AUC with our samples and Dr. Sarah Lee (University of Birmingham, UK) for guiding and training on AUC data analysis. Special thanks to MRC, UK and Warwick Medical School (WMS) for funding this project, and School of Life Sciences (SLS) for providing lab space and other facilities.

All references are included above at the end of main Chapters (Chapter 6).

Supplementary Information:

Expression of empty vectors (Controls)



Heterologous expression of *S. pneumoniae* FtsE, FtsX, FtsA and PcsB in *E. coli*

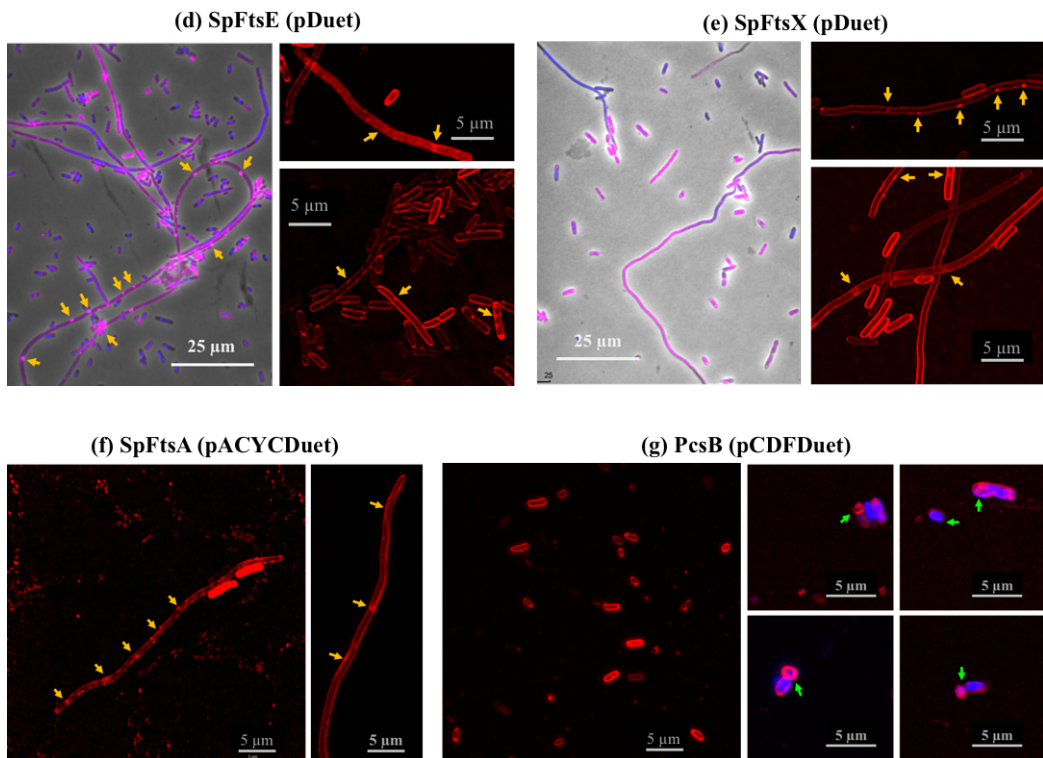


Fig. S1: Heterologous expression of *S. pneumoniae* divisome proteins. FM4-64 (red) and DAPI (blue) stained *E. coli* cells at 100x magnification transformed with empty vector pETDuet (a), pACYCDuet (b) and pCDFDuet (c) plasmids compared to the same cell line harbouring their respective above expression constructs for SpFtsE (d), SpFtsX (e), SpFtsA (f) and PcsB (g). Merged phase contrast micrograph with FM4-64 and DAPI channels at 40x magnification shows the cell surface morphology of SpFtsE (d: left panel) and SpFtsX (e: left) overproduced cells; whereas 100x magnification micrographs with FM4-64 staining of SpFtsE (d: right panel; top and

bottom), *SpFtsX* (e: right panel; top and bottom) and *SpFtsA* (f: left and right) shows patchy staining pattern (yellow arrows) in elongated cells. In contrast, *PcsB* overproduced cells with FM4-64 staining (g: left and right) shows normal cells, but some were observed with minicell formation pointed with green arrows (g: top and bottom images of centre and left panel).

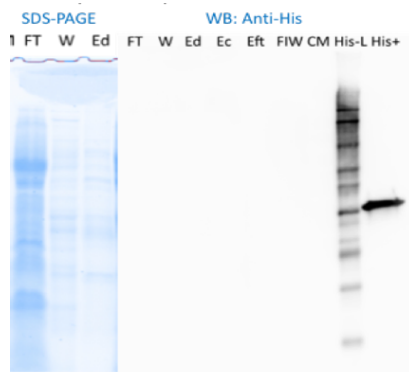


Fig. S2: An empty vector (*pDuet1*) was transformed and purified using SMALP extraction, IMAC and SEC. SDS-PAGE shows flow-through (FT) contain many proteins, which dilutes out with low imidazole wash (W) and elute (Ed) with high imidazole (500 mM). However, no detectable His-tagged protein was observed in Western blot and immunoassay with monoclonal anti-his-tag antibody that detects a his-tag positive control correctly with His+ sample as well as His-tagged ladder (His-L). CM: Colour marker.

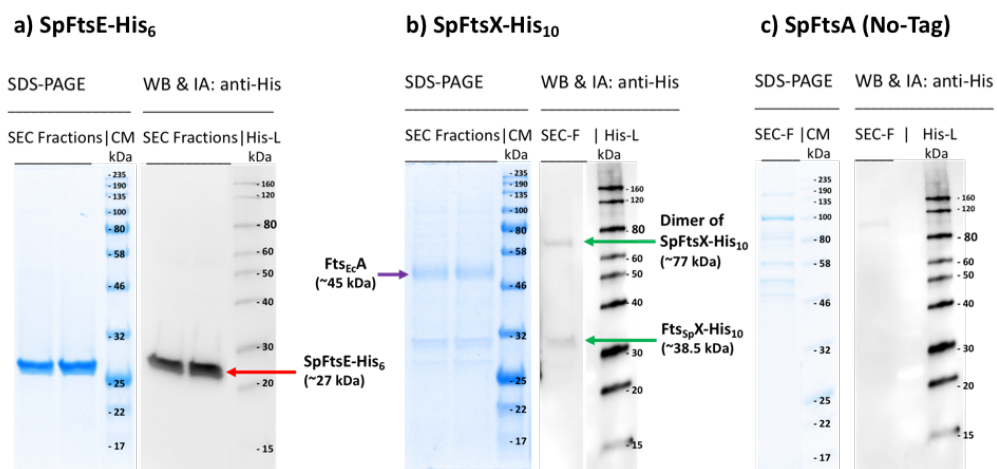


Fig. S3: *SpFtsE-His*, *SpFtsX-His* and untagged *SpFtsA* when purified individually following standard SMALP extraction, IMAC and SEC purification, we observed *SpFtsE-His* purified as single protein and migrated as single band (~27 kDa) upon SDS-PAGE and western blot (WB) and immunoassay (IA) against its his-tag (a); *SpFtsX-His* (~32 kDa) co-purified with another band around 46 kDa as observed in SDS-PAGE gel (b), however the same band is not detected in WB and IA with anti-his antibody. The 46 kDa band contain traces of *E. coli* *FtsA* peptides as found through mass spectrometry. In case of *SpFtsA* (untagged) expression and purification, no detectable and strong band is observed for *SpFtsA* in SDS-PAGE as well as in WB and IA (c).

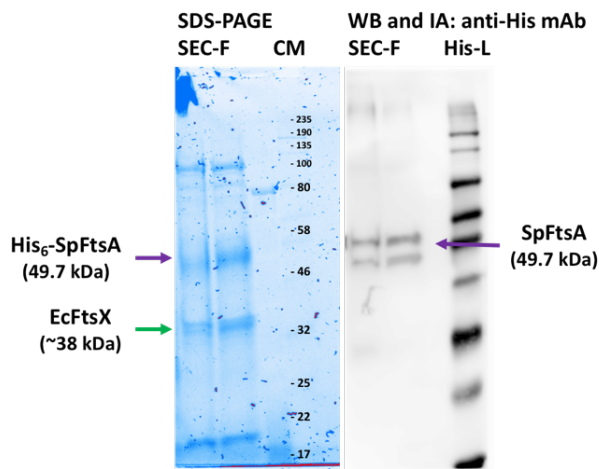


Fig. S4: Extraction and purification of *SpFtsA* (~49 kDa) that is his-tagged at N-terminally co-purified with traces of *E. coli FtsX* (~32 kDa) in the absence of cognate *S. pneumoniae FtsX*, as observed on SDS-PAGE but on WB and IA only His-tagged *SpFtsA* is detected.

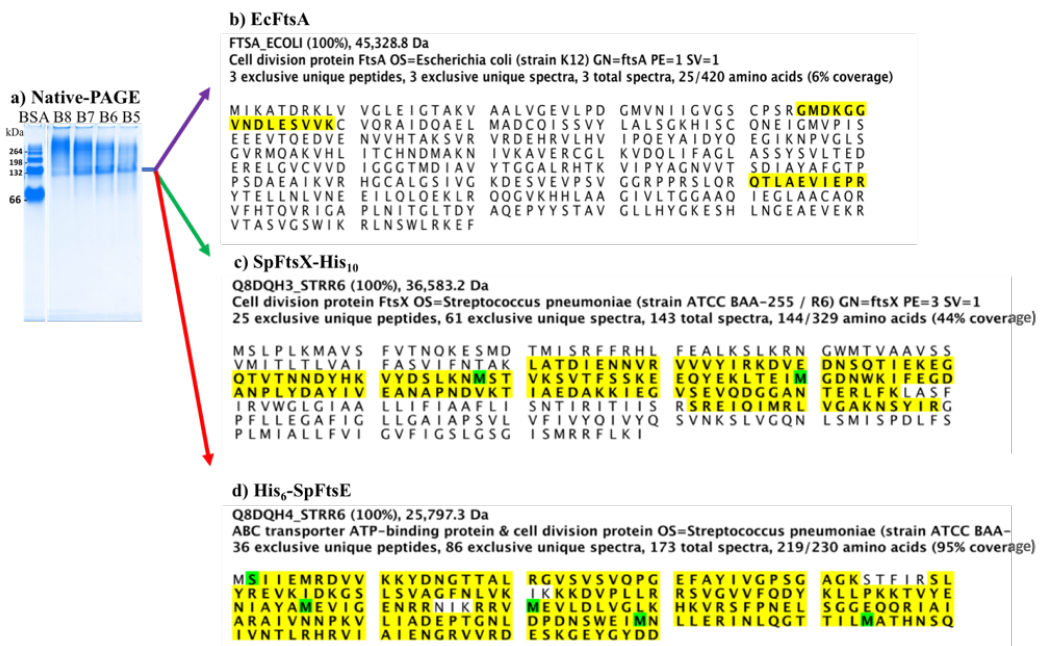


Fig. S5: SMALP extraction and purification of *SpFtsEX* copurify traces of *E. coli FtsA* as observed when the Native-PAGE bands (a) for the complex were analysed and sequenced through LC-MS/MS mass spectrometry. Yellow lines indicate sequence coverage by exclusive unique peptides. Overall 6%, 44% and 95% coverages were achieved with *EcFtsA* (b), *SpFtsX* (c) and *SpFtsE* (d) exclusive unique peptides respectively.

Co-expression : FtsX-His₁₀ and FtsA

Purification : His-Tag/Ni²⁺-NTA

SDS-PAGE

Sequence identification by Mass Spectrometry

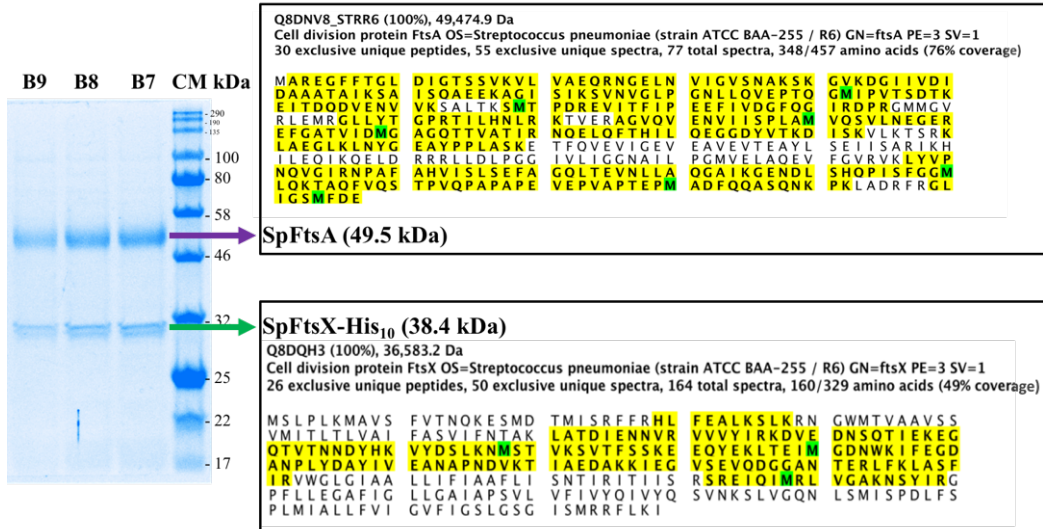


Fig. S8: Sequence identification of purified *SpFtsA* (untagged, ~ 49 kDa band) and *SpFtsX* (his-tagged, ~ 32 kDa band) on SDS-PAGE, using mass-spectrometry (LC-MS/MS) analysis.

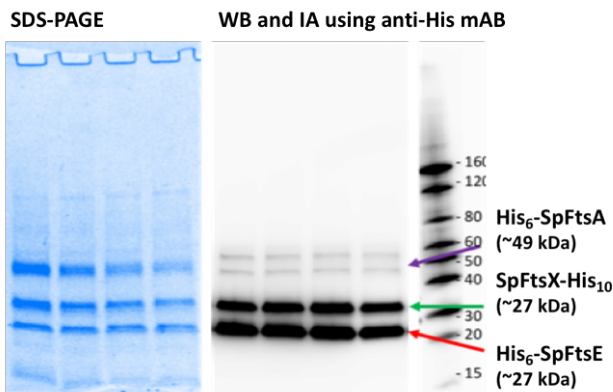


Fig. S9: His-tagged (*N*-terminal) *SpFtsA* in *pHETIS-ACYC* vector when co-transformed *E. coli* cells with *pHETIS-Duet2::SpFtsEX* (his-tagged). All three proteins co-expressed and co-purified as detected upon SDS-PAGE, WB and IA. His₆-*SpFtsA* detected with two close bands, which also observed in a previous study²⁵, indicates a possible *C*-terminal truncation.

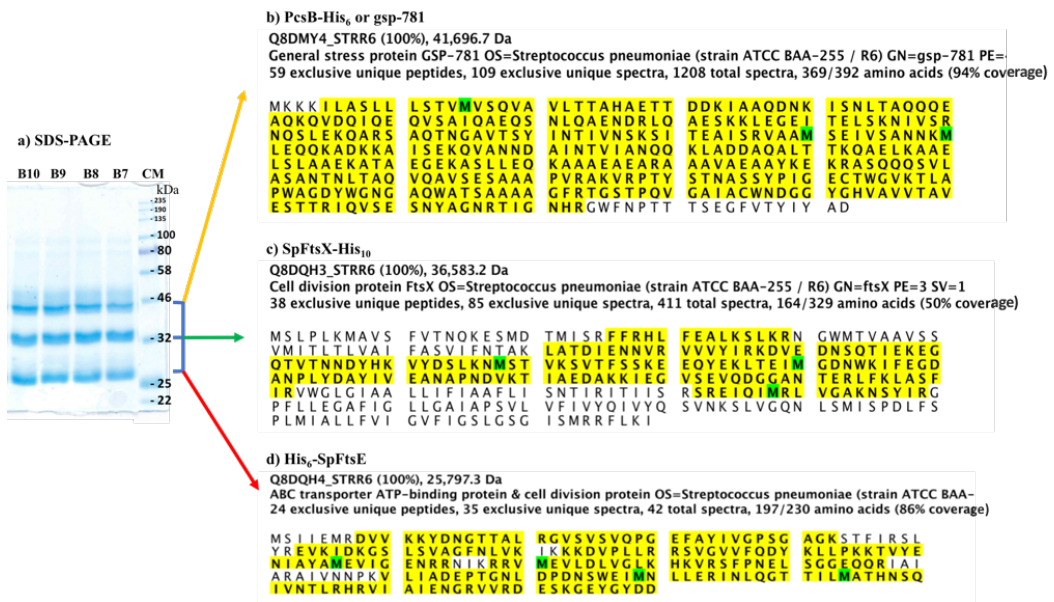


Fig. S10: SMALP extraction and purification of SpFtsEX-PcsB complex when separated upon SDS-PAGE (a) three bands (~ 42 kDa, 36 kDa and 27 kDa) were detected through Coomassie staining. These bands are analysed and sequenced through LC-MS/MS mass spectrometry, which them as PcsB (b), SpFtsX (c) and SpFtsE (d) with overall 94%, 50% and 86% sequence coverage respectively with their corresponding exclusive unique peptides. Yellow lines indicate sequence coverage by exclusive unique peptides.

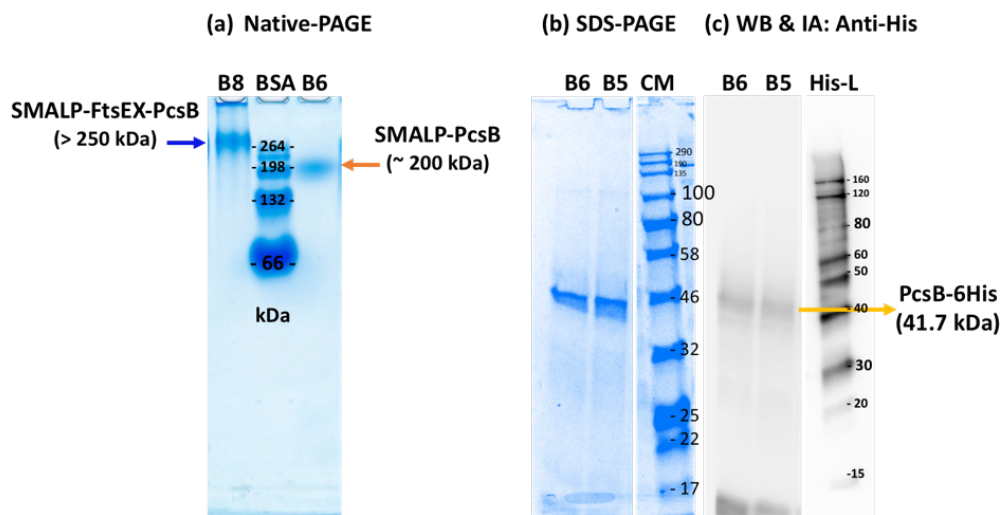


Fig. S11: Purified SMALP-PcsB protein migrate further compared to purified SMALP-SpFtsEX-PcsB complex upon non-reducing Native-PAGE (a), SDS-PAGE of the same SMALP-PcsB sample shows good purity of PcsB as single band around 42 kDa (b), the same band also detected on WB and IA (c).

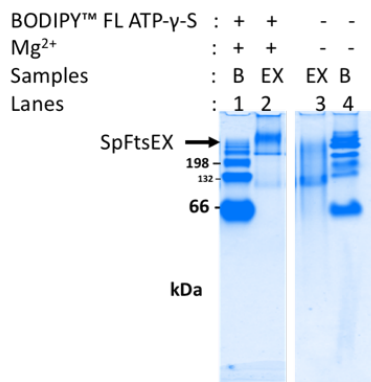


Fig. S12: Coomassie stained Native-PAGE of the same gel that analysed for BODIPY-ATP-γ-S binding as shown in main Fig. 5a.

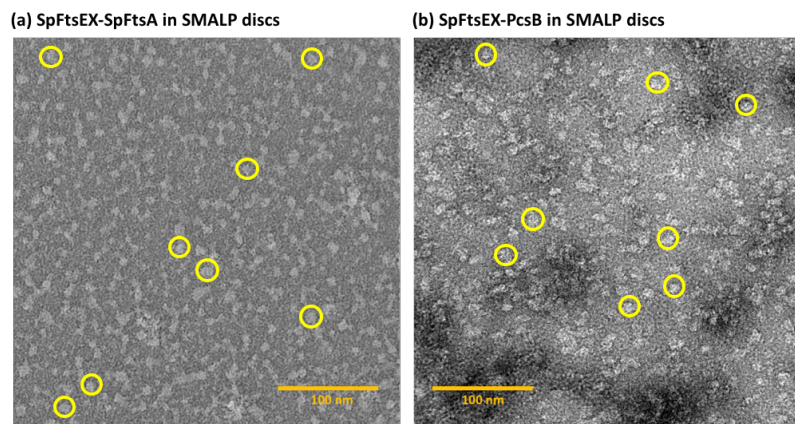


Fig. S13: Negative stain (UA 2%) electron micrograph of SpFtsEX-SpFtsA complex (a), and SpFtsEX-PcsB complex (b) in SMALP discs, sizes between 12 nm – 20 nm, shows monodispersed. Yellow circles are directing few of those disc like structure. Scale bar 100 nm.

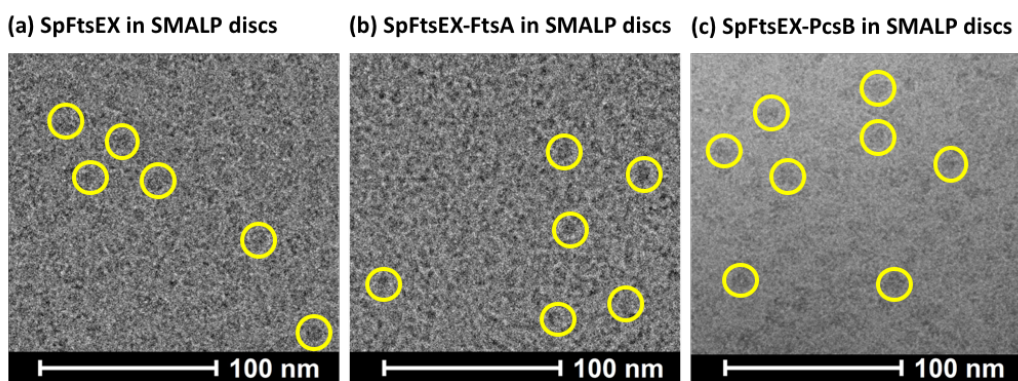


Fig. S14: Cryo-electron micrograph of SpFtsEX complex (a), SpFtsEX-SpFtsA complex (b), and SpFtsEX-PcsB complex (b) in SMALP discs, shows good contrast of monodispersed particles. Yellow circles are directing few of those disc like structure. Scale bar 100 nm.